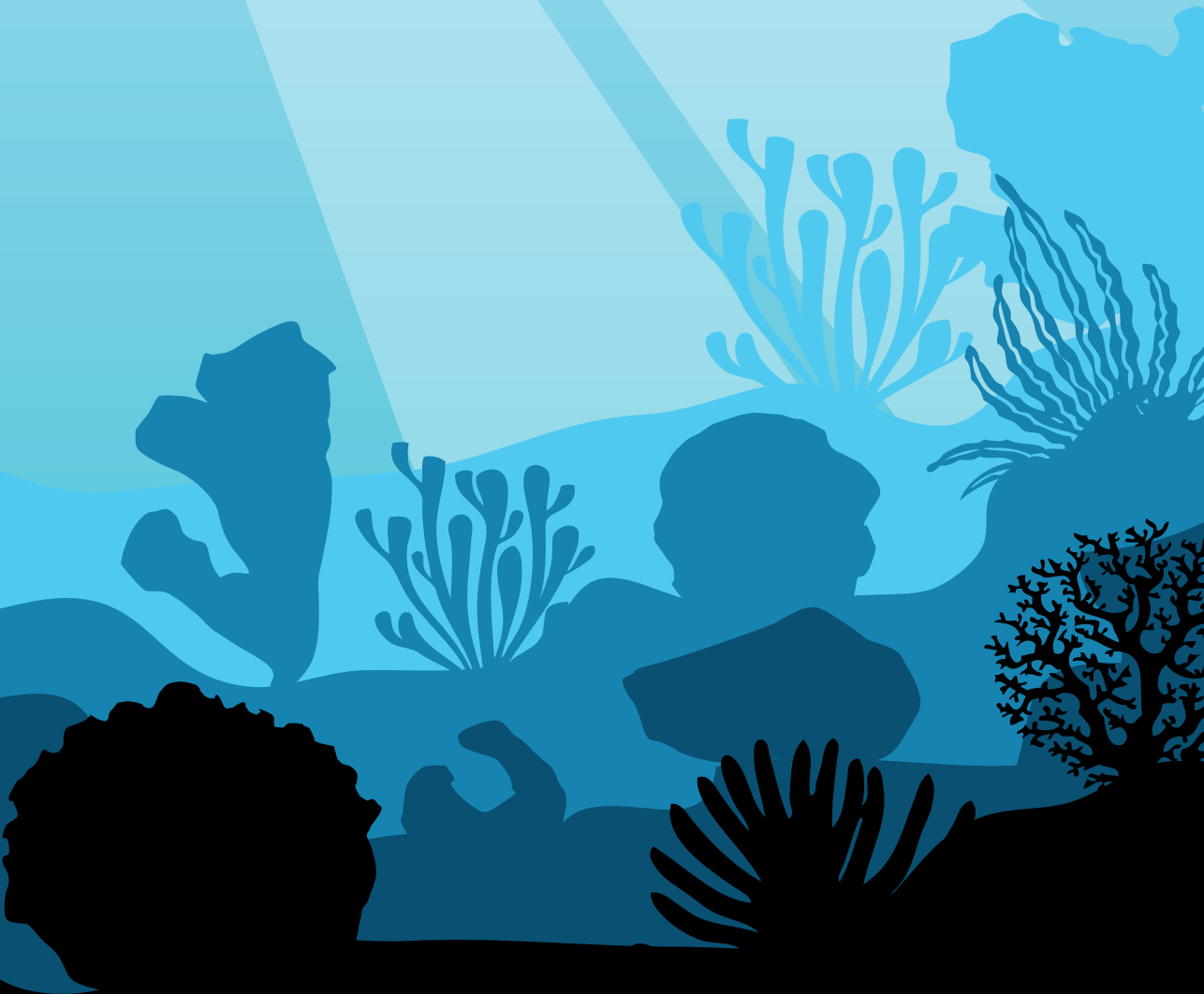


Depth Matters: (anti) Microbial Diversity of Marine Sponges



ANAK AGUNG GEDE INDRANINGRAT

Propositions

1. Sponges inhabiting shallow water yield stronger antibacterial activities compared to their deep-water counterparts.
(this thesis)
2. In marine sponges, host-identity plays a more significant role in determining prokaryotic community composition than the impact of depth.
(this thesis)
3. Writing a popular science article should be included in every PhD curriculum.
4. Offline courses offer a more comprehensive and interactive understanding of a subject compared to Massive Open Online Courses (MOOCs).
5. Multitasking leads to procrastination.
6. The introduction of video assistant referees (VARs) makes football less attractive to watch.

Propositions belonging to the thesis, entitled:

“Depth Matters: (anti) Microbial Diversity of Marine Sponges”

Anak Agung Gede Indraningrat
Wageningen, 29 May 2019

Depth Matters: (anti) Microbial Diversity of Marine Sponges

Anak Agung Gede Indraningrat

Thesis committee

Promotor

Prof. Dr Hauke Smidt

Personal chair at the Laboratory of Microbiology
Wageningen University & Research, The Netherlands

Co-promotors

Dr Detmer Sipkema

Associate professor at the Laboratory of Microbiology
Wageningen University & Research, The Netherlands

Dr Leontine E. Becking

Assistant professor at the Marine Animal Ecology Group
Wageningen University & Research, The Netherlands

Other members

Prof. Dr Shirley A. Pomponi, Wageningen University & Research

Prof. Dr Peter J. Schupp, Carl von Ossietzky Universität Oldenburg, Germany

Prof. Dr Jos Raaijmakers, NIOO-KNAW

Prof. Dr Nicole J. de Voogd, Naturalis, Leiden

This research was conducted under the auspices of the Graduate School VLAG
(Advanced studies in Food Technology, Agrobiotechnology, Nutrition and Health Sciences)

Depth Matters: (anti) Microbial Diversity of Marine Sponges

Anak Agung Gede Indraningrat

Thesis

submitted in fulfilment of the requirements for the degree of doctor
at Wageningen University

by the authority of the Rector Magnificus,

Prof. Dr A.P.J. Mol,

in the presence of the

Thesis Committee appointed by the Academic Board

to be defended in public

on Wednesday 29 May 2019

at 4 p.m. in the Aula

Anak Agung Gede Indraningrat
Depth Matters: (anti) Microbial Diversity of Marine Sponges,
222 pages.

PhD thesis, Wageningen University, Wageningen, the Netherlands (2019)
With references, with summaries in English, Dutch and Bahasa Indonesia

ISBN: 978-94-6343-944-2

DOI: <https://doi.org/10.18174/475461>

This thesis is dedicated to my parents, my sister and my wife

Table of contents

Chapter 1	General Introduction	9
Chapter 2	Bioprospecting sponge-associated microbes for antimicrobial compounds	23
Chapter 3	Depth affects sponge prokaryotic communities and their antimicrobial activities in two Demosponges, <i>Xestospongia muta</i> and <i>Agelas sventres</i>	69
Chapter 4	Cultivation and antimicrobial screening of sponge-associated bacteria from the marine sponges <i>Agelas sventres</i> and <i>Xestospongia muta</i> collected from different depths	101
Chapter 5	Quantifying variations of microbiota and metabolome composition in deep-sea sponges - implications for chemical ecology and bioprospecting	141
Chapter 6	General discussion	173
	References	188
	Thesis Summary	208
Appendices	Nederlandse Samenvatting	210
	Ringkasan Bahasa Indonesia	212
	Acknowledgements	214
	Co-author affiliations	218
	About the author	219
	List of publications	220
	Overview of completed training activities	221
	Colophon	222



Chapter 1

General Introduction



Marine sponges: a brief overview of biology and ecology

Sponges (phylum Porifera) are the oldest metazoans, and radiocarbon dating has revealed that these animals have existed since the Precambrian era, approximately 650 million years ago [1]. Sponges mostly inhabit marine habitats, and only a small number of species can be found in fresh water habitats including e.g. lakes or rivers [2,3]. The morphologies of sponges are highly diverse ranging from flat, tube, barrel, encrusting tissue to branching, along with different colours, and their sizes can span from a few millimetres to several metres [3]. Depending on the type of sponge, skeletal components may consist of calcium carbonate, silicate, chitin or spongin [3,4]. These skeletal components are also the basis for taxonomic identification of sponges, which have been classified for decades into three major classes: Demospongiae (common sponges), Hexactinellida (glass sponges) and Calcarea (calcareous sponges) [5]. Only recently, Homoscleromorpha has been suggested as a new class, since the comprehensive analysis of molecular marker genes revealed deviation of this sub-class from the initial grouping within the Demospongiae [3,6]. Up to now, over 8500 sponge species have been described, and 80% of those are classified into the Demospongiae [3,7].

Sponges are sessile animals that display a simple organizational body plan without specialized tissues or organs (Figure 1). Their outer part (pinacoderm) consists of many small pores (ostia) to filter seawater from the surrounding environment [3]. Briefly, the incoming seawater is filtered through aquiferous systems by choanocytes, the function of which is to capture food particles such as bacteria, archaea, viruses and unicellular algae [4]. Subsequently, these captured particles are transported to the inner part (mesohyl) to be either digested by archaeocytes via phagocytosis or retained in the mesohyl as associated microbes [8,9]. Finally, the nearly sterile seawater is extruded via the main large opening (osculum) [3]. With their remarkable pumping ability, sponges are estimated to be able to filter up to 24,000 litres of seawater per kg per day [10].

Sponges occupy marine habitats across different biogeographical regions and are pivotal for marine ecosystem functioning [11]. Firstly, sponges contribute to stabilizing reef structure via calcification, cementation and bio-erosion. Secondly, sponges and their associated microbiomes are prominent players in various biogeochemical cycles in marine habitats, including e.g. the carbon, nitrogen, sulphur, silicon, and phosphorus cycles [12]. Thirdly, sponges capture dissolved organic matter from the surrounding seawater and subsequently

make these nutrients accessible for higher trophic levels [13,14]. Lastly, sponges affect the water column by their filtering capacity and deter predators by producing secondary metabolites [11].

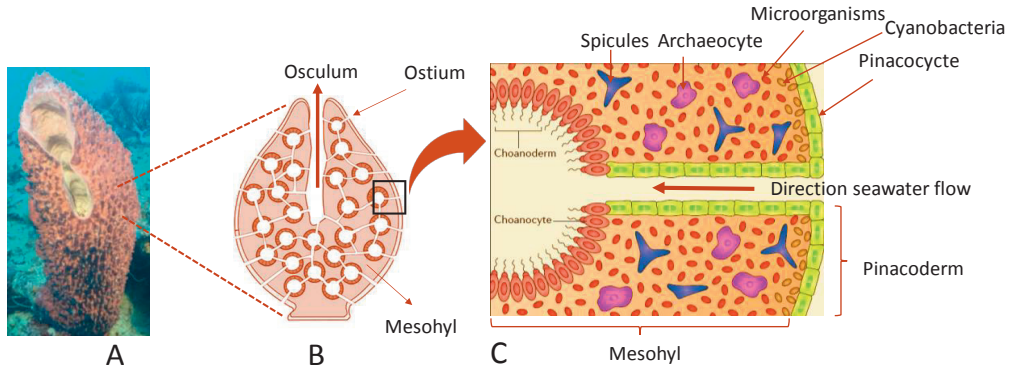


Figure 1. An example of sponge body structure (A, underwater photograph of *Xestospongia muta* taken during the field trip near Curaçao), along with an illustration of a typical canal system (B, adapted from [15]) and an overview of internal structure of Demosponges (C, adapted from [4] with permission from Nature Publisher Group).

Sponge-associated microbes

The association of sponges and microorganisms has been recognised since decades when early electron microscopy studies showed that some sponge species harbour a great amount of microbes in their tissues [16]. Further investigation showed that some of these microbes remain undigested since they are protected by a capsule-like structure to hide from phagocytosis by archaeocytes [17]. In terms of density, prokaryotic communities within sponge tissues vary, depending on the sponge species. Some species have prokaryotic densities in the range of 10^8 – 10^{10} cells per gram of sponge wet weight, and they often are referred to as high microbial abundance (HMA) sponges [9]. Other sponges may harbour only 10^5 – 10^6 prokaryotic cells per gram of sponge wet weight, which is similar to the abundance of microbes in seawater, and thus they are grouped as low microbial abundance (LMA) sponges [18,19]. Sponge-associated microbes have attracted increasing attention since evidence has accumulated that these prokaryotic assemblages contribute to their hosts by their involvement in nutrient metabolism in the holobiont, such as the carbon, nitrogen, sulphur and phosphorus cycles [19–21]. In addition, sponges-associated microbes also play an important role in host-defence by producing various secondary metabolites to reduce predation by fish, biofouling organisms and bacterial infections [4,19].

The advance of molecular tools in the past decades has paved the way to study prokaryotic assemblages of marine sponges without requiring direct cultivation, given that the majority of these bacteria and archaea remain uncultivable [4,19]. In 2002, Hentschel and co-workers conducted phylogenetic analyses of 190 sponge-derived 16S ribosomal RNA (rRNA) gene sequences that led to the identification of 14 unique monophyletic clusters from seven bacterial phyla that were coined as “sponge-specific clusters” [22]. Sponge-specific clusters were defined to have 16S rRNA gene-sequences from (1) at least three sponge species; (2) from different geographic locations; (3) and are more similar to each other than to non-sponge derived sequences [22]. Simister and co-workers expanded the analysis of sponge-specific clusters using 7500 publicly available sponge-derived 16S rRNA gene sequences and identified that such clusters were present in 14 phyla, with most clusters being assigned to the phyla Proteobacteria, Acidobacteria, Chloroflexi, Cyanobacteria, Poribacteria and Thaumarchaeota [23]. Recently, the Global Sponge Microbiome Project analyzed prokaryotic communities of 804 samples from 81 sponge species and identified 41 bacterial and archaeal phyla (including candidate phyla) associated with sponges [24]. Recent evidence, however, showed that sequences of these sponge-specific clusters could also be retrieved in minute numbers from environmental sources e.g. seawater or sediment, and thus the term “sponge-enriched cluster” was introduced to accommodate these observations [24,25]. Many sponge-associated bacteria that make part of sponge-enriched clusters are phylogenetically only distantly related to bacteria found in other environments. For example, Fieseler and co-workers discovered a 16S rRNA gene sequence that only shares 75% similarity with known bacterial sequences, which led to the proposition of the candidate phylum Poribacteria [26]. Compelling evidence confirmed that Poribacteria are present almost exclusively in sponges and consist of different phlotypes [27,28].

Despite the advance of molecular methods to investigate prokaryotic community composition, culture-dependent methods remain essential to gain insight in metabolic capacities of microorganisms. Furthermore, the ability to culture allows small-scale production of secondary metabolites, and to build strain collections [29]. The fact that sponge-associated bacteria are the potential sources of pharmaceutically relevant products has indeed been the main inspiration to culture these microbes in synthetic media [30,31]. In the past decade, several attempts have been made to increase cultivability of sponge-associated bacteria such as by designing various types of growth media [32,33], supplementing growth media with sponge extracts[32,34], and *in situ* cultivation by designing diffusion growth chambers [35], and the I-

tip [36]. Although, several novel isolates have been obtained [32], most of these only represented a small fraction of the total prokaryotic community of marine sponges and mainly represented four phyla only: Actinobacteria, Proteobacteria, Bacteroidetes, and Firmicutes [29]. In fact, most of these cultivable bacteria are not affiliated with any of the sponge-enriched clusters, but they likely represent opportunistic bacteria that are present in the sponge's canal system [29,32,33].

Sponges and their associated microbes as source for antimicrobial compounds

Nowadays, resistance of microorganisms against antimicrobial drugs, which is triggered by misuse and overuse of antimicrobial drugs in the medical and veterinary sectors, increasingly poses challenges in medical treatments [37,38]. Pathogenic microbes acquire resistance via several mechanisms e.g. mutation, transduction and transformation [39]. Antimicrobial resistance is a serious global threat, which is expected to attribute to 10 million deaths worldwide in 2050 and to trigger an economic loss of up to 100 trillion US dollars because of a decrease of 2-3% in the gross domestic product [40]. In recent decades, only a limited number of new antimicrobial drugs have been introduced on the market, and this does not keep pace with the increasing rate of morbidity and mortality due to infections by resistant pathogenic strains [41]. Therefore, increasing efforts to search for novel antimicrobial substances are urgently needed.

The oceans harbour a largely untapped source of secondary metabolites with approximately 15,000 marine natural compounds described so far [42]. Among all the investigated marine organisms, sponges contribute to almost 30% of the known marine natural products, including for example alkaloids, polyketides, non-ribosomal peptides, sterols, and terpenes [42,43]. These sponge derived compounds exhibit a broad array of biological activities including antimicrobial, antitumor, anticancer, anti-inflammation, immunosuppressive, and neuro-suppressive activity [42-45]. Bioassay-guided investigations of sponge extracts against clinically relevant bacteria, viruses, protozoa and fungal pathogens have led to identification of potent molecules with antimicrobial activity, such as lasonolide A (anti *Candida albicans*), manzamine A (antimalaria, anti HIV-1), and psammaphin A (anti methicillin-resistant *Staphylococcus aureus*) [46].

Although many bioactive molecules have been derived from sponges, sustainable supply is a major bottleneck for these complex biomolecules to enter preclinical and clinical trials [31,47].

As an illustration, 300 mg of the anticancer compound Halicondrin B requires 1 metric tonne of the sponge *Lissodendoryx* sp [48]. Obviously, with such low yield, clinical trials with patients become unfeasible. Therefore, different approaches need to be taken to overcome the supply issues. One of the alternative avenues would be to search for these bioactive molecules among sponge-associated microbes since many sponge natural products are of microbial origin [49,50]. Tremendous efforts to search for antimicrobial compounds from sponge-associated microbes via direct cultivation have led to the discovery of some potent antimicrobial compounds *in vitro* such as the antiviral sorbicillactone A [51], the antibacterial subtilomycin [52], the antifungal saadamycin [53] and the antiprotozoal manzamine A [54]. Additionally, metagenomics based strategies have also been applied to complement culture dependent approaches in order to explore the biochemical potential of the uncultivable fraction of sponge-associated microbes for producing novel drugs [55-58]. Through heterologous expression, the identified gene clusters can be expressed in a suitable hosts [59]. As an example, three novel antibacterial proteins have been identified from the microbiome of the sponge *Cymbastela concentrica* using a metagenomics approach [60].

While drug discovery in the past decade has focused on shallow sponges, deep-sea sponges have been shown to also harbour as much potential as their shallow counterparts with respect to the diversity of antimicrobial substances. For example, the compounds fascioquinol A and B (antibacterial), 3-O-methyl massadine chloride (antibacterial and antifungal) and alisiaquinone C (antimalaria) were obtained from deep-sea sponges [61,62]. Additionally, prokaryotic communities of deep-sea sponges also possess an array of secondary metabolite gene clusters that are predicted to encode pharmaceutically relevant compounds including many classes of antibiotics [63].

Despite the number of antimicrobial compounds reported from sponges and their associated microbes, unfortunately, none of these compounds that show high potency *in vitro* has currently entered preclinical/clinical assessment nor have they been approved as drugs on the market [47]. In many cases, pharmaceutical companies tend to invest more on cancer research since this field has a larger market potential than antimicrobials [60,62]. For instance, sponge-derived anticancer compounds cytarabine and eribulin mesylate have been approved by the US FDA for clinical use and are now available on the market as anticancer drugs [66]. Irrespective of these bottlenecks, sponges and their associated microbes have proven themselves as prominent producers of secondary metabolites and with respect to their antimicrobial activity. Thus, they

indeed may provide a valuable resource for discovery of novel antimicrobial compounds to overcome infections with resistant pathogens when the urgency further grows.

Diversity of sponges and their associated microbes along depth gradients

Sponges occupy a wide range of marine habitats across a broad bathymetric range starting from shallow waters (< 30 m), the mesophotic zone (30 – 200 m) to the deep sea (> 200 m). Mesophotic environments are below shallow coral reefs and are defined as reef communities present in the low-light zone at intermediate depths ranging from 30 to 200 m [34,64]. The upper limit of the mesophotic zone is often determined based on the depth limit of recreational SCUBA diving, while the lower limit can vary depending on local environmental factors (mainly light intensity and temperature) [65,66]. The deep sea approximately starts from around 200 m and is generally characterized by dark conditions with high pressures, primarily cold and well-oxygenated environments [67]. In the past decade, numerous studies have been undertaken to investigate sponges from shallow reefs and have advanced our understanding on ecology and biotechnological aspects of the sponge-microbiome holobiont. Conversely, knowledge of sponges beyond shallow habitats is rather limited, which is mainly constrained by technical issues and costs to obtain those samples [66,68,69]. The advances of scuba diving, submersibles and remotely operated vehicles in the past decades, however, provided new opportunities to further explore the marine environment beyond shallow water [70]. For example, the Bonaire Deep Reef Expedition that covered the lower mesophotic and upper dysphotic (99.5 m to 242 m) zones using a manned submersible collected 52 sponge specimens belonging to 31 species of which 13 were identified as new species [71]. Furthermore, the Spanish/EU bottom trawl ground fish surveys at a depth range of 40 – 1500 m at the Flemish Cap, Flemish Pass and the Grand Banks Northwest Atlantic Ocean have reported large sponges communities with at least 30 different sponge species. These two studies underlined the differences in community structure and abundance of sponges between shallow and deep habitats, which has been mainly linked to the difference in ecological conditions connected to depth.

Differences in terms of environmental conditions that prevail in habitats beyond shallow water with respect to fluctuations of physicochemical factors (e.g. light, nutrient, temperature) [66,72] and stressors (e.g. predators and pathogens) [66,73] could possibly be linked to changes in prokaryotic composition of sponges. From studies conducted in shallow water, sponges have

been reported to maintain their prokaryotic composition irrespective of different season, temperature, and biogeographical distances [74-76]. A transplantation study of sponges *Tethya bergquistae* and *Ecionemia alata* from high-light to low-light habitats and vice versa showed changes in sponge morphology, but surprisingly, a stable prokaryotic composition was retained [77]. Similarly, a transplantation study of the sponge *Aplysina cavernicola* from below 40 m depth to a high-light intensity habitat (7 – 15 m) had no effect on microbiota and metabolome profile of the sponge [78]. Conversely, analysis of prokaryotic communities from the three Caribbean sponges *Plakortis angulospiculatus*, *Agelas conifera*, and *Xestospongia muta* from shallow waters to the mesophotic zone highlighted that depth influenced cyanobacterial composition of sponges [79]. Moreover, a depth gradient study of *X. muta* from 10 – 90 m depth showed that prokaryotic composition of *X. muta* was impacted by environmental factors associated with depth (light and the level of inorganic nutrition) [80]. A depth gradient study on *Callyspongia* spp. indicated substantial differences in prokaryotic community composition with respect to members of the Cyanobacteria and Betaproteobacteria between shallow reef slopes to deep drop-off reefs, however, the actual environmental conditions that drive for such difference remain uncertain [81].

Exploration of deep-sea sponges provides a glimpse on their prokaryotic community composition. A microbial community survey of the Caribbean sponge *Polymastia* cf. *corticata* from a depth of approximately 1100 m indicated presence of abundant sponge-specific sulfur-oxidizing Gammaproteobacteria and Alphaproteobacteria and a sulfate-reducing archaeon, which was previously reported to be present in shallow water sponges [82]. A comparative study of deep *Geodia* spp. and sediment samples indicated similarity of microbiota composition between the two biotopes including the presence of anaerobic ammonium oxidizing (anammox) bacteria and sulfate-reducing bacteria, suggesting that deep-sea sponges have recruited these specific functional guilds from the surrounding environments [83]. Investigations on four sponges (*Lissodendoryx diversichela*, *Poecillastra compressa*, *Inflatella pellicula*, and *Stelletta normani*) collected from a depth of approximately 700 m showed that these deep species shared similar archaeal populations with their shallow counterparts but that the deep sponges had a distinct bacterial community including Gammaproteobacteria from the Chromatiales group [84]. The deep sea is also a habitat for carnivorous sponges from the family Cladorhizidae, which are typically host to methane-producing bacteria [85,86]. Given that the deep sea covers a wide bathymetric range, however, none of these deep-sea explorations to date focused on prokaryotic composition along a depth gradient. Thus, we generally know very

little to what extent vertical distribution affects prokaryotic community of sponges and to which extent it influences metabolite compositions of sponges, especially of those that occupy deep-sea habitats.

Research aim

It has become clear that sponges and their associated prokaryotic communities are important both for marine ecology and for biotechnological purposes. However, as previously mentioned, relatively limited information is available on the impact of depth on prokaryotic community composition and the variability of metabolite profiles, including the production of antimicrobial compounds in sponges. Therefore, with this thesis I aim to characterize prokaryotic composition, antimicrobial activity and the metabolome of marine sponges along different depth gradients. Overall, the research described in this thesis is expected to expand our knowledge on ecological aspects of sponge-associated microbes beyond shallow habitats and to provide additional insight on bioprospecting with respect to the discovery of novel compounds with antimicrobial activities and other therapeutic applications from sponges and their symbionts. Figure 2 provides a brief overview of research described in this thesis.

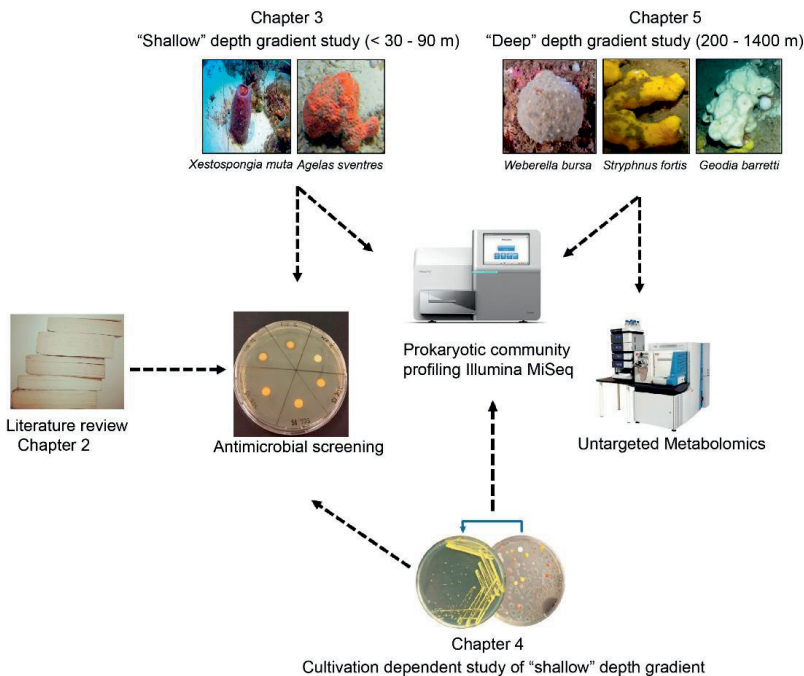


Figure 2. A schematic representation of each research chapter described in this thesis. The direction of arrows indicates methods used in each of research chapter. Underwater pictures of *Agelas sventres* and *Xestospongia muta* were taken in the Curaçao Sea during a sampling trip. Underwater photograph of *Weberella bursa* was provided by Peter Leopold, University of

Tromsø, Norway, taken at 40 m at Svalbard. Underwater images of *Stryphnus fortis* and *Geodia barretti* were taken at the West Shetland Channel by courtesy of K. Howell, Plymouth University, UK.

Study objects

Sponge species that are present and relatively abundant with a considerable depth range were selected for this work. *Xestospongia muta* and *Agelas sventres* were selected since they are abundant from shallow water to mesophotic depths and were sampled in the Curaçao sea in the Dutch Caribbean. In addition, the three boreal sponges *Weberella bursa*, *Stryphnus fortis* and *Geodia barretti* represent sponges that occupy deep-sea habitats and were sampled in the David strait during a sea expedition conducted by the Department of Fisheries and Oceans, Canada. In the following section, these target sponge species are described to provide a brief overview of our current knowledge with respect to their morphology, prokaryotic community composition and secondary metabolites.

Agelas sventres, Lehnert & van Soest, 1996 (Demospongiae, Agelasida, Agelasidae) is distributed around the tropical western Atlantic and spans a depth range from around 20 m to 125 m [87]. *A. sventres* (Figure 2) was previously named “*Agelas* species 3”, and received its specific epithet by combination of “Sven” and “Tres” to acknowledge Sven Zea, a marine scientist who had dubbed this *Agelas* species [88,89]. *A. sventres* is characterised by a bulbous, massive-lobate to ball form with a diameter of around 10-40 cm. Its external structure colour is orange while the internal colour ranges from orange to orange yellow [87]. *A. sventres* can be confused with the smaller *Agelas clathrodes* (Schmidt, 1870) based on morphological characteristics, but *A. sventres* usually displays a softer, cavernous lobes crown with holes or oscules and acanthostyles type of spicules [90]. *Agelas* extracts have a wide range of biological activities [91]. To date, one bioactive substance has been reported from *A. sventres*, namely sventrin, a bromopyrrole alkaloid, which serves as a feeding deterrent against the omnivorous reef fish *Thalassoma bifasciatum* [92]. Up to now, the prokaryotic community of *A. sventres* is unknown. However, previous prokaryotic community profiling of other *Agelas* species, e.g. *A. conifera*, *A. dispar* and *A. oroides* has consistently grouped them as HMA sponges [79,93,94].

Xestospongia muta, Schmidt, 1870 (Demospongiae, Haplosclerida, Petrosiidae), often referred to as the “great barrel sponge”, is a conspicuous sponge species and abundantly distributed in

the Caribbean sea, Bermuda, the Bahamas, Florida and the Gulf of Mexico over a wide depth range starting from 10 m to around 100 m [80,89,90,95]. *X. muta* (Figure 2) is characterised by a typical barrel-shape and even surface [89,90]. Individuals are often very large, with heights and diameters that can reach over 1 m [96]. *X. muta* is well studied for its secondary metabolites, and isolated compounds include antitumor (dibromo acetylenic acid) [97], anti HIV (brominated polyacetylenic acid) [98], and antifungal (ene-yne tetrahydrofurans) molecules [99]. A recent metabolite profiling study showed that *X. muta* harbours many brominated polyunsaturated fatty acids [100]. In addition, a transcriptomic analysis suggested that the microbiota associated with *X. muta* plays a pivotal role in nitrogen cycling in coral reef habitats, indicated by detection of multiple nitrogen transformation pathways [101].

Weberella bursa, Linnaeus, 1758 (Demospongiae, Polymastiida, Polymastiidae) is distributed in the northeastern Atlantic Ocean from the Arctic to the iberomoroccan Gulf and has a depth range from 130 - 1500 m [102,103]. *W. bursa* (Figure 2) is characterised by a globular or ovoid shape with a firm consistency and a finely hispid surface [89,102]. The exhalant papillae are numerous (50 – 100 per specimen) and very small. *W. bursa* has similar morphological characteristics as *Polymastia thielei* and *Polymastia uberrima*, but can be distinguished from the two *Polymastia* species by the pale colouration of both the cortex and the choanosome, a much thinner cortex, the reticulate choanosomal skeleton and the presence of just two size categories of spicules [104]. There are no studies on the prokaryotic composition and metabolite profiles of *W. bursa*. However, sponges within the family of Polymastiidae e.g. *Polymastia* sp. have been reported to have a low number of associated microorganisms [93], to indicate that *W. bursa* is likely an LMA sponge.

Stryphnus fortis, Vosmaer, 1885 (Demospongiae, Tetractinellida, Ancorinidae) is a typical deep-sea sponge with reported depth range of 200-2598 m and is dominantly found from the boreo-arctic region to the Azores to Northern Norway [105]. *S. fortis* (Figure 2) is characterised by a rough and radial organization of the skeleton at the surface, naturally white colour, but a yellow appearance is often observed in nature due to coverage by the yellowish deep-sea sponge *Hexadella detritifera* [106,107]. To date, no studies on prokaryotic community composition of *S. fortis* are available. Ianthelline was the first described bioactive compound from *S. fortis*, and *in vitro* tests showed that the compound exhibited both antifouling and cytotoxic activities [108,109]. However, the actual producer of Ianthelline is unclear since a recent finding suggested that ianthelline is actually produced by *Hexadella detritifera* and not

S. fortis [106]. Additionally, another compound coined stryphnusin has recently been isolated from *S. fortis* with anti-acetylcholinesterase activity [110].

Geodia barretti, Bowerbank, 1858 (Demospongiae, Astrophorida, Geodiidae) is a massive deep-sea sponge species that is typically found in boreal waters at a temperature from 3-9°C across the Northern and North-western Atlantic Ocean at depths ranging from 30-2000 m [103,111,112]. *G. barretti* (Figure 2) is characterised by a large, usually globular, smooth surface with a hard consistency, and its cortex is approximately 0.5 mm thick, formed out of terrasters (ball-shaped microscleres) [113]. *G. barretti* is rich in secondary metabolites, and some compounds are bioactive. For instance, antifouling activity against barnacle larvae (*Balanus improvisus*) was reported from barrettin, 8, 9-dihydrobarrettin, barretide A and barretide B [114-116]. The compound 2-O-acetyl-1-O-hexadecylglycero-3-phosphocholine was reported to be toxic to human solid tumor cells [117]. *G. barretti* is an HMA sponge, with Proteobacteria, Acidobacteria and Chloroflexi among the dominant phyla [118,119]. In addition, bacterial and archaeal communities in *G. barretti* have been reported to be involved in the sulphur cycle [120] and nitrogen cycle [113,121].

Thesis outline

Chapter 2 provides a comprehensive literature review of antiviral, antibacterial, antifungal and antiprotozoal compounds that have been reported from sponge-associated microbes. In this review, 35 bacterial and 12 fungal genera associated with sponges that produce antimicrobials were identified. Finally, a culture-independent approach to exploit the genetic richness of antimicrobial compound producing-pathways is discussed.

Chapter 3 describes studies of the prokaryotic diversity of the two sponges *A. sventres* and *X. muta* along a depth gradient off the coast of Curaçao. Samples used were divided into three depth categories: shallow (< 30 m), middle (30 – 60 m) and deep (60 – 90 m). In addition, antimicrobial properties of the sponges were assessed by screening crude extracts against a panel of microbial indicator strains covering Gram positive bacteria, Gram negative bacteria, a yeast and an oomycete.

Chapter 4 entails a cultivation experiment in which the cultivable bacterial fraction was studied from the *A. sventres* and *X. muta* specimens described in Chapter 3. Bacterial populations growing on different agar media were identified using 16S rRNA gene amplicon sequencing to observe whether sponges collected from different depths yielded different

isolates. Subsequently, representative isolates growing on agar plates were picked based on morphological characteristics, and these isolates were screened for their antimicrobial activities.

Chapter 5 describes the prokaryotic community composition and metabolite profiles of the three Arctic deep-sea sponges *Weberella bursa*, *Stryphnus fortis* and *Geodia barretti* using 16S rRNA gene Illumina MiSeq sequencing and metabolomics. OTUs of which the relative abundance was significantly correlated with depth were determined and the impact of depth on metabolic profiles of these sponges was investigated.

Chapter 6 summarizes and integrates the research described in this thesis and further discusses the impact of depth on the composition of prokaryotic communities, antimicrobial activity and secondary metabolites present in marine sponges.



Chapter 2

Bioprospecting sponge-associated microbes for antimicrobial compounds

Anak Agung Gede Indraningrat, Hauke Smidt and Detmer Sipkema

Published in Marine Drugs (doi:10.3390/md14050087)



Abstract

Sponges are the most prolific marine organisms with respect to their arsenal of bioactive compounds including antimicrobials. However, the majority of these substances are probably not produced by the sponge itself, but rather by bacteria or fungi that are associated with their host. This review for the first time provides a comprehensive overview of antimicrobial compounds that are known to be produced by sponge-associated microbes. We discuss the current state-of-the-art by grouping the bioactive compounds produced by sponge-associated microorganisms in four categories: antiviral, antibacterial, antifungal and antiprotozoal compounds. Based on *in vitro* activity tests, identified targets of potent antimicrobial substances derived from sponge-associated microbes include: human immunodeficiency virus 1 (HIV-1) (2-undecyl-4-quinolone, sorbicillactone A and chartarutine B); influenza A (H1N1) virus (truncateol M); nosocomial Gram positive bacteria (thiopeptide YM-266183, YM-266184, mayamycin and kocurin); *Escherichia coli* (sydonic acid), *Chlamydia trachomatis* (naphthacene glycoside SF2446A2); *Plasmodium* spp. (manzamine A and quinolone 1); *Leishmania donovani* (manzamine A and valinomycin); *Trypanosoma brucei* (valinomycin and staurosporine); *Candida albicans* and dermatophytic fungi (saadamycin, 5,7-dimethoxy-4-*p*-methoxyphenylcoumarin and YM-202204). Thirty-five bacterial and 12 fungal genera associated with sponges that produce antimicrobials were identified, with *Streptomyces*, *Pseudovibrio*, *Bacillus*, *Aspergillus* and *Penicillium* as the prominent producers of antimicrobial compounds. Furthermore culture-independent approaches to more comprehensively exploit the genetic richness of antimicrobial compound-producing pathways from sponge-associated bacteria are addressed.

Keywords: antimicrobial compounds; sponges; sponge-associated microbes

Introduction

Antimicrobial resistance (AMR) is an emerging global threat, decreasing the possibilities for prevention and treatment of infectious diseases caused by viruses, bacteria, parasites and fungi [40,122]. A global surveillance report by the World Health Organization (WHO) [122] indicated an increase of morbidity and mortality of infectious diseases due to AMR, which could lead to a world-wide economic loss of up to 100 trillion US dollars (USD) in 2050 as the result of a 2%–3% reduction in the gross domestic product (GDP) [40]. A conservative estimation is that AMR now annually attributes to 700,000 deaths globally, with a potential leap to 10 million in 2050 [40]. AMR is a response of microorganisms against antimicrobial compounds, which can arise via several mechanisms such as chromosomal mutations [40], binding site modifications [122] or horizontal transfer of genes conferring resistance [37]. For several pathogenic bacteria such as *Staphylococcus aureus* [123], *Pseudomonas aeruginosa* [40,124], and *Mycobacterium tuberculosis* [125], the emergence of multi drug resistant (MDR) strains has been reported, which make infections with these strains increasingly difficult to treat with currently available antibiotics [37].

In the context of the arms race between humans and infectious agents, the discovery and development of new types of antimicrobial compounds with pronounced bioactivity and clinical significance are urgent [123,124]. The efforts to modify existing drugs are often not effective to overcome the mutation rate of pathogens and do not lead to the introduction of new classes of antimicrobial compounds [125]. The terrestrial environment has been the main focus of microbial-derived drug discovery since the first report on Penicillin in 1929 [126], followed by the booming of new classes of antibiotics in 1960s [38]. Although novel antimicrobials are still being discovered from the soil niche, e.g., turbomycin A and B [127] and teixobactin [128], there are issues with de-replication, which significantly reduces the discovery rate of new compounds from heavily screened environments [129].

In comparison with soils, the marine environment has been largely neglected for discovery of antibiotics until recently, mainly because of accessibility issues, but yet hold a huge biodiversity and potential novelty of antimicrobial compounds [130]. Of many marine organisms, sponges (phylum Porifera) are considered as the most prolific source of therapeutic compounds as these animals harbour a large variety of secondary metabolites, many of which are beneficial for human health purposes [13–17]. The “Supply Issue” is the main obstacle to exploit the biological activity of sponges’ metabolites since a large quantity of biomaterial is

required for experimental purposes. Interestingly, in recent years an increasing number of studies highlighted that many active substances from sponges are of bacterial origin due to similarity to chemical structures found in terrestrial microorganisms [19,31,131]. Furthermore, several studies have reported a wide diversity of antimicrobial activities from sponge-associated microbes, which make these microbial communities a valuable source for novel antimicrobials [46,131-135].

This review highlights the current knowledge of antimicrobial compounds produced by sponge-associated microbes. Our definition of “antimicrobial” is not limited to antibacterial agents, but also includes compounds active against viruses, fungi and infectious protozoa. For each of the four biological activities, a few substances are highlighted because of their high activity, along with the most complete overview to date of other known compounds with antimicrobial activity from sponge-associated microorganisms. To compare different bioactive compounds and crude extracts, inhibitory concentrations of substances reviewed have been as much as possible expressed in the same unit ($\mu\text{g/mL}$). Original articles use minimum inhibitory concentrations (MIC), half maximum inhibitory concentrations (IC_{50}) and the concentration of a drug that give the half-maximal response (EC_{50}). As they are not easily converted, we stuck to the original measures.

Moreover, we analyzed the distribution of bacterial and fungal genera associated with sponges that have been reported to produce antimicrobial compounds to identify the most prolific genera. In addition, the potential for application of metagenomics to complement culture-dependent antimicrobial screening strategies is also discussed.

Antiviral compounds

New antiviral compounds are needed due to the increased occurrence of diseases caused by viral infections and because of antiviral escape strategies [47]. Marine organisms, and sponges in particular, have been shown to be a valuable source for antivirals. For example, the discovery of the nucleosides spongothymidine and spongouridine from the sponge *Tethya crypta* was the basis for the compound Ara-A (vidarabine) that is active against the herpes simplex virus [47,136-138].

Screening of sponge-associated microbes yielded several prospective anti-HIV-1 (human immunodeficiency virus-1) compounds (Table 1 and Figure 1). Bultel-Poncé *et al.* [139] isolated *Pseudomonas* sp. 1531-E7 from the marine sponge *Homophymia* sp. resulting in the

discovery of the antiviral compound 2-undecyl-4-quinolone (**1**) (Figure 1). The compound had an IC_{50} concentration as low as 10^{-3} $\mu\text{g/mL}$ *in vitro* against HIV-1. Bringmann *et al.* [51] elucidated the chemical structure of sorbicillactone A (**2**) which was isolated from *Penicillium chrysogenum*, a fungus associated with the sponge *Ircinia fasciculata*. Sorbicillactone A displayed cytoprotective effects on HIV-1-infected cells of the human cell line H9 at concentrations of 0.1–1 $\mu\text{g/mL}$. In addition, *in vitro* testing using H9 cells indicated that sorbicillactone A reduced the appearance of the HIV-1 protein up to 70% at a concentration of 0.3 $\mu\text{g/mL}$ [51]. The sponge-associated fungus *Stachybotrys chartarum* MXH-X73 produces the compound stachybotrin D (**3**), which exhibited anti-HIV-1 activity by targeting reverse transcriptase [140]. At EC_{50} concentrations from 2.73 $\mu\text{g/mL}$ to 10.51 $\mu\text{g/mL}$, stachybotrin D was active not only against the wild type HIV-1 but also against several non-nucleoside reverse transcriptase inhibitor (NNRTI) resistant HIV-1 strains. Li *et al.* [141] reported identification of three other anti-HIV-1 compounds from *Stachybotrys chartarum*: chartarutine B, G, and H. Of these three chartarutine compounds, chartarutine B (**4**) showed the lowest concentration that resulted in 50% inhibition of HIV-1 (IC_{50} of 1.81 $\mu\text{g/mL}$), followed by chartarutine G (IC_{50} of 2.05 $\mu\text{g/mL}$) and chartarutine H (IC_{50} of 2.05 $\mu\text{g/mL}$), respectively.

Sponge-associated microbes have also been found to produce anti-influenza compounds (Table 1). Zhao *et al.* [142] elucidated 14 new isoprenylated cyclohexanols coined as truncateols A-N from the sponge-associated fungus *Truncatella angustata*, and these compounds were tested *in vitro* against the influenza A (H1N1) virus. Truncateols C, E and M displayed bioactivity against H1N1, with truncateol M (**5**) being the most potent inhibitor, as shown by its IC_{50} value of 2.91 $\mu\text{g/mL}$. This inhibitory concentration was almost six fold lower than that of the positive control oseltamivir at 14.52 $\mu\text{g/mL}$. Truncateol M was predicted to be active at the late stage of the virus infection, likely during the assembly or release step of the virion [142] due to resemblance of the inhibition patterns observed for neuraminidase-inhibitor drugs, e.g., zanamivir and oseltamivir [143]. In addition, the presence of a chlorine atom in the chemical structure of truncateol M is of particular interest since halogenation often enhances bioactivity of a given compound [144,145].

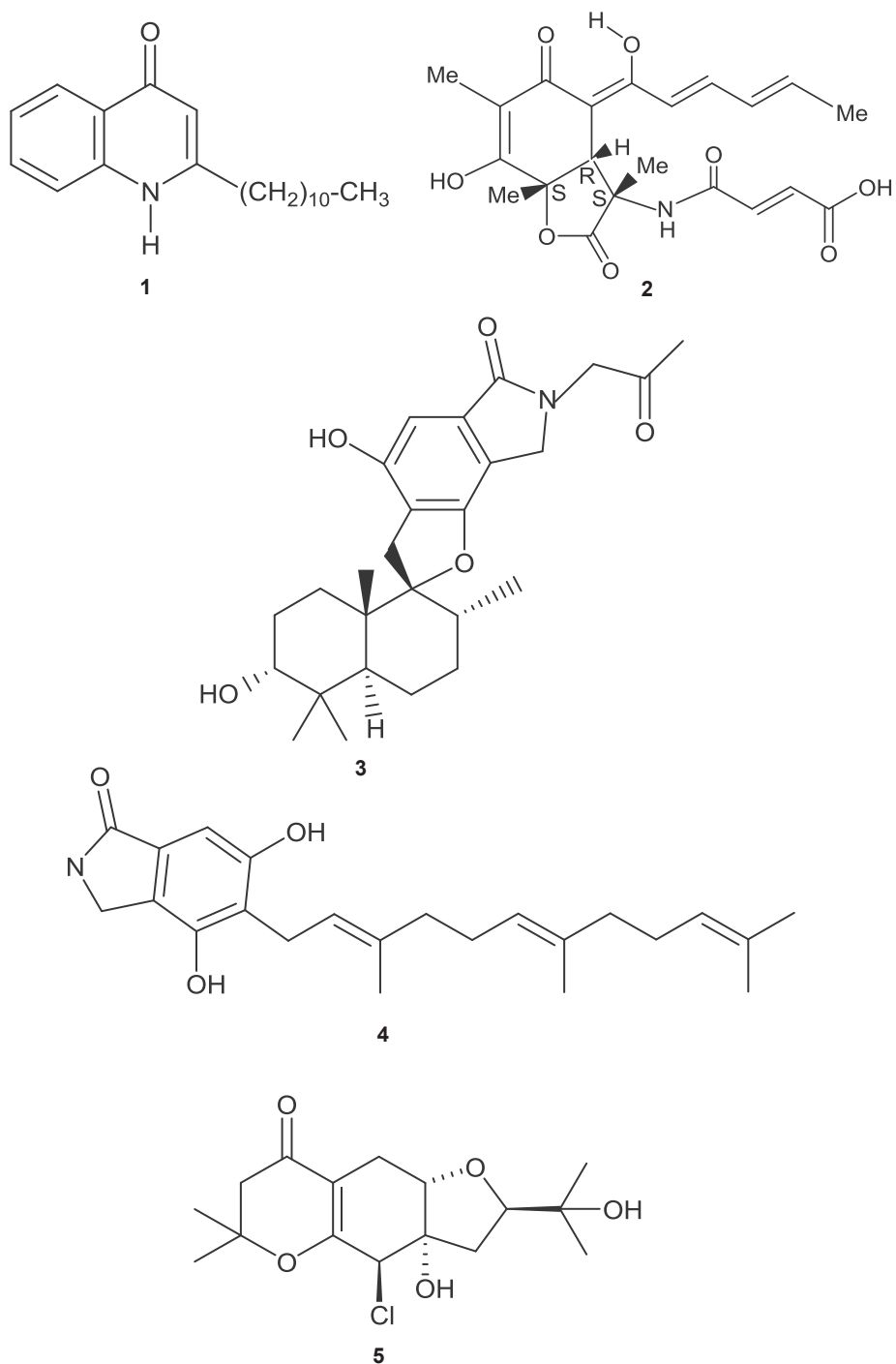


Figure 1. Chemical structures of the antiviral compounds 2-undecyl-4-quinolone (1), sorbicillactone A (2), stachybotrin D (3), chartarutine B (4), and truncateol M (5).

Table 1. Bioactive compounds with antiviral activity from sponge-associated microbes.

Sponge	Origin (Depth)	Microorganism	Phylum	Compound	Property	Target	Reference
<i>Homophymia</i> sp.	Touho, New Caledonia (ND)	<i>Pseudomonas</i> sp. 1531-E7	Proteobacteria	2-undecyl-4-quinolone	IC ₅₀ (10 ⁻³ µg/mL)	HIV-1	[139]
<i>Ircinia fasciculata</i>	Bight of Fetovaia, Italy (17.5 m)	<i>Penicillium chrysogenum</i>	Ascomycota	Sorbicillactone A	Reducing protein expression and activity of reverse transcriptase (0.3–1 µg/mL)	HIV-1	[51]
<i>Xestospongia testudinaria</i>	Paracel Islands (ND)	<i>Stachybotrys chartarum</i> MXH-X73	Ascomycota	Stachybotrin D	EC ₅₀ (3.71 µg/mL)	HIV-1	[140]
<i>Xestospongia testudinaria</i>	Paracel Islands (ND)	<i>Stachybotrys chartarum</i> MXH-X73	Ascomycota	Stachybotrin D	EC ₅₀ (3.09 µg/mL)	Non-nucleoside reverse transcriptase inhibitor (NNRTI) resistant HIV-1 strain_1RT-K103N	[140]
<i>Xestospongia testudinaria</i>	Paracel Islands (ND)	<i>Stachybotrys chartarum</i> MXH-X73	Ascomycota	Stachybotrin D	EC ₅₀ (10.51 µg/mL)	NNRTI resistant HIV-1RT-L100L,K103N	[140]
<i>Xestospongia testudinaria</i>	Paracel Islands (ND)	<i>Stachybotrys chartarum</i> MXH-X73	Ascomycota	Stachybotrin D	EC ₅₀ (5.87 µg/mL)	NNRTI resistant HIV-1RT-K103N,V108I	[140]
<i>Xestospongia testudinaria</i>	Paracel Islands (ND)	<i>Stachybotrys chartarum</i> MXH-X73	Ascomycota	Stachybotrin D	EC ₅₀ (6.27 µg/mL)	NNRTI resistant HIV-1RT-K103N,G190A	[140]
<i>Xestospongia testudinaria</i>	Paracel Islands (ND)	<i>Stachybotrys chartarum</i> MXH-X73	Ascomycota	Stachybotrin D	EC ₅₀ (2.73 µg/mL)	NNRTI resistant HIV-1RT-K103N,P225H	[140]
<i>Niphates</i> sp.	Beibuwan Bay, China (10 m)	<i>Stachybotrys chartarum</i>	Ascomycota	Chartarutine B	IC ₅₀ (1.81 µg/mL)	HIV-1	[141]
<i>Niphates</i> sp.	Beibuwan Bay, China (10 m)	<i>Stachybotrys chartarum</i>	Ascomycota	Chartarutine G	IC ₅₀ (2.05 µg/mL)	HIV-1	[141]
<i>Niphates</i> sp.	Beibuwan Bay, China (10 m)	<i>Stachybotrys chartarum</i>	Ascomycota	Chartarutine H	IC ₅₀ (2.05 µg/mL)	HIV-1	[141]
<i>Amphimedon</i> sp.	Yongxin island, China (10 m)	<i>Truncatella angustata</i>	Ascomycota	Truncateol M	IC ₅₀ (2.91 µg/mL)	H1N1	[142]

<i>Calyspongia</i> sp.	Sanya, China (ND)	<i>Epicoccum</i> sp. JY40	Ascomycota	Pyronopolylene C-glycoside iso-D8646-2-6	IC ₅₀ (56.06 µg/mL)	H1N1	[146]
<i>Calyspongia</i> sp.	Sanya, China (ND)	<i>Epicoccum</i> sp. JY40	Ascomycota	Pyronopolylene C-glycoside, 8646-2-6	IC ₅₀ (62.07 µg/mL)	H1N1	[146]
Unidentified	Naozhou Sea, China (ND)	<i>Aspergillus terreus</i> MXH-23	Ascomycota	Butyrolactone III	Percentage of inhibition (53.9% ± 0.53% at 50 µg/L)	H1N1	[147]
Unidentified	Naozhou Sea, China (ND)	<i>Aspergillus terreus</i> MXH-23	Ascomycota	5-[(3,4-dihydro-2,2-dimethyl-2H-1-benzopyran-6-yl)-methyl]-3-hydroxy-4-(4-hydroxyphenyl)-2(5H)-furanone	Percentage of inhibition (57.8% ± 1.99% at 50 µg/L)	H1N1	[147]
Unidentified	Paracel Islands (ND)	<i>Aspergillus sydowii</i> ZSDS1-F6	Ascomycota	(Z)-5-(Hydroxymethyl)-2-(60)-methylhept-20-en-20-yl)-phenol	IC ₅₀ (14.30 µg/mL)	H3N2	[148]
Unidentified	Paracel Islands (ND)	<i>Aspergillus sydowii</i> ZSDS1-F6	Ascomycota	Diorcinol	IC ₅₀ (15.31 µg/mL)	H3N2	[148]
Unidentified	Paracel Islands (ND)	<i>Aspergillus sydowii</i> ZSDS1-F6	Ascomycota	Cordyol C	IC ₅₀ (19.33 µg/mL)	H3N2	[148]
Unidentified	Paracel Islands (ND)	<i>Stachybotrys</i> sp. HH1 ZSDS1F1-2	Ascomycota	Stachybotrisphenone B	IC ₅₀ (10.2 µg/mL)	Enterovirus 71 (EV71)	[149]
Unidentified	Paracel Islands (ND)	<i>Stachybotrys</i> sp. HH1 ZSDS1F1-2	Ascomycota	Grisephenone A	IC ₅₀ (16.94 µg/mL)	Enterovirus 71 (EV71)	[149]
Unidentified	Paracel Islands (ND)	<i>Stachybotrys</i> sp. HH1 ZSDS1F1-2	Ascomycota	3,6,8-Trihydroxy-1-methylxanthone	IC ₅₀ (10.4 µg/mL)	Enterovirus 71 (EV71)	[149]
<i>Petromica citrina</i>	Saco do Poço, Brazil (5–15 m)	<i>Bacillus</i> sp. B555	Firmicutes	Unidentified	IC ₅₀ (27.35 µg/mL) EC ₅₀ (>500 µg/mL)	Bovine viral diarrhoea virus	[150]
<i>Petromica citrina</i>	Saco do Poço, Brazil (5–15 m)	<i>Bacillus</i> sp. B584	Firmicutes	Unidentified	IC ₅₀ (10.24 µg/mL) EC ₅₀ (277 µg/mL)	Bovine viral diarrhoea virus	[150]
<i>Petromica citrina</i>	Saco do Poço, Brazil (5–15 m)	<i>Bacillus</i> sp. B616	Firmicutes	Unidentified	IC ₅₀ (47 µg/mL) EC ₅₀ (1500 µg/mL)	Bovine viral diarrhoea virus	[150]

Table 1 is organised according to the target viruses. IC₅₀: half maximum inhibitory concentration; EC₅₀: the concentration of a drug that give the half-maximal response; ND: not determined; HIV: human immunodeficiency virus; H1N1 and H3N2 are influenza A virus subtypes.

Antibacterial compounds

The screening procedure for antibacterial activity often includes both Gram positive and Gram negative target strains, including, e.g., *Staphylococcus* spp., *Streptococcus* spp., *Bacillus* spp., *Clostridium* spp., *Escherichia* spp., and *Pseudomonas* spp. From a medical point of view, these genera receive attention because they are well represented among the causative agents for human infectious diseases, such as pneumonia, urinary tract and blood stream infections [151,152]. Microbial isolates from marine sponges have been shown to exhibit bioactivity against a wide spectrum of pathogenic bacteria (Table 2). The novel thiopeptide antibiotics YM-266183 (**6**) and YM-266184 (**7**) (Figure 2), which were isolated from the sponge-associated bacterium *Bacillus cereus* QN03323, showed antibacterial activity against nosocomial infectious Gram positive bacteria *in vitro* [153,154]. Both YM-266183 and YM-266184 effectively inhibited *Staphylococcus aureus* and vancomycin-resistant *Enterococcus faecium* as indicated by minimal inhibition concentration (MIC) values as low as 0.025 µg/mL. In addition, compound YM-266184 was found particularly active against methicillin resistant *Staphylococcus aureus* (MRSA) with a MIC of 0.39 µg/mL. Compound YM-266183 also inhibited MRSA but required a two-fold higher concentration of the pure compound. Bioactivity of these thiopeptides was also observed against *Streptococcus epidermidis* and *Enterococcus* spp. (Table 2). The compound kocurin (**8**) was identified from three sponge-associated actinobacteria: *Kocuria marina* F-276,310, *Kocuria palustris* F-276,345, and *Micrococcus yunnanensis* F-256,446 [155,156]. Kocurin is a new member of the thiazolyl peptide family and exhibited anti-MRSA activity with an MIC of 0.25 µg/mL, which to date is the most potent anti-MRSA compound reported from sponge-associated microbes. Scheenemaan *et al.* [157] isolated *Streptomyces* sp. HB202 from the sponge *Haliclona simulans*, which lead to discovery of the polyketide mayamycin. *In vitro* assays with mayamycin (**9**) showed bioactivity against *S. aureus* and MRSA with IC₅₀ values of 1.16 µg/mL and 0.58 µg/mL respectively, along with an IC₅₀ of 0.14 µg/mL against *Staphylococcus epidermidis* [158].

Although many studies on antibacterial activity from sponge-associated microbes included Gram negative strains (Table 2), reports on pronounced antibacterial compounds active against Gram negative bacteria are limited in comparison to those that inhibit Gram positive strains. One of the examples of an inhibitor of a Gram negative bacterium is the compound naphthacene glycoside SF2446A2 (**10**) isolated from *Streptomyces* sp. RV15 that was originally obtained from the marine sponge *Dysidea tupa* [159]. Naphthacene glycoside SF2446A2 (**10**) inhibited

the Gram-negative bacterium *Chlamydia trachomatis* at an IC₅₀ value of 2.81 ± 0.24 µg/mL. Reimer *et al.* [159] underlined that compound **10** not only effectively inhibited the formation of chlamydial inclusion bodies during the primary infection but also affected the ability of *C. trachomatis* in producing viable progeny during the developmental cycle. *Chlamydia trachomatis* is an obligate intracellular Gram negative bacterium which is a leading cause of sexually transmitted diseases, and currently no methods are available to treat this infectious microorganism [159,160]. Li *et al.* [161] isolated four new bisabolane-typesesquiterpenoids: aspergiterpenoid A, (-)-sydonol, (-)-sydonic acid, (-)-5-(hydroxymethyl)-2-(2',6',6'-trimethyltetrahydro-2H-pyran-2-yl)phenol and a known compound (Z)-5-(Hydroxymethyl)-2-(6'-methylhept-2'-en-2'-yl)phenol from a sponge-associated *Aspergillus* sp. (Table 2). Of these five substances, the compound sydonic acid (**11**) exhibited the lowest MIC value against *Escherichia coli* at 1.33 µg/mL. This is the lowest inhibition concentration against *E.coli* reported from a compound produced by sponge-associated microbes although the inhibition concentration is still higher than the positive control ciprofloxacin (0.21 µg/mL) (Table 2).

Pruksakorn *et al.* [162] reported three prospective anti-tuberculosis compounds: trichoderin A (**12**), A1 and B from the sponge-associated fungus *Trichoderma* sp. 05FI48. Both under standard aerobic growth and dormancy-inducing hypoxic conditions, these three compounds inhibited *Mycobacterium smegmatis*, *M. bovis* BCG, and *M. tuberculosis* H37Rv with MIC values in the range of 0.02–2.0 µg/mL. Of these three compounds, trichoderin A was the most potent compound indicated by the lowest MIC values against those *Mycobacterium* strains. Additional analysis revealed that bioactivity of trichoderin A is based on its ability to inhibit adenosine triphosphate (ATP) synthesis of mycobacteria [163]. Compounds such as trichoderin A are particularly important because in many cases, pathogens such as *Campylobacter* spp., *Helicobacter pylori*, and *Legionella pneumophila* are difficult to treat due to the fact that they are present in a dormant state [164]. Such physiologically inactive cells highly contribute to the need for prolonged antibiotic treatments, which may lead to the emergence of resistant strains [165,166]

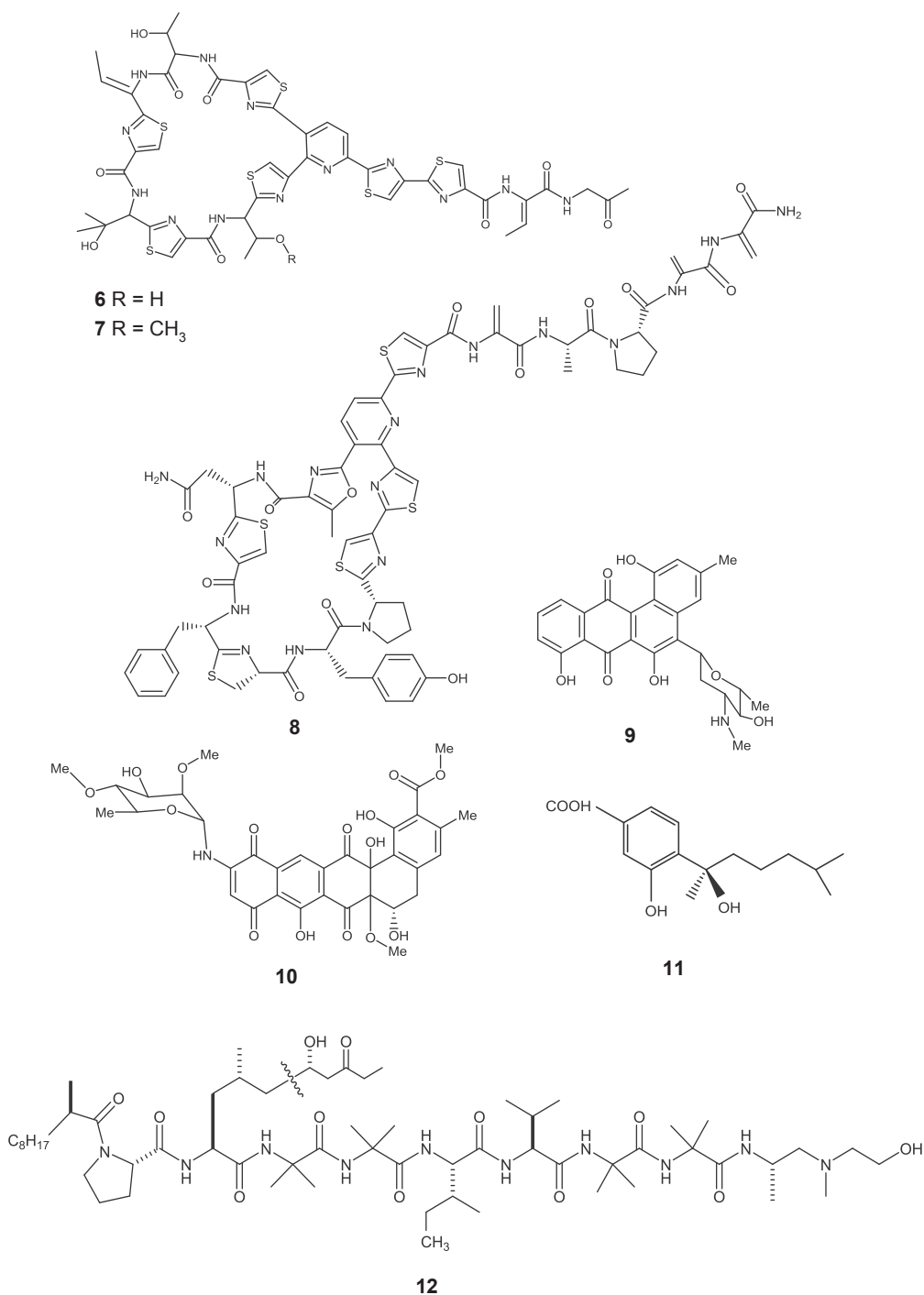


Figure 2. Chemical structures of the antibacterial compounds YM-266183 (**6**), YM-266184 (**7**), kocurin (**8**), mayamycin (**9**), naphthacene glycoside SF2446A2 (**10**), symonic acid (**11**) and trichoderin A (**12**).

Table 2. Bioactive compounds with antibacterial activity from sponge-associated microbes.

Sponge	Origin (Depth)	Microorganism	Phylum	Compound	Property	Target	References
<i>Halichondria japonica</i>	Iriomote island, Japan (ND)	<i>Bacillus cereus</i> QNO3323	Firmicutes	Thiopeptide YM-266183	MIC (0.025 µg/mL)	<i>Staphylococcus aureus</i>	[153,154]
<i>Halichondria japonica</i>	Iriomote island, Japan (ND)	<i>Bacillus cereus</i> QNO3323	Firmicutes	Thiopeptide YM-266184	MIC (0.025 µg/mL)	<i>S. aureus</i>	[153,154]
<i>Halichondria panicea</i>	Kiel Fjord, Baltic Sea, Germany (ND)	<i>Streptomyces</i> sp. HB202	Actinobacteria	Mayamycin	IC ₅₀ (1.16 µg/mL)	<i>S. aureus</i>	[158]
<i>Sphectospongia vagabunda</i>	Red Sea (ND)	<i>Micrococcus</i> sp. EG45	Actinobacteria	Microfuside A	MIC (12.42 µg/mL)	<i>S. aureus</i> NCTC 8325	[167]
<i>Isodictya setifera</i>	Ross island, Antarctica (30–40 m)	<i>Pseudomonas aeruginosa</i>	Proteobacteria	Phenazine-1-carboxylic acid	MIC (>4.99 µg/mL)	<i>S. aureus</i>	[168]
<i>Isodictya setifera</i>	Ross island, Antarctica (30–40 m)	<i>Pseudomonas aeruginosa</i>	Proteobacteria	Phenazine-1-carboxamide	MIC (>4.99 µg/mL)	<i>S. aureus</i>	[168]
<i>Hymeniacidon perleve</i>	Bohai Sea, China (ND)	<i>Aspergillus versicolor</i> MF359	Ascomycota	5-Methoxydihydrosterigmatocystin	MIC (12.5 µg/mL)	<i>S. aureus</i>	[169]
<i>Melophus</i> sp.	Lau group, Fiji islands (10 m)	<i>Penicillium</i> sp. FF001	Ascomycota	Citrinin	MIC (1.95 µg/mL)	<i>S. aureus</i>	[170]
<i>Petrosia</i> sp.	Jeju island, Korea (20 m)	<i>Aspergillus versicolor</i>	Ascomycota	Averantin	MIC (3.13 µg/mL)	<i>S. aureus</i> SG511	[171]
<i>Petrosia</i> sp.	Jeju island, Korea (20 m)	<i>Aspergillus versicolor</i>	Ascomycota	Nidurufin	MIC (6.25 µg/mL)	<i>S. aureus</i> SG511	[171]
<i>Petrosia</i> sp.	Jeju island, Korea (20 m)	<i>Aspergillus versicolor</i>	Ascomycota	Averantin and nidurufin	MIC (3.13 µg/mL)	<i>S. aureus</i> 285	[171]
<i>Petrosia</i> sp.	Jeju island, Korea (20 m)	<i>Aspergillus versicolor</i>	Ascomycota	Averantin	MIC (1.56 µg/mL)	<i>S. aureus</i> 503	[171]
<i>Petrosia</i> sp.	Jeju island, Korea (20 m)	<i>Aspergillus versicolor</i>	Ascomycota	Nidurufin	MIC (3.13 µg/mL)	<i>S. aureus</i> 503	[171]
<i>Hymeniacidon perleve</i>	Nanji island, China (ND)	<i>Pseudoalteromonas piscicida</i> NJ6-3-1	Ascomycota	Norharman (beta-carboline alkaloid)	MIC (50 µg/mL)	<i>S. aureus</i>	[172]

<i>Halichondria panicea</i>	Bogil island, Korea (ND)	<i>Exophiala</i> sp.	Ascomycota	Chlorohydroaspyrones A	MIC (62.5 µg/mL)	<i>S. aureus</i>	[173]
<i>Halichondria panicea</i>	Bogil island, Korea (ND)	<i>Exophiala</i> sp.	Ascomycota	Chlorohydroaspyrones B	MIC (62.5 µg/mL)	<i>S. aureus</i>	[173]
<i>Axinella</i> sp.	South China Sea, China (ND)	<i>Eupenicillium</i> sp.	Ascomycota	αβ-Dehydrocurvularin	MIC (375 µg/mL)	<i>S. aureus</i>	[174]
<i>Halictolona</i> sp.	Cagaras Archipelago, Brazil (4–20 m)	<i>Pseudomonas fluorescens</i> H40, H41 and <i>Pseudomonas aeruginosa</i> H51	Proteobacteria	Diketopiperazine	MIC (512 µg/mL)	<i>S. aureus</i>	[175]
<i>Spongia officinalis</i>	Southeast Coast India (10–15 m)	<i>Streptomyces</i> sp. MAPS15	Actinobacteria	2-pyrrolidone	MIC (500 µg/mL)	<i>S. aureus</i> PC6	[176]
unidentified	South China Sea (10 m)	<i>Nocardopsis</i> sp. 13-33-15 and 13-12-13	Actinobacteria	1,6-Dihydroxyphenazine	DOI (25 ± 0.6 mm)	<i>S. aureus</i> SJ51	[177]
Unidentified	Atlantic coast, USA (ND)	<i>Kocuria palustris</i> F-276,310; <i>Kocuria marina</i> F-276,345 <i>Micrococcus yunnanensis</i> F-256,446	Actinobacteria	Kocurin	DOI (21 ± 0.1 mm)	methicillin-resistant <i>Staphylococcus aureus</i> (MRSA)	[155,156]
<i>Halichondria japonica</i>	Iriomote island, Japan (ND)	<i>Bacillus cereus</i> QNO3323	Firmicutes	Thiopeptide YM-266183	MIC (0.78 µg/mL)	MRSA	[153,154]
<i>Halichondria japonica</i>	Iriomote island, Japan (ND)	<i>Bacillus cereus</i> QNO3323	Firmicutes	Thiopeptide YM-266184	MIC (0.39 µg/mL)	MRSA	[153,154]
<i>Halichondria panicea</i>	Kiel Fjord, Baltic Sea, Germany (ND)	<i>Streptomyces</i> sp. HB202	Actinobacteria	Mayamycin	IC50 (0.58 µg/mL)	MRSA	[158]
<i>Melophus</i> sp.	Lau group, Fiji islands (10 m)	<i>Penicillium</i> sp. FF001	Ascomycota	Citrinin	MIC (3.90 µg/mL)	MRSA	[170]
<i>Halichondria panicea</i>	Bogil island, Korea (ND)	<i>Exophiala</i> sp.	Ascomycota	Chlorohydroaspyrones A	MIC (125 µg/mL)	MRSA	[173]
				Chlorohydroaspyrones B	MIC (62.5 µg/mL)	MRSA	

<i>Xestospongia testudinaria</i>	Bidong Island, Malaysia (ND)	<i>Serratia marcescens</i> IBRL USM 84	Proteobacteria	Prodiginosin	DOI (22.5 mm)	MRSA	[178]
<i>Halichondria panicea</i>	Bogil island, Korea (ND)	<i>Exophiala</i> sp.	Ascomycota	Chlorohydroaspyrones A	MIC (125 µg/mL)	multi drug-resistant <i>S. aureus</i>	[173]
				Chlorohydroaspyrones B	MIC (125 µg/mL)	multi drug-resistant <i>S. aureus</i>	[173]
<i>Melophus</i> sp.	Lau group, Fiji islands (10 m)	<i>Penicillium</i> sp. FF001	Ascomycota	Citrinin	MIC (0.97 µg/mL)	rifampicin-resistant <i>S. aureus</i>	[170]
<i>Halichondria panicea</i>	Baltic Sea (ND)	<i>Streptomyces</i> sp. HB202	Actinobacteria	Mayamycin	IC ₅₀ (0.14 µg/mL)	<i>Staphylococcus epidermidis</i>	[158]
<i>Halichondria panicea</i>	Kiel Fjord, Baltic Sea, Germany (ND)	<i>Streptomyces</i> sp. HB202	Actinobacteria	Streptophenazines G	IC ₅₀ (3.57 ± 0.21 µg/mL)	<i>S. epidermidis</i>	[179]
<i>Halichondria panicea</i>	Kiel Fjord, Baltic Sea, Germany (ND)	<i>Streptomyces</i> sp. HB202	Actinobacteria	Streptophenazines K	IC ₅₀ (6.16 ± 0.85 µg/mL)	<i>S. epidermidis</i>	[179]
unidentified sponge	Vizhijam coast (10–12 m)	<i>Aspergillus clavatus</i> MFD15	Ascomycota	1 <i>H</i> -1,2,4-Triazole-3-carboxaldehyde 5-methyl	MIC (800 ± 10 µg/mL)	<i>S. epidermidis</i>	[180]
<i>Spongia officinalis</i>	Southeast Coast India (10–15 m)	<i>Streptomyces</i> sp. MAPS15	Actinobacteria	2-Pyrrolidone (Z)-5-(Hydroxymethyl)-2-(6'-methylhept-2-en-2'-yl)phenol	MIC (500 µg/mL)	<i>S. epidermidis</i> PC5	[176]
<i>Xestospongia testudinaria</i>	Weizhou coral reef, China (ND)	<i>Aspergillus</i> sp.	Ascomycota	Aspergiterpenoid A	MIC (1.24 µg/mL)	<i>Staphylococcus albus</i>	[161]
				(-)-5-(Hydroxymethyl)-2-(2',6',6'-trimethyltetrahydro-2 <i>H</i> -pyran-2-yl)phenol	MIC (1.26 µg/mL)		
<i>Halichondria panicea</i>	Kiel Fjord, Baltic Sea, Germany (ND)	<i>Streptomyces</i> sp. HB202	Actinobacteria	Mayamycin	IC ₅₀ (3.71 µg/mL)	<i>Staphylococcus lentus</i>	[158]

<i>Halichondria japonica</i>	Iriomote island, Japan (ND)	<i>Bacillus cereus</i> QNO3323	Firmicutes	Thiopeptide YM-266183	MIC (1.56 µg/mL)	Methicillin-Resistant <i>Streptococcus epidermidis</i> (MRSE)	[153,154]
<i>Halichondria japonica</i>	Iriomote island, Japan (ND)	<i>Bacillus cereus</i> QNO3323	Firmicutes	Thiopeptide YM-266184	MIC (0.2 µg/mL)	MRSE	[153,154]
<i>Petrosia</i> sp.	Jeju island, Korea (20 m)	<i>Aspergillus versicolor</i>	Ascomycota	Averantin	MIC (0.78 µg/mL)	<i>Streptococcus pyogenes</i> 308A	[171]
<i>Petrosia</i> sp.	Jeju island, Korea (20 m)	<i>Aspergillus versicolor</i>	Ascomycota	Nidurufin	MIC (3.13 µg/mL)	<i>Streptococcus pyogenes</i> 308A	[171]
<i>Petrosia</i> sp.	Jeju island, Korea (20 m)	<i>Aspergillus versicolor</i>	Ascomycota	Averantin	MIC (3.13 µg/mL)	<i>Streptococcus pyogenes</i> 77A	[171]
<i>Petrosia</i> sp.	Jeju island, Korea (20 m)	<i>Aspergillus versicolor</i>	Ascomycota	Nidurufin	MIC (6.25 µg/mL)	<i>Streptococcus pyogenes</i> 77A	[171]
<i>Halichondria japonica</i>	Iriomote island, Japan (ND)	<i>Bacillus cereus</i> QNO3323	Firmicutes	Thiopeptide YM-266183	MIC (1.56 µg/mL)	<i>Bacillus subtilis</i> ATCC 633	[153,154]
<i>Halichondria japonica</i>	Iriomote island, Japan (ND)	<i>Bacillus cereus</i> QNO3323	Firmicutes	Thiopeptide YM-266184	MIC (1.56 µg/mL)	<i>B. subtilis</i> ATCC 633	[153,154]
<i>Halichondria panicea</i>	Kiel Fjord, Baltic Sea, Germany (ND)	<i>Streptomyces</i> sp. HB202	Actinobacteria	Mayamycin	IC ₅₀ (3.71 µg/mL)	<i>B. subtilis</i>	[158]
<i>Halichondria panicea</i>	Kiel Fjord, Baltic Sea, Germany (ND)	<i>Streptomyces</i> sp. HB202	Actinobacteria	Streptopenazines G	IC ₅₀ (3.49 ± 0.38 µg/mL)	<i>B. subtilis</i>	[179]
<i>Halichondria panicea</i>	Kiel Fjord, Baltic Sea, Germany (ND)	<i>Streptomyces</i> sp. HB202	Actinobacteria	Streptopenazines K	IC ₅₀ (9.18 ± 2.89 µg/mL)	<i>B. subtilis</i>	[179]
<i>Callyspongia</i> sp.	Kyung-Po beach, Korea (12 m)	<i>Brevibacterium</i> sp. KMD 003	Actinobacteria	6-Hydroxymethyl-1-phenazine-carboxamide 1,6-	MIC (5.06 µg/mL)	<i>B. subtilis</i>	[181]
		<i>Brevibacterium</i> sp. KMD 003	Actinobacteria	Phenazinedimethanol	MIC (4.80 µg/mL)	<i>B. subtilis</i>	[181]
<i>Halictona simulans</i>	Gurraig Sound Kilkieran Bay, Ireland (15 m)	<i>Streptomyces</i> sp. SM8	Actinobacteria	Mixture Kitamycin A or B and Antimycin A3 or A7	MIC (7.42 µg/mL)	<i>B. subtilis</i>	[182]
			Actinobacteria	Antimycin A2, A8, A11 or A17	MIC (9.40 µg/mL)		

		Antimycin A3 or A7		MIC (400 µg/mL)		
		Antimycin A2, A8, A11 or A17, antimycin A3 or A7		MIC (400 µg/mL)		
<i>Hymeniacidon perleve</i>	Bohai Sea, China (ND)	<i>Aspergillus versicolor</i> MF359	Ascomycota	MIC (3.125 µg/mL)	<i>B. subtilis</i> [169]	
<i>Hymeniacidon perleve</i>	Nanji island, China (ND)	<i>Pseudoalteromonas piscicida</i> NJ6-3-1	Proteobacteria	MIC (50 µg/mL)	<i>B. subtilis</i> [172]	
<i>Xestospongia testudinaria</i>	Weizhou coral reef, China (ND)	<i>Aspergillus</i> sp.	Ascomycota	MIC (0.66 µg/mL)	<i>B. subtilis</i> [161]	
				(Z)-5-(Hydroxymethyl)-2-(6'-methylhept-2'-en-2'-yl)phenol		MIC (2.33 µg/mL)
				(Hydroxymethyl)-2-(2',6',6'-trimethyltetrahydro-2H-pyran-2-yl)phenol		MIC (0.62 µg/mL)
<i>Hyrtyos altum</i>	Aragusuku island, Japan (ND)	<i>Vibrio</i> sp.	Proteobacteria	DOI (17 mm)	<i>B. subtilis</i> [183]	
<i>Isodictya setifera</i>	Ross island, Antarctica (30–40 m)	<i>Pseudomonas aeruginosa</i>	Proteobacteria	MIC (<0.49 µg/mL)	<i>Bacillus cereus</i> [168]	
<i>Xestospongia testudinaria</i>	Weizhou coral reef, China (ND)	<i>Aspergillus</i> sp.	Ascomycota	MIC (2.33 µg/mL)	<i>B. cereus</i> [161]	
<i>Xestospongia testudinaria</i>	Bidong Island, Malaysia (ND)	<i>Serratia marcescens</i> IBRL USM 84	Proteobacteria	DOI (10–14 mm)	<i>B. cereus</i> [178]	
<i>Xestospongia testudinaria</i>	Bidong Island, Malaysia (ND)	<i>Serratia marcescens</i> IBRL USM 84	Proteobacteria	DOI (10–14 mm)	<i>Bacillus licheniformis</i> [178]	

unidentified	South China Sea (10 m)	<i>Nocardioopsis</i> sp. 13-33-15 and 13-12-13	Actinobacteria	1,6-Dihydroxyphenazine	DOI (16 ± 0.5 mm)	<i>Bacillus mycoloides</i> SJ14	[177]
<i>Dysidea avara</i>	Mediterranean sea (ND)	<i>Actinokinetespora</i> sp. EG49	Actinobacteria	1,6-Dimethoxyphenazine	DOI (20 ± 0.4 mm)		
<i>Sphacelosporgia vagabunda</i>	Red Sea (ND)	<i>Nocardioopsis</i> sp. RV163	Actinobacteria	Dihydroxyphenazine (result of the co-culture)	DOI (11 mm)	<i>Bacillus</i> sp. P25	[184]
<i>Halocondria japonica</i>	Iriomote island, Japan (ND)	<i>Bacillus cereus</i> QNO3323	Firmicutes	Thiopeptide YM-266183	MIC (0.1 µg/mL)	<i>E. faecalis</i> CAY 04_1	[153,154]
<i>Halocondria japonica</i>	Iriomote island, Japan (ND)	<i>Bacillus cereus</i> QNO3323	Firmicutes	Thiopeptide YM-266184	MIC (0.025 µg/mL)	<i>E. faecalis</i> CAY 04_1	[153,154]
<i>Sphacelosporgia vagabunda</i>	Red Sea (ND)	<i>Micrococcus</i> sp. EG45	Actinobacteria	Microfuside A	MIC (9.55 µg/mL)	<i>E. faecalis</i> JH212	[167]
<i>Halocondria japonica</i>	Iriomote island, Japan (ND)	<i>Bacillus cereus</i> QNO3323	Firmicutes	Thiopeptide YM-266183	MIC 0.2 µg/mL	<i>Enterococcus faecium</i> CAY 09_1	[153,154]
<i>Halocondria japonica</i>	Iriomote island, Japan (ND)	<i>Bacillus cereus</i> QNO3323	Firmicutes	Thiopeptide YM-266184	MIC (0.05 µg/mL)	<i>E. faecium</i> CAY 09_1	[153,154]
<i>Halocondria japonica</i>	Iriomote island, Japan (ND)	<i>Bacillus cereus</i> QNO3323	Firmicutes	Thiopeptide YM-266183	MIC (0.025 µg/mL)	Vancomycin-Resistant <i>E. faecium</i> CAY 09_2	[153,154]
<i>Halocondria japonica</i>	Iriomote island, Japan (ND)	<i>Bacillus cereus</i> QNO3323	Firmicutes	Thiopeptide YM-266184	MIC (0.025 µg/mL)	Vancomycin-Resistant <i>E. faecium</i> CAY 09_2	[153,154]
<i>Melophus</i> sp.	Lau group, Fiji islands (10 m)	<i>Penicillium</i> sp. FF001	Ascomycota	Citrinin	MIC (1.95 µg/mL)	Vancomycin-resistant <i>E. faecium</i>	[170]
<i>Callyspongia</i> sp.	Kyung-Po beach, Korea (12 m)	<i>Brevibacterium</i> sp. KMD 003	Actinobacteria	6-Hydroxymethyl-1-phenazine-carboxamide	MIC (1.26 µg/mL)	<i>Enterococcus hirae</i>	[181]
		<i>Aspergillus</i> sp.	Ascomycota	1,6-Phenazinedimethanol (–)-Sydonic acid	MIC (1.20 µg/mL)	<i>E. hirae</i>	[181]
					MIC (1.33 µg/mL)	<i>Escherichia coli</i>	[161]

		(Z)-5-(Hydroxymethyl)-2-(6'-methylhept-2'-en-2'-yl)phenol	
		MIC (4.72 µg/mL)	MIC (2.33 µg/mL)
<i>Xestospongia testudinaria</i>	Weizhou coral reef, China (ND)	Aspergiterpenoid A	MIC (4.72 µg/mL)
		(-)-Sydonol	MIC (5.04 µg/mL)
<i>Halocondria japonica</i>	Iriomote island, Japan (ND)	<i>Bacillus cereus</i> QNO3323	MIC (>100 µg/mL)
<i>Halocondria japonica</i>	Iriomote island, Japan (ND)	<i>Bacillus cereus</i> QNO3323	MIC (>100 µg/mL)
unidentified sponge	Vizhijam coast (10–12 m)	<i>Aspergillus clavatus</i> MFD15	MIC (800 ± 10 µg/mL)
<i>Spongia officinalis</i>	Southeast Coast India (10–15 m)	<i>Streptomyces</i> sp. MAPS15	MIC (400 µg/mL)
<i>Hyrtios altum</i>	Aragusuku island, Japan (ND)	<i>Vibrio</i> sp.	DOI (16 mm)
<i>Niphates olemda</i>	Bali Bata National Park, Indonesia (ND)	<i>Curvularia lunata</i>	DOI (11 mm)
<i>Niphates olemda</i>	Bali Bata National Park, Indonesia (ND)	<i>Curvularia lunata</i>	DOI (11 mm)
<i>Halichondria panicea</i>	Kiel Fjord, Baltic Sea, Germany (ND)	<i>Streptomyces</i> sp. HB202	IC50 (1.16 µg/mL)
<i>Spongia officinalis</i>	Southeast Coast India (10–15 m)	<i>Streptomyces</i> sp. MAPS15	MIC (700 µg/mL)
<i>Halichondria panicea</i>	Kiel Fjord, Baltic Sea, Germany (ND)	<i>Streptomyces</i> sp. HB202	IC50 (1.16 µg/mL)
<i>Haliclona</i> sp.	Cagaras Archipelago, Brazil (4–20 m)	<i>Pseudomonas fluorescens</i> H40, H41 and <i>Pseudomonas aeruginosa</i> H51	MIC (512 µg/mL)

<i>Callispongia</i> sp.	Kyung-Po beach, Korea (12 m)	<i>Brevibacterium</i> sp. KMD 003	Actinobacteria	6-Hydroxymethyl-1-phenazine-carboxamide	MIC (1.26 µg/mL)	<i>Micrococcus luteus</i>	[181]
<i>Isodictya setifera</i>	Ross island, Antarctica (30–40 m)	<i>Pseudomonas aeruginosa</i>	Proteobacteria	Phenazinedimethanol Phenazine-1-carboxylic acid and phenazine-1-carboxamide	MIC (1.20 µg/mL) MIC (>4.99 µg/mL)	<i>M. luteus</i> <i>M. luteus</i>	[181] [168]
unidentified	South China Sea (10 m)	<i>Nocardioopsis</i> sp. 13-33-15 and 13-12-13	Actinobacteria	1,6-Dihydroxyphenazine	DOI (18 ± 0.9 mm)	<i>M. luteus</i> SJ47	[177]
unidentified	South China Sea (10 m)	<i>Nocardioopsis</i> sp. 13-33-15 and 13-12-13	Actinobacteria	1,6-Dimethoxyphenazine	DOI (23 ± 0.5 mm)	<i>M. luteus</i> SJ47	[177]
<i>Xestospongia testudinaria</i>	Weizhou coral reef, China (ND)	<i>Aspergillus</i> sp.	Ascomycota	(-)-Sydonic acid	MIC (5.33 µg/mL)	<i>Micrococcus tetragenus</i>	[161]
<i>Xestospongia testudinaria</i>	Weizhou coral reef, China (ND)	<i>Aspergillus</i> sp.	Ascomycota	(Z)-5-(Hydroxymethyl)-2-(6'-methylhept-2-en-2'-yl)phenol	MIC (2.33 µg/mL)	<i>M. tetragenus</i>	[161]
<i>Xestospongia testudinaria</i>	Weizhou coral reef, China (ND)	<i>Aspergillus</i> sp.	Ascomycota	Aspergiterpenoid A	MIC (2.36 µg/mL)	<i>M. tetragenus</i>	[161]
<i>Xestospongia testudinaria</i>	Weizhou coral reef, China (ND)	<i>Aspergillus</i> sp.	Ascomycota	(-)-Sydonol	MIC (0.32 µg/mL)	<i>M. tetragenus</i>	[161]
<i>Halichondria panicea</i>	Kiel Fjord, Baltic Sea, Germany (ND)	<i>Streptomyces</i> sp. HB202	Actinobacteria	Mayamycin	IC50 (3.45 µg/mL)	<i>Brevibacterium epidermidis</i>	[158]
<i>Halichondria panicea</i>	Kiel Fjord, Baltic Sea, Germany (ND)	<i>Streptomyces</i> sp. HB202	Actinobacteria	Mayamycin	IC50 (3.89 µg/mL)	<i>Dermabacter hominis</i>	[158]
<i>Halichondria panicea</i>	Kiel Fjord, Baltic Sea, Germany (ND)	<i>Streptomyces</i> sp. HB202	Actinobacteria	Mayamycin	IC50 (14.48 µg/mL)	<i>Propionibacterium acnes</i>	[158]
<i>Halichondria panicea</i>	Kiel Fjord, Baltic Sea, Germany (ND)	<i>Streptomyces</i> sp. HB202	Actinobacteria	Mayamycin	IC50 (13.92 µg/mL)	<i>Xanthomonas campestris</i>	[158]
<i>Dysidea tupha</i>	Rovinj, Croatia (ND)	<i>Streptomyces</i> sp. RV15	Actinobacteria	Naphthacene glycoside SF2446A2	IC50 (2.81 ± 0.24 µg/mL)	<i>Chlamydia trachomatis</i>	[159]

<i>unidentified</i>	ND	<i>Trichoderma</i> sp. 05F148	Ascomycota	Trichoderin A	MIC (0.1 µg/mL)	<i>Mycobacterium smegmatis</i>	[162]
<i>unidentified</i>	ND	<i>Trichoderma</i> sp. 05F148	Ascomycota	Trichoderin A1	MIC (1.56 µg/mL)	<i>M. smegmatis</i>	[162]
<i>unidentified</i>	ND	<i>Trichoderma</i> sp. 05F148	Ascomycota	Trichoderin B	MIC (0.63 µg/mL)	<i>M. smegmatis</i>	[162]
<i>unidentified</i>	ND	<i>Trichoderma</i> sp. 05F148	Ascomycota	Trichoderin A	MIC (0.02 µg/mL)	<i>Mycobacterium bovis</i> BCG	[162]
<i>unidentified</i>	ND	<i>Trichoderma</i> sp. 05F148	Ascomycota	Trichoderin A1	MIC (0.16 µg/mL)	<i>M. bovis</i> BCG	[162]
<i>unidentified</i>	ND	<i>Trichoderma</i> sp. 05F148	Ascomycota	Trichoderin B	MIC (0.02 µg/mL)	<i>M. bovis</i> BCG	[162]
<i>unidentified</i>	ND	<i>Trichoderma</i> sp. 05F148	Ascomycota	Trichoderin A	MIC (0.12 µg/mL)	<i>Mycobacterium tuberculosis</i> H37rv	[162]
<i>unidentified</i>	ND	<i>Trichoderma</i> sp. 05F148	Ascomycota	Trichoderin A1	MIC (2.0 µg/mL)	<i>M. tuberculosis</i> H37rv	[162]
<i>unidentified</i>	ND	<i>Trichoderma</i> sp. 05F148	Ascomycota	Trichoderin B	MIC (0.13 µg/mL)	<i>M. tuberculosis</i> H37rv	[162]
<i>Xestospongia testudinaria</i>	Weizhou coral reef, China (ND)	<i>Aspergillus</i> sp.	Ascomycota	(-)-Sydonic acid	MIC (2.66 µg/mL)	<i>Vibrio parahaemolyticus</i>	[161]
<i>Xestospongia testudinaria</i>	Weizhou coral reef, China (ND)	<i>Aspergillus</i> sp.	Ascomycota	(-)-Sydonic acid	MIC (1.33 µg/mL)	<i>Vibrio anguillarum</i>	[161]
<i>Dysidea avara</i>	Mediterranean sea (ND)	<i>Actinokinetespora</i> sp. EG49	Actinobacteria	1,6-Dihydroxyphenazine (result of co-culture)	DOI (15 mm)	<i>Actinokinetespora</i> sp. EG49	[184]
<i>Spherospongia vagabunda</i>	Red Sea (ND)	<i>Nocardia</i> sp. RV163	Actinobacteria				
<i>Xestospongia testudinaria</i>	Weizhou coral reef, China (ND)	<i>Aspergillus</i> sp.	Ascomycota	(-)-Sydonic acid	MIC (0.66 µg/mL)	<i>Sarcina lutea</i>	[161]

Table 2 is organised according to the target bacteria. IC₅₀: half maximum inhibitory concentration; MIC: minimum inhibitory concentration; DOI: diameter of inhibition; ND: not determined. Susceptible to [186]: amp = ampicillin; atm = aztreonam; azm = azithromycin; caz = ceftazidime; cef = cefalotin; chl = chloramphenicol; cip = ciprofloxacin; cpd = ceftiofloxime; fox = ceftiofloxime; gen = gentamicin; oxa = oxacillin; pen = penicillin; sxt = trimethoprim/sulfamethoxazole; tet = tetracycline; tzp = piperacillin/tazobactam; van = vancomycin.

Antifungal activity

The incidence rate of fungal infections has increased significantly over the past decades. This is mainly caused by clinical use of antibacterial drugs and immunosuppressive agents after organ transplantation, cancer chemotherapy, and advances in surgery [187,188]. Several fungal species that often cause human infections include *Candida albicans*, *Candida glabrata*, *Cryptococcus neoformans* and *Aspergillus fumigatus* [187,189,190]. The story becomes more complex as many of these pathogenic fungi develop resistance against available antifungal drugs, which will prolong duration of treatments [191].

Screening for antifungals is often focused on finding compounds active against *Candida albicans*, the prominent agent for candidiasis (Table 3). Invasive candidiasis is accounted as the most common nosocomial fungal infection resulting in an average mortality rate between 25%–38% [188]. El-Gendy *et al.* [192] isolated *Streptomyces* sp. Hedaya 48 from the sponge *Aplysina fistularis* and identified two compounds: the novel compound saadamycin (**13**) and the known compound 5,7-dimethoxy-4-*p*-methoxylphenylcoumarin (**14**) (Figure 3). Bioassays indicated that both saadamycin and 5,7-dimethoxy-4-*p*-methoxylphenylcoumarin displayed pronounced antifungal activity against *Candida albicans* with MIC values of 2.22 µg/mL and 15 µg/mL, respectively. In addition, both compounds displayed bioactivity against some pathogenic dermatophytes (skin-infecting fungi), such as *Epidermophyton floccosum*, *Trichophyton rubrum*, *Trichophyton mentagrophytes*, *Microsporium gypseum*, *Aspergillus niger*, *Aspergillus fumigatus*, *Fusarium oxysporum*, and *Cryptococcus humicolus* (Table 3). Further analysis showed that saadamycin displayed a more potent bioactivity indicated by a 3875 fold lower MIC than that of the reference compound, miconazole, whereas 5,7-dimethoxy-4-*p*-methoxylphenylcoumarin was around a 200 fold more potent than miconazole.

Antifungal activity was also detected from the sponge-associated fungus *Phoma* sp. Q60596. The sponge-derived fungus produced a new lactone compound, YM-202204 (**15**) [193], which was effective against *C. albicans* (IC₈₀ of 6.25 µg/mL), along with *Cryptococcus neoformans* (IC₈₀ of 1.56 µg/mL), *Saccharomyces cerevisiae* (IC₈₀ of 1.56 µg/mL) and *Aspergillus fumigatus* (IC₈₀ of 12.5 µg/mL). Furthermore, Nagai *et al.* [193] showed that YM-202204 was able to block the glycoposphatidylinositol (GPI) anchor, an important structure for protein attachment in the membrane of eukaryotic cells and one of the targets in developing antifungal drugs [194,195].

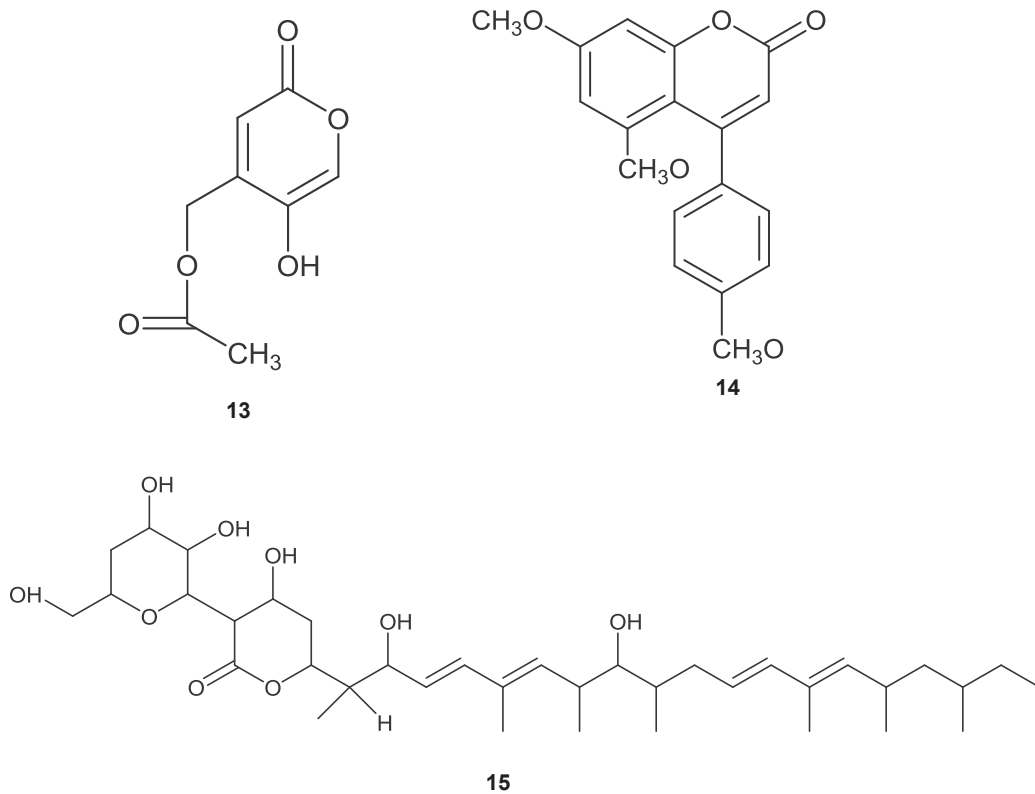


Figure 3. Chemical structures of the antifungal compounds saadamycin (**13**), 5,7-dimethoxy-4-*p*-methoxyphenylcoumarin (**14**) and YM-202204 (**15**).

Table 3. Bioactive compounds with antifungal activity from sponge-associated microbes.

Sponge	Origin (Depth)	Microorganism	Phylum	Compound	Property	Target	Reference
<i>Aplysina fistularis</i>	Sharm El-Sheikh, Egypt (ND)	<i>Streptomyces</i> sp. Hedaya48	Actinobacteria	Saadamycin	MIC (2.22 µg/mL)	<i>Candida albicans</i>	[192]
<i>Aplysina fistularis</i>	Sharm El-Sheikh, Egypt (ND)	<i>Streptomyces</i> sp. Hedaya48	Actinobacteria	5,7-Dimethoxy-4-p-methoxyphenylcoumarin	MIC (15 µg/mL)	<i>C. albicans</i>	[192]
<i>Halichondria japonica</i>	Iriomote island, Japan (ND)	<i>Phoma</i> sp. Q60596	Ascomycota	YM-202204	IC ₈₀ (6.25 µg/mL)	<i>C. albicans</i>	[193]
<i>Haliclona simulans</i>	Gurraig Sound Kilkieran Bay, Ireland (15 m)	<i>Streptomyces</i> sp. SM8	Actinobacteria	Mixture of kitamycin A or B, and antimycin A3 or A7	MIC (240 µg/mL)	<i>C. albicans</i>	[182]
<i>Haliclona simulans</i>	Gurraig Sound Kilkieran Bay, Ireland (15 m)	<i>Streptomyces</i> sp. SM8	Actinobacteria	Antimycin A2, A8, A11, or A17	MIC (210 µg/mL)	<i>C. albicans</i>	[182]
<i>Haliclona simulans</i>	Gurraig Sound Kilkieran Bay, Ireland (15 m)	<i>Streptomyces</i> sp. SM8	Actinobacteria	Antimycin A3 or A7	MIC (80 µg/mL)	<i>C. albicans</i>	[182]
<i>Haliclona simulans</i>	Gurraig Sound Kilkieran Bay, Ireland (15 m)	<i>Streptomyces</i> sp. SM8	Actinobacteria	Antimycin A2, A8, A11, or A17, antimycin A3 or A7	MIC (90 µg/mL)	<i>C. albicans</i>	[182]
<i>Halichondria</i> sp.	West Coast of India (10 m)	<i>Bacillus</i> sp. SAB1	Firmicutes	3-Phenylpropionic acid	DOI (7–10 mm) at 50µg/disk	<i>C. albicans</i>	[196]
<i>Halichondria</i> sp.	West Coast of India (10 m)	<i>Bacillus</i> sp. SAB1	Firmicutes	4,4'-Oxybis(3-phenylpropionic acid)	DOI (4–6 mm) at 50µg/disk	<i>C. albicans</i>	[196]
<i>Xestospongia exigua</i>	Bali Sea, Indonesia (ND)	<i>Penicillium</i> cf. <i>montanense</i>	Ascomycota	Xestodecalactone B	MIC (28.03 µg/disk)	<i>C. albicans</i>	[197]
unidentified	Iriomote island, Japan (ND)	<i>Streptomyces</i> sp. Ni-80	Actinobacteria	Urauchimycins A and B	MIC (10 µg/mL)	<i>C. albicans</i>	[198]
<i>Haliclona</i> sp.	Tateyama, Japan (ND)	<i>Streptomyces bambbergensis</i>	Actinobacteria	Unidentified	DOI (5 mm)	<i>C. albicans</i>	[199]
<i>Haliclona</i> sp.	Tateyama, Japan (ND)	<i>Streptomyces javensis</i>	Actinobacteria	Unidentified	DOI (11 mm)	<i>C. albicans</i>	[199]
unidentified	Nagura Bay, Ishigaki, Japan (ND)	<i>Streptomyces albidoflavus</i>	Actinobacteria	Unidentified	DOI (16 mm)	<i>C. albicans</i>	[199]
unidentified	Nagura Bay, Ishigaki, Japan (ND)	<i>Streptomyces variabilis</i>	Actinobacteria	Unidentified	DOI (19 mm)	<i>C. albicans</i>	[199]
unidentified	Nagura Bay, Ishigaki, Japan (ND)	<i>Streptomyces luteosporus</i>	Actinobacteria	Unidentified	DOI (24 mm)	<i>C. albicans</i>	[199]
<i>Sphaciospongia vagabunda</i>	Rovinj, Croatia (3–20 m)	<i>Actinokineospora</i> sp. EG49	Actinobacteria	Unidentified	DOI (12 mm)	<i>C. albicans</i>	[200]
<i>Dysidea tupa</i>	Rovinj, Croatia (3–20 m)	<i>Streptomyces</i> sp. RV15	Actinobacteria	Unidentified	DOI (4–6 mm)	<i>C. albicans</i>	[200]

<i>Sigmadocia fibulatus</i>	Hare Island, India (5-10 m)	<i>Bacillus</i> sp. SC3	Firmicutes	Unidentified	DOI (15 mm)	<i>C. albicans</i>	[201]
<i>Sigmadocia fibulatus</i>	Hare Island, India (5-10 m)	<i>Pseudomonas</i> sp. SC11	Proteobacteria	Unidentified	DOI (7 mm)	<i>C. albicans</i>	[201]
<i>Echinodictyum</i> sp.	Hare Island, India (5-10 m)	<i>Idiomarina baltica</i> SA7	Proteobacteria	Unidentified	DOI (10 mm)	<i>C. albicans</i>	[201]
<i>Spongia</i> sp.	Hare Island, India (5-10 m)	<i>Staphylococcus equorum</i> SB11	Firmicutes	Unidentified	DOI (10 mm)	<i>C. albicans</i>	[201]
<i>Aphysina aerophoba</i>	Banyuls-sur-Mer, France (5-15 m)	<i>Bacillus subtilis</i> A184	Firmicutes	Surfactin, iturin, and fengycin	ND	<i>C. albicans</i>	[202]
<i>Aphysina aerophoba</i>	Banyuls-sur-Mer, France (5-15 m)	<i>Bacillus subtilis</i> A190	Firmicutes	Surfactin	ND	<i>C. albicans</i>	[202]
<i>Aphysina aerophoba</i>	Banyuls-sur-Mer, France (5-15 m)	<i>Bacillus subtilis</i> A202	Firmicutes	Iturin	ND	<i>C. albicans</i>	[202]
<i>Leucosolenia</i> sp.	Lough Hyne, Co. Cork, Ireland (15 m)	<i>Vibrio</i> sp. SC-C1-5	Proteobacteria	Unidentified	ND	<i>C. albicans</i>	[203]
<i>Leucosolenia</i> sp.	Lough Hyne, Co. Cork, Ireland (15 m)	<i>Vibrio</i> sp. BSw21697	Proteobacteria	Unidentified	ND	<i>C. albicans</i>	[203]
<i>Leucosolenia</i> sp.	Lough Hyne, Co. Cork, Ireland (15 m)	<i>Vibrio splendidus</i> LGP32	Proteobacteria	Unidentified	ND	<i>C. albicans</i>	[203]
<i>Leucosolenia</i> sp.	Lough Hyne, Co. Cork, Ireland (15 m)	<i>Bacillus amyloliquefaciens</i>	Proteobacteria	Unidentified	ND	<i>C. albicans</i>	[203]
<i>Leucosolenia</i> sp.	Lough Hyne, Co. Cork, Ireland (15 m)	<i>Vibrio</i> sp. SC-C1-5	Proteobacteria	Unidentified	ND	<i>Candida glabrata</i>	[203]
<i>Leucosolenia</i> sp.	Lough Hyne, Co. Cork, Ireland (15 m)	<i>Vibrio</i> sp. BSw21697	Proteobacteria	Unidentified	ND	<i>C. glabrata</i>	[203]
<i>Leucosolenia</i> sp.	Lough Hyne, Co. Cork, Ireland (15 m)	<i>Vibrio splendidus</i> LGP32	Proteobacteria	Unidentified	ND	<i>C. glabrata</i>	[203]
<i>Leucosolenia</i> sp.	Lough Hyne, Co. Cork, Ireland (15 m)	<i>Bacillus amyloliquefaciens</i>	Firmicutes	Unidentified	ND	<i>C. glabrata</i>	[203]
<i>Leucosolenia</i> sp.	Lough Hyne, Co. Cork, Ireland (15 m)	<i>Pseudoalteromonas</i> sp. A2B10	Proteobacteria	Unidentified	ND	<i>C. glabrata</i>	[203]
<i>Leucosolenia</i> sp.	Lough Hyne, Co. Cork, Ireland (15 m)	<i>Pseudoalteromonas</i> sp. K2B-2	Proteobacteria	Unidentified	ND	<i>C. glabrata</i>	[203]
<i>Leucosolenia</i> sp.	Lough Hyne, Co. Cork, Ireland (15 m)	<i>Pseudoalteromonas</i> sp. LJ1	Proteobacteria	Unidentified	ND	<i>C. glabrata</i>	[203]
<i>Leucosolenia</i> sp.	Lough Hyne, Co. Cork, Ireland (15 m)	<i>Pseudoalteromonas</i> sp. S3178	Proteobacteria	Unidentified	ND	<i>C. glabrata</i>	[203]

<i>Aphysina fistularis</i>	Sharm El-Sheikh, Egypt (ND)	<i>Streptomyces</i> sp. Hedaya48	Actinobacteria	Saadamycin	MIC (5 µg/mL)	<i>Trichophyton rubrum</i>	[192]
<i>Aphysina fistularis</i>	Sharm El-Sheikh, Egypt (ND)	<i>Streptomyces</i> sp. Hedaya48	Actinobacteria	5,7-Dimethoxy-4- <i>p</i> -methoxyphenylcoumarin	MIC (7.5 µg/mL)	<i>T. rubrum</i>	[192]
<i>Aphysina fistularis</i>	Sharm El-Sheikh, Egypt (ND)	<i>Streptomyces</i> sp. Hedaya48	Actinobacteria	Saadamycin	MIC (1.5 µg/mL)	<i>Trichophyton mentagrophyte</i>	[192]
<i>Aphysina fistularis</i>	Sharm El-Sheikh, Egypt (ND)	<i>Streptomyces</i> sp. Hedaya48	Actinobacteria	5,7-Dimethoxy-4- <i>p</i> -methoxyphenylcoumarin	MIC (90 µg/mL), MIC (1.25 µg/mL)	<i>T. mentagrophyte</i>	[192]
<i>Aphysina fistularis</i>	Sharm El-Sheikh, Egypt (ND)	<i>Streptomyces</i> sp. Hedaya48	Actinobacteria	Saadamycin	MIC (100 µg/mL)	<i>Microsporium gypseum</i>	[192]
<i>Aphysina fistularis</i>	Sharm El-Sheikh, Egypt (ND)	<i>Streptomyces</i> sp. Hedaya48	Actinobacteria	5,7-Dimethoxy-4- <i>p</i> -methoxyphenylcoumarin	MIC (10 µg/mL)	<i>M. gypseum</i>	[192]
<i>Aphysina fistularis</i>	Sharm El-Sheikh, Egypt (ND)	<i>Streptomyces</i> sp. Hedaya48	Actinobacteria	Saadamycin	MIC (1.0 µg/mL)	<i>Epidermophyton floccosum</i>	[192]
<i>Aphysina fistularis</i>	Sharm El-Sheikh, Egypt (ND)	<i>Streptomyces</i> sp. Hedaya48	Actinobacteria	5,7-Dimethoxy-4- <i>p</i> -methoxyphenylcoumarin	MIC (50 µg/mL)	<i>E. floccosum</i>	[192]
<i>Aphysina fistularis</i>	Sharm El-Sheikh, Egypt (ND)	<i>Streptomyces</i> sp. Hedaya48	Actinobacteria	Saadamycin	MIC (1.2 µg/mL)	<i>Fusarium oxysporum</i>	[192]
<i>Aphysina fistularis</i>	Sharm El-Sheikh, Egypt (ND)	<i>Streptomyces</i> sp. Hedaya48	Actinobacteria	5,7-Dimethoxy-4- <i>p</i> -methoxyphenylcoumarin	MIC (22 µg/mL)	<i>F. oxysporum</i>	[192]
<i>Aphysina fistularis</i>	Sharm El-Sheikh, Egypt (ND)	<i>Streptomyces</i> sp. Hedaya48	Actinobacteria	Saadamycin	MIC (5.16 µg/mL)	<i>Cryptococcus humicola</i>	[192]
<i>Aphysina fistularis</i>	Sharm El-Sheikh, Egypt (ND)	<i>Streptomyces</i> sp. Hedaya48	Actinobacteria	5,7-Dimethoxy-4- <i>p</i> -methoxyphenylcoumarin	MIC (10 µg/mL)	<i>C. humicola</i>	[192]
<i>Halichondria japonica</i>	Iriomote island, Japan (ND)	<i>Phoma</i> sp. Q60596	Ascomycota	YM-202204	IC ₈₀ (1.56 µg/mL)	<i>Cryptococcus neoformans</i>	[193]
<i>Aphysina fistularis</i>	Sharm El-Sheikh, Egypt (ND)	<i>Streptomyces</i> sp. Hedaya48	Actinobacteria	Saadamycin	MIC (1.6 µg/mL)	<i>Aspergillus fumigatus</i>	[192]
<i>Aphysina fistularis</i>	Sharm El-Sheikh, Egypt (ND)	<i>Streptomyces</i> sp. Hedaya48	Actinobacteria	5,7-Dimethoxy-4- <i>p</i> -methoxyphenylcoumarin	MIC (10 µg/mL)	<i>A. fumigatus</i>	[192]
<i>Halichondria japonica</i>	Iriomote island, Japan (ND)	<i>Phoma</i> sp. Q60596	Ascomycota	YM-202204	IC ₈₀ (12.5 µg/mL)	<i>A. fumigatus</i>	[193]
<i>Leucosolenia</i> sp.	Lough Hyne, Co. Cork, Ireland (15 m)	<i>Staphylococcus saprophyticus</i>	Firmicutes	Unidentified	ND	<i>A. fumigatus</i>	[203]
<i>Leucosolenia</i> sp.	Lough Hyne, Co. Cork, Ireland (15 m)	<i>Staphylococcus</i> sp. HJB003	Firmicutes	Unidentified	ND	<i>A. fumigatus</i>	[203]

<i>Leucosolenia</i> sp.	Lough Hyne, Co. Cork, Ireland (15 m)	<i>Vibrio littoralis</i> MANO22P	Proteobacteria	Unidentified	ND	<i>A. fumigatus</i>	[203]
<i>Leucosolenia</i> sp.	Lough Hyne, Co. Cork, Ireland (15 m)	<i>Vibrio</i> sp. SC-C1-5	Proteobacteria	Unidentified	ND	<i>A. fumigatus</i>	[203]
<i>Leucosolenia</i> sp.	Lough Hyne, Co. Cork, Ireland (15 m)	<i>Vibrio</i> sp. BSw21697	Proteobacteria	Unidentified	ND	<i>A. fumigatus</i>	[203]
<i>Leucosolenia</i> sp.	Lough Hyne, Co. Cork, Ireland (15 m)	<i>Vibrio splendidus</i> LGP32	Proteobacteria	Unidentified	ND	<i>A. fumigatus</i>	[203]
<i>Leucosolenia</i> sp.	Lough Hyne, Co. Cork, Ireland (15 m)	<i>Bacillus amyloliquefaciens</i> Hedaya48	Firmicutes	Unidentified	ND	<i>A. fumigatus</i>	[203]
<i>Aphysina fistularis</i>	Sharm El-Sheikh, Egypt (ND)	<i>Streptomyces</i> sp. Hedaya48	Actinobacteria	Saadamycin	MIC (1.0 µg/mL)	<i>Aspergillus niger</i>	[192]
<i>Aphysina fistularis</i>	Sharm El-Sheikh, Egypt (ND)	<i>Streptomyces</i> sp. Hedaya48	Actinobacteria	5,7-Dimethoxy-4- <i>p</i> -methoxyphenylcoumarin	MIC (20 µg/mL)	<i>A. niger</i>	[192]
<i>Halichondria</i> sp.	West Coast of India (10 m)	<i>Bacillus</i> sp. SAB1	Firmicutes	3-Phenylpropionic acid	DOI (1–3 mm) at 50 µg/disc	<i>A. niger</i>	[196]
<i>Halichondria</i> sp.	West Coast of India (10 m)	<i>Bacillus</i> sp. SAB1	Firmicutes	4,4'-Oxybis(3-phenylpropionic acid)	DOI (4–6 mm) at 50 µg/disc	<i>A. niger</i>	[196]
<i>Halichondria</i> sp.	West Coast of India (10 m)	<i>Bacillus</i> sp. SAB1	Firmicutes	3-Phenylpropionic acid	DOI (4–6 mm) at 50 µg/disc	<i>Rhodotorula</i> sp.	[196]
<i>Halichondria</i> sp.	West Coast of India (10 m)	<i>Bacillus</i> sp. SAB1	Firmicutes	4,4'-Oxybis(3-phenylpropionic acid)	DOI (7–10 mm) at 50 µg/disc	<i>Rhodotorula</i> sp.	[196]
<i>Halichondria japonica</i>	Iriomote island, Japan (ND)	<i>Phoma</i> sp. Q60596	Ascomycota	YM-202204	IC ₈₀ (1.56 µg/mL)	<i>Saccharomyces cerevisiae</i>	[193]
<i>Hymeniacion perleve</i>	Nanji island, China (ND)	<i>Pseudoalteromonas piscicida</i> NJ6-3-1	Proteobacteria	Norharman (a beta-carboline alkaloid)	DOI (3–5 mm)	<i>S. cerevisiae</i>	[172]
<i>Hymeniacion perleve</i>	Nanji island, China (ND)	<i>Bacillus megaterium</i> NJ6-3-2	Firmicutes	Unidentified	DOI (3–5 mm)	<i>S. cerevisiae</i>	[172]
<i>Leucosolenia</i> sp.	Lough Hyne, Co. Cork, Ireland (15 m)	<i>Vibrio littoralis</i> MANO22P	Proteobacteria	Unidentified	ND	<i>S. cerevisiae</i>	[203]
<i>Leucosolenia</i> sp.	Lough Hyne, Co. Cork, Ireland (15 m)	<i>Vibrio</i> sp. SC-C1-5	Proteobacteria	Unidentified	ND	<i>S. cerevisiae</i>	[203]
<i>Leucosolenia</i> sp.	Lough Hyne, Co. Cork, Ireland (15 m)	<i>Vibrio</i> sp. BSw21697	Proteobacteria	Unidentified	ND	<i>S. cerevisiae</i>	[203]
<i>Leucosolenia</i> sp.	Lough Hyne, Co. Cork, Ireland (15 m)	<i>Vibrio splendidus</i> LGP32	Proteobacteria	Unidentified	ND	<i>S. cerevisiae</i>	[203]
<i>Leucosolenia</i> sp.	Lough Hyne, Co. Cork, Ireland (15 m)	<i>Bacillus amyloliquefaciens</i>	Firmicutes	Unidentified	ND	<i>S. cerevisiae</i>	[203]

<i>Psammocinia</i> sp.	Sdot-Yam, Israel (ND)	<i>Aspergillus insuetus</i>	Ascomycota	Insuetolides A	MIC (60.09 µg/mL)	<i>Neurospora crassa</i>	[204]
<i>Psammocinia</i> sp.	Sdot-Yam, Israel (ND)	<i>Aspergillus insuetus</i>	Ascomycota	Strobilactone A	MIC (69.97 µg/mL)	<i>N. crassa</i>	[204]
<i>Psammocinia</i> sp.	Sdot-Yam, Israel (ND)	<i>Aspergillus insuetus</i>	Ascomycota	(<i>E,E</i>)-6-(60,70-Dihydroxy-20,40-octadienoyl)-strobilactone A	MIC (71.79 µg/mL)	<i>N. crassa</i>	[204]
<i>Myxilla incrustans</i>	The Caribbean Island of Dominica (ND)	<i>Microsphaeropsis</i> sp.	Ascomycota	Microsphaeropsisin	ND	<i>Eurotium repens</i>	[205]
<i>Myxilla incrustans</i>	The Caribbean Island of Dominica (ND)	<i>Microsphaeropsis</i> sp.	Ascomycota	(<i>R</i>)-Mellein	ND	<i>E. repens</i>	[205]
<i>Myxilla incrustans</i>	The Caribbean Island of Dominica (ND)	<i>Microsphaeropsis</i> sp.	Ascomycota	(3 <i>R</i> ,4 <i>R</i>)-Hydroxymellein	ND	<i>E. repens</i>	[205]
<i>Myxilla incrustans</i>	The Caribbean Island of Dominica (ND)	<i>Microsphaeropsis</i> sp.	Ascomycota	4,8-Dihydroxy-3,4-dihydro-2 <i>H</i> -naphthalen-1-one	ND	<i>E. repens</i>	[205]
<i>Ectyoplasia ferox</i>	The Caribbean Island of Dominica (ND)	<i>Coniothyrium</i> sp.	Ascomycota	(3 <i>R</i>)-6-Methoxymellein	ND	<i>E. repens</i>	[205]
<i>Ectyoplasia ferox</i>	The Caribbean Island of Dominica (ND)	<i>Coniothyrium</i> sp.	Ascomycota	(3 <i>R</i>)-6-Methoxy-7-chloromellein	ND	<i>E. repens</i>	[205]
<i>Ectyoplasia ferox</i>	The Caribbean Island of Dominica (ND)	<i>Coniothyrium</i> sp.	Ascomycota	(<i>p</i> -Hydroxyphenyl) ethanol	ND	<i>E. repens</i>	[205]
<i>Ectyoplasia ferox</i>	The Caribbean Island of Dominica (ND)	<i>Coniothyrium</i> sp.	Ascomycota	Phenylethanol	ND	<i>E. repens</i>	[205]
<i>Myxilla incrustans</i>	The Caribbean Island of Dominica (ND)	<i>Microsphaeropsis</i> sp.	Ascomycota	Microsphaeropsisin	ND	<i>Ustilago violacea</i>	[205]
<i>Myxilla incrustans</i>	The Caribbean Island of Dominica (ND)	<i>Microsphaeropsis</i> sp.	Ascomycota	(<i>R</i>)-Mellein	ND	<i>U. violacea</i>	[205]
<i>Myxilla incrustans</i>	The Caribbean Island of Dominica (ND)	<i>Microsphaeropsis</i> sp.	Ascomycota	(3 <i>R</i> ,4 <i>R</i>)-Hydroxymellein	ND	<i>U. violacea</i>	[205]
<i>Myxilla incrustans</i>	The Caribbean Island of Dominica (ND)	<i>Microsphaeropsis</i> sp.	Ascomycota	4,8-Dihydroxy-3,4-dihydro-2 <i>H</i> -naphthalen-1-one	ND	<i>U. violacea</i>	[205]
<i>Ectyoplasia ferox</i>	The Caribbean Island of Dominica (ND)	<i>Coniothyrium</i> sp.	Ascomycota	(3 <i>R</i>)-6-Methoxymellein	ND	<i>U. violacea</i>	[205]
<i>Ectyoplasia ferox</i>	The Caribbean Island of Dominica (ND)	<i>Coniothyrium</i> sp.	Ascomycota	(3 <i>R</i>)-6-Methoxy-7-chloromellein	ND	<i>U. violacea</i>	[205]
<i>Ectyoplasia ferox</i>	The Caribbean Island of Dominica (ND)	<i>Coniothyrium</i> sp.	Ascomycota	(<i>p</i> -Hydroxyphenyl) ethanol	ND	<i>U. violacea</i>	[205]

<i>Echyoplasia ferox</i>	The Caribbean Island of Dominica (ND)	<i>Coniothyrium</i> sp.	Ascomycota	Phenylethanol	ND	<i>U. violacea</i>	[205]
<i>Echyoplasia ferox</i>	The Caribbean Island of Dominica (ND)	<i>Coniothyrium</i> sp.	Ascomycota	(3 <i>S</i>)-(3',5'-Dihydroxyphenyl)butan-2-one	ND	<i>U. violacea</i>	[205]
<i>Echyoplasia ferox</i>	The Caribbean Island of Dominica (ND)	<i>Coniothyrium</i> sp.	Ascomycota	(3 <i>S</i>)-(3',5'-Dihydroxyphenyl)butan-2-one	ND	<i>Mycotypha microspora</i>	[205]

Table 3 is organised according to the target fungi. IC₅₀: half maximum inhibitory concentration; IC₈₀: 80% inhibitory concentration; MIC: minimum inhibitory concentration; DOI: diameter of inhibition; ND: not determined.

Antiprotozoal activity

Malaria, caused by *Plasmodium* spp. infections, represents the most devastating protozoal disease worldwide, and results in both mortality and economic loss, mainly in developing countries [206]. Developing drugs with a better therapeutic profile against the parasite is one of the key aims of current malaria research, which includes screening for antimalarial substances from marine organisms [45,207].

Manzamine A (16) (Figure 4), first reported by Sakai and co-workers [208] from the sponge *Haliclona* sp., is a promising substance against *Plasmodium* spp. Initially, its antitumor property was of main interest, but subsequently diverse antimicrobial activities such as: anti-HIV, antibacterial, and antifungal were identified from the compound [209]. Currently the antimalaria properties of manzamine A are considered its most promising bioactivity. Manzamine A was shown to inhibit *P. falciparum* D6 and W3 clonal cell lines that are sensitive and resistant against the antimalarial chloroquine [210], with IC₅₀ values of 0.0045 and 0.008 µg/mL, respectively [211]. Furthermore, *in vivo* screening by Ang *et al.* [206] showed that manzamine A at concentration of 0.008 µg/mL inhibited 90 % growth of the parasite *Plasmodium berghei* that causes malaria in rodents. In addition, Rao *et al.* reported [211] that manzamine A displayed anti-*Leishmania* activity, indicated by IC₅₀ and IC₉₀ values of 0.9 µg/mL and 1.8 µg/mL, respectively, against *Leishmania donovani*.

Isolation of manzamine A from several other sponge species [209] raised the hypothesis that it was of microbial origin [212,213]. Hill *et al.* [214] confirmed this hypothesis by isolating *Micromonospora* sp. M42 as the microbial producer of manzamine A from the Indonesian sponge *Acanthostrongylophora ingens*. A series of analyses using molecular-microbial community analysis, and Matrix Assisted Laser Desorption Ionization-Mass Spectrometry (MALDI-MS) corroborated that indeed the strain *Micromonospora* sp. M42 synthesizes manzamine A [215,216]. Considering the therapeutic potential of manzamine A for treating malaria and leishmaniasis, *Micromonospora* sp. M42 could be a sustainable provider of the substance, because the “Sponge Supply Problem” has been overcome [216]. Moreover, identification of several manzamine-derivatives e.g. manzamine E, F, J, and 8-hydroxymanzamine A, from marine sponges which displayed antibacterial, antifungal and antiprotozoal activity [211,213], could also lead to isolation of associated microbial producers in the future.

Pimentel-Elardo *et al.* [217] identified three compounds with anti-*Leishmania* and anti-*Trypanosoma* activity from a sponge-associated *Streptomyces* sp, namely the cyclic depsipeptide valinomycin (17), the indolocarbazole alkaloid staurosporine (18) and butenolide (19) (Table 4). Valinomycin and staurosporine inhibited the growth of *L. major* with IC₅₀ values of 0.12 µg/mL and 1.24 µg/mL, respectively. In addition, the three compounds displayed bioactivity against *Trypanosoma brucei* with IC₅₀ values of 0.0036 µg/mL for valinomycin, 0.0051 µg/mL for staurosporine and 7.92 µg/mL for butenolide.

Scopel *et al.* [218] isolated two sponge-associated fungi, namely *Hypocrea lixii* F02 and *Penicillium citrinum* F40 (Table 4) that were active against the protozoal parasite *Trichomonas vaginalis*, which causes trichomoniasis, a sexually transmitted disease [219]. Culture filtrates of both isolates inhibited *T. vaginalis* ATCC 30236 and fresh clinical isolates, including the metronidazole-resistant TV-LACM2, with MIC values of 2.5 mg/mL. Further observation indicated that culture filtrates of these two fungi had no haemolytic effect against mammalian cells, which is one of the important criteria to further develop anti-protozoal drugs [218].

Table 4. Bioactive compounds with antiprotozoal activity from sponge-associated microbes.

Sponge	Origin (Depth)	Microorganism	Phylum	Compound	Property	Target	References
<i>Homophymia</i> sp.	Touho, New Caledonia (ND)	<i>Pseudomonas</i> sp. 1531-E7	Proteobacteria	2-Undecyl-4-quinolone	IC ₅₀ (1 µg/mL)	<i>Plasmodium falciparum</i>	[139]
<i>Acanthostromylophora ingens</i>	Manado, Indonesia (ND)	<i>Micromonospora</i> sp. M42	Actinobacteria	Manzamine A	IC ₅₀ (0.0045 µg/mL)	<i>P. falciparum</i>	[213-216]
<i>Hyattella intestinalis</i>	Palk strait, Tamil Nadu, India (ND)	unidentified bacterial isolate THB20	Unidentified	Unidentified	IC ₅₀ (41.88 µg/mL)	<i>P. falciparum</i>	[220]
<i>Stylissa carteri</i>	Palk strait, Tamil Nadu, India (ND)	unidentified bacterial isolate THB17	Unidentified	Unidentified	IC ₅₀ (20.56 µg/mL)	<i>P. falciparum</i>	[221]
<i>Clathria indica</i>	Palk strait, Tamil Nadu, India (ND)	unidentified bacterial isolate THB23	Unidentified	Unidentified	IC ₅₀ (28.80 µg/mL)	<i>P. falciparum</i>	[222]
<i>Clathria vulpina</i>	Palk strait, Tamil Nadu, India (ND)	unidentified bacterial isolate THB15	Unidentified	Unidentified	IC ₅₀ (20.73 µg/mL)	<i>P. falciparum</i>	[223]
<i>Haliclona grant</i>	Palk strait, Tamil Nadu, India (ND)	unidentified bacterial isolate THB14	Unidentified	Unidentified	IC ₅₀ (11.98 µg/mL)	<i>P. falciparum</i>	[224]
<i>Acanthostromylophora ingens</i>	Manado, Indonesia (ND)	<i>Micromonospora</i> sp. M42	Actinobacteria	Manzamine A	<i>In vivo</i> inhibition (90%) at concentration of 0.008 µg/mL	<i>Plasmodium berghei</i>	[206,214-216]
<i>Aplysina aerophoba</i>	Rovinj, Croatia (3–20 m)	<i>Micromonospora</i> sp. RV1115	Actinobacteria	Diazepinomicin	IC ₅₀ (6.29 µg/mL)	<i>Trypanosoma brucei</i>	[225]
<i>Sphaestospongia vagabunda</i>	Rovinj, Croatia (3–20 m)	<i>Actinokineospora</i> sp. EG49	Actinobacteria	Unidentified	Percentage of growth inhibition (48%)	<i>T. brucei</i>	[200]
unidentified	Rovinj, Croatia (3–20 m)	<i>Brevibacterium</i> sp. EG10	Actinobacteria	Unidentified	Percentage of growth inhibition growth inhibition (30%)	<i>T. brucei</i>	[200]
unidentified	Rovinj, Croatia (3–20 m)	<i>Gordonia</i> sp. EG50	Actinobacteria	Unidentified	Percentage of growth inhibition growth inhibition (28%)	<i>T. brucei</i>	[200]

<i>Dysidea tupa</i>	Rovinj, Croatia (3–20 m)	<i>Kocuria</i> sp. RV89	Actinobacteria	Unidentified	Percentage of growth inhibition growth inhibition (19%)	<i>T. brucei</i>	[200]
<i>Dysidea avara</i>	Mediterranean sea (ND)	<i>Nocardioopsis</i> sp. RV163	Actinobacteria	Dihydroxyphenazine (produced from co-culture)	IC ₅₀ (4.03 µg/mL)	<i>T. brucei</i>	[184]
<i>Sphectospongia vagabunda</i>	Red Sea (ND)	<i>Actinokinetespora</i> sp. EG49	Actinobacteria	Actinosporin A	IC ₅₀ (19.19 µg/mL)	<i>T. brucei brucei</i>	[226]
<i>Aplysina polyoides</i>	Rovinj, Croatia (3–20 m)	<i>Streptomyces</i> sp. 34	Actinobacteria	Valinomycin	IC ₅₀ (0.0036 µg/mL)	<i>T. brucei brucei</i>	[217]
<i>Axinella aerophoba</i>	Rovinj, Croatia (3–20 m)	<i>Streptomyces</i> sp. 22	Actinobacteria	Valinomycin	IC ₅₀ (0.0036 µg/mL)	<i>T. brucei brucei</i>	[217]
<i>Tedania</i> sp.	Rovinj, Croatia (3–20 m)	<i>Streptomyces</i> sp. 11	Actinobacteria	Staurosporine	IC ₅₀ (0.0051 µg/mL)	<i>T. brucei brucei</i>	[217]
<i>Tethya</i> sp.	Rovinj, Croatia (3–20 m)	<i>Streptomyces</i> sp. T03	Actinobacteria	Butenolide	IC ₅₀ (7.92 µg/mL)	<i>T. brucei brucei</i>	[217]
<i>Petrosia ficiformis</i>	Milos, Greece (ND)	<i>Streptomyces</i> sp. SBT344	Actinobacteria	Unidentified	IC ₅₀ (<10 µg/mL)	<i>T. brucei brucei</i>	[227]
<i>Sarcostragus foetidus</i>	Milos, Greece (ND)	<i>Modestobacter</i> sp. SBT363	Actinobacteria	Unidentified	IC ₅₀ (<10 µg/mL)	<i>T. brucei brucei</i>	[227]
<i>Sarcostragus foetidus</i>	Milos, Greece (ND)	<i>Nonomuraea</i> sp. SBT364	Actinobacteria	Unidentified	IC ₅₀ (<10 µg/mL)	<i>T. brucei brucei</i>	[227]
<i>Phorbas tenacior</i>	Crete, Greece (ND)	<i>Micromonospora</i> sp. SBT687	Actinobacteria	Unidentified	IC ₅₀ (14.87 µg/mL)	<i>T. brucei brucei</i>	[227]
<i>Petrosia ficiformis</i>	Milos, Greece (ND)	<i>Streptomyces</i> sp. SBT348	Actinobacteria	Unidentified	IC ₅₀ (16.52 µg/mL)	<i>T. brucei brucei</i>	[227]
<i>Ircinia variabilis</i>	Milos, Greece (ND)	<i>Geodermatophilus</i> sp. SBT381	Actinobacteria	Unidentified	IC ₅₀ (18.60 µg/mL)	<i>T. brucei brucei</i>	[227]
<i>Spirastrella cunctatrix</i>	Milos, Greece (ND)	<i>Modestobacter</i> sp. SBT362	Actinobacteria	Unidentified	IC ₅₀ (19.34 µg/mL)	<i>T. brucei brucei</i>	[227]
<i>Spirastrella cunctatrix</i>	Milos, Greece (ND)	<i>Rhodococcus</i> sp. SBT367	Actinobacteria	Unidentified	IC ₅₀ (19.97 µg/mL)	<i>T. brucei brucei</i>	[227]
<i>Axinella polyoides</i>	Banyuls-sur-Mer, France (ND)	<i>Streptomyces axinellae</i> Po1001T	Actinobacteria	Tetromycin 1	IC ₅₀ (26.02 µg/mL)	<i>T. brucei brucei</i>	[228]
<i>Axinella polyoides</i>	Banyuls-sur-Mer, France (ND)	<i>Streptomyces axinellae</i> Po1001T	Actinobacteria	Tetromycin 2	IC ₅₀ (40.35 µg/mL)	<i>T. brucei brucei</i>	[228]

<i>Axinella polypoides</i>	Banyuls-sur-Mer, France (ND)	<i>Streptomyces axinellae</i> Po1001T	Actinobacteria	Tetromycin 3	IC ₅₀ (23.18 µg/mL)	<i>T. brucei brucei</i>	[228]
<i>Axinella polypoides</i>	Banyuls-sur-Mer, France (ND)	<i>Streptomyces axinellae</i> Po1001T	Actinobacteria	Tetromycin 4	IC ₅₀ (32.17 µg/mL)	<i>T. brucei brucei</i>	[228]
<i>Axinella polypoides</i>	Banyuls-sur-Mer, France (ND)	<i>Streptomyces axinellae</i> Po1001T	Actinobacteria	Tetromycin B	IC ₅₀ (17.20 µg/mL)	<i>T. brucei brucei</i>	[228]
<i>Aphysina polypoides</i>	Rovinj, Croatia (3–20 m)	<i>Streptomyces</i> sp. 34	Actinobacteria	Valinomycin	IC ₅₀ (<0.12 µg/mL)	<i>Leishmania major</i>	[217]
<i>Axinella aerophoba</i>	Rovinj, Croatia (3–20 m)	<i>Streptomyces</i> sp. 22	Actinobacteria	Valinomycin	IC ₅₀ (<0.12 µg/mL)	<i>L. major</i>	[217]
<i>Tedania</i> sp.	Rovinj, Croatia (3–20 m)	<i>Streptomyces</i> sp. 11	Actinobacteria	Staurosporine	IC ₅₀ (1.24 µg/mL)	<i>L. major</i>	[217]
<i>Axinella polypoides</i>	Banyuls-sur-Mer, France (ND)	<i>Streptomyces axinellae</i> Po1001T	Actinobacteria	Tetromycin 3	IC ₅₀ (31.72 µg/mL)	<i>L. major</i>	[228]
<i>Sphinctospongia vagabunda</i>	Rovinj, Croatia (3–20 m)	<i>Actinokineospora</i> sp. EG49	Actinobacteria	Unidentified	growth inhibition (48%)	<i>L. major</i>	[200]
unidentified	Rovinj, Croatia (3–20 m)	<i>Gordonia</i> sp. EG50	Actinobacteria	Unidentified	growth inhibition (28%)	<i>L. major</i>	[200]
<i>Axinella corrugata</i>	The Arvoredo Biological Marine Reserve, Brazil	<i>Hypocrea lixii</i> F02	Ascomycota	Unidentified	MIC (250 µg/mL)	<i>Trichomonas vaginalis</i> ATCC 30236	[218]
<i>Axinella corrugata</i>	The Arvoredo Biological Marine Reserve, Brazil	<i>Hypocrea lixii</i> F02	Ascomycota	Unidentified	MIC (250 µg/mL)	<i>T. vaginalis</i> fresh isolate	[218]
<i>Axinella corrugata</i>	The Arvoredo Biological Marine Reserve, Brazil	<i>Hypocrea lixii</i> F02	Ascomycota	Unidentified	MIC (250 µg/mL)	<i>T. vaginalis</i> metronidazole-resistant LACM2	[218]
<i>Stoeba</i> sp.	The Arvoredo Biological Marine Reserve, Brazil	<i>Penicillium citrinum</i> F40	Ascomycota	Unidentified	MIC (250 µg/mL)	<i>T. vaginalis</i> ATCC 30236	[218]
<i>Stoeba</i> sp.	The Arvoredo Biological Marine Reserve, Brazil	<i>Penicillium citrinum</i> F40	Ascomycota	Unidentified	MIC (250 µg/mL)	<i>T. vaginalis</i> fresh isolate	[218]

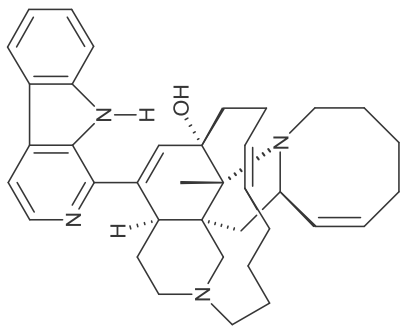
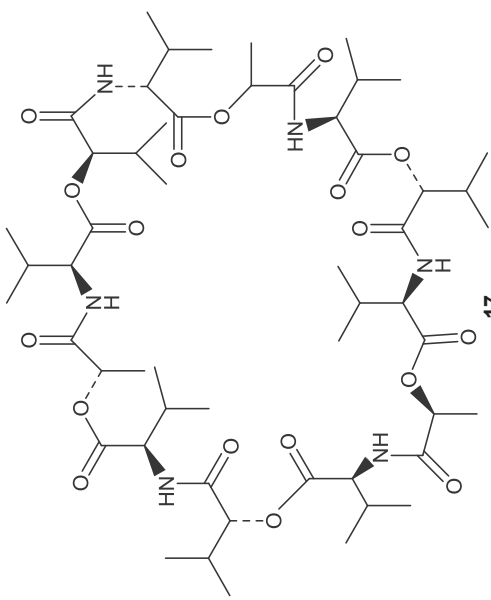
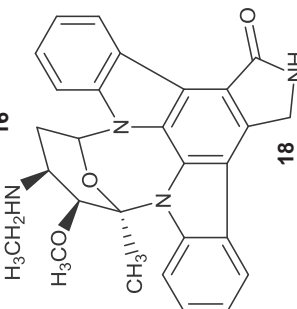

<i>Stoeba</i> sp.	The Arvoredo Biological Marine Reserve, Brazil (ND)	<i>Penicillium citrinum</i> F40	Ascomycota	Unidentified	MIC (250 µg/mL)	<i>T. vaginalis</i> metronidazole-resistant LACM2	[218]
							
							
							

Table 4 is organised according to the target protozoa. IC₅₀: half maximum inhibitory concentrations; MIC: minimum inhibitory concentration; ND: not determined.

Figure 4. Chemical structures of the antiprotozoal compounds manzamine A (16), valinomycin (17), staurosporine (18) and butenolide (19).

Discussion

Antimicrobial compounds from sponge-associated microbes: What we learned so far

Bioprospecting is the effort to discover natural compounds with therapeutic and biological applications [229]. In line with this definition, sponge-associated microbes offer a huge potential as the source of antimicrobial substances as shown by many microbial isolates being reported to inhibit pathogenic reference strains *in vitro* and to synthesize active substances against one or several groups of infectious agents. Based on our review, antimicrobial compounds produced by sponge-associated microbes with the most pronounced bioactivity include: 2-undecyl-4-quinolone, sorbicillactone A, stachybotrin D and chartarutine B against HIV-1; truncateol M against H1N1 M; YM-266183, YM-266184, kocurin, mayamycin, sydonic acid, naphthacene glycoside SF2446A2 and trichoderin A against a variety of bacterial strains; saadamycin and YM-202204 against fungi; manzamine-A against malaria; and valinomycin against Trypanosoma. In this case the most pronounced activity is solely based on reported inhibition data and does not yet take potential side effects into account. Therefore the most promising compounds may be ones that have higher IC₅₀ values, but cause less side effects. As these data are not available for the majority of the reported compounds, we have focused on the most potent compounds.

Sponge-associated bacteria and fungi are the two groups of microorganisms that have been found to produce antimicrobial compounds (Figure 5). The large majority of the antimicrobial compounds found in sponge-associated microbiota is produced by bacteria (90%), while fungi account for approximately 10% of the compounds reported. Sponge-associated bacteria derived antimicrobial compounds were found from 35 genera (Figure 5B). At a higher taxonomic level, these 35 bacterial genera can be classified into the four phyla Actinobacteria, Proteobacteria, Firmicutes and Cyanobacteria with percentages of 48.8%, 36.6%, 11.4% and 0.4% respectively. In contrast, sponge-associated fungi that have been found to produce antimicrobials are affiliated solely to the phylum Ascomycota.

Streptomyces is the most prominent genus as indicated by 30% of sponge bacteria-derived compounds. *Streptomyces* has become a main target for screening for bioactive compounds both from terrestrial and marine environments due to the high diversity of secondary metabolites they produce [230,231]. Of the many sponge-associated *Streptomyces* isolates reported, *Streptomyces* sp. HB202 and *Streptomyces* sp. RV15 are of particular interest in term

of producing antibacterial compounds. *Streptomyces* sp. HB202, isolated from the sponge *Halichondria panicea* has been documented to produce three antibacterial substances: mayamycin, streptophenazine G and K, which are mainly active against Gram positive pathogenic bacteria (Table 2). *Streptomyces* sp. RV15, on the other hand, produces the compound naphthacene glycoside which up to now is the only anti-Chlamydia reported from sponge-associated microbes [159]. In addition, the report on crude extract inhibition of *Streptomyces* sp. RV15 against *S. aureus* and *E. faecalis* [200] may give a hint to discover other antibacterial substances from this strain. *Streptomyces* sp. Hedaya48 is currently the most potent sponge-associated bacterial isolate for antifungal activities with the production of saadamycin and 5,7-dimethoxy-4-*p*-methoxyphenylcoumarin [192]. In addition, isolation of the anti-Trypanosoma and anti-Leishmania compounds valinomycin, staurosporine and butenolide from *Streptomyces* sp. 43, 21 and 11 [217], affirms *Streptomyces* as the currently most prominent producer of antimicrobial substances from sponges.

Pseudovibrio follows as the second most prolific bacterial genus isolated from sponges (20%) with respect to antimicrobial activities. Reports on *Pseudovibrio* spp. are concentrated on antibacterial activity and are mainly based on screening of crude extracts. Up to now, tropodithetic acid is the only antibacterial compound that has been identified from *Pseudovibrio* [232]. Although representing a lower percentage of the sponge-associated bacteria found to produce antimicrobials than *Streptomyces* and *Pseudovibrio*, 9% of the currently known bioactives was found to be produced by sponge-associated *Bacillus* spp., with activities against viruses, bacteria and fungi. *Bacillus cereus* QNO3323 is currently the most prominent antimicrobial producer from this genus with the very potent thiopeptides YM-266183 and YM-266184 that are active against Gram positive bacteria.

Sponge-associated Ascomycota found to produce antimicrobials can be further classified into 12 genera. Of these 12 fungal genera, *Aspergillus* (30%) and *Penicillium* (23%) are currently the two most prominent groups of sponge-associated fungi reported as antimicrobial producers. This finding is not surprising since both *Aspergillus* and *Penicillium* are known prolific producers of secondary metabolites from other sources [233]. *Aspergillus versicolor* [171] and an unidentified *Aspergillus* sp. isolated from the sponge *Xestospongia testudinaria* [161] showed a strong antibacterial activity as indicated by potent inhibition of pathogenic bacteria. The antimicrobial activities found from sponge-associated *Penicillium* spp. are particularly remarkable as it is the only fungal genus that is found to produce antivirals, antibacterials, antifungals and antiprotozoals. *Penicillium chrysogenum* [51] and *Penicillium* sp. FF01 [170]

are to date the most promising sponge-associated *Penicillium* isolates for which anti-HIV activity (sorbicillactone) and antibacterial activity (citrinin) were reported, respectively. Sponge-derived *Stachybotrys* spp. are only known for antiviral activity, particularly against HIV and enterovirus 71 (EV71), and there are no reports of other antimicrobial activities. Generally, although the number of produced antimicrobials is outnumbered by those of sponge-associated bacteria, sponge-associated fungi should be considered as an important reservoir of antimicrobial compounds.

When the chemical structures of sponge-microbe-derived compounds are considered, a rather diverse array of structures is observed, including peptides, terpenoids, phenazines, indoles, phenoles and polyketides. Sixty percent of the antivirals from sponge-associated microbes are ketone derivatives (quinolone, sorbicillactone, isoindolinone, butyrolactone, furanone, xanthone, methanone, phenone). Peptide derivatives constitute 19% of the total identified antibacterial substances and roughly 12.5% from the total antimicrobial compounds reviewed here. Phenazine derivatives are the second most frequently isolated class of antibacterial compounds from sponge-associated microbes (15%) as exemplified in this review by the antibacterial compounds streptophenazine [179], phenazine alkaloid antibiotics [168], 6-hydroxymethyl-1-phenazine-carboxamide and 1,6-phenazinedimethanol [181]. Phenazine is a nitrogen-containing heterocyclic compound with a wide range of biological activities [177,234], and several studies from terrestrial environments and chemically synthesized phenazines have been reported as antiviral [235], antibacterial [236], and antimalaria [237]. Moreover, this group of compounds is attractive for therapeutic application since their structures are relatively small and hence can easily reach tissues and organs [177,238].

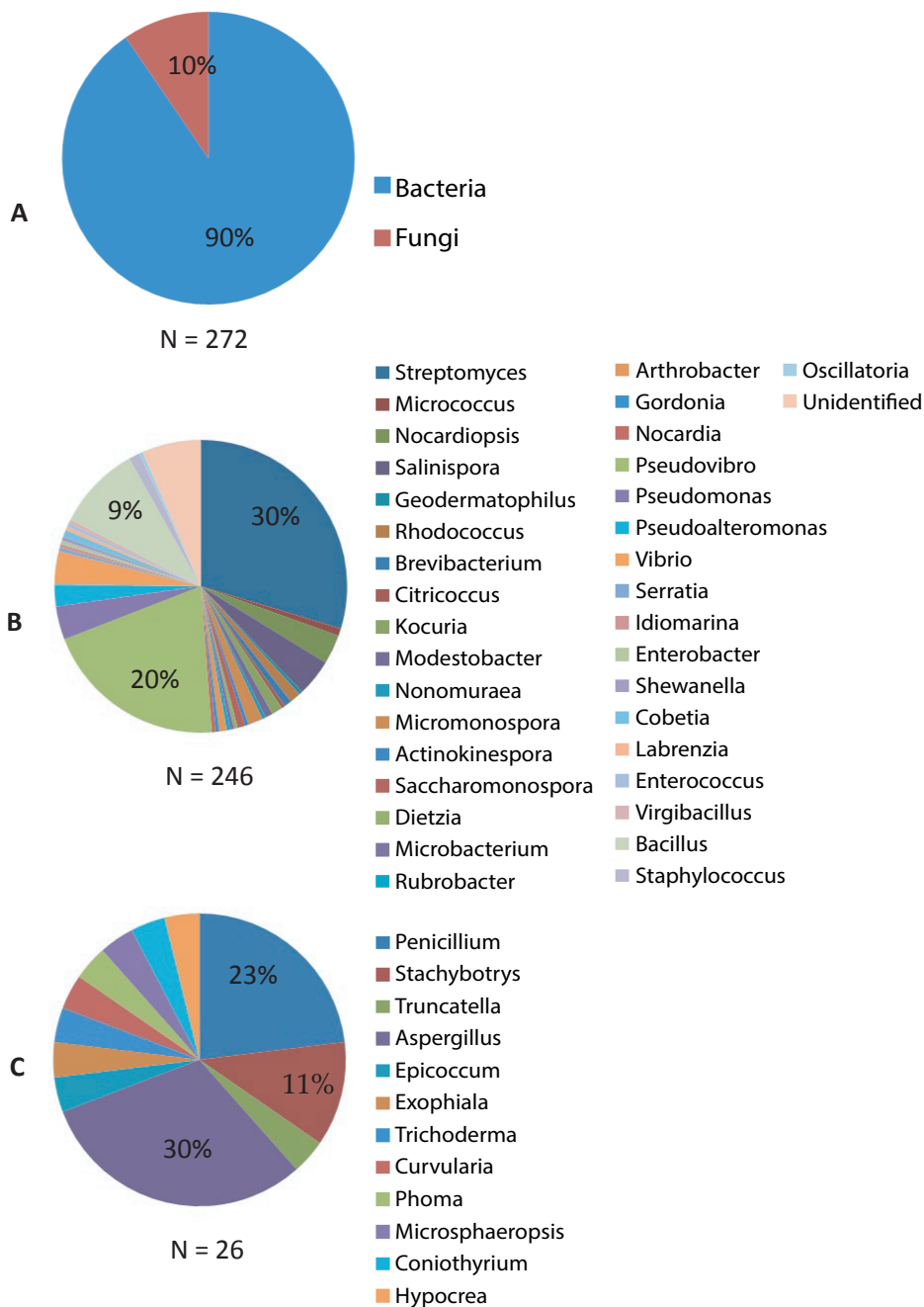


Figure 5. Distribution of sponge-associated microorganisms found to produce antimicrobial compounds: (A) Bacteria and Fungi; (B) Bacterial genera; and (C) Fungal genera. Figure 5 was made based on the summary of the taxonomic affiliations of sponge-associated microbes ($N = 272$) that were found to produce antimicrobials.

Discovering antimicrobial compounds from sponge-associated microbes: From culture-dependent to culture-independent methods

Isolation of antimicrobial producers provides a valuable basis for assessing the biotechnological potential of sponge-associated microbes. In a wider perspective, however, only a small fraction of this sponge-microbial community has been isolated under laboratory conditions leaving the majority resistant to *in vitro* growth with current cultivation approaches [4,19,29]. Several studies have focused on improving cultivability of sponge-associated microbes. Some of the approaches include using low nutrient media [239], floating filter cultures [32], employing different carbon sources, e.g., lectin [240], sponge extracts [32], and *in situ* cultivation using a diffusion growth chamber [35]. Furthermore, flow-cytometry and density gradient centrifugation have been applied to separate sponge cells from their associated bacteria to enrich the inoculum [21,241]. Additionally, co-cultivation through mixing of two or more microbial isolates *in vitro* [242] is an approach proposed to discover more natural compounds from sponge-associated microbes. The idea behind co-culture lies in the fact that many biosynthetic gene clusters found in microorganisms remain cryptic under standard laboratory conditions, and co-cultivation might provide a possibility to activate these silent genes [243,244]. As an example, the co-culture by Dashti *et al.* [184] of the sponge-associated Actinobacteria, *Actinokinespora* sp. EG49 and *Nocardiopsis* sp. RV163, resulted in isolation of the antibacterial compound 1,6-dihydroxyphenazine, which was not found from the individual isolates. However, even if the cultivability of sponge-associated microbes is improved, there is a long way ahead to reach a point that we will be able to isolate and routinely cultivate 50% of the microbes that are found in sponges. At the same time, the advance of genetic and molecular studies has resulted in the development of tools to study genes, transcripts and proteins by directly analyzing environmental DNA, RNA and proteins, thus bypassing cultivation procedures [242]. In relation to screening for antimicrobial activity, metagenomics has been applied to identify antimicrobials of uncultivated microorganisms from terrestrial environments, such as the antimycobacterial nocardamine, the putative antibacterial activity of terragines A–E [245], violacein that is active against *S. aureus*, *Bacillus* sp. and *Streptococcus* sp. [246] and a polyketide with activity against the yeast *Saccharomyces cerevisiae* [247].

Two main metagenomic approaches, functional screening and sequence homology-based methods, are generally distinguished [248]. Functional screening relies on detection of the metabolic activities of metagenomic library clones without requiring any prior sequence

information [248-250]. Gillespie *et al.* [127] applied function-based metagenomics with *E. coli* as expression host, to identify the antibiotics turbomycin A and B from a soil sample. MacNeil *et al.* [251] identified the antimicrobial indirubin by constructing a BAC (bacterial artificial chromosome) library in *E. coli*. Yung *et al.* [60] reported two hydrolytic enzymes from fosmid clones CcAb1 and CcAb2, which were derived from a metagenome of the sponge *Cymbastela concentrica* using *E. coli* as the host. Both fosmid clones inhibited the growth of *Bacillus* sp. with an inhibition diameter of 20 mm, and clone CcAb1 showed additional inhibition of *S. aureus* and an *Alteromonas* sp. with diameters of inhibition of 50 mm and 60 mm, respectively. Further phylogenetic analysis showed that active genes encoding for these enzymes were of microbial origin [60]. He *et al.* [252] constructed a fosmid library of the sponge *Discodermia calyx* using *E. coli* as the host and identified antimicrobial activity of the enzyme 3-hydroxypalmitic acid against *B. cereus* and *C. albicans*. In addition, using the same approach He *et al.* [253] observed an active clone, pDC113, that displayed a clear inhibition zone against *B. cereus*. Subsequently, 11 cyclodipeptides were identified from this clone. Generally, it can be stated that although a number of antimicrobials have been discovered through functional screening of metagenomic libraries from sponges, the expression of large gene clusters such as those encoding PKS (Polyketide Synthase) and NRPS (Non-ribosomal Peptide Synthetase) is still a difficult hurdle to take. Several key elements need to be considered to achieve successful expression of biosynthetic gene clusters; namely mobilizing the biosynthetic pathway into a suitable vector, selecting an appropriate heterologous host and stably maintaining the gene clusters in the host [254]. The size of many of these gene clusters requires the use of cloning vectors that can accept large inserts, such as fosmids, or BACs if the required insert size is over 100 kb [255]. Selection of heterologous expression systems in particular is a crucial factor before applying functional metagenomics to identify antimicrobials, because expression hosts are microbes as well and especially clones that express genes encoding for enzymes involved in production of antimicrobials may therefore be non-viable. Ongley *et al.* [254] pointed out some considerations in selecting an expression host such as relatedness to the native producer, availability of genetic tools and precursors, a high growth rate, and suitability for fermentation at a large scale. *E. coli*, the most commonly used expression host, has limitations for expressing parts of metagenomes because, e.g., of the sheer size of some gene clusters, genes with deviating codon usage, incompatible regulatory elements, lack of biosynthesis precursors or unavailability of posttranslational modifications [249,256]. Therefore, in order to make screening for antimicrobials through metagenomic libraries more efficient, it is of utmost importance to diversify the suite of expression hosts used. Several non-*E. coli* hosts, such as

Agrobacterium tumefaciens, *Bacillus subtilis*, *Burkholderia graminis*, *Caulobacter vibrioides*, *Pseudoalteromonas haloplanktis*, *Pseudomonas putida*, *Ralstonia metallidurans*, *Rhizobium leguminosarum*, *Streptomyces avermitilis*, *S. albus*, *Pseudomonas putida*, *Sulfolobus solfataricus*, *Thermus thermophilus*, *Thiocapsa roseopersicina* and *Saccharopolyspora* sp. have been developed and should be more seriously considered as expression hosts when performing metagenomic screenings for antimicrobials [249,256,257].

Sequence-based screening, on the other hand, requires information on the sequence of genes involved in the production of a natural product as guidance to search for similar sequences in a sequenced metagenomic library or scaffolds reconstructed from direct metagenomic sequencing [258]. Homology-based screening is suitable to identify a compound with highly conserved biosynthesis pathways, e.g., those mediated by PKS and NRPS [259]. Piel and colleagues [260-264] applied this method, and identified the antitumor polyketide onnamide from uncultivated bacteria of the sponge *T. swinhoei*. Sequence-based screening was applied by Fisch [265] to unravel the complete pathway of the polyketide psymberin that was found to possess a potent antitumor activity, from uncultivated sponge-associated microbes. By sequence-based screening of metagenomic libraries, Schirmer *et al.* [266] reported diverse polyketide gene clusters in microorganisms from the sponge *Discodermia dissoluta*. The development of techniques that yield longer read lengths, such as Pacific Biosciences (PacBio) RS II SMRT (Single Molecule Real-Time) sequencing technology, in which a single read can be extended over 10 kbp [267], can be instrumental in increasing the accuracy in assembling large gene clusters. Application of PacBio for secondary metabolite gene clusters has been reported by Alt and Wilkinson [59], who identified the 53,253 bp genomic fragment encoding the transacyltransferase (trans-AT) polyketide synthase (PKS) from a marine *Streptomyces* sp responsible for the production of the antibiotic anthracimycin (atc). Furthermore, using *Streptomyces coelicolor* as heterologous expression host, the authors confirmed production of anthracimycin [59]. Furthermore, single cell analysis by combining cell separation and fluorescence-assisted cell sorting (FACS) could be a strategy to overcome the complexity of the microbial community in sponges since this method can be used to select for genomes from microbes that are present in low abundance in the sponge leading to a simplified reconstruction of secondary metabolite gene clusters present in these bacteria [268]. This strategy has been applied by Wilson *et al.* [58] for resolving the gene clusters encoding the machinery needed for the production of the polytheonamides produced by the candidate genus *Entotheonella* from the sponge *Theonella swinhoei*.

Inspired by these examples, homology-based screening could be further exploited to identify biosynthesis gene sequences that could lead to the identification of novel antimicrobial substances from Nature's excessive diversity. Moreover, application of homology-based screening can benefit from publicly available metagenomic sequencing data and prediction tools for analyzing biosynthesis gene clusters, e.g., AntiSMASH (Antibiotics and Secondary Metabolite Analysis Shell) [269,270]. Application of sequence-based screening, however, is limited by the fact that the found sequences need to be related to known compounds, inherently limiting the potential for novelty. Furthermore, information on gene sequences is no guarantee that the acquisition of a complete gene pathway has been obtained [271]. Therefore, sequence-based metagenomics should ideally be complemented by chemical analysis to confirm whether the predicted compound exists and is fully functional (Figure 6).

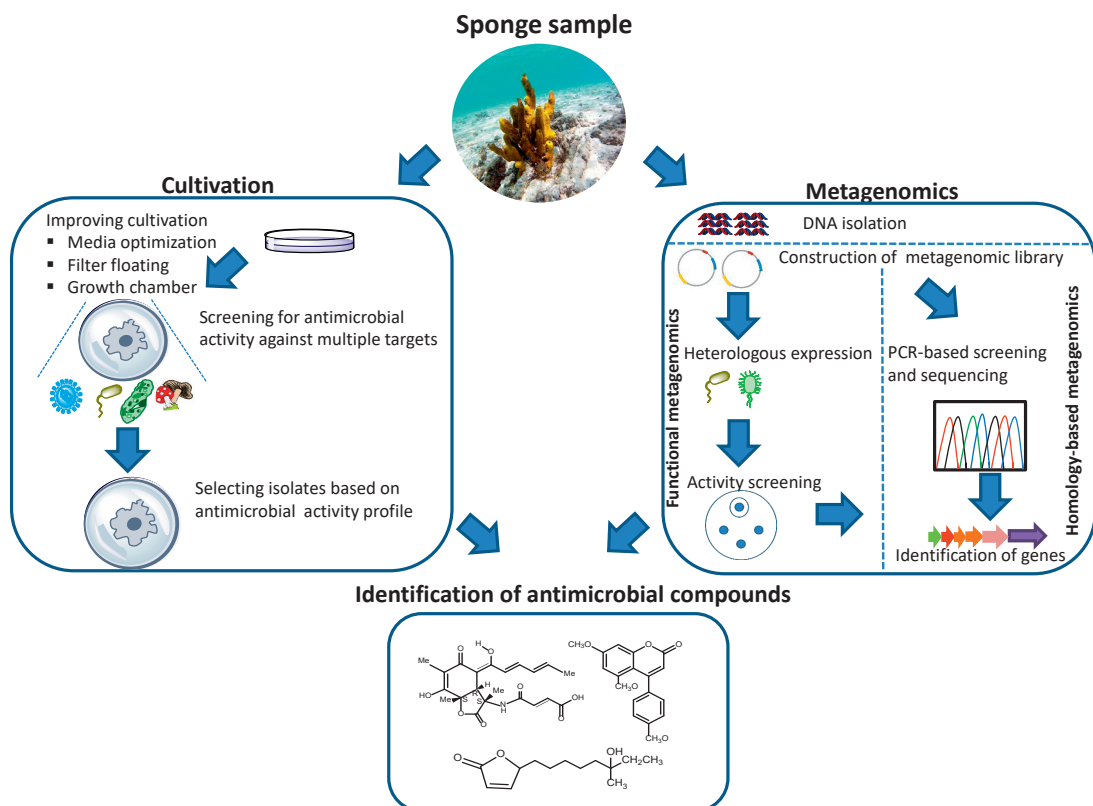


Figure 6. General overview of the strategies used to discover antimicrobial compounds from sponge-associated microorganisms.

Conclusion and outlook

Sponge-associated microbes already offer a rich source of potent antimicrobial compounds against viruses, bacteria, protozoa and fungi, and currently available compounds are predominantly active against HIV-1, H1N1, nosocomial Gram positive bacteria, *Escherichia coli*, *Plasmodium* spp, *Leishmania donovani*, *Trypanosoma brucei*, *Candida albicans* and dermatophytic fungi. *Streptomyces*, *Pseudovibrio*, *Bacillus*, *Aspergillus* and *Penicillium* are the microbial genera associated with sponges from which potent antimicrobial compounds are most frequently isolated. However, none of the antimicrobial compounds highlighted in this review have been successfully marketed as pharmaceuticals. To clearly translate bioactivity of these important compounds it is crucial to further unravel their mode of actions and measure their level of toxicity, since the majority of these studies has been focused on *in vitro* bioassays and elucidation of the chemical structures only.

The known versatility of antimicrobial activities found in sponge-associated microorganisms could easily be expanded even without considering additional sponge sampling campaigns. Bioactivity screens of identified compounds or undefined sponge extracts is often restricted to a specific antimicrobial activity. The selection, for instance, relies on the specific research activities of the groups involved in isolating the microbes [45]. Consequently, it is probably safe to assume that other potent antimicrobial properties from many sponge isolates and their bioactive compounds remain undetected. Therefore, known antimicrobial compounds and producer strains are a valuable source for additional antimicrobial activities screenings using different target types (viruses, bacteria, fungi, protozoa and beyond). In addition, sponge-derived strain collections that comprise isolates that tested negative for antimicrobial activity at first may have done so, because the compound of interest is not produced under standard laboratory conditions. Exposure of these strains to potential microbial targets may lead to recovery of bioactivity that would otherwise go unnoticed.

Ideally, researchers who isolate microbes from sponges will deposit them to publicly available culture collections so that laboratories with complementary expertise and interests could benefit and screen the deposited isolates for different antimicrobial activities. This will make exchange of materials and knowledge that can be obtained much more efficient. Importantly, a fair agreement on intellectual property rights needs to be established for translating this into reality. Lastly, the revolutionary advance of next generation sequencing technologies combined with more diversified heterologous expression systems (Figure 6) are expected to open up the

large unexplored reservoir of antimicrobials produced by yet uncultivated sponge-associated microbes.

Acknowledgments

Anak Agung Gede Indraningrat receives a PhD fellowship from the Indonesia Endowment Fund for Education (LPDP), grant number 20140812021557. This work was also supported by the EC grant “BluePharmTrain” (grant agreement no. 607786).



Chapter 3

Depth affects sponge prokaryotic communities and their antimicrobial activities in two Demosponges, *Xestospongia muta* and *Agelas sventres*

Anak Agung Gede Indraningrat, Georg Steinert, Leontine E. Becking, Benjamin Mueller, Jasper de Goeij, Hauke Smidt, Detmer Sipkema

Manuscript in preparation

The background of the page features a stylized, light gray illustration of a coral reef. It includes various types of coral, such as branching corals and large, rounded sponges, set against a backdrop of soft, wavy lines representing the reef's structure. The overall aesthetic is clean and scientific.

Abstract

Marine sponges are important members of marine ecosystems and host various and diverse microbiota. While the large majority of studies on microbial composition and antimicrobial activity of marine sponges are from shallow water, it is largely unknown how microbiota and antimicrobial activity are affected by depth. The latter is of importance for marine ecology studies as well as future bioprospecting. In the present study, we investigated the prokaryotic composition and antimicrobial activity associated with the sponges *Xestospongia muta* and *Agelas sventres* collected from three depth ranges: shallow (< 30 m), middle (30 - 60 m), and deep (60 - 90 m). The prokaryotic community was assessed by employing 16S rRNA gene amplicon sequencing, and antimicrobial activity was evaluated by screening crude extracts of the sponges against a set of Gram-positive bacteria, Gram-negative bacteria, a yeast and an oomycete. For both sponges, there was a significant difference in prokaryotic community composition between the deep and shallow specimens. Specific OTUs assigned to the phyla Cyanobacteria, Chloroflexi, Acidobacteria, Actinobacteria, Proteobacteria and Thaumarchaeota were significant contributors for the variance observed along the depth gradient. Antibacterial activities were generally higher from shallow extracts, whereas there were limited or no antibacterial activities from deep-water sponges. Conversely, a strong anti-oomycete activity was found in deep and shallow specimens, but without clear pattern along the depth gradient. Using the piphillin prediction tool, nine putative pathways related to the production of antibiotics and secondary metabolites were predicted for both sponges based on 16S rRNA gene data and publicly available genomes of closely related organisms. Overall, this work reports how depth influences prokaryotic assemblages in marine sponges and antimicrobial activity.

Keywords: sponge, prokaryotic community, antimicrobial, depth gradient

Introduction

Marine sponges (phylum Porifera) occupy a wide range of habitats ranging from tropical to polar regions [3,272]. In line with their abundance, sponges have prominent roles in coral reef ecosystems, such as seafloor structuring, involvement in various biogeochemical cycles and to provide shelter for other marine fauna [11]. Sponges convert dissolved organic matter to particulate organic matter via the “sponge loop” to provide organic carbon to higher trophic levels [13]. Sponges host dense and diverse prokaryotic communities, and for some species, prokaryotes may constitute more than one-third of their biomass [273]. Most sponges-associated microbes generally maintain stable relationships with their host across space, time and generations [75,76,274-277]. Furthermore, a substantial proportion of these microbes is enriched in sponges as compared to the surrounding environment, which indicates their specificity for co-inhabitation with sponges [23,24,278]. Sponge-associated microbes do not squat their home; instead, these prokaryotic communities contribute to their host by involvement in nutrient cycles within the host tissue [19-21,279] and in defence mechanisms [4,280,281]. Marine sponges and their associated microbes are prominent producers of secondary metabolites, with over 5000 described compounds, many of which display unique features and are potentially applicable for therapeutic purposes [43,282].

While ecological and biotechnological studies on sponges and their associated microbes come dominantly from shallow reef habitats, similar information from the mesophotic zone is rather scarce [79-81]. Mesophotic ecosystems are low-light adapted reefs starting from 30 m depth and extending to 200 m of depth and span the region between the bright light from shallow waters and the ever dark deeper waters. These mesophotic habitats are therefore also referred to as the twilight zone [68]. Mesophotic ecosystems are generally less exposed to environmental changes and anthropogenic disturbances and therefore are often proposed to be a refuge for fauna from shallow habitats including sponges [65,68]. From a biotechnological perspective, the functional diversity of primary and secondary metabolism-associated gene clusters beyond shallow water is relatively underexplored and is yet expected to harbour truly different sources of novel compounds for therapeutic and industrial applications [61]. As an example, unique and diverse polyketide synthase and non-ribosomal peptide synthetase gene clusters of microbial origin were reported from the three deep-sea sponges *Inflatella pellicula*, *Poecillastra compressa*, and *Stelletta normani*, which may provide hints to novel compounds [63]. Furthermore, the TARA Ocean study underlined the sharp increase of unknown functional genes as depth increased from shallow to deeper sea zones [283], which further

reinforces the potential for bioprospecting for novel compounds in mesophotic habitats and beyond.

Differences in the ecological settings between the mesophotic zone and shallow water related to light intensity, temperature, nutrient availability, predation and human impact may lead to changes in prokaryotic composition in marine invertebrates including sponges [73,79-81]. Prokaryotic community analysis of samples from three common Caribbean sponges taken from depths ranging from 10 to 100 m suggested that each sponge species maintains a core microbiota, but that sponge-associated microbiota varies with depth [79]. In addition, a study from the Pacific indicated a significant change of the prokaryotic community composition of the sponge *Callyspongia* sp. from shallow to mesophotic habitats. However, the exact environmental factor(s) responsible for such differences could not be determined [81]. Additionally, more comprehensive studies on corals have indicated morphological adaptations and symbiont specializations with greater depth, with species inhabiting the mesophotic zone harbouring a specific photosynthetic endosymbiont (*Symbiodinium*) community to adapt to low light conditions [284-288].

As commonly reported, sponges harbor various chemical defenses to deter predation and fouling and to compete for space with other benthic marine organisms [289-291]. In some cases, these compounds also serve as general antimicrobial substances [292-294]. Little is known as to what extent the metabolome of marine sponges is affected by depth. A transplantation study of individuals of the sponge *Aplysina cavernicola* from deep (40 m) to shallow areas with more light exposure (7-15 m) over a period of three months did not alter metabolite profiles of the sponge, suggesting that the corresponding gene clusters were expressed constitutively [78]. Conversely, transplantation (from 10 m depth to 75 m and vice versa) and a feeding assay by exposing tissues of the sponge *Plakortis angulospiculatus* to the pufferfish *Canthigaster rostrata* showed that shallow sponges displayed a much stronger deterrent effect compared to individuals from the mesophotic zone, plausibly due to higher exposure of predating fish in shallow habitats [73].

The Caribbean Sea harbors a large diversity of marine sponges, where *Xestospongia muta* and *Agelas sventres* are two species commonly found [89,90]. *X. muta* in particular is a dominant member of sponge communities throughout the Caribbean Sea, characterized by a large amount of biomass with some individuals having a diameter and height of over 1 m [96,295]. A report from the Florida Keys showed that the population of *X. muta* increased by 122% over 12 years,

which mainly was triggered by shifting of genetic structure between populations of the two distinct *X. muta* clusters (cluster 1 and 2) due to unequal reproduction and higher recruitment of cluster 2 over cluster 1. However, the selective force(s) responsible for such a shift remain unclear [296]. Prokaryotic communities of *X. muta* have been well studied. *X. muta* is classified as high microbial abundance sponge, and various studies on organic extracts of *X. muta* have highlighted potential predator deterrent and antimicrobial activities [79,80,98,99,297,298]. Previously, an investigation on prokaryotic community of *X. muta*, complemented with measurement of inorganic nutrients along a depth gradient (10-90 m) in Little Cayman, showed a change of microbiota composition, mainly due to a reduced percentage of Cyanobacteria in the lower mesophotic zone due to decline of irradiance and nutrients [80]. In contrast to *X. muta*, the prokaryotic composition of *A. sventres* has not been studied, and up to now, the feeding deterrent compound sventrin is the only bioactive compound that has been reported from *A. sventres* [80,87,92].

Given that both *X. muta* and *A. sventres* have a depth span from shallow water to mesophotic habitats and are known to produce bioactive secondary metabolites, these sponge species were selected to study the impact of depth on prokaryotic community composition and antimicrobial activities. To address this aim, we employed Illumina MiSeq 16S rRNA gene amplicon sequencing to investigate prokaryotic community composition of the sponges and the surrounding sea water samples collected from three depth categories: shallow (< 30 m), middle (30 – 60 m) and deep (60 – 90 m). In addition, antimicrobial activity of tissue extracts of the two sponge species along the depth gradient was examined against six microbial indicator strains, which included Gram-positive and Gram-negative bacteria, a yeast and an oomycete. Finally, using 16S rRNA gene data as input, the Piphillin prediction tool [299] was used to predict whether a trend regarding distribution of secondary metabolite pathways related to antibiotics biosynthesis was observed with respect to depth.

Materials and Methods

Sample collection and sponge tissue processing

Xestospongia muta and *Agelas sventres* samples were collected in front of Substation Curaçao (12°05'04.4"N 68°53'53.7"W) from 4 – 22 November 2015. Samples were collected from three depth categories; shallow (< 30 m), middle (30 – 60 m) and deep (60 – 90 m). From each of the depth categories, five sponge specimens were collected for each of the two species. Shallow

sponge specimens were collected via SCUBA diving, while middle and deep specimens were taken using a submersible vehicle, the “Curasub”. Seawater samples (n = 3, 1 L) were collected from each depth using a Niskin bottle. Upon arrival in the laboratory, sponge specimens were cleaned from any visible debris, rinsed three times using artificial seawater (ASW, 33 g / L synthetic sea salt [Instant Ocean Reef Crystals, Aquarium Systems, Sarrebourg, France]) and were cut into pieces of ~ 0.1 cm³. Pieces of tissue from each specimen were preserved in a 15 mL tube containing 10 mL of RNA*later* stabilization solution (Thermo Fisher Scientific). Additionally, seawater samples were filtered through 0.2 µm pore size nitrocellulose filters (Sigma-Aldrich). The preserved sponge tissues and filters were stored at -20°C until further use.

DNA extraction

DNA was extracted from sponge samples (~ 200 mg biomass/sample) and seawater filters using the Fast DNA Spin kit for soil (MP biomedical) following manufacturer’s instructions with the slight modification of conducting 2 times 45 s bead beating (Precellys 24 Bertin Instruments, Montigny-le-Bretonneux, France). DNA concentrations were checked using a spectrophotometer (DeNovix DS-11, Wilmington, USA) and were visualized on a 1% agarose gel.

Sponge molecular taxonomy

Molecular identification of sponge samples was conducted by amplifying cytochrome oxidase subunit 1 (COI) encoding genes using primers dgLCO1490F (5’-GGT CAA CAA ATC ATA AAG ATA TTG G-3’) and dgHCO2198R (5’-TAA ACT TCA GGG TGA CCA AAA AAT CA-3’) [300]. PCR amplification of the COI fragment was performed in a volume of 50 µL containing 28.75 µL nuclease free water, 10 µL 5x Green Gotaq Flexi buffer, 1 µL 10mM dNTPs, 1 µL forward primer (10 µM), 1 µL reverse primer (10 µM), 3µL MgCl₂ (25 mM), 4 µL Bovine Serum Albumin (BSA), 0.25 µL Gotaq HotStart DNA Polymerase (5 U/µL) and 1 µL DNA (10–20 ng), following the protocol as described by Meyer *et al* [301]. PCR products were visualised on a 1% agarose gel, purified using the Thermo Scientific GeneJET PCR Purification Kit and Sanger sequenced in both directions (GATC Biotech AG, Germany).The chromatograms of forward and reverse COI sequences of each specimen were assembled and quality checked manually using Geneious [302] version10.0.9. Additionally, six and four reference COI sequences of *X. muta* and *A. sventres*, respectively, were retrieved from the

Sponge Gene Tree server [303], along with COI sequences of other sponge species as outgroups. All COI sequences were aligned using MEGA6 [304] with the MUSCLE algorithm resulting in a final sequence length of 644 nt and 707 nt for *X. muta* and *A. sventres*, respectively. Subsequently, phylogenetic trees were generated in MEGA6 based on the COI sequences by applying the maximum likelihood algorithm.

Prokaryotic community profiling using 16S rRNA gene amplicon sequencing

Prokaryotic community composition was assessed by Illumina MiSeq amplicon sequencing of the V4 region of the 16S rRNA gene using a two-step amplification procedure. PCR was conducted by using the 2nd version of the EMP (Earth Microbiome Project) primer pair 515FY(5'GTGYCAGCMGCCGCGGTAA3')[305] and 806RB (5'GGACTACNVGGGTWTCTAAT 3') [306]. Subsequently, Unitag 1 and Unitag 2 were added to the forward and reverse primer, respectively, as previously described [307]. In the first step PCR, 25 μ L PCR reactions contained 16.55 μ L nuclease free water (Promega, Madison, USA), 5 μ L of 5 \times HF buffer, 0.2 μ L of 2 U/ μ L Phusion hot start II high fidelity polymerase (Thermo Fisher Scientific AG), 0.75 μ L of 10 μ M stock solutions of each primer, 0.75 μ L 10 mM dNTPs (Promega) and 1 μ L template DNA (10 – 20 ng/ μ L). Amplification was performed at 98°C for 3 min, followed by 25 cycles at 98°C for 25 s, 50°C for 20 s, 72°C for 20 s and a final extension of 7 min at 72°C. PCR products were visualized on a 1% (w/v) agarose gel. Subsequently, 5 μ L of these first-step PCR products were used as template in the second PCR reaction to incorporate 8 nt sample specific barcodes. The second step PCR was performed in triplicate for each sample in 50 μ L PCR reactions which contained 31 μ L nuclease free water (Promega), 10 μ L of 5 \times HF buffer, 0.5 μ L of 2 U/ μ L Phusion hot start II high fidelity polymerase (Thermo Fisher Scientific AG), 5 μ L equimolar mixes of 10 μ M forward primer (barcode-linker-Unitag1) and reverse primer (barcode-linker-Unitag2), 1 μ L 10mM dNTPs (Promega) and 2.5 μ L of the first PCR product as template. The PCR products were purified following a method as previously described [308], and the purified library was sequenced at the GATC Biotech AG (Germany) by Illumina Miseq sequencing.

Raw sequence processing

Raw sequence data were processed using a previously described protocol [308] with slight modifications. Specifically, raw data was analyzed using NG-Tax (Galaxy version 1.0) [309] with forward and reverse paired-end reads being trimmed to 70 nucleotides. Subsequently, both reads were concatenated, resulting in sequences of 140 bp that were used for further sequence

data processing. Taxonomic assignment was done by utilizing a customized version of the SILVA 128 SSU database [310], and OTUs classified as Chloroplasts were removed from the analysis.

Prokaryotic community analysis

Data analyses were performed in R version 3.5.0 (<https://www.r-project.org/>) and Microsoft Excel. Community 16S rRNA gene abundance data processing and analyses in R were performed using the following R packages: phyloseq version 1.21.0 [311], microbiome version 0.99.90 [312], and ggplot2 version 2.2.1 [313]. The NG-Tax generated phylogenetic OTU tree was processed using the ape package version 4.1 [314], and phylogenetic diversity was calculated using the picante package version 1.6-2 [315]. Phylogenetic diversity of each group of samples was analyzed using Kruskal-Wallis and Wilcoxon rank sum test to assess significance of potential differences among groups of samples for the parameters “sample types” (i.e., *X. muta*, *A. sventres*, and seawater) and “depth” (i.e., shallow, middle, deep). The raw p-values were adjusted using the Benjamin-Hochberg method. The prokaryotic community composition was visualized by principal coordinate analysis (PCoA) based on Hellinger transformed relative abundances of OTUs using Bray–Curtis distances. The *adonis* and *betadisper* functions as implemented in *vegan* package version 2.5.2 [316] were employed to estimate the variance and dispersion of beta diversity, by applying two factors: “sample type” and “depth”. Community composition at phylum level was calculated based on average relative abundance among specimens.

A heatmap was generated in R using *pheatmap* version 1.0.8 [316] for the most abundant OTUs ($\geq 0.25\%$, $n = 100$) based on average relative abundance across all samples. Subsequently, the most abundant OTUs listed in the heatmap ($n=100$) were used to identify OTUs which were significantly enriched in the 3569 sponge specimens (comprising 269 sponge species) from the sponge microbiome project [25]. Sequence comparison was done based on a method described by Dat *et al* [308]. Briefly, sponge microbiome project subOTU sequences were selected based on having no more than one nucleotide mismatch with sequences of the most abundant OTUs observed in this study. The selected subOTU sequences were then uploaded to the spongeEMP online server (www.spongeemp.com) to identify OTUs that were significantly enriched in sponges. Furthermore, the most abundant OTUs were checked by a G-test using the script *group_significance.py* in QIIME version 1.9.1, and raw p-values were adjusted using the Benjamin-Hochberg FDR correction for multiple comparisons.

Functional capacities of prokaryotic communities of all sponge samples were predicted using the Piphillin prediction tool [299] version 6.0 based on the OTU table containing raw count data of each OTU and the fasta file containing the representative sequence of each OTU. Briefly, the representative sequence for each OTU (query) was searched against the Kyoto Encyclopedia of Genes and Genomes (KEGG, May 2017 release) database using 97% cut-off sequence identity. Statistical analysis was performed in STAMP [317] ($p \leq 0.05$ was considered significant, parameters: Kruskal-Wallis, Post-hoc test Games-Howell, and Storey FDR for multiple correction methods) focusing on KEGG pathways related to antibiotics and secondary metabolites biosynthesis.

Preparation of crude extract of sponge tissue and antimicrobial activity screening

Crude extracts of sponge tissues were prepared based on the method by Rohde *et al* [318] with a slight modification on the amount of starting tissue samples. Briefly, 0.3 g of freeze-dried sponge sample was transferred to a 35 mL glass tube (Kimax) and dissolved in 10 mL methanol/ethyl acetate (1:1). The tube was incubated at room temperature (20°C) and shaken at 150 rpm for 20 min, followed by 10 min of centrifugation at 1400 rpm. Crude extracts were transferred into pre-weighed glass tubes and evaporated till they were completely dried with a speed-vac (Eppendorf Vacufuge Concentrator, Hamburg, Germany). Extraction of each sponge sample was conducted three times, and obtained crude extracts from each of the extractions were pooled in the same pre-weighed glass tube and stored at -20°C until further use.

Six microbes were used as indicator strains to evaluate antimicrobial activity of sponge extracts, namely the Gram positive bacteria *Bacillus subtilis* DSM 402 and *Staphylococcus simulans* DSM 20037, Gram negative bacteria *Escherichia coli* K12MG1655 and *Aeromonas salmonicida* DSM 19634, the yeast *Candida oleophila* DSM 70763, and the oomycete *Saprolegnia parasitica* CBS223.65. Briefly, bacterial strains and the yeast strain were grown in liquid Lysogeny Broth medium (LB, Oxoid) for *E. coli*, Nutrient broth (Oxoid) for *A. salmonicida* and *B. subtilis*, Trypticase Soy Yeast Extract for *S. simulans* (DSMZ medium no. 92) and Universal Medium for Yeast (DSMZ medium no. 186) for *C. oleophila* until an optical density of 0.5 was reached, measured at 660 nm. Subsequently, 200 μ L of each active culture was spread with a sterile hockey stick on agar media with the same composition as the corresponding liquid media. *S. parasitica* was prepared by inoculating agar plugs of 1x1 cm from a lawn of fresh *S. parasitica* culture plate on one-fifth strength of Potato Dextrose Agar (PDA, Oxoid) plates supplemented with 1% of Bacto agar (Oxoid).

Antimicrobial properties of each crude extract were examined using the disc diffusion assay [318] by adding 20 μ L extract (0.5 mg / disc) to three 6 mm cellulose paper discs (Whatman). Paper discs containing the crude extract were air-dried for 30 min. As negative control, triplicate discs containing 20 μ l methanol/ethyl acetate (1:1) were included. Paper discs containing sponge crude extracts were tested against indicator strains on agar plates. Plates containing sponge extracts and indicator strains were incubated at 37°C for *E. coli* and *S. simulans*, at 30°C for *A. salmonicida*, *B. subtilis* and at 20°C for *C. oleophila* for 48 h. The plates containing extracts and *S. parasitica* were incubated at 20°C for 96 h. After incubation, the radius of the zone of inhibition (ZOI) surrounding each disc was measured to the nearest mm using a digital calliper (Perel, Gavere, Belgium), and the average ZOI radius for each extract was calculated from triplicate discs. In addition, to differentiate the level of inhibition from each crude extract, the recorded ZOI radius was grouped into three categories: weak (0 – 5 mm), moderate (5 – 10 mm) and strong (> 10 mm). Analysis of variance (ANOVA) was done to compare average ZOIs formed by sponge crude extracts against indicator strains. Subsequently Tukey Post-Hoc test was applied to assess significance in ANOVA.

Data availability

Illumina MiSeq raw sequence data can be accessed via the NCBI Sequence Read Archive (SRA) ID: SRP142603 with accession numbers SRX3998987 – SRX3998883. The COI gene sequences can be accessed at GenBank under the accession numbers: MH285785 – MH285814. The Biom table containing OTU abundance (number of reads) combined with the NG-Tax classification for each individual OTU can be accessed at the FigShare online repository <https://figshare.com/s/3e3864567ca36749c38f>). In addition, metadata of individual samples is available at the FigShare online repository (<https://figshare.com/s/01aa248292580571a360>) and the phylogenetic tree of OTUs is available in the Newick tree format at the FigShare online repository (<https://figshare.com/s/5c73b425ac3b7af9261e>). R Scripts are provided as a pdf file and can be accessed via <https://figshare.com/s/f930079547dbddbed5b4>.

Results

Molecular sponge taxonomy

Genetic analysis of the COI gene sequences obtained from all sponge samples used for this study showed that all COI sequences of suspected *X. muta* samples could be assigned to the same species (Supplementary Figure 1A). On the other hand, four out of five of the suspected deep *A. sventres* samples formed a separate clade from the other *A. sventres* samples and *A. sventres* reference COI gene sequences. These four deep samples may therefore represent a new *Agelas* species or another known *Agelas* species for which no COI gene sequence is available (Supplementary Figure 1B). Hence, all deep *Agelas* samples were excluded from further analysis as taxonomy could not be unequivocally established.

The impact of depth on sponge-associated microbial communities

Across 34 samples (25 sponge and 9 seawater samples), 2,277,222 high quality reads were clustered into 4,394 Operational Taxonomic Units (OTUs) (Table 1, Supplementary Table 1). *X. muta* samples yielded the highest number of observed OTUs on average, followed by seawater and *A. sventres* samples. In total 23 phyla (20 bacterial and 3 archaeal phyla) were identified, and the prokaryotic community patterns of the sponges *X. muta* and *A. sventres* were more similar to each other, than to those of seawater samples (Figure 1). Some phyla were consistently found in all *A. sventres* and *X. muta* samples: Acidobacteria, Actinobacteria, Chloroflexi, Gemmatimonadetes, Nitrospirae, Proteobacteria (Alpha-, Gamma- and Delta-), Spirochaetae, SBR1093 and Thaumarchaeota. Bacteroidetes, Cyanobacteria and Tectomicrobia were present in *X. muta* samples, but absent in *A. sventres* samples. Euryarchaeota, and Marinimicrobia were only observed in seawater samples.

At OTU level the two sponge species had different prokaryotic communities that also differed from the community in the surrounding seawater (Figure 2). Of the 100 most abundant OTUs, only five OTUs were shared between *X. muta* and *A. sventres*: OTU254 (*Albidovulum*, Deltaproteobacteria), OTU9 and OTU49 (uncultured Gammaproteobacteria), OTU147 (Sva0996, Actinobacteria) and OTU75 (uncultured bacterium, PAUC34f) (Figure 3). Furthermore, 20 (of the 100) OTUs were related to sponge-enriched clusters in the sponge EMP database (Figure 3). These belong to Actinobacteria (Sva0996), Acidobacteria (PAUC26f, Subgroup 9, TK85), Chloroflexi (TK10, S085, SAR202, Caldilineaceae), Cyanobacteria (SubsectionI), Nitrospirae (*Nitrospira*), Nitrospinae (MD2898-B26), Gemmatimonadetes

(PAUC43f) and Thaumarchaeota (*Candidatus Nitrosopumilus*). The sample type (*X. muta*, *A. sventres*, seawater) contributed to 74 % of the variance of the prokaryotic community composition (PERMANOVA, $p = 0.001$) (Table 2). Furthermore, prokaryotic data was distributed heterogeneously (betadisper, $p = 0.001$). Analysis using the factor depth contributed to only 10% of the variance found in prokaryotic community composition ($p = 0.1$).

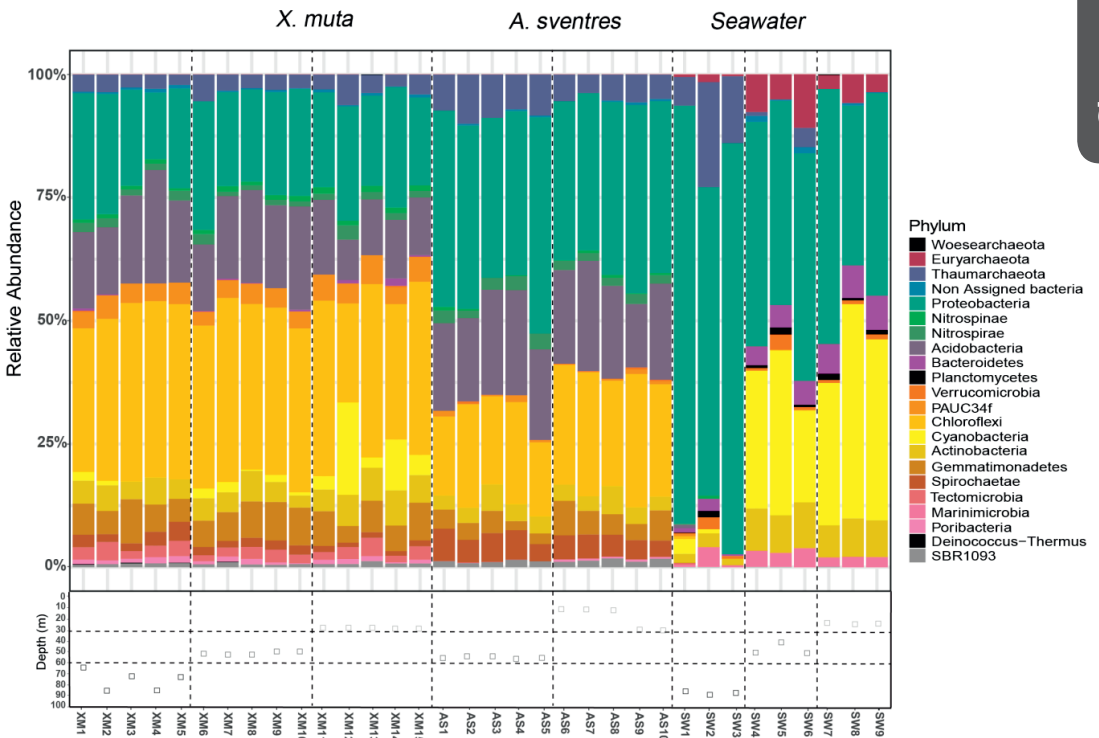
When the impact of depth on prokaryotic community composition was analysed per sponge species it contributed to 32% of the variation in prokaryotic community composition for *X. muta* ($p = 0.001$) and 18% of the variation in *A. sventres* ($p = 0.009$). Likewise, depth contributed to 66% ($p = 0.003$) of the differences in prokaryotic community composition in seawater samples (Figure 2, Table 2). Additionally, prokaryotic composition of deep *X. muta*, middle *A. sventres* and deep seawater were significantly different compared to prokaryotic composition of other depth categories within the same sample type ($p < 0.05$, Supplementary Table 3). Similar to beta diversity analyses, alpha diversity analyses also indicated that sample type significantly affected phylogenetic diversity (PD) (Kruskal-Wallis, $p = 0.003$), with *X. muta* being the sample type with the highest PD. Conversely, the impact of depth on alpha diversity was not significant (Supplementary Table 2 and Supplementary Figure 2)

Table 1. An overview of sample data with sample identifiers (ID), sponge species, average actual depth and depth category, average number of reads, average number of OTUs, and average phylogenetic diversity. All values are given with their corresponding standard deviation. A more detailed description of individual specimens is available in Supplementary Table 1.

Sample ID	Species	Average depth (m) and depth category	Average number of reads	Average number of OTUs	Average Phylogenetic Diversity
XM-XM5	<i>X. muta</i>	78.20±8.78 m (deep)	53,595± 51,996	174±18	17.54±1.11
XM6-XM10	<i>X. muta</i>	50.20±2.05 (middle)	54,253±61,518	179±10	18.28±0.24
XM11-XM15	<i>X. muta</i>	27±0 (shallow)	89,129±69,868	163±14	17.72±0.57
AS1-AS5	<i>A. sventres</i>	53±1 (middle)	63,389±30,710	70±6	11.94±0.86
AS6-AS10	<i>A. sventres</i>	18±8.21 (shallow)	74,756±52,091	70±6	12.38±0.53
SW1-SW3	Seawater	87±4.35 (deep)	93,275±35,371	102±50	12.74±2.78
SW4-SW6	Seawater	46.67±5.77 (middle)	48,825±17,635	148±14	15.36±0.43
SW7-SW9	Seawater	20.33±0.57 (shallow)	58,438±8,580	123±5	14.52±0.30

Table 2. Multivariate analysis of prokaryotic community data after Hellinger transformation based on parameter sample types (sponge and seawater), depth (sponge and seawater) and depth for subsets *X. muta*, *A. sventres* and seawater. Df, degrees of freedom

Parameter	OTUs	Df	PERMANOVA		Betadisper	
			R^2	p -value	F	p -value
Sample types (sponges and sea water)	4394	2	0.74	0.001	4.46	0.02
Depth (sponges and sea water)	4394	2	0.09	0.17	1.02	0.4
Depth (<i>X. muta</i> only)	2576	2	0.32	0.001	1.89	0.2
Depth (<i>A. sventres</i> only)	699	1	0.18	0.009	0.35	0.54
Depth (seawater only)	1119	2	0.66	0.003	7.19	0.006

**Figure 1.** Prokaryotic composition of sponge specimens and seawater samples at the phylum level based on relative abundance of assigned 16S rRNA gene OTUs. Phyla with average relative abundance lower than 0.25% in all samples (Woesearchaeota, Deinococcus-Thermus, Planctomycetes) were coloured in black. Sampling depth of each sponge specimen and seawater sample is indicated below each bar. Individual samples were labelled based on sample type: XM (*X.muta*), AS (*A. sventres*), SW (seawater), followed by sample number.

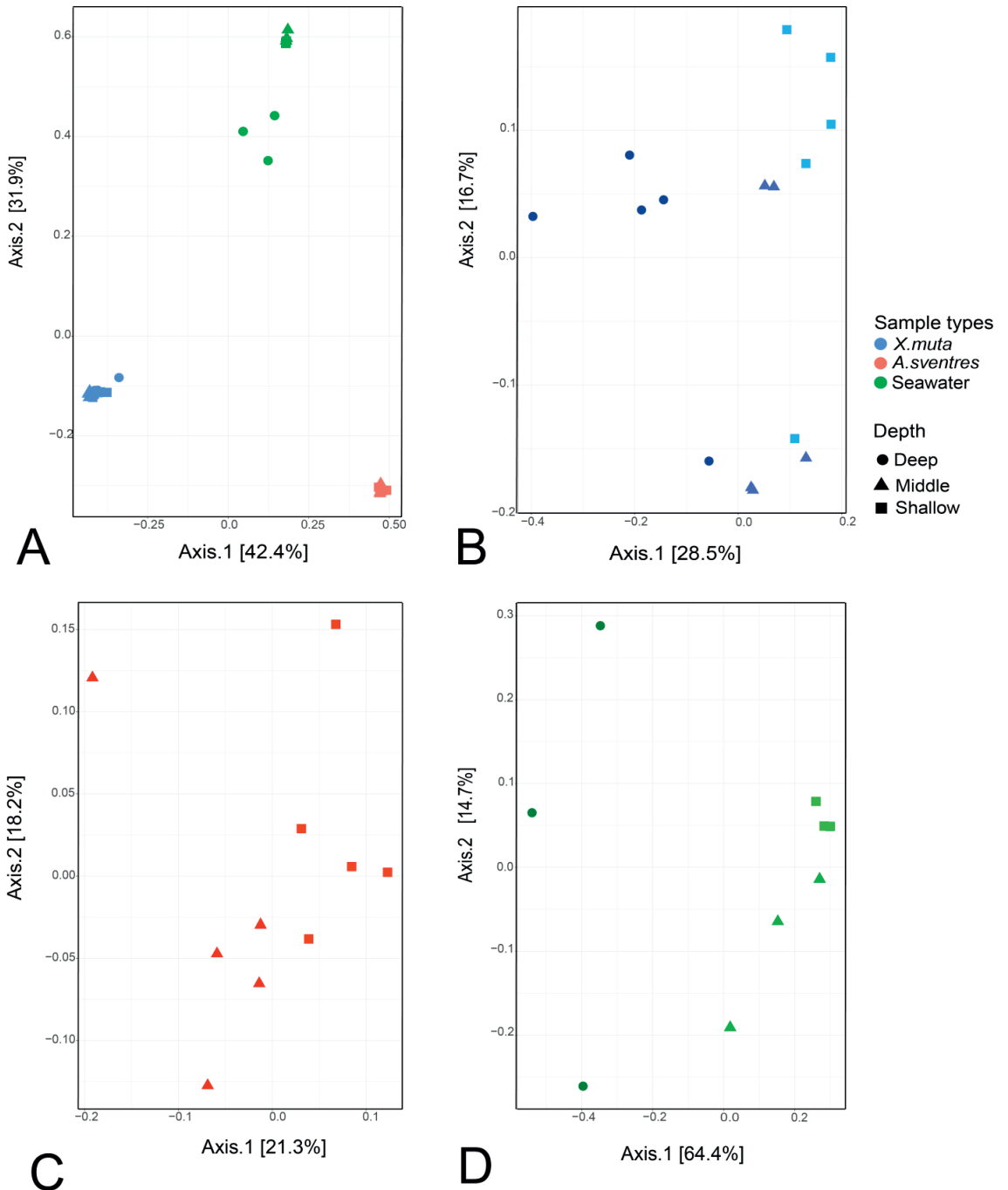


Figure 2. Principal Coordinate Analysis (PCoA) of prokaryotic community of (A) sponges and seawater samples using Bray-Curtis distance based on relative abundance of OTUs after Hellinger transformation. Additionally, the PCoA was done separately for each sample type: (B) *X. muta*, (C) *A. sventres* and (D) seawater.

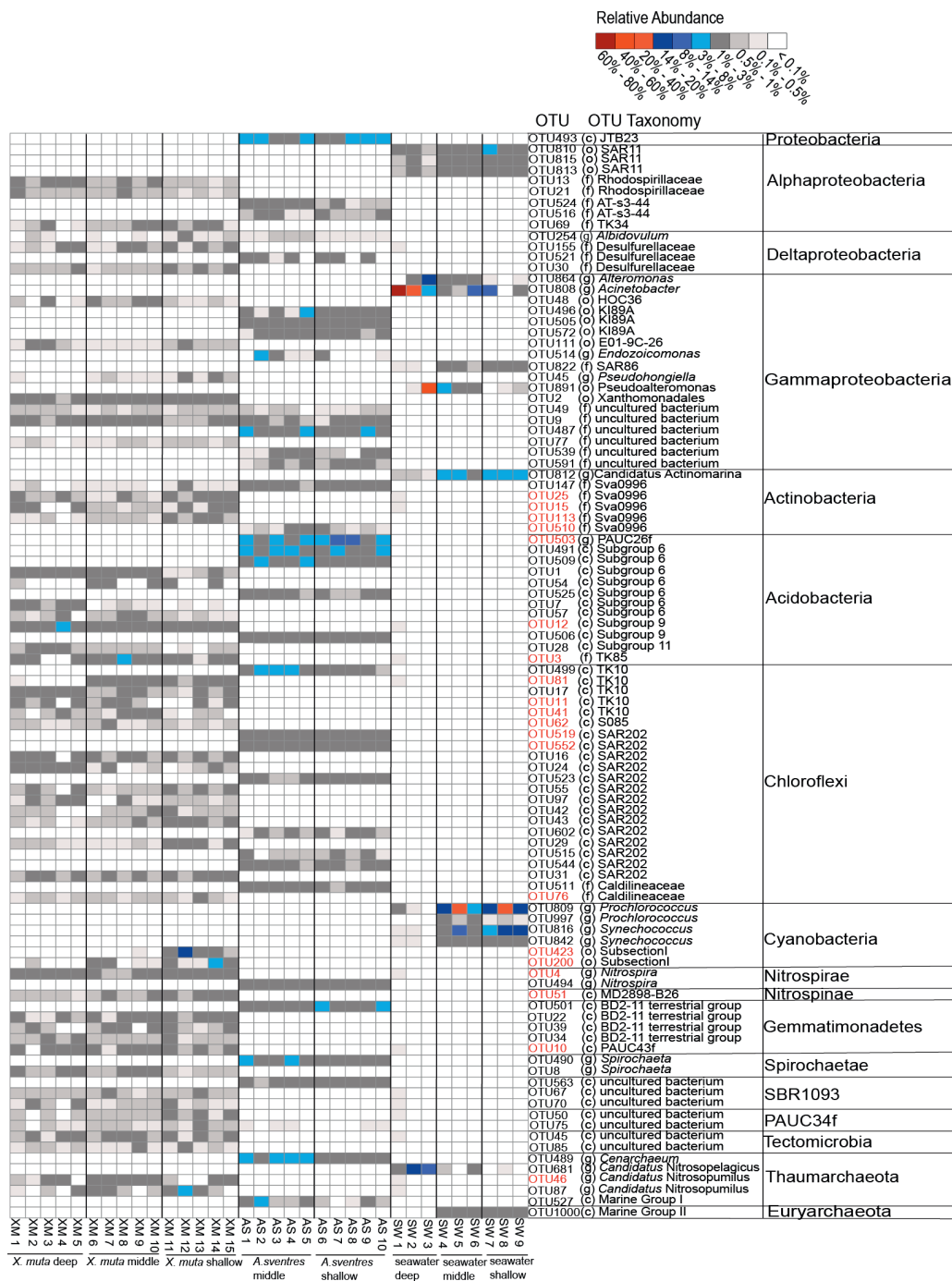


Figure 3. Heatmap of OTUs with average relative abundance $\geq 0.25\%$ among all samples. OTUs were grouped at phylum level. OTUs highlighted in red were identified as “sponge-enriched” in the sponge EMP database. The letter in parentheses for OTU taxonomy indicates the lowest taxonomic rank that was obtained: c (class), o (order), f (family), g (genus).

The impact of depth was evident as indicated by differences in relative abundance in a number of predominant OTUs between the different depth zones. In shallow *X. muta*, the relative abundance of OTU200 and OTU423 both belonging to Cyanobacteria Subsection I was significantly higher than in deeper samples where OTU423 was completely absent (Supplementary Table 4). Additionally, a significant decrease of relative abundance from shallow to the deeper *X. muta* individuals was observed for OTU87 (Thaumarchaeota, *Candidatus* Nitrosopumilus), OTU113 (Actinobacteria, Sva0996 marine group), OTU29 (Chloroflexi, SAR202) and OTU81 (Chloroflexi, TK10) (Supplementary Table 4). Conversely, acidobacterial OTU7 (subgroup 6) and OTU28 (subgroup 11) had a significantly higher relative abundance in deep *X. muta* samples compared to their middle and shallow counterparts.

In *A. sventres*, four OTUs had a significantly higher relative abundance in shallow specimens than in the middle depth specimens: OTU503 (Acidobacteria, PAUC26f), OTU552, OTU602 (Chloroflexi, SAR202) and OTU591 (Gammaproteobacteria). In contrast, OTU514 (Proteobacteria, *Endozoicomonas*) and OTU527 (Thaumarchaeota, Marine group I) displayed a significantly higher relative abundance in middle depth *A. sventres* specimens compared to their shallow counterparts (Supplementary Table 4).

For the seawater OTUs assigned to Cyanobacteria, members of the genera *Prochlorococcus* (OTU809 and OTU997) and *Synechococcus* (OTU 816 and OTU 842) were present at significantly higher relative abundance in shallow and middle samples than in the deep seawater samples (Supplementary Table 4). These cyanobacterial OTUs in seawater were different ones than those observed in *X. muta*. The same trend was observed for OTU812 (Actinobacteria, *Candidatus* Actinomarina). On the other hand, a significantly increased relative abundance in deep seawater samples was seen for OTU681 (Thaumarchaeota, *Candidatus* Nitrosopelagicus) and OTU808 (Gammaproteobacteria, *Acinetobacter*) as compared to middle and shallow seawater samples.

Antimicrobial activity of sponge tissue samples

All 15 *X. muta* and 10 *A. sventres* tissue samples were screened for antimicrobial activity against six different indicator strains (Figure 4). For *X. muta*, recorded antibacterial activity came mainly from four shallow specimens of which XM14 was the only crude extract that weakly inhibited three of the four bacterial strains: *Bacillus subtilis*, *Staphylococcus simulans*, and *Aeromonas salmonicida* (Supplementary Table 5). Crude extracts from shallow specimens XM11, XM13 and XM15 produced small ZOI radii against *E. coli*. The only non-shallow *X.*

muta specimen with antibacterial activity was XM7 (middle) that was found active against *S. simulans*, whereas none of the deep *X. muta* specimens showed antibacterial activity. On the other hand, inhibition of *Saprolegnia parasitica* was most prominent for the deep *X. muta* specimens with two extracts with an intermediate ZOI radius (XM2 and XM4), whereas a large ZOI radius was displayed by XM3 and XM5 extracts. In addition, two shallow crude extracts of *X. muta* (XM11 and XM12) displayed a strong inhibition against *S. parasitica*. All *X. muta* extracts were inactive against the yeast *C. oleophila*. Overall, statistical analysis (Supplementary Table 5) showed that the impact of depth was significant when the average ZOI radii of shallow *X. muta* extracts against *E. coli* were compared with those produced by the middle and deep crude extracts (Tukey post hoc test, $p = 0.03$, Supplementary Table 5). Additionally, the average ZOI radius of deep *X. muta* extracts against *S. parasitica* was larger compared to that of the middle crude extracts (Tukey post hoc test, $p = 0.04$). For the remaining antimicrobial activities, sampling depth had no significant impact (anova, $p > 0.05$).

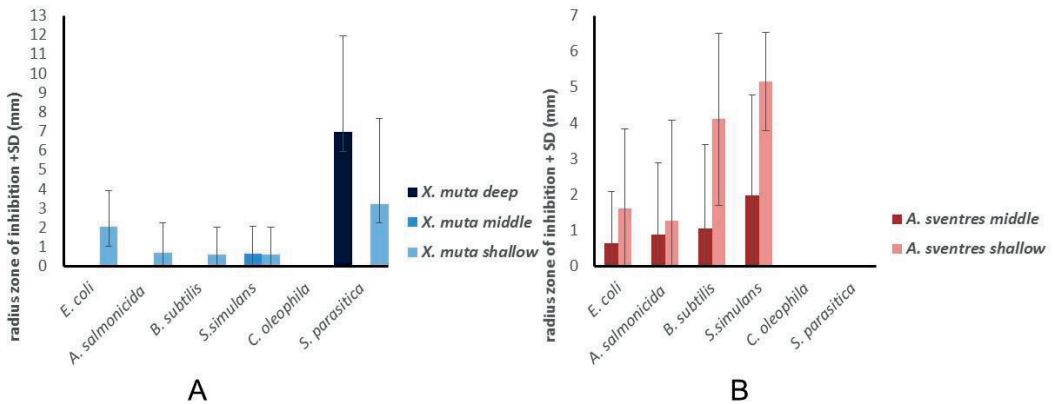


Figure 4. Average radius of the zone of inhibition and standard deviation of *X. muta* (A) and *A. sventres* (B) crude extracts against indicator strains.

For *A. sventres*, all crude extracts from shallow specimens were active against *S. simulans*, with weak activities shown for AS7 and AS8 and moderate inhibition for AS6, AS9, and AS10 (Supplementary Table 5). From the crude extracts from specimens from the middle depth zone, only AS4 (weak) and AS5 (moderate) were active against *S. simulans*. For inhibition of the other bacteria, always the same trend was observed, in that extracts from shallow *A. sventres* individuals were more active than extracts from the middle *A. sventres* individuals (Figure 4b), but differences between depth categories were never significant (Supplementary Table 5). No

inhibition of the yeast *C. albicans* or the oomycete *S. parasitica* by *A. sventres* crude extracts was observed.

Antibiotics and secondary metabolite synthesis pathway prediction

The potential functional roles of sponge-associated prokaryotic populations were investigated using Piphillin, which is an algorithm that applies nearest-neighbor matching between 16S rRNA amplicons and genomes to predict the represented genomes [299]. The proportion of OTUs from our query sequence data that matched with the KEGG database at 97% cut-off sequence similarity was only 3.5%. This low percentage is mainly caused by the fact that Piphillin is not optimized to predict genomes from environmental samples [299].

Based on prokaryotic diversity profiles, nine putative pathways related to biosynthesis of secondary metabolites were predicted to be present in both *X. muta* and *A. sventres*. These predicted pathways were: i) ansamycin, ii) butirosin and neomycin, iii) indole alkaloid, iv) novobiocin, v) tropane piperidine and pyridine alkaloid, vi) streptomycin, vii) penicillin and cephalosporin, viii) siderophore group non-ribosomal peptides, and ix) vancomycin group antibiotics ($p < 0.05$, Supplementary Figure 3). In *X. muta*, four putative biosynthesis pathways had an average relative abundance above 0.1%: streptomycin (0.5%), novobiocin (0.3%), tropane piperidine and pyridine alkaloid (0.25%), and ansamycine (0.15%). The other five predicted pathways showed average relative abundances in the range of 0.01 – 0.1%.

For *A. sventres*, three predicted biosynthesis pathways yielded average relative abundances above 0.1%, namely streptomycin (0.6%), novobiocin (0.24%), tropane piperidine and pyridine alkaloid (0.18%). Four predicted biosynthesis pathways with relative abundances in the range of 0.01 – 0.1% were butirosin and neomycin, indole alkaloid, vancomycin group antibiotics, and ansamycins. Siderophore group non-ribosomal peptides and penicillin and cephalosporin biosynthesis pathways were predicted to be present in minute quantities. Overall, relative abundances of these predicted pathways were slightly higher in *X. muta* samples than in *A. sventres* samples (Supplementary Figure 3). However, in both sponges the relative abundance of these putative biosynthesis pathways was generally low, and no correlation between the predicted metabolic pathways and depth was observed (Supplementary Figure 3).

Discussion

In this study, we analysed prokaryotic composition of two sponge species, *X. muta* and *A. sventres*, that are commonly found in the Curaçao Sea with a depth range from near surface shallow waters to the mesophotic zone. Sample type specific subset analyses showed that deep *X. muta* specimens harboured significantly different prokaryotic communities as compared to middle and shallow *X. muta* specimens, and middle *A. sventres* harboured different communities than shallow *A. sventres*. In addition, prokaryotic communities in deep seawater samples were significantly different from those in shallower seawater samples. Seawater temperature, light intensity and nutrient availability are connected with depth and could cause the change of prokaryotic community composition in marine habitats from shallow water to the mesophotic zone [66,319]. A recent depth-gradient study of *X. muta* prokaryotic communities covering a shallow depth range (9 – 28 m) and two seasons (autumn and spring) underlined differences in prokaryotic composition across different depths at this smaller scale in autumn, but such differences were absent in spring. The observed changes of prokaryotic composition across different depths in autumn are likely triggered by differences in temperature, light, nutrient, and turbidity between seasons [100]. In our study, the recorded average temperature at shallow (27°C) and deep (23°C) areas during sampling in October – November was similar to the temperatures along a depth gradient coral-endosymbiont study that was conducted during the given months at the same area [284]. While temperature could be a factor that influences prokaryotic composition in marine habitats [319], temperature differences within this range are not likely to lead to different prokaryotic assemblages within sponges as shown in other studies [320,321]. Thus, other environmental factors, such as light intensity or nutrient availability may affect prokaryotic communities in sponges as from other studies it is known that there is a strong reduction of light intensity and nutrients for the depth range covered in our study [80,286,322].

At OTU level declining relative abundance of Cyanobacteria was evident as depth increased for *X. muta* and seawater. The two dominant OTUs found in seawater were assigned to the genera *Prochlorococcus* and *Synechococcus* that are among the abundant Cyanobacteria in many shallow ocean regions and that decrease drastically in abundance in deeper areas due to the decrease of light intensity [323,324]. The dominant cyanobacterial OTUs (OTU200 and 423) found in *X. muta* were different from the ones in seawater and could only be identified at class level (SubsectionI), but showed the same decline in relative abundance with depth as the

cyanobacteria in seawater. In addition, these two cyanobacterial OTUs found in *X. muta* were affiliated with sponge-enriched clusters and likely contribute to carbon fixation in sponges. Seminal shading experiments of other marine sponges have shown that reduced exposure to light significantly reduced the proportion of chlorophyll a and b in cyanobacterial symbionts, which consequently reduced the biomass of sponges, reinforcing the importance of these photosynthetic symbionts for nutrient acquisition to their hosts [55,325-327]. Furthermore, this result is in line with findings reported from a prokaryotic community study of *X. muta* across different depths (10 – 90 m) conducted at Little Cayman, where relative abundance of Cyanobacteria declined in deeper regions as light intensity and inorganic nutrient level (N and C) decreased [80]. Conversely, such a trend was not observed from the study in the Lee Stocking Island despite a similar decrease of light irradiance within the same depth range for the two sites. However, given that the inorganic nutrient level steadily increased with depth at Lee Stocking Island, it is suggested that cyanobacterial symbionts in *X. muta* shift to heterotrophy for compensating the decline in irradiance [80].

In the same way as Cyanobacteria, OTUs from Chloroflexi, Acidobacteria, Actinobacteria, Thaumarchaeota and Proteobacteria contributed significantly to differences between prokaryotic assemblages across different depths in both sponges. Marine sponges are considered as hot spots for Chloroflexi, which are especially prevalent in HMA sponges [328,329]. Among the most abundant Chloroflexi OTUs identified in both sponges, OTU81 (SAR202) and OTU552 (TK10) in *X. muta* and *A. sventres*, respectively, were identified as members of sponge-enriched clusters, and their relative abundances declined with depth. Although ecological functions of Chloroflexi in sponges remain unclear, in shallow habitats they may be phototrophic given that members of this phylum possess Reaction Centre II to capture and utilize sunlight for energy [330,331]. In *X. muta*, relative abundance of the two most abundant acidobacterial OTUs, OTU7 (Subgroup 6) and OTU28 (Subgroup 11), increased in deep specimens, however, these OTUs do not belong to sponge-enriched clusters. In contrast, in *A. sventres*, acidobacterial OTU503 (PAUC26f) was found to be associated with a sponge-enriched cluster, and increasing relative abundance was observed in middle specimens. Acidobacteria are among the prevalent bacterial taxa in marine sponges and often regarded for their versatile metabolic capacity such as degradation of pollutants [332,333]. Although it is unclear whether an increasing trend is evident in deep *A. sventres* specimens due to lack of samples, it is plausible that the abundance of Acidobacteria following the increase

of depth might be related to degradation of recalcitrant organic substrates which often accumulate in deep water habitats [334].

Actinobacteria (Sva0996) were represented by members of sponge-enriched clusters in both sponges, with higher relative abundance being observed in shallow specimens of *X. muta* (OTU113). A specific role of Sva0996 in marine sponges is unknown, however, previous studies suggested this taxon to be present at high nitrate concentrations and in high primary productivity areas [335-337]. The archaeal phylum of Thaumarchaeota is mainly linked to ammonia oxidation in marine sponges and has been reported as dominant phylum in sponges both from shallow and deep water [308,338,339]. A contradictory trend was observed for the most dominant thaumarchaeotal OTUs in each sample type, with OTU87 (*Candidatus Nitrosopumilus*) being most abundant in *X. muta* in shallow specimens, whereas the relative abundance of OTU527 (Marine group I) in *A. sventres* and OTU681 (*Candidatus Nitrosopelagicus*) in seawater was most prominent in middle and deep samples, respectively. Despite the fact that these dominant thaumarchaeotal OTUs do not belong to sponge-enriched clusters, the observed trend in relative abundance suggests that different members of this phylum specialized to adapt to distinctive ammonia concentrations and related physical factors (temperature, light intensity, and dissolved oxygen) along depth gradients such as those investigated in this study [340]. Lastly, the most abundant gammaproteobacterial OTUs that changed with depth in *A. sventres*, OTU591 (non assigned) and OTU514 (*Endozoicomonas*), do not affiliate with any sponge-enriched cluster. While genus level information of OTU591 is unavailable, some possible roles assigned to members of the genus *Endozoicomonas* in sponges include antibiotic production, nitrate reduction and production of bromopyrrole as a feeding deterrent compound [341].

Sponges, as many other marine fauna in reef habitats, need to defend themselves against fouling and predatory organisms or pathogenic bacteria [292,318]. Therefore, sponges biosynthesize various antimicrobial and deterrent compounds [342]. *Agelas* species are among chemically well-defended sponges by producing a group of brominated-pyrrole-containing alkaloids and are unpalatable for a typical spongivorous fish such as *Thalassoma bifasciatum* [343,344]. *X. muta* is also dominated by brominated compounds, with a stable pattern over a narrow depth range (9 – 24 m) in spring, whereas separate clustering of metabolite profiles was evident between shallow and deep *X. muta* specimens in autumn [100]. Additionally, feeding frequency of *X. muta* by parrot fishes, including *Sparisoma aurofrenarum*, *Scarus croicensis* and *Scarus laeniopterus*, was evidently increased in bleached individuals, and the reduced level

of cyanobacterial symbionts has been suggested to be responsible for decreasing chemical defence in these bleached *X. muta* individuals [345]. In this study, we observed a general trend that antimicrobial activity against the four bacterial indicator strains was higher for shallow sponge extracts than for specimens collected at middle and deep habitats, but this difference was generally not significant due to large intraspecific variation between biological replicates. In addition, extracts of *A. sventres* specimens showed generally more diverse and stronger antibacterial activities than *X. muta* extracts.

Different types of natural products have been described from *X. muta* including antifungals [99,346]. *Saprolegnia* spp. are fungal-like eukaryotic microorganisms that are parasitic to fish and fish eggs and are resistant to a wide range of antifungals, making infections with *Saprolegnia* a serious threat in the aquaculture industries [347,348]. Malachite green is the chemical most used to prevent *Saprolegnia* infections, but since the compound is toxic, also to other organisms it has been banned world-wide [349,350]. Therefore, development of novel anti-*Saprolegnia* drugs is urgent [347,351]. Moderate to strong inhibition of *S. parasitica* was observed solely from *X. muta* crude extracts (and not *A. sventres*), and only from deep (4/5) and shallow (2/5) specimens, whereas no activity was observed with extracts from middle specimens. As such, no clear trend could be observed, but the trend of decreasing antimicrobial activity with depth appears not to be true for anti-*Saprolegnia* activity. Recently, Takahashi and co-workers highlighted a potential anti-saprolegniasis compound from the fungus *Penicillium coralligerum* isolated from a deep-sea sea cucumber [352], which underlines the potential of deeper waters to discover novel bioactive compounds.

Nine putative metabolic pathways related to biosynthesis of antibiotics and secondary metabolites were predicted based on the 16S rRNA gene amplicon data from both *A. sventres* and *X. muta* using the Piphillin prediction tool [299]. Piphillin was selected over other similar tools because the software does not require a particular data pre-processing protocol and does not depend on a specific functional database compared to other prediction tools such as PICRUSt [353] and Tax4fun [354]. Ansamycins belong to a polyketide family with potent antibiotics, such as rifamycin and geldanamycin [355]. Many polyketide compounds have been reported from sponges, and likely most of them are of microbial origin as highlighted in previous studies [356-358]. Butirosin and neomycin are related to aminoglycoside antibiotics [359], and four pathways were related to novobiocin, penicillin and cephalosporin, streptomycin and vancomycin pathways, which are commonly prescribed antibiotics. The pathway related to indole alkaloids is linked to various indole-derived compounds such as

aaptamine, carbazole and piperidine, all of which have been reported to have antibacterial activities [360]. Compounds synthesized via tropane, piperidine and pyridine alkaloid pathways have been shown to have antiprotozoal activities against *Trypanosoma brucei* [361]. It is important to note that the current predictions most likely do not fully reflect the actual pathways, given that the Piphillin database lacks near neighbor reference genomes and are mostly based on reference genomes from human microbiomes [299]. However, the predicted presence of these secondary metabolic pathways in prokaryotic communities of *X. muta* and *A. sventres* supports the hypothesis that some compounds associated with these sponges are likely of microbial origin, and metagenomic analyses should confirm the presence of these biosynthetic gene clusters in these sponge species.

Conclusion

We investigated the impact of depth on prokaryotic community composition and antimicrobial activity associated with the tropical sponges *X. muta* and *A. sventres* from shallow water to mesophotic depth. For both species depth had a significant impact on the associated prokaryotes with respect to different relative abundances of specific OTUs assigned to Cyanobacteria, Chloroflexi, Acidobacteria, Actinobacteria, Proteobacteria and Thaumarchaeota. Although the actual environmental parameters that cause the shift in prokaryotic communities with increasing depth remain unclear, we speculate that light and nutrient availability may at least play a role. Additionally, crude extracts of shallow sponge specimens in general showed stronger and more diverse antibacterial activities compared to extracts from mesophotic depths, but these differences were not significant.

Acknowledgments

Anak Agung Gede Indraningrat received a PhD fellowship from the Indonesia Endowment Fund for Education (LPDP), grant number 20140812021557. The submersible dive was financed by the Substation Curaçao and field trip expenses and sample processing were supported by the Rufford Foundation under grant number 17660-1 and the People Programme (Marie Curie Actions) of the European Union's Seventh Framework Programme FP7 under REA grant agreement no. 607786 (BluePharmTrain). Furthermore, we thank Adriaan "Dutch" Schrier, Laureen Schenk and the submersible team and staff at the Substation Curaçao: Bruce Brandt, Barbara van Bebber, Tico Christiaan, Barry Brown, Manuel Jove and Joe Oliver for all facilities and help. We would also like to thank Mark. J.A. Vermeij from CARMABI for providing laboratory equipment and a supporting letter to transport sponge samples from

Curaçao to the Netherlands. We also would like to thank Irene de Bruijn and Joost M. Raaijmakers from NIOO KNAW for providing *Saprolegnia parasitica*.

Supplementary Information

Supplementary Table 1. Detailed overview of each sponge specimen and seawater sample arranged from deep to shallow, including information regarding 16S rRNA amplicon sequence data.

Core ID	Species	Actual Depth (m)	Depth Category	Number of Reads	Number of OTUs	Phylogenetic Diversity
XM1	<i>X.muta</i>	66	Deep	47230	200	19.15
XM2	<i>X.muta</i>	86	Deep	27517	165	17.28
XM3	<i>X.muta</i>	72	Deep	13666	180	18
XM4	<i>X.muta</i>	85	Deep	35555	153	16.16
XM5	<i>X.muta</i>	82	Deep	144005	170	17.11
XM6	<i>X.muta</i>	51	Middle	21932	166	18.25
XM7	<i>X.muta</i>	52	Middle	18902	186	18.63
XM8	<i>X.muta</i>	52	Middle	25927	171	18.11
XM9	<i>X.muta</i>	48	Middle	41288	188	18.02
XM10	<i>X.muta</i>	48	Middle	163216	182	18.38
XM11	<i>X.muta</i>	27	Shallow	40656	160	17.9
XM12	<i>X.muta</i>	27	Shallow	60677	146	16.93
XM13	<i>X.muta</i>	27	Shallow	136515	165	17.75
XM14	<i>X.muta</i>	27	Shallow	186619	185	18.51
XM15	<i>X.muta</i>	27	Shallow	21179	159	17.52
AS1	<i>A.sventres</i>	54	Middle	104359	64	10.88
AS2	<i>A.sventres</i>	52	Middle	53094	71	13.06
AS3	<i>A.sventres</i>	52	Middle	70372	64	11.47
AS4	<i>A.sventres</i>	54	Middle	69361	76	11.77
AS5	<i>A.sventres</i>	53	Middle	19759	74	12.54
AS6	<i>A.sventres</i>	12	Shallow	47923	68	12.06
AS7	<i>A.sventres</i>	12	Shallow	20605	63	11.69
AS8	<i>A.sventres</i>	12	Shallow	114551	67	12.34
AS9	<i>A.sventres</i>	27	Shallow	144184	75	13.03
AS10	<i>A.sventres</i>	27	Shallow	46515	77	12.76
SW1	seawater	84	Deep	111117	77	13.18
SW2	seawater	92	Deep	52537	160	15.28
SW3	seawater	85	Deep	116171	70	9.76
SW4	seawater	50	Middle	36066	137	14.9
SW5	seawater	40	Middle	68949	143	15.43
SW6	seawater	50	Middle	41461	164	15.76
SW7	seawater	20	Shallow	49916	125	14.48
SW8	seawater	21	Shallow	58323	117	14.25
SW9	seawater	20	Shallow	67075	126	14.85

Supplementary Table 2. Statistical analysis on phylogenetic diversity of sponge and seawater samples tested using Kruskal Wallis and Wilcoxon rank sum test based on parameters sample types and depth.

Category		<i>A. sventres</i>	Seawater
Sample types (sponges and sea water)	<i>X. muta</i>	0.003	0.003
	<i>A.sventres</i>	-	0.003
Depth (<i>X. muta</i>)		Middle	Shallow
	Deep	0.015	0.024
	Middle	-	0.174
Depth (<i>A. sventres</i>)		Shallow	
	Middle	0.007	
Depth (sea water)		Middle	Shallow
	Deep	0.3	0.3
	Middle	-	0.3

Supplementary Table 3. Pairwise comparison on sample types and subset of sample types based on depth categories.

A	Depth (sponge and seawater) pairs	F.Model	R2	p.value	p.adjusted sig
	Deep vs Middle	2.14		0.10	0.08
	Deep vs shallow	2.51		0.12	0.04
	Middle vs shallow	0.27		0.01	0.87
B	Sample type (sponge pairs)	F.Model	R2	p.value	p.adjusted sig
	<i>X.muta</i> vs <i>A.sventres</i>	66.00		0.74	0.00
	<i>X.muta</i> vs Seawater	32.89		0.60	0.00
	<i>A.sventres</i> vs Seawater	37.06		0.69	0.00
C	Depth (<i>X. muta</i>) pairs	F.Model	R2	p.value	p.adjusted sig
	Deep vs Middle	2.78		0.26	0.01
	Deep vs Shallow	3.75		0.32	0.01
	Middle vs Shallow	1.82		0.19	0.06
D	Depth (<i>A. sventres</i>)	F.Model	R2	p.value	p.adjusted sig
	Middle vs Shallow	1.786981	0.1825876	0.007	0.007
E	Depth (Seawater) pairs	F.Model	R2	p.value	p.adjusted sig
	Deep vs Middle	4.924592	0.5518003	0.1	0.001
	Deepvs Shallow	7.989329	0.66637	0.1	0.001
	Middle vs Shallow	2.980473	0.4269729	0.1	0.7

Supplementary Table 4. The most abundant OTUs in each sample type (*X. muta*, *A. sventres* and seawater) that change with depth (> 0.25% relative abundance). Means of relative abundances of OTUs in each depth category are highlighted in bold. Microbial taxonomy is provided based on NG-TAX output (SILVA database 128) from Phylum to the lowest level (if applicable). Fold difference indicate changes of abundance between different depths.

A. *A. sventres*

OTU	<i>A. sventres</i> middle		<i>A. sventres</i> shallow		Microbial Taxonomy	Fold differences (shallow/middle)
	FDR	P	mean	mean		
otu503	0.0005		3058.60	4445	Acidobacteria, PAUC26f	1.45
otu552	0.0005		975.80	2416.60	Chloroflexi, SAR202	2.48
otu602	0.0005		505.20	1231.40	Chloroflexi, SAR202	2.44
otu591	0.0005		537.00	1126.40	Proteobacteria,	2.10
otu514	0.02		1179.20	436.80	Gammaaproteobacteria	0.37
otu527	0.001		1322.8	559.6	Proteobacteria, <i>Endozoicomonas</i>	0.42
					Thaumarchaeota, Marine Group I	

B. *X. muta*

OTU	FDR	P	<i>X.muta</i> middle		<i>X.muta</i> deep		<i>X.muta</i> shallow		Taxonomy	Fold difference (shallow/middle)	Fold difference (shallow/deep)
			deep	middle	deep	middle	mean				
otu87	0.03		382.20	372.00	372.00	1831.60	Thaumarchaeota, Candidatus	4.92	4.79		
otu113	0.001		92.20	296.80	296.80	1081.60	Nitrosopumilus	3.64	11.73		
otu423	0.001		0.00	19.00	19.00	3299.20	Actinobacteria, Sva0996 marine group	173.64	NA		
otu200	0.002		50.00	324.00	324.00	2868.00	Cyanobacteria, SubsectionI	8.85	57.36		
otu29	0.001		280.40	139.20	139.20	737.00	Cyanobacteria, SubsectionI	5.29	2.63		
otu81	0.001		36.40	1438.00	1438.00	2331.80	Chloroflexi, TK10	1.62	64.06		
otu145	0.001		16.60	151.80	151.80	1322.60	Proteobacteria, Pseudohongiella	8.71	79.67		
otu7	0.004		1186.20	150.60	150.60	138.40	Acidobacteria, Subgroup 6	0.92	0.12		
otu28	0.002		600.40	385.20	385.20	302.00	Acidobacteria, Subgroup 11	0.78	0.50		

C. seawater

OTU	FDR	seawater		seawater	seawater	Taxonomy	Fold difference	
		deep mean	middle mean	shallow mean	(shallow/middle)		(shallow/deep)	
otu809	0.001	617.67	7299.00	11181.67		Cyanobacteria, Prochlorococcus	1.53	18.10
otu816	0.001	193.67	3156.33	7847.33		Cyanobacteria, Synechococcus Actinobacteria, Candidatus Actinomarina	2.49	40.52
otu812	0.001	553.67	2490.33	3401.00		Actinomarina	1.37	6.14
otu842	0.001	91.67	1008.67	961.00		Cyanobacteria, Synechococcus	0.95	10.48
otu997	0.001	0.00	925.33	355.67		Cyanobacteria, Prochlorococcus	0.38	N/A
otu808	0.001	34672.33	2481.33	2004.33		Proteobacteria, Acinetobacter Thaumarchaeota, Candidatus Nitrosopelagicus	0.81	0.06
otu681	0.002	7519.67	633.67	22.67			0.036	0.003

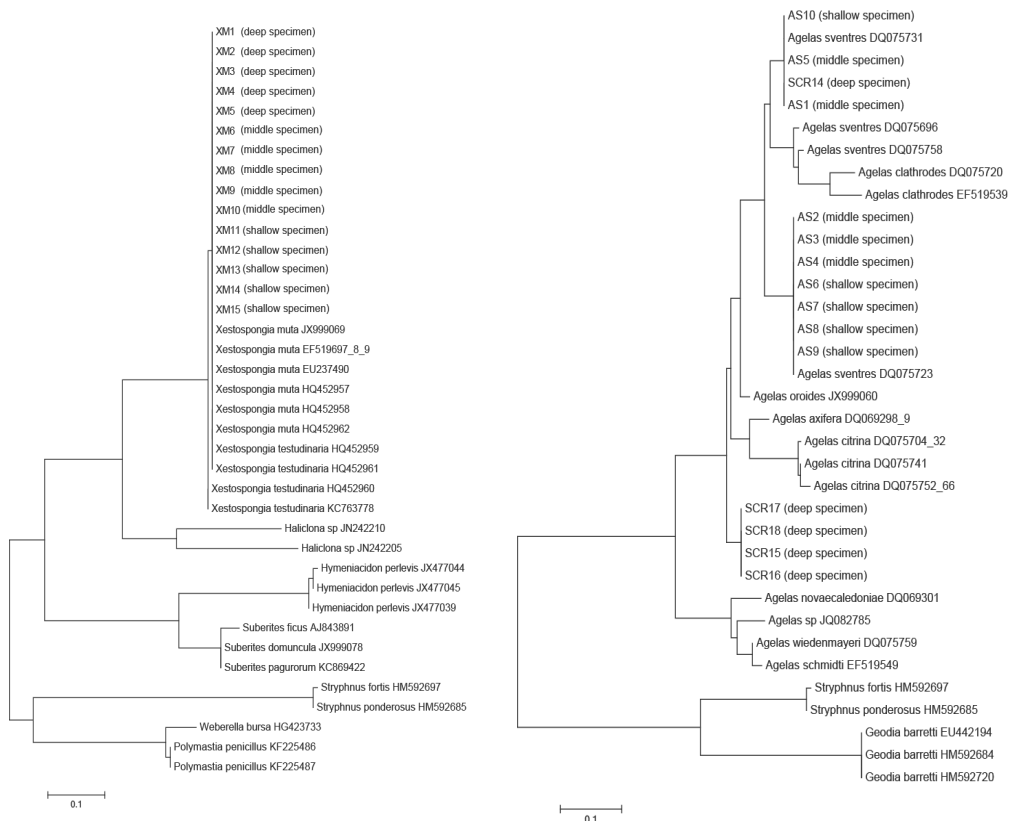
Supplementary Table 5. Statistical test on the radius of the radius zone of inhibition (mm) of sponge crude extracts against microbial indicator strains. Panel A: Comparison of ZOI radii of sponge extracts of *X. muta* from different depths. Panel B: Comparison of ZOI radii of sponge extracts of *A. sventres* from different depths. In both tables, recorded ZOIs for each crude extract are provided, along with average inhibition and standard deviation per depth category. Analysis of variance (anova) was applied with p-values <0.05 being indicative of significant differences (highlighted in bold). Subsequently, only values found significant were tested using the Tukey post hoc test to determine which pair-wise comparison of sponge crude extracts gave a statistically significant result (highlighted in bold). Non-significant anova results were not tested in Tukey post hoc test (N/A, not applicable). ZOI radii were grouped into three categories, namely weak (0 -5 mm), moderate (5-10 mm), strong (> 10 mm).

A. *X. muta*

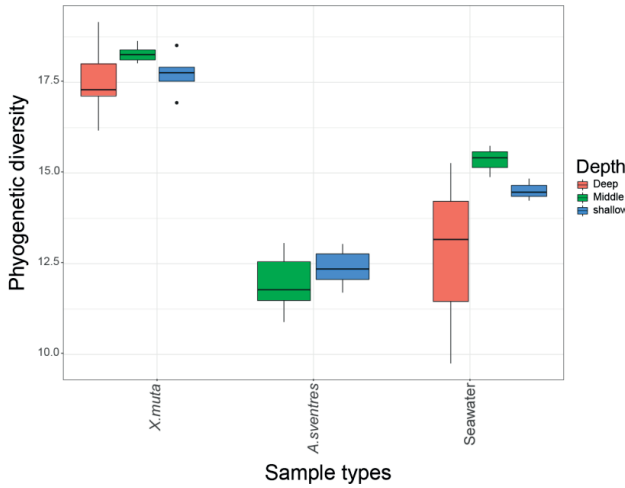
		radius zone of inhibition (mm)					
Sponge extracts		<i>E. coli</i>	<i>A. salmo- nicida</i>	<i>B. subtilis</i>	<i>S. simulans</i>	<i>C. oleo- phila</i>	<i>S. para- sitica</i>
	XM1	0	0	0	0	0	0
deep	XM2	0	0	0	0	0	5.55
deep	XM3	0	0	0	0	0	13.43
deep	XM4	0	0	0	0	0	6.51
deep	XM5	0	0	0	0	0	9.38
	mean inhibition and standard deviation	0±0	0±0	0±0	0±0	0±0	6.97±4.96
middle	XM6	0	0	0	0	0	0
middle	XM7	0	0	0	3.2	0	0
middle	XM8	0	0	0	0	0	0
middle	XM9	0	0	0	0	0	0
middle	XM10	0	0	0	0	0	0
	mean inhibition and standard deviation	0±0	0±0	0±0	0.64±1.43	0±0	0±0
shallow	XM11	3.72	0	0	0	0	8.14
shallow	XM12	0	0	0	0	0	8.09
shallow	XM13	3.27	0	0	0	0	0
shallow	XM14	0	3.47	3.14	3.1	0	0
shallow	XM15	3.28	0	0	0	0	0
	mean inhibition and standard deviation	2.05±1.88	0.69±1.55	0.63±1.40	0.62±1.39	0±0	3.25±4.44
	ANOVA (p-value)	0.02	0.40	0.40	0.60	0.04	N/A
Tukey	pvalue_deep_middle	1	N/A	N/A	N/A	0.04	N/A
Post hoc	pvalue_deep_shallow	0.03	N/A	N/A	N/A	0.3	N/A
test	pvalue_middle_shallow	0.03	N/A	N/A	N/A	0.4	N/A

B. *A. sventres*

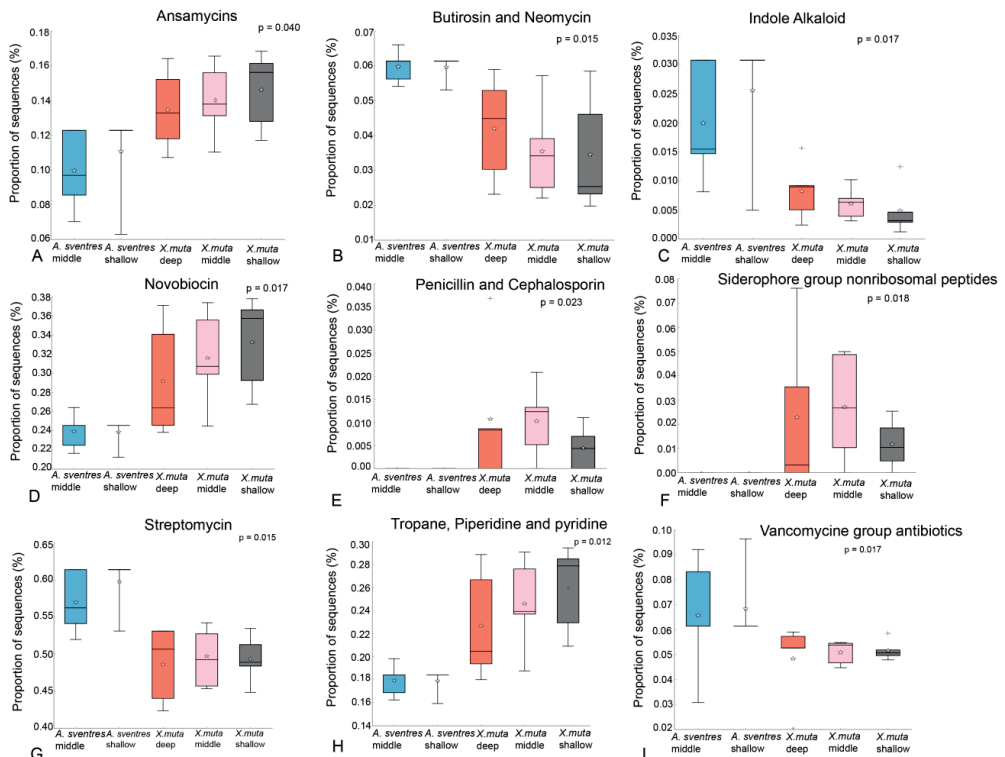
radius zone of inhibition (mm)							
Depths	Sponge extracts	<i>E. coli</i>	<i>A. salmonicida</i>	<i>B. subtilis</i>	<i>S. simulans</i>	<i>S. parasitica</i>	<i>C. oleophila</i>
middle	AS1	0	0	0	0	0	0
middle	AS2	0	0	0	0	0	0
middle	AS3	0	0	0	0	0	0
middle	AS4	0	0	0	4.07	0	0
middle	AS5	3.22	4.47	5.27	5.86	0	0
mean inhibition and standard deviation		0.64±1.44	0.89±2.00	1.05±2.36	1.99±2.79	0±0	0±0
shallow	AS6	4.15	0	5.59	6.86	0	0
shallow	AS7	0	0	0	3.15	0	0
shallow	AS8	0	0	4.01	4.68	0	0
shallow	AS9	3.96	6.32	5.93	5.5	0	0
shallow	AS10	0	0	5	5.63	0	0
mean inhibition and standard deviation		1.62±2.22	1.26±2.83	4.11±2.41	5.16±1.37	0±0	0±0
ANOVA (p-value)	pvalue_middle_shallow	0.4	0.8	0.08	0.05	N/A	N/A



Supplementary Figure 1. (A). Phylogenetic tree of *X. muta* specimens and (B) *A. sventres* specimens based on the COI gene. The number (0.01) below the reference bar indicates percentage distance of sequence.



Supplementary Figure 2. Phylogenetic diversity (PD) of prokaryotic communities in *X. muta*, *A. sventres* and seawater at different depths.



Supplementary Figure 3. Proportion of sequences predicted to be related to secondary metabolites pathways according to KEGG in *X. muta* and *A. sventres*. Stars denote mean and plus (+) symbol indicate outliers as identified by STAMP.



Chapter 4

Cultivation and antimicrobial screening of sponge-associated bacteria from the marine sponges *Agelas sventres* and *Xestospongia muta* collected from different depths

Anak Agung Gede Indraningrat, Sebastian Micheller, Mandy Runderkamp, Ina Sauerland, Leontine. E. Becking, Hauke Smidt and Detmer Sipkema

Manuscript in preparation

The background of the page features a stylized, light gray illustration of a coral reef. It includes various types of coral, such as branching corals and large, rounded sponges, set against a backdrop of soft, wavy lines representing the reef's topography. The overall aesthetic is clean and scientific.

Abstract

Prokaryotic communities constitute a significant fraction of sponges' tissues. Cultivation of sponge-associated bacteria from shallow water (≤ 30 m) are the focus of many studies, whereas limited information is available from their deeper counterparts. This study aimed to assess the cultivability of bacteria from two marine sponges *Xestospongia muta* and *Agelas sventres* collected from three depth ranges (< 30, 30-60, 60-90 m). Sponge-associated bacteria were cultivated on six different culture media, and replicate plates were used either to pick individual colonies or to scrape off the entire biomass. We applied Illumina MiSeq sequencing of 16S rRNA gene amplicons for prokaryotic community analysis of the original sponge samples as well as the biomass scraped from agar plates. In total 144 bacterial isolates were picked based on a colony morphology coding scheme. Subsequently, 16S rRNA gene sequence analysis of these isolates led to selection of 41 and 20 bacterial isolates from *X. muta* and *A. sventres*, respectively, for antimicrobial screening. Cell-free supernatants obtained from liquid cultures of these 61 isolates were screened against four bacterial indicator strains, a yeast and an oomycete. In this study we found that sponge individuals at each depth range harboured specific cultivable bacteria that were not retrieved from sponge individuals collected at other depth ranges. Furthermore, bacteria from the genera *Pseudovibrio*, *Ruegeria* and *Microbulbifer* were among the most abundant OTUs detected in the scraped prokaryotic communities. At the prokaryotic community level, the source of inoculum (sponge species) and the cultivation medium had more impact on the prokaryotic community recovered by cultivation than the depth from which the sample was collected. Although no clear pattern was observed regarding the influence of depth on the bioactivity of isolates, ten isolates from *X. muta* and eight isolates from *A. sventres* showed antibacterial activities against *Escherichia coli*, *Aeromonas salmonicida*, *Bacillus subtilis*, and *Staphylococcus simulans*.

Keywords: sponges, cultivation, depth, antimicrobial activity

Introduction

Bacteria constitute a major fraction of the prokaryotic community of most marine sponges, and many of these sponge-associated bacteria are of ecological and biotechnological importance [4,19]. One of the functional roles attributed to sponge-associated bacteria is their involvement in host-defence by producing biologically active compounds to protect their host from predation, fouling organisms and microbial infections [4,19]. The microbial origin of these compounds is based on the observation that some compounds produced by sponges share structural similarity with substances known to be produced by microorganisms [49,50]. A number of studies showed that indeed sponge-associated bacteria synthesized some compounds that were previously reported from sponges [58,362-364]. Many of these substances display remarkable biological activities, such as anticancer, anti-inflammatory, antitumor and antimicrobial activity that are of pharmaceutical interest, reinforcing the importance of sponge-associated bacteria as a treasure trove for drug discovery [30,132].

In recent years, the increasing pace at which microorganisms, including pathogens, develop antimicrobial resistance has fuelled the quest for novel drugs, including isolation of sponge-associated bacteria for their capacity to produce antimicrobial compounds [4,157,203,365,366]. Despite the fact that currently only a small percentage of sponge-associated bacteria is accessible through culturing, cultivation remains an important approach to assess physiological and biochemical properties of a strain to materialise its biotechnological properties [29,367]. To date, the cultivable sponge-associated bacteria are mainly members of the phyla Actinobacteria, Bacteroidetes, Firmicutes, Proteobacteria (Alpha- and Gamma-) and to a lesser extent also Deltaproteobacteria), Planctomycetes and Verrucomicrobia [29,32,365,368-370]. Of these phyla, members of the Actinobacteria are recognized as prominent producers of antimicrobial substances and account for almost 30% of the sponge bacteria-derived bioactive compounds [30,132]. In addition, antimicrobial activities also are frequently detected from cultivable Proteobacteria and Firmicutes, represented mainly by the genera *Pseudovibrio* and *Bacillus* [30].

The majority of studies on marine sponge prokaryotic community composition and bioprospecting for their antimicrobial potential was done with samples collected at shallow depth (< 30 m) [23,24,31,278], while data generated from sponges from greater depth (> 30 m) is sparse [79-81]. This discrepancy is mainly caused by technical constraints to obtain sponge samples from greater depth, as specialized equipment such as technical diving gear and

submersibles are required, which in most cases are expensive or even inaccessible [66,68,69]. The few studies that have reported on deeper sponge prokaryotic community composition using culture-independent studies showed that the composition changes when depth increases, which is mainly explained by environmental factors related to depth, such as light intensity and nutrient availability [79,80]. Additionally, unique microbial gene clusters encoding for the biosynthesis of secondary metabolites have been detected from deep-sea sponges [63]. This implies that the deeper sponges harbour an additional biotechnological potential beyond their shallow counterparts [61].

Xestospongia muta and *Agelas sventres* are conspicuous sponges in the Caribbean Sea and have a considerable depth span, ranging from 2 m to reach down to approximately 100 m [71,80,87]. These two species are characterized by dense and diverse bacterial communities and are classified as “High Microbial Abundance sponges” [79,80]. Both sponges are also rich in secondary metabolites with a remarkable array of biological activities including antimicrobial activity [91,371]. A previous cultivation study aiming to grow bacteria from *X. muta* from shallow water recovered bacterial isolates assigned to Actinobacteria, Bacteroidetes, Firmicutes and Proteobacteria [372]. Conversely, no bacterial cultivation study has been reported for *A. sventres*.

In this study we aimed to investigate the cultivability of sponge-associated bacteria of *X. muta* and *A. sventres* collected across a depth gradient to assess to what extent sponges from different depths yield different bacterial isolates. Different types of cultivation media were used to capture as much variation of cultivable bacteria from sponge inocula as possible. Furthermore, to be able to perform high-throughput identification of the isolates, we collected total colony material for each growth medium used and performed “community” 16S ribosomal RNA (rRNA) gene amplicon sequencing. In addition, antimicrobial activities of pure bacterial isolates were evaluated by testing growth inhibition of a panel of Gram positive bacteria (*Bacillus subtilis* and *Staphylococcus simulans*), Gram negative bacteria (*Escherichia coli* and *Aeromonas salmonicida*), a yeast (*Candida oleophila*) and an oomycete (*Saprolegnia parasitica*).

Material and Methods

Sample collection

Xestospongia muta and *Agelas sventres* samples were collected in front of Substation Curaçao (12°05'04.4"N 68°53'53.7"W) from 4-22 November 2015. For the described study, samples were grouped into three categories; shallow (0-30 m), middle (30-60 m) and deep (60-90 m). From each of the depth categories, three individual sponge specimens were collected for each of the two species (Supplementary Table 1). Shallow sponge specimens were collected via SCUBA diving, while middle and deep specimens were taken using a submersible vehicle, the “Curasub”. Upon arrival in the laboratory at Substation Curaçao, any visible debris was removed from the sponge specimens, and they were rinsed three times using artificial seawater (ASW, 33 g/L synthetic sea salt [Instant Ocean Reef Crystals, Aquarium Systems, Sarrebourg, France]) and were cut into pieces of ~0.1 cm³. Pieces of tissue from each specimen were preserved in a 15 mL tube containing 10 mL of RNAlater stabilization solution (Thermo Fisher Scientific, Waltham, Massachusetts, USA) and stored at -20°C. All sponge samples were identified by sequence analysis of the cytochrome oxidase I (COI) gene amplified by PCR from DNA extracted from these pieces (see below for details). The deep *A. sventres* samples were excluded from the dataset since they formed a different clade from the other *A. sventres* samples based on the COI sequence and may represent a different *Agelas* species. The remaining tissue pieces of each sponge specimen were homogenized with mortar and pestle, and two tissue volumes of sterile artificial seawater were added to obtain a homogeneous cell suspension. The suspensions were aliquoted into sterile cryo-tubes (Corning, New York, USA) by mixing 1 mL of cell suspension with 0.6 mL of 50% sterile glycerol in ASW before storage at -80°C.

Cultivation conditions

For each sponge specimen, material from the original glycerol stock was serially diluted to 10⁻³ in ASW. One hundred fifty microliters of dilutions 10⁻¹ to 10⁻³ were spread in duplicates onto different agar-based growth media. The following six media were used: (I) marine agar 1/10 (MA1/10) (1 L ddH₂O, 3.74 g marine broth 2216 (Difco, Detroit, USA), pH 7.6 ± 0.1) [33]; (II) M3 (1 L ddH₂O, 2 g peptone, 0.1 g asparagine, 4 g sodium propionate, 0.5 g K₂HPO₄, 0.1 g MgSO₄, 0.01 g FeSO₄, 5 g glycerol, 20 g NaCl, 0.05 g K₂Cr₂O₇ and 0.015 g nalidixic acid, pH: 7.0 ± 0.1) [373]; (III) OLIGO (1 L ASW, 0.5 g tryptone, 0.1 g sodium glycerol phosphate, 0.05 g yeast extract, pH: 7.6 ± 0.1) [374]; (IV) Gram Positive (GP) (1 L ddH₂O, 10 g tryptose, 5 g NaCl, 3 g beef extract, 2.5 mL (2-)phenylethanol, pH 7.3 ± 0.1) [375]; (V) Mucin (1 L ASW,

1.0 g Mucin, pH 7.5 ± 0.1) [376]; (VI) Crenarchaeota (1 L ASW, 0.124 g $\text{Na}_2\text{CO}_3 \cdot 2\text{H}_2\text{O}$, 0.053 g NH_4Cl , 1 mL tungsten-selenite solution, pH 7.0 ± 0.1) [32]. After autoclaving, media V and VI were supplemented with 1 mL trace metal solution [376], 1 mL phosphate solution [376] and 1 mL vitamin solution (BME vitamins, [diluted 10-fold]; Sigma). All media contained 15 g/L of Noble agar (Difco) to produce solid media. Petri dishes were sealed with parafilm and incubated in the dark at 30°C for 28 days. For each medium, three negative controls were included and inoculated with sterile artificial seawater. The colonies on all plates were counted every five days. Replicate plates were subsequently used to either pick individual colonies or to scrape off the entire biomass. Individual colonies were picked based on their colony morphology code (CMC) (Figure 1) [377]. The CMCs consisted of five-digit numbers that were derived from four main criteria and one sub-criterion: a) Form (1 = circular, 2 = irregular, 3 = filamentous, 4 = rhizoid), b) Surface (0 = no surface variation, 1 = veined, 2 = rough, 3 = dull, 4 = wrinkled, 5 = wet), c) Color (1 = opaque, 2 = cloudy, 3 = translucent, 4 = iridescent), d) Elevation (1 = flat, 2 = raised, 3 = umbonate, 4 = crateriform, 5 = convex, 6 = pulvinate). A sub-criterion was made for the surface criterion since bacterial colonies may combine different appearances. Therefore, two digit numbers were used to describe the cell surface either based on a single sub-criterion e.g. 02 = rough) or combination of sub-criteria (e.g. 15 = veined and wet).







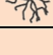



Colony morphology specifications				
Consecutive numbering	FORM	SURFACE	COLOR	ELEVATION
1		veined	opaque	
2		rough	cloudy	
3		dull	translucent	
4		wrinkled	iridescent	
5		wet		
6				
CMC	1	2 3	1	4
				12314

Figure 1. Colony morphology code (CMC, adapted from [377]) to categorise the morphology of picked bacterial colonies. For example a bacterial colony with CMC 12314 would be described as circular (form), rough and dull (surface), opaque (color) and crateriform (elevation).

Colonies (>1 mm in diameter) with different morphologies (CMCs) were isolated from agar plates dedicated for “picking” using sterile toothpicks. A picked colony was labelled based on

the medium, the order of picking on the agar plate, and the source of sponge inoculum. Subsequently, selected colonies were transferred to a fresh agar plate and subsequently grown in liquid culture (same media as their original cultivation media without Noble agar). Bacterial isolates were cryopreserved in sterile cryotubes (Corning) by mixing 0.6 mL of growing cultures at an $OD_{600} \geq 0.2$ with 0.4 mL of 50% sterile glycerol in ASW and stored at -80°C . From a second replicate plate, total biomass was harvested by adding 1.5 mL of sterile ASW to each agar plate and scraping off the biomass using an L-shaped spreader. Six hundred microliters of the obtained suspension of each dilution from the same inoculum and medium was pooled and equally mixed to be used as the starting material for DNA extraction.

DNA extraction

The FastDNA Spin kit for soil (MP biomedical, California, USA) DNA was used to extract total DNA from the sponge inocula as well as from scraped colony material according to the manufacturer's instructions with the slight modification of conducting 2 times 45 s bead beating (Precellys 24, Montigny-le-Bretonneux, France). Concentration and quality of extracted DNA was checked using a spectrophotometer (DeNovix DS-11, Wilmington, USA), and by electrophoresis on a 1% agarose gel.

Prokaryotic community profiling using 16S rRNA gene amplicon sequencing

The composition of sponge inocula and colony material was assessed by Illumina MiSeq amplicon sequencing of 16S rRNA gene fragments using a two-step amplification procedure [305]. PCR was conducted by using the primer pair 515FY (5'GTGYCAGCMGCCGCGGTAA 3') and 806RB (5'GGACTACNVTGGGTWTCTAAT 3') [306] where Unitag 1 and Unitag 2 were added to the forward and reverse primer (Supplementary Table 2), respectively, as previously described [307]. In the first step PCR, 25 μL PCR reactions contained 16.55 μL nuclease free water (Promega, Madison, USA), 5 μL of 5 \times HF buffer, 0.2 μL of 2 U/ μL Phusion hot start II high fidelity polymerase (Thermo Fisher Scientific AG), 0.75 μL of 10 μM stock solutions of each primer, 0.75 μL 10 mM dNTPs (Promega) and 1 μL template DNA (10–20 ng/ μL). Amplification was performed at 98°C for 3 min, followed by 25 cycles at 98°C for 25 s, 50°C for 20 s, 72°C for 20 s and a final extension of 7 min at 72°C . PCR products were visualized on a 1% (w/v) agarose gel. Subsequently, 5 μL of these first-step PCR products were used as template in the second PCR reaction to incorporate 8 nt sample specific barcodes as previously described [307]. The second step PCR was performed in triplicate for each sample in 50 μL PCR reactions which contained 31 μL nuclease free water (Promega), 10 μL of 5 \times HF

buffer, 0.5 μL of 2 U/ μL Phusion hot start II high fidelity polymerase (Thermo Fisher Scientific AG), 5 μL equimolar mixes of 10 μM forward primer (barcode-linker-Unitag1) and reverse primer (barcode-linker-Unitag2), 1 μL 10mM dNTPs (Promega) and 2.5 μL of the first PCR product. The PCR products were purified using the HighPrepTM PCR clean-up kit (Magbio, London, UK), and quantified using the Quant-iTdsDNA high-sensitivity assay kit (Invitrogen) and the Qubit fluorometer 2.0 (Invitrogen, Grand Island, NY, USA). Samples were pooled in equimolar concentrations to ensure equal representation of each sample [307]. The pooled library was purified, concentrated, and quantified again with the HighPrepTM PCR clean-up kit (Magbio) and the Quant-iTdsDNA high-sensitivity assay kit (Invitrogen). Finally, the library was sequenced at GATC Biotech AG (Germany) by Illumina MiSeq sequencing.

Sequence data processing

Raw DNA sequence data was analyzed using the NG-Tax pipeline (Galaxy version 1.0) [309]. NG-tax was used as previously described [308] with some modifications with respect to the final length of trimmed and concatenated sequences and the version of SILVA database used for taxonomic assignment. Briefly, paired-end libraries were combined, and only read pairs with matching primers and barcodes were retained. Forward and reverse reads were trimmed to 70 nucleotides to avoid overlap in forward and reverse reads. Paired-end trimmed forward and reverse reads were concatenated, and the resulting 140 bp were subsequently used for sequence data processing. Demultiplexing, assignment of Operational Taxonomic Units (OTUs), chimera removal, and taxonomic assignment were performed using default settings of the NG-tax pipeline (Galaxy version 1.0). Reads were ranked per sample by abundance and OTUs (at a 100% identity level) were added to an initial OTU table for that sample starting from the most abundant sequence until the relative abundance was lower than 0.1%. The final OTU table was created by clustering the reads that were initially discarded as they represented OTUs with relative abundances < 0.1% with the OTUs from the initial OTU table with allowing 1 nucleotide mismatch (98.5% similarity) [309]. Finally, taxonomic assignment was done by utilizing the SILVA 128 SSU database [310]. OTUs classified as Chloroplasts were removed from the analysis.

Prokaryotic diversity analyses

The bar plots of community composition at the phylum level were generated with Microsoft Excel 2016. Other prokaryotic diversity data analyses were performed in R (version 3.4.2) (<https://www.r-project.org>). Prokaryotic community beta diversity was visualized by principal

coordinate analysis (PCoA) based on relative abundance of OTUs after Hellinger transformation and generated using Bray–Curtis distance as implemented in the microbiome package (version 1.1.10013) [312]. To estimate the variance and dispersion of beta diversity of three experimental factors: “Sponge” (*X. muta*, *A. sventres*), “Depth” (deep, middle and shallow) and “Media type” (MA1/10, M3, OLIGO, GP, Mucin, Crenarchaeota), permutation ANOVA (PERMANOVA) was performed with 999 permutations using the *adonis* and *betadisper* functions, respectively, as implemented in the *vegan* package (version 2.5.2) [378]. Furthermore, a heatmap was generated in R using *pheatmap* (version 1.0.8) [316] for the overall most abundant OTUs ($\geq 0.25\%$ relative abundance, $n=32$) across the scraped communities.

Regrowth, identification and antimicrobial activity screening of picked isolates

Regrowth and identification of picked isolates

The glycerol stocks of picked colonies were re-grown in 5 mL of the liquid media that were used for their initial isolation. Regrown strains were identified by colony PCR. Briefly, cell lysis was conducted by centrifuging 2 mL of the liquid cultures at 14,000 g, and subsequently the obtained pellet was suspended in a sterile PCR tube with 50 μ L nuclease-free water (Promega). Furthermore, the cell suspension was stored at -20°C for 2 h, followed by incubation at 98°C for 10 min in a PCR thermocycler (BIOKÉ, SensoQuest GmbH, Goettingen, Germany). The colony identity was determined by amplifying the 16S rRNA gene in a 50 μ L PCR reaction mixture containing 32.5 μ L nuclease-free water (Promega), 10 μ L $5\times$ Phusion Green Buffer (Promega), 1 μ L 10 mM dNTPs (Promega), 0.5 μ L Phusion HotStart Polymerase (5u/ μ L, Promega), 1 μ L 10 μ M forward primer 27F (5'-GTTTGATCCTGGCTCAG-3') [379], 1 μ L 10 μ M reverse primer 1492R (5'-GGACTACNVGGGTWTCTAAT-3') [379], and 1 μ L template from the pre-lysis cell suspension. The PCR program consisted of initial denaturation at 98°C for 3 min; 30 cycles of denaturation at 98°C for 30 s, annealing at 52°C for 40 s and extension at 72°C for 90 s, and final extension at 72°C for 7 min in a PCR thermocycler (BIOKÉ). PCR products were Sanger-sequenced at GATC Biotech (Cologne, Germany) with sequencing primer 806RB [306] to facilitate alignment with the Illumina MiSeq sequencing reads.

Despite of the morphological differences observed on agar plates, it turned out that a substantial number of isolates with different morphologies had highly similar 16S rRNA genes ($\geq 97\%$ sequence identity) after alignment using MEGA 6 [304], which indicated that they belong to similar taxa. To conduct an efficient antimicrobial screening, a selection of isolates based on their 16S rRNA gene sequence identity was done. All Sanger sequences from isolates were

processed in ContigExpress version 10.3.0 (Vector NTI 10, New York, USA) using a threshold for secondary base calling of 70%. Subsequently, the first 30 nucleotides from the 5' end and first 20 nucleotides from the 3' end were trimmed from all sequences. Furthermore, the 5' end and 3' end were further trimmed until fewer than three ambiguous nucleotides were found within the first (or last) 25 nucleotides of the sequence. Finally sequences with a total length of >600 bp were aligned and clustered based on a cut-off of 97% sequence similarity. Selection of isolates for the antimicrobial activity screening was done by taking one representative isolate from each contig (based on 97% sequence similarity) and including isolates with sequences that did not cluster with any other sequence (singletons).

Antimicrobial activity screening of picked isolates

The representative isolates selected based on their 16S rRNA gene similarity were grown in 30 mL of the same liquid media used for the initial isolation. These cultures were incubated under aerobic conditions on a rotary shaker (180 rpm) at 30°C until they reached the stationary phase. Subsequently, the cultures were centrifuged at 4,122 g for 20 min and filtered using a 0.22- μ m filter to obtain cell-free supernatants. These cell-free supernatants were stored at 4°C for three days until the antimicrobial activity screening was performed.

Antimicrobial activity of all selected isolates was tested against six indicator strains: Gram positive bacteria: *Bacillus subtilis* DSM 402 and *Staphylococcus simulans* DSM 20037, Gram negative bacteria: *Escherichia coli* K12MG1655 and *Aeromonas salmonicida* DSM 19634, the yeast *Candida oleophila* DSM 70763, and the oomycete *Saprolegnia parasitica* CBS223.65. *E. coli* and *S. simulans* were grown in liquid Lysogeny Broth medium (Oxoid, Hampshire, UK) and in liquid Trypticase Soy Yeast Extract (DSMZ medium no. 92), respectively. Both *A. salmonicida* and *B. subtilis* were grown in Nutrient broth (Oxoid), while *C. oleophila* was grown in liquid Universal Medium for Yeast (DSMZ medium no. 186). All indicator strains were grown aerobically on a rotary shaker (150 rpm) until an OD₆₆₀ of 0.5 was reached. Subsequently, 200 μ L of these actively growing cultures were spread with a sterile hockey stick on agar media with the same composition as the corresponding liquid media. To prepare *S. parasitica* agar plates, one agar plug of 1x1 cm was transferred from a lawn of fresh *S. parasitica* grown in one-fifth strength of Potato Dextrose Agar (PDA, Oxoid) plates supplemented with 1% of Bacto agar (Oxoid) to a new agar plate with the same composition. Subsequently, antimicrobial properties of the isolates were examined using the disc diffusion assay by adding 20 μ L of each cell free supernatant of an isolate onto 6 mm cellulose paper

discs (Whatman, Maidstone, UK). Paper discs containing extracts were air-dried for 30 min to let excess liquid evaporate. As a negative control, 20 μ L of the respective sterile, uninoculated liquid media was added to the paper discs and included in the screening test. All discs were prepared and assayed in triplicate on top of the agar for each of the indicator strains. Agar plates of the antimicrobial screening assay were incubated at 37°C for *E. coli* and *S. simulans*, 30°C for *A. salmonicida* and *B. subtilis* and at 20°C for *C. oleophila* for 48 h. While, the agar plates with *S. parasitica* were incubated at 20°C for 96 h. After incubation, the radius of the zone of inhibition (ZOI) surrounding each paper disc was measured from the edge of the disc to the end of the clear zone to the nearest mm using a digital calliper (Perel, Gavere, Belgium). The ZOI radius for each extract was calculated as the average value of triplicate discs.

Data availability

Filtered and demultiplexed Illumina MiSeq sequence data can be accessed via the NCBI Sequence Read Archive (SRA) ID PRJNA453745 with accession numbers SRX3998987–SRX3998883. Sequences of individual isolates are available in the NCBI database under project number SUB4990620. The biom table containing OTU abundance (absolute read numbers) combined with the classification for each individual OTU can be accessed at the FigShare online repository (<https://figshare.com/s/4afa290522bd8d6a5611>). A metadata file connected to the individual samples is available via the FigShare online repository (<https://figshare.com/s/c2f78daf6d5962f56fd7>). The phylogenetic tree of all OTUs, available in the Newick tree format Phylogenetic tree file can be accessed at the FigShare online repository (<https://figshare.com/s/5c73b425ac3b7af9261e>).

Results

Cultivated bacteria of X. muta and A. sventres along a depth gradient

Agar plates dedicated for scraping of six different agar-based growth media cumulatively yielded 650 and 3024 bacterial colonies from nine *X. muta* samples of three depth categories (deep, middle, shallow) and six *A. sventres* samples of two depth categories (middle and shallow), respectively (Table 1). Illumina MiSeq sequencing of sponge sample inocula and the bacterial colonies scraped from agar plates yielded a total of 5,545,747 high-quality reads, which clustered into 791 OTUs, with 371 OTUs being identified from scraped plates (Supplementary Table 3).

Table 1. Total number of colonies observed from all agar media obtained from individual inocula that were scraped off the plates for sequencing for (A) *X. muta* and (B) *A. sventres*. The numbers highlighted in red indicate samples for which 16S rRNA gene amplicon products were obtained and sent for Illumina MiSeq sequencing.

A. Total number of colonies from *X. muta* samples

Scraping isolates	<i>X. muta</i> deep			<i>X. muta</i> middle			<i>X. muta</i> shallow			Total per medium
	XM3	XM4	XM5	XM7	XM8	XM9	XM12	XM14	XM15	
MA1/10 agar	2	0	13	0	1	22	1	0	1	40
M3 agar	0	0	0	0	1	0	43	3	0	47
OLIGO agar	56	0	0	1	1	82	0	0	24	164
GP agar	0	0	0	1	1	0	7	3	0	12
Mucin agar	87	3	12	66	13	5	5	1	22	214
Crenarchaeota agar	61	4	11	51	1	3	2	0	40	173
Total per sample	206	7	36	119	18	112	58	7	87	650
Total per depth	249			249			152			

B. Total number of colonies from *A. sventres* samples

Scraping isolates	<i>A. sventres</i> middle			<i>A. sventres</i> shallow			Total per medium
	AS2	AS3	AS4	AS7	AS8	AS11	
MA1/10 agar	3	0	2	6	0	0	11
M3 agar	0	0	4	1	0	2	7
OLIGO agar	19	513	131	45	69	126	903
GP agar	0	0	0	0	4	0	4
Mucin agar	57	377	127	19	53	399	1032
Crenarchaeota agar	32	648	130	49	63	125	1067
Total per sample	111	1558	394	120	189	652	3024
Total per depth	2063			961			

The scraped community of *X. muta* consisted mainly of representatives of four phyla, namely Proteobacteria (Alpha- and Gamma-), Firmicutes, Actinobacteria and Bacteroidetes (Figure 2). A high relative abundance (> 40%) of the class Alphaproteobacteria was observed for all scraped bacterial communities of *X. muta*, whereas isolates belonging to the remaining phyla/classes varied more with depth. Firmicutes was the second most abundant phylum with 13.6 ± 1.3 % of the reads in the scraped community of the deep *X. muta* samples, 34.1 ± 3.1 % in middle and 26.0 ± 1.5 % in shallow samples. The class Gammaproteobacteria represented 39.0 ± 1.1 % from the reads of the deep samples and lower relative abundances of 6.5 ± 0.2 % and 18.5 ± 0.7 % in the middle and shallow samples, respectively. Furthermore, the percentage of Actinobacteria among the cultured fraction was 12.0 ± 1.1 % in shallow samples and decreased to 6.4 ± 0.7 % and 0.66 ± 0.07 % as depth increased.

Among scraped bacterial communities of *X. muta*, 13 OTUs were obtained from all depth categories (Figure 3A), which were predominantly affiliated with the genus *Pseudovibrio* and a few other genera (Supplementary Table 4). OTUs classified as *Mycobacterium* (Actinobacteria), *Salagentibacter*, *Tenacibacillum* (Bacteroidetes), *Fictibacillus*, *Marinococcus*, Planococcaceae (Firmicutes), *Mameliella*, *Roseomonas* (Alphaproteobacteria), *Alteromonas* and *Alcanivorax* (Gammaproteobacteria) were present in the scraped bacterial community of deep *X. muta*, and were absent from their middle and shallow *X. muta* counterparts. Furthermore, OTUs assigned to Caulobacteraceae, *Brevundimonas* and *Paracoccus* (Alphaproteobacteria) were only present in scraped bacterial communities of middle *X. muta* samples. Lastly, OTUs assigned to *Brachybacterium*, *Arthrobacter*, *Kocuria* (Actinobacteria), *Labrenzia*, *Altererythrobacter* (Alphaproteobacteria), *Parahaliea*, *Exiguobacterium*, and *Lactobacillus* (Firmicutes) were only found in scraped bacterial communities of shallow samples. The only overlapping OTU between deep *X. muta* inocula and the corresponding scraped community on agar plates was OTU194 (*Halomonas*) (Supplementary Table 4). However, this single overlapping OTU was represented only by 131 reads in one inoculum (XM14) and accounted for 0.0014% of the total reads in that inoculum.

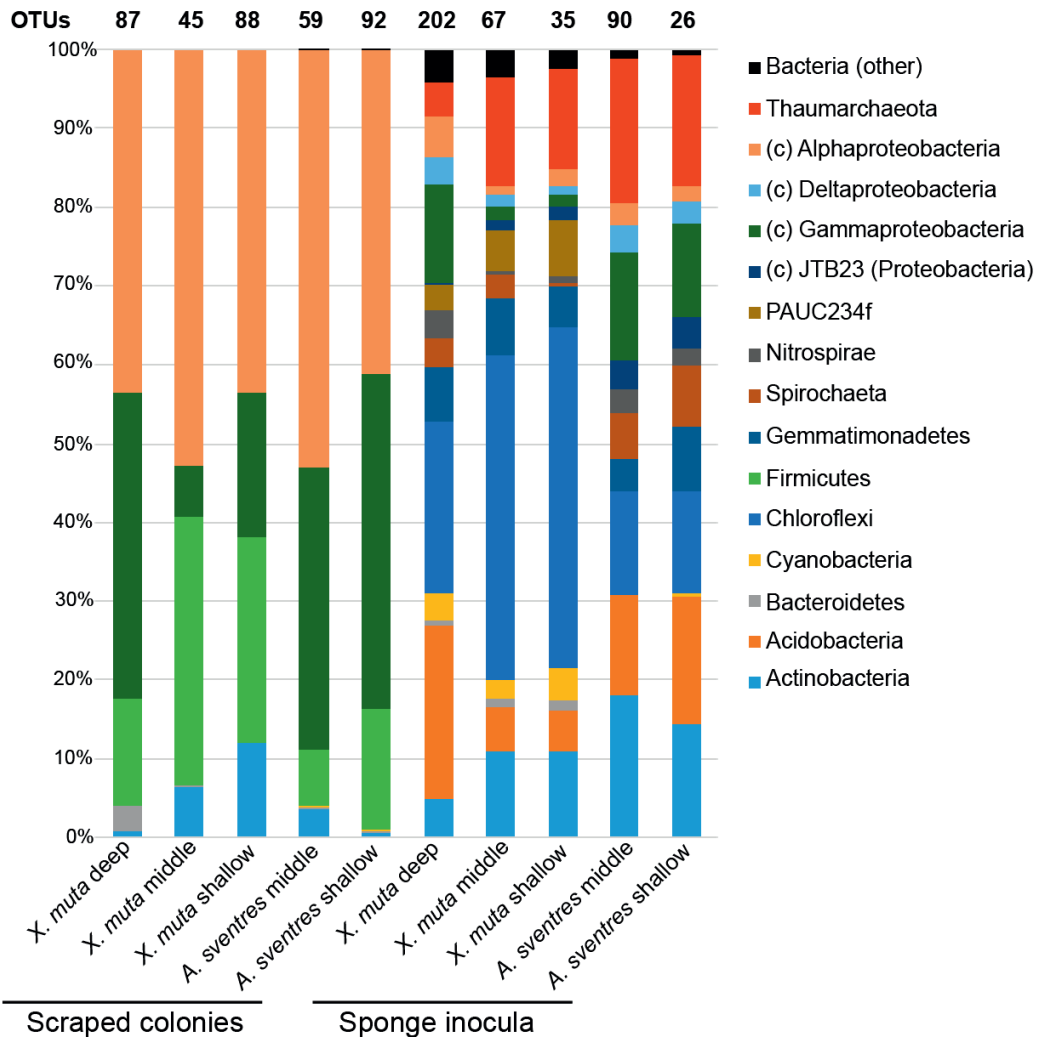


Figure 2. Distribution of prokaryotic phyla based on total reads obtained from Illumina MiSeq sequencing of 16S rRNA genes amplified from scraped colonies and sponge inocula. Reads derived from scraped microbial communities and sponge inocula were pooled per depth category. The total numbers of OTUs per pool are indicated on top of each bar. Phyla with an average relative abundance lower than 0.5% in all samples (Poribacteria, SBR1093, Tectomicrobia, Nitrospirae, Deinococcus Thermus, Verrucomicrobia, Betaproteobacteria (class level) and non-assigned bacterial phyla) were collapsed under “Bacteria (Other)”. The phylum Proteobacteria is displayed at the class level (Alpha-, Gamma-, Delta- and JTB23).

The scraped communities of *A. sventres* collected from shallow and middle depth comprised three phyla: Proteobacteria (Alpha- and Gamma-), Firmicutes and Actinobacteria, which cumulatively contributed to 99.5% of the total bacterial community. The relative abundance of the class Alphaproteobacteria and the phylum Actinobacteria increased from 41.0±1.7 % and

0.45±0.04 % in shallow specimens, respectively, to 53.0±1.9 % and 3.6±0.2 %, in the middle specimens. Conversely, the percentages of Gammaproteobacteria and Firmicutes decreased from 42.6±1.2 % and 15.4±1.7 % in shallow specimens to 35.8±1.7 % and 7.3±0.7 %, respectively, in the middle depth specimens. The remaining 0.5±0.01 % of the bacterial reads in both shallow and middle scraped bacterial community from *A. sventres* belonged to Bacteroidetes, Betaproteobacteria, Cyanobacteria and Verrucomicrobia.

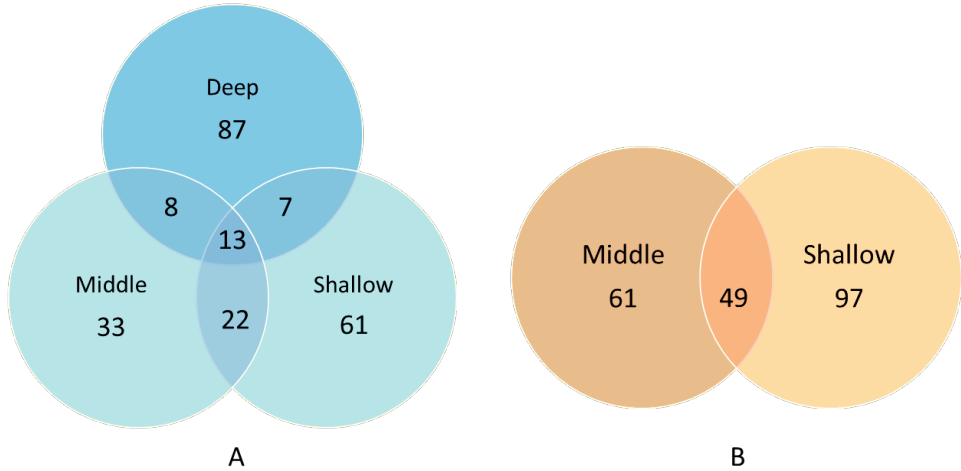


Figure 3. Venn diagrams with the numbers of OTUs retrieved from colonies scraped off agar media shared between different depth categories in *X. muta* (A) and *A. sventres* (B).

Forty-nine OTUs were shared between middle and shallow scraped communities of *A. sventres* (Figure 3B), which were assigned to genera *Janibacter* (Actinobacteria), *Synechococcus* (Cyanobacteria), *Labrenzia*, *Pseudovibrio*, *Ruegeria* (Alphaproteobacteria), *Limnobacter* (Betaproteobacteria), *Microbulbifer* and *Endozoicomonas* (Gammaproteobacteria). OTUs assigned to Corynebacteriales, *Nocardia*, *Rhodococcus* (Actinobacteria), *Aureivirga*, *Muricauda*, Flavobacteriaceae (Bacteroidetes), *Paracoccus*, *Sphingomonas* (Alphaproteobacteria) and *Alcanivorax* (Gammaproteobacteria) were present in middle scraped bacterial communities of *A. sventres* and absent from their shallow counterparts, whereas OTUs assigned to Brucellaceae, *Erythrobacter*, *Mesorhizobium*, *Rhizobium*, *Phyllobacterium* (Alphaproteobacteria), Enterobacteriaceae, Vibrionaceae, *Vibrio*, *Escherichia-Shigella* (Gammaproteobacteria) were only found in scraped bacterial communities of shallow *A. sventres* samples (Supplementary Table 4). Limited overlap was found between OTUs in the inocula and scraped bacterial communities of *A. sventres*. OTU1404 (*Pseudovibrio*), and OTU514 and OTU620 (*Endozoicomonas*) were the three OTUs that overlapped between inocula

and the scraped bacterial community from the middle depth, whereas OTU514 and OTU816 (*Synechococcus*) were the two OTUs shared between inocula and scraped bacterial communities for the shallow samples.

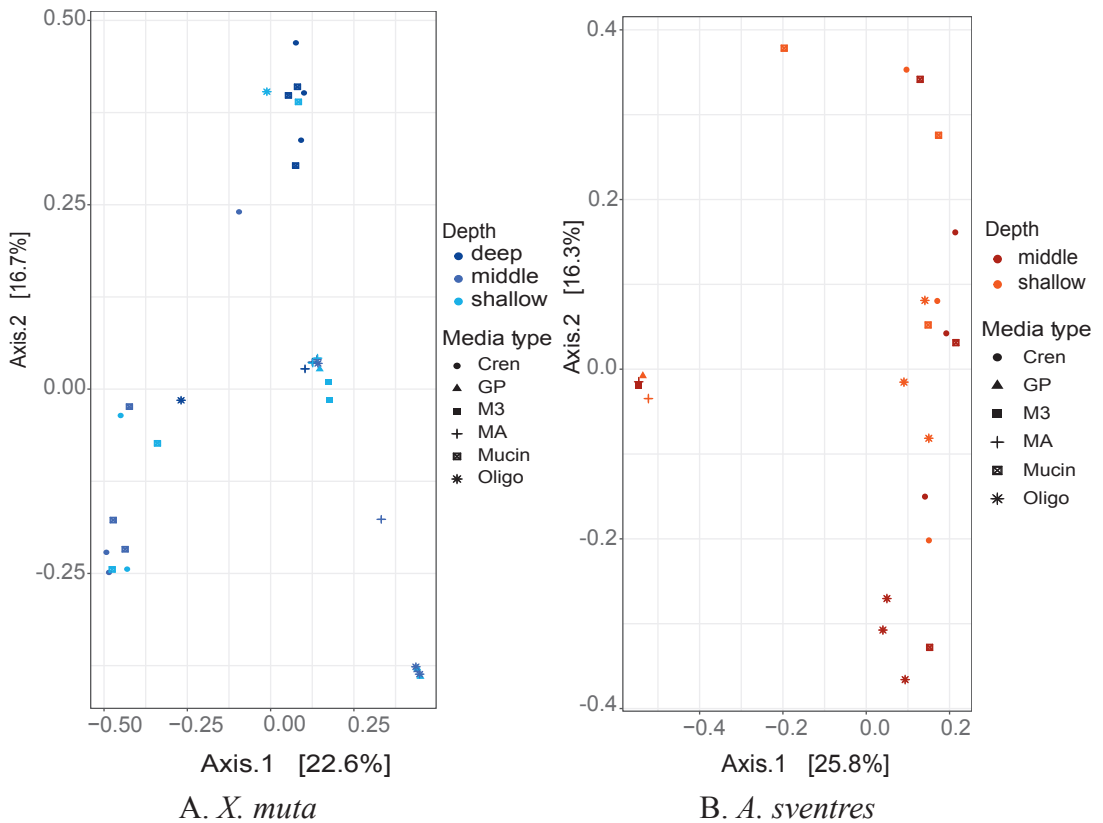


Figure 4. Principal Coordinate Analysis (PCoA) plots based on Bray-Curtis distance of bacterial composition coloured based on depth range from scraped bacterial communities of (A) *X. muta* and (B) *A. sventres*. Media type indicates the agar media on which these bacterial communities were grown (OLIGO, Mucin, Crenarchaeota, M3, GP, MA1/10).

Table 2. Multivariate analysis of the influence of sponge species, depth and media type on scraped bacterial communities of *X. muta* and *A. sventres*. Significant differences are highlighted in bold.

Samples	Parameter	OTUs	df	PERMANOVA		Betadisper	
				R2	p-value	F	p-value
All scraped bacterial colonies (excluding inocula of <i>X. muta</i> and <i>A. sventres</i>)	Sponge (<i>X. muta</i> and <i>A. sventres</i>)	371	1	0.10	0.001	23.84	0.001
	Media type (MA1/10, M3, OLIGO, GP, Mucin, Crenarchaeota)	371	5	0.28	0.001	2.43	0.06
	Depth (deep, middle, shallow)	371	2	0.08	0.003	0.16	0.84
Scraped bacterial colonies of <i>X. muta</i> (excluding inoculum <i>X. muta</i>)	Depth (deep, middle and shallow)	220	2	0.10	0.038	0.84	0.45
	Media type (MA1/10, M3, OLIGO, GP, Mucin, Crenarchaeota)	220	5	0.31	0.001	1.20	0.33
Scraped bacterial colonies of <i>A. sventres</i> (excluding inoculum <i>A. sventres</i>)	Depth (middle and shallow)	151	1	0.06	0.146	0.05	0.83
	Media type (MA1/10, M3, OLIGO, GP, Mucin, Crenarchaeota)	151	5	0.60	0.001	4.00	0.04

Multivariate analysis using PCoA based on pairwise Bray-Curtis distances showed overlapped of microbiota composition among different cultivation media irrespective of depth origin of the sponge (Figure 4). The sponge (source of inocula) contributed to 10% (PERMANOVA, $p = 0.001$) of the difference in the scraped bacterial communities (Table 2). In addition, depth explained 10% and 6% of the differences in the scraped prokaryotic communities in *X. muta* and *A. sventres*, respectively. The growth medium used significantly affected the bacterial community recovered by cultivation ($p=0.001$) and explained 31% and 60% of the variation observed within scraped bacterial communities in *X. muta* and *A. sventres*, respectively. This is partly explained by the uneven distribution of the number of colonies obtained on different growth media. For example GP, M3 and 1/10 MA accumulatively yielded only 1% of the total colonies found in *A. sventres*, and 10% of total bacterial colonies of *X. muta*. From both sponges, the highest numbers of colonies were obtained from CR, OLIGO and Mucin agar media (Table 2 and Supplementary Table 5).

The replicate plates dedicated for picking yielded a comparable total number of colonies as the plates for scraped bacterial community (Supplementary Table 4). Overall, 76 bacterial colonies from *X. muta* and 68 bacterial colonies of *A. sventres* were picked from agar media and survived after re-streaking on agar media and cultivation in corresponding liquid media. These 144 colonies represented 40 and 16 CMCs, respectively (Supplementary Table 6). In *X. muta*, *Pseudovibrio* (22 isolates) and *Ruegeria* (16) were the two most common genera picked from all agar plates (Figure 5). Likewise in *A. sventres*, the three most frequently picked genera were *Pseudovibrio* (38), *Microbulbifer* (7) and *Ruegeria* (7). Furthermore, sequence comparison of these picked isolates with Illumina MiSeq sequences showed matches only with OTUs from the scraped community, but not with OTUs found in sponge inocula (data not shown). Among the most abundant OTUs (Figure 6), a number of bacterial taxa were consistently detected irrespective of the media used for cultivation, including Rhodobacteraceae (OTU512 and OTU1265), *Pseudovibrio* (OTU1234 and OTU1255), and *Ruegeria* (OTU592).

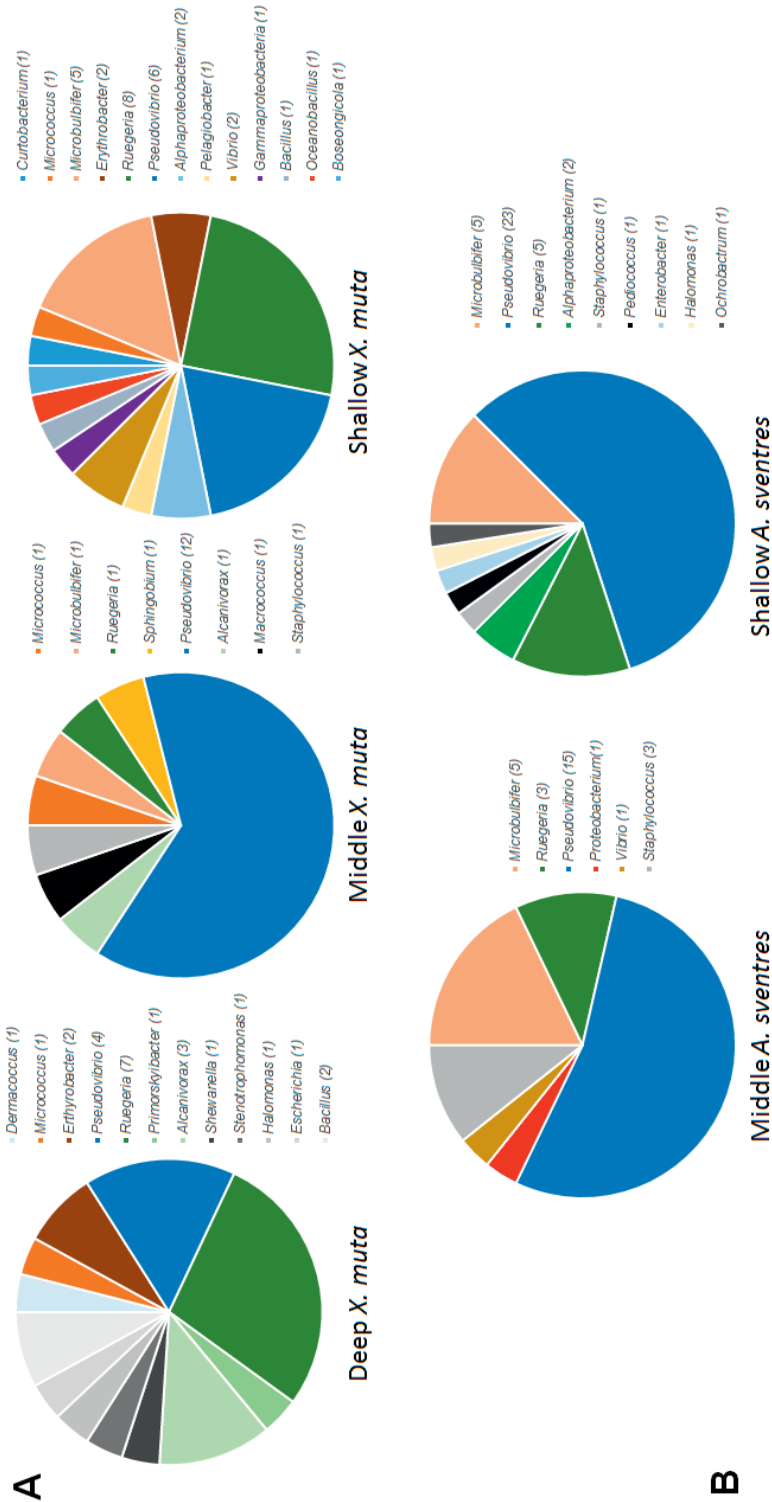


Figure 5. Distribution of picked bacterial colonies from agar plates at genus level based on 16 S rRNA gene sequences. The numbers in parentheses following genus names indicate the number of isolates. Panel A shows the distribution of colonies in *X. muta* and panel B represents colonies from *A. sventres*.

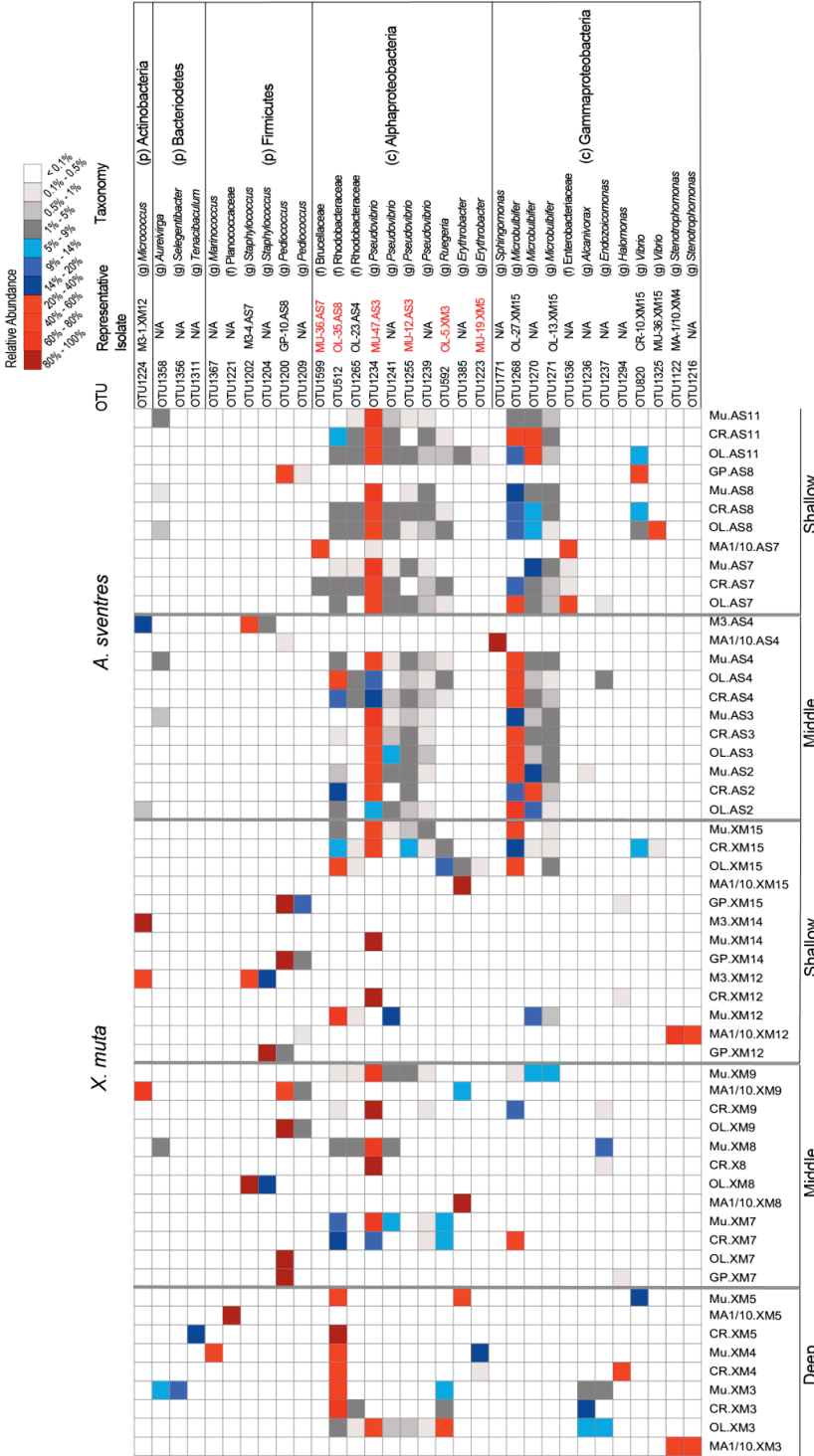


Figure 6. Heatmap representing the most abundant OTUs (average relative abundance $\geq 0.25\%$) across all samples derived from scraped bacterial communities on agar plates of *X. muta* and *A. sventres*. Samples were labelled based on their cultivation media (e.g. OL = OLIGO, CR = Crenarchaeota and Mu = Mucin) followed by their sponge specimen code and subsequently were grouped according to their depth category (depth, middle, shallow). For each OTU, a representative isolate from picked colonies is indicated if recovered by picking colonies (otherwise NA). Isolates highlighted in red were included in the antimicrobial screening. The letter in parentheses indicates the best taxonomy assignment available for each OTU: g (genus), f (family), c (class), p (phylum).

Antimicrobial activity screening of sponge-associated bacteria

Of the 144 picked isolates (Supplementary Table 6), a selection for antimicrobial activity screening was made based on sequence identity and led to a total of 61 bacterial isolates (41 from *X. muta* and 20 from *A. sventres*) (Supplementary Table 7). Subsequently, cell free supernatants of liquid cultures of these 61 isolates were screened against six microbial indicator strains. Eighteen isolates displayed inhibition against bacterial indicator strains (Table 3). However, none of the strains inhibited the growth of the yeast *Candida oleophila* or the oomycete *Saprolegnia parasitica*.

The 41 isolates from *X. muta* were mainly isolated from Mucin (18), OLIGO (13), and MA1/10 (7), while the remaining media: GP, CR and M3 were only represented by one isolate. However, it is important to note that these selected isolates were representatives of contigs which also contain isolates from other media or depths as well. The ten bacterial isolates that displayed antibacterial activities came from three media: MU (n=5), MA1/10 (n=3) and OLIGO (n=2). The majority of these active isolates inhibited only one-indicator strain with *E. coli* and *S. simulans* as the most frequently inhibited strains. Isolates with antibacterial activities from *X. muta* were assigned to nine bacterial genera namely: *Alcanivorax*, *Bacillus*, *Erythrobacter*, *Escherichia*, *Micrococcus*, *Pseudovibrio*, *Ruegeria*, *Sphingobium*, and *Vibrio*. Five out of ten of these isolates came from deep specimens, one was derived from a middle depth specimen and the remaining four isolates were from shallow specimens. Three isolates from deep specimens inhibited two indicator strains: Mucin-6.XM5 (against *E. coli* and *A. salmonicida*), MA1/10-6.XM5 (against *E. coli* and *B. subtilis*), and Mucin-19.XM5 (against *A. salmonicida* and *B. subtilis*).

The 20 selected isolates from *A. sventres* were obtained from media OLIGO (n =8), Mucin (n=7), GP (4) and M3 (n=1). Eight isolates showed antibacterial activities, they were isolated from media Mucin (n=6) and OLIGO (n=2) and represent isolates originating from shallow (4) and middle (4) *A. sventres* specimens. Isolates were assigned to the genera *Microbulbifer*, *Pseudovibrio*, *Ruegeria* and *Vibrio*. The cell-free supernatant of isolate OLIGO-35.AS8 was found active against *A. salmonicida* and *B. subtilis*, while the other cell-free supernatants were active against only one indicator bacterial strain (Table 3).

Table 3. List of isolates with antimicrobial activity against bacterial indicator strains. Inhibition zone radii (mm) were calculated by subtracting the radius of the paper disc from the radius of the inhibition zone. Average and standard deviations are based on triplicate measurements. N/D (Not Detected) indicates that no inhibition was observed. Abbreviations used for bacterial indicator strains are: EC (*Escherichia coli*), AS (*Aeromonas salmonicida*), BS (*Bacillus subtilis*), SS (*Staphylococcus simulans*).

Isolate	Sponge individual and depth	Closest BLAST hit; Accession no	Identity	Radius ZOI (mm)			
				EC	AS	BS	SS
OLIGO-3.XM3	XM3 (deep)	<i>Ruegeria</i> sp. CECT 5091; MH023307.1	98%	N/D	N/D	0.83±0.0	N/D
OLIGO-2.XM3	XM3 (deep)	<i>Pseudovibrio denitrificans</i> strain Ab134; KX990273.1	99%	0.42±0.0	N/D	N/D	N/D
Mucin-23.XM5	XM5 (deep)	<i>Alcanivorax</i> sp. MCCC 1A00973; KU681505.1	99%	N/D	N/D	N/D	0.53±0.25
MA1/10-10.XM5	XM5 (deep)	<i>Bacillus licheniformis</i> strain HRBL-15TDI7; CP014781.1	99%	0.56±0.11	N/D	N/D	N/D
Mucin-6.XM5	XM5 (deep)	<i>Micrococcus luteus</i> strain trpE16 genome; CP007437.1	99%	0.50±0.0	0.40±0.0	N/D	N/D
MA1/10-6.XM5	XM5 (deep)	<i>Escherichia coli</i> strain E41-1; CP028483.1	99%	0.83±0.32	N/D	0.87±0.08	N/D
Mucin-19.XM5	XM5 (deep)	<i>Erythrobacter</i> sp. DSW98; DQ395681.1	99%	N/D	0.60±0.0	0.40±0.0	N/D
MA1/10-2.XM7	XM7 (middle)	<i>Sphingobium yanoikuyae</i> strain S72; CP023741.1	100%	N/A	0.42±0.03	N/D	N/D

Mucin-33.XM15	XM15 (shallow)	<i>Pseudovibrio denitrificans</i> strain SCSIO_43753; KY887758.1	100%	0.43±0.0	N/D	N/D	N/D	N/D
Mucin-36.XM15	XM15 (shallow)	<i>Vibrio</i> sp. VibC-Oc-063;KF577116.1	97%	N/D	N/D	N/D	1.32±0.30	N/D
Mucin-46.AS2	AS2 (middle)	<i>Ruegeria</i> sp. JZ11IS69; KC429844.1	99%	N/D	N/D	N/D	0.94±0.32	N/D
Mucin-12.AS3	AS3 (middle)	<i>Pseudovibrio</i> sp. strain RKSG039; MG799441.1	99%	N/D	N/D	N/D	0.98±0.10	N/D
Mucin-47.AS3	AS3 (middle)	<i>Pseudovibrio</i> sp. strain RKSG039; MG799441.1	100%	N/D	N/D	N/D	0.25±0.0	N/D
Mucin-16.AS4	AS4 (middle)	<i>Vibrio campbellii</i> strain BoB-90;CP026315.1	98%	N/D	N/D	N/D	0.51±0.06	N/D
OLIGO-27.AS7	AS7 (shallow)	<i>Microbulbifer variabilis</i> strain Ni-2088; NR_041021.1	99%	N/D	0.6±0.0	N/D	N/D	N/D
Mucin-56.AS8	AS8 (shallow)	<i>Pseudovibrio</i> sp. FO-BEG1;KY671135.1	100%	0.62±0.12	N/D	N/D	N/D	N/D
OLIGO-35.AS8	AS8 (shallow)	<i>Ruegeria</i> sp. WJ45-6; JX853816.1	98%	N/D	0.63±0.0	0.63±0.0	N/D	N/D
Mucin-41.AS11	AS11 (shallow)	<i>Pseudovibrio</i> sp. strain RKSG039;MG799441.1	100%	N/D	N/D	N/D	0.42±0.25	N/D

Discussion

Cultivable bacteria from X. muta and A. sventres collected from different depths

This study aimed to investigate the impact of depth on the cultivability of bacteria associated with the sponges *X. muta* and *A. sventres* collected from shallow (0-30 m) areas to greater depths (30-60 m and 60-90 m), and to screen for antimicrobial activities of the isolated bacteria. Irrespective of their depth category, Proteobacteria (Alpha- and Gamma-), Actinobacteria and Firmicutes were bacterial phyla dominantly detected from the cultivable fraction of both sponges. This observation is in contrast to a cultivation-independent assessment of the prokaryotic communities of these sponges where depth was found to have a significant impact on the associated communities. However, this discrepancy can be explained by the lack of similarity between the isolates obtained and the bacteria present in the original sponge inocula. The latter is a recurring issue in attempts to isolate dominant representatives of sponge-associated bacteria [29,33,372,380-382] and has often been explained by the recovery of isolates that were present in low numbers in the canal systems and choanocyte chambers of sponges before processing [29,32,380].

Some genera were exclusively detected in the scraped bacterial community from deep specimens of *X. muta*, such as *Alcanivorax* and *Alteromonas*. These genera have also previously been isolated from deep-sea sponges and deep marine habitats [383,384] and have been associated with oil and mucus degradation [385]. On the other hand, some OTUs assigned to *Altererythrobacter*, *Arthrobacter*, *Brachybacterium*, *Rothia* and *Kocuria* were exclusively detected in the scraped community of shallow *X. muta* specimens. This implies that the depth from which sponge samples are collected may impact the bacteria recovered in cultivation. This is in line with the observation that depth significantly affected the composition of biomass scraped off the agar plates when both sponges were analyzed together, and when *X. muta* derived samples were analyzed alone, although it should be noted that the effect of sponge species and media used was more pronounced (Table 2). Overall, the bacteria recovered were mainly affected by the cultivation media used. Although this difference may in part be explained by the disparity in the number of colonies obtained for different media, a similar impact of cultivation conditions on the recovery of sponge-associated bacteria has been previously observed [32]. Another aspect that may have affected the cultivable bacteria from different sponge samples, is the viability of the bacteria in the original samples [386].

Isolates of the genus *Pseudovibrio* were consistently detected in the scraped bacterial communities of all samples. *Pseudovibrio* spp. can be vertically transmitted via sponge larvae [277] and have been recovered from a large number of different sponges across the globe [387]. Our results show that also along vertical gradients *Pseudovibrio* spp are generally recovered from sponges. In addition to *Pseudovibrio*, members of the genera *Ruegeria* and *Microbulbifer* were also among the most abundant OTUs in all sponge specimens, and these two genera have also been frequently reported from other cultivation studies of marine sponges [388,389]. *Ruegeria* has been associated to facilitating cell-to-cell communication between bacteria and the sponge host [390,391], but the fact that these bacteria were not detected in the original samples casts some doubt on this hypothesis. The genus *Microbulbifer* has been associated with the production of paraben (*para*-hydroxybenzoate) compounds that play a role as chemical mediator of interactions between microbial associates in marine sponges [392].

Antibacterial activity of sponge-associated bacteria

The role of sponge-associated microbes as source of various secondary metabolites has motivated the quest to search for isolates that produce potent bioactive compounds, and a number of promising results *in vitro* have been documented [30,157,382]. It is generally taken for granted that many microbial secondary metabolites are biosynthesized during the stationary phase, and that their production is affected by the type of growth media and growth conditions applied [382,393]. Although the cell-free supernatants from our isolates were collected from the stationary phase, the recorded inhibition zones against the bacterial indicator strains were rather small. This is most likely due to low biomass densities that were achieved for most isolates and corresponding low secondary metabolite concentrations in the supernatant. In addition, short-term storage of cell-free extracts (3-5 days at 4°C) may have affected the bioactivity (Supplementary Table 7). We observed that a prolonged storage for 2 more days reduced the ZOI radius for a number of the cell-free supernatants. Previous studies confirmed that storage temperature and duration could influence stability of antimicrobial activities of plant crude extracts [394,395] and bacteriocin from lactic acid bacteria [396]. Furthermore, no inhibition against the yeast and oomycete were observed from these isolates, while direct extractions from these sponges showed potent activity especially against the oomycete *S. parasitica* (Chapter 3 of this thesis).

The impact of cultivation media was most pronounced and active isolates were obtained only from three media: OLIGO, 1/10 diluted Marine Agar (MA), and Mucin, although it should be

noted that some of these isolates chosen as representatives were also obtained from other media and samples. *Pseudovibrio* strains were the most frequently isolated bioactive strains and were obtained from both sponges from different depths. *Pseudovibrio* spp. have received considerable interest from a biotechnological point of view especially for their antimicrobial activity, and a large number of secondary metabolite biosynthetic gene clusters have been identified for this genus [365,380,397,398]. Our finding therefore confirms that *Pseudovibrio* is a cosmopolitan genus that occupies a wide range of marine sponges as previously described, but apparently is also found at different depths. The remaining isolates showing antimicrobial activity were assigned to genera *Alcanivorax*, *Ruegeria*, *Vibrio*, *Bacillus*, *Micrococcus*, *Microbulbifer* and *Sphingobium*, all of which are common inhabitants of various marine habitats including sponges with existing records of antibacterial activities [167,203,399-401].

Conclusion

Using six different agar media, we investigated the cultivability of sponge-associated bacteria of the two marine sponges *X. muta* and *A. sventres* collected at different depths. The most dominant OTUs recovered from plates from all depths and both sponge species included *Pseudovibrio*, *Ruegeria* and *Microbulbifer*. Sponge species and type of media used during cultivation, and for *X. muta* also depth, contributed significantly to the variation in the scraped bacterial biomass. Furthermore, we identified ten isolates from *X. muta* and eight isolates from *A. sventres* that displayed antibacterial activities. However, for antimicrobial activity, no clear pattern regarding antibacterial activities related to depth of the original samples was observed.

Acknowledgements

Anak Agung Gede Indraningrat received a PhD fellowship from the Indonesia Endowment Fund for Education (LPDP), grant number 20140812021557. The submersible dives were financed by Substation Curaçao and field trip expenses were supported by the Rufford Foundation under grant number 17660-1. Furthermore, we thank Adriaan “Dutch” Schrier, Laureen Schenk and the submersible team and staff at the Substation Curaçao: Bruce Brandt, Barbara van Bebber, Tico Christiaan, Barry Brown, Manuel Jove and Joe Oliver for all facilities and help. We would also like to thank Mark. J.A. Vermeij from CARMABI for providing laboratory equipment. We also would like to thank Irene de Bruijn and Jos M. Raaijmakers from NIOO KNAW for providing *Saprolegnia parasitica*.

Supplementary Material

Supplementary Table 1. Sponge specimens that were used as inocula for cultivation.

No	Species	Sample Code	Actual Depth (m)	Depth category
1	<i>X. muta</i>	XM3	72	Deep
2	<i>X. muta</i>	XM4	85	Deep
3	<i>X. muta</i>	XM5	82	Deep
4	<i>X. muta</i>	XM7	52	Middle
5	<i>X. muta</i>	XM8	52	Middle
6	<i>X. muta</i>	XM9	48	Middle
7	<i>X. muta</i>	XM12	27	Shallow
8	<i>X. muta</i>	XM14	27	Shallow
9	<i>X. muta</i>	XM15	27	Shallow
10	<i>A. sventres</i>	AS2	54	Middle
11	<i>A. sventres</i>	AS3	52	Middle
12	<i>A. sventres</i>	AS4	52	Middle
13	<i>A. sventres</i>	AS7	12	Shallow
14	<i>A. sventres</i>	AS8	12	Shallow
15	<i>A. sventres</i>	AS11	27	Shallow

Supplementary Table 2, Supplementary Table 3 and Supplementary Table 4 are available via the following link <https://figshare.com/s/f724e9047f4347af58a0>

Supplementary Table 5. Number of colonies counted from each sponge per agar medium from agar plates dedicated for picking. Panel A shows colonies from *X.muta* and Panel B indicates colonies from *A. sventres*.

A. *X. muta*

Picked isolates	<i>X. muta</i> deep			<i>X. muta</i> middle			<i>X. muta</i> shallow		
	XM3	XM4	XM5	XM7	XM8	XM9	XM12	XM14	XM15
Marine agar 1/10 (10x diluted)	0	1	15	1	0	32	1	0	0
M3 agar	0	0	0	0	0	0	14	0	0
OLIGO agar	57	0	0	11	0	68	5	1	45
GP agar	0	0	0	3	35	39	3	0	1
Mucin agar	101	3	18	79	65	5	1	0	29
Crenarchaeota agar	58	3	9	59	4	9	4	0	24

B. *A. sventres*

Picked isolates	<i>A. sventres</i> middle			<i>A. sventres</i> shallow		
	AS2	AS3	AS4	AS7	AS8	AS11
Marine agar 1/10 (10x diluted)	0	0	1	3	0	2
M3 agar	1	0	1	2	0	0
OLIGO agar	36	524	151	59	62	128
GP agar	0	0	94	0	4	0
Mucin agar	36	382	143	99	100	40
Crenarchaeota agar	29	728	149	44	63	147

Supplementary Table 6. Colonies picked from *X. muta* (panel A) and *A. sventres* (panel B) with their Colony Morphology Code (CMC), contig number or singleton (based on 16S rRNA gene sequence). In columns 4, 5, 6, and 7 taxonomic information of isolates based on a BLAST search with 16S rRNA genes is provided. Finally, the depth range of the origin sponge samples is provided in the last column.

A. *X. muta*

Isolate Code	CMC	Contig/singleton	Phylum/Class	Closest relative	Acc number	% identity	Depth
Mucin-18.XM4	22522	1	Alphaproteobacteria	<i>Erythrobacter flavus</i> strain VG1 chromosome, complete genome	CP022528.1	100%	deep
Mucin-6.XM5	10512	2	Actinobacteria	<i>Micrococcus luteus</i> strain tpE16 genome	CP007437.1	99%	deep
Mucin-23.XM5	10512	3	Gammaaproteobacteria	<i>Alcanivorax</i> sp. MCCC 1A00973 16S ribosomal RNA gene, partial sequence	KU681505.1	99%	deep
Mucin-17.XM4	10531	7	Firmicutes	<i>Bacillus firmus</i> strain KP 16S ribosomal RNA gene, partial sequence	MH071301.1	99%	deep
Mucin-16.XM3	20321	10	Alphaproteobacteria	<i>Ruegeria</i> sp. CECT 5091 16S ribosomal RNA gene, partial sequence	MH023307.1	99%	deep
OLIGO-9.XM12	10512	11	Alphaproteobacteria	<i>Ruegeria pomeroyi</i> strain LS80 16S ribosomal RNA gene, partial sequence	FJ937909.1	99%	shallow
OLIGO-2.XM3	12313	15	Alphaproteobacteria	<i>Pseudovibrio denitrificans</i> strain Ab134 16S ribosomal RNA gene, partial sequence	KX990273.1	99%	deep
Mucin-19.XM5	20511	singleton	Alphaproteobacteria	<i>Erythrobacter</i> sp. DSW98 16S ribosomal RNA gene, partial sequence	DQ395681.1	99%	deep
OLIGO-3.XM3	10513	singleton	Alphaproteobacteria	<i>Ruegeria</i> sp. CECT 5091 16S ribosomal RNA gene, partial sequence	MH023307.1	98%	deep
MA1/10-6.XM5	10523	singleton	Firmicutes	<i>Escherichia coli</i> strain E41-1 chromosome, complete genome	CP028483.1	99%	deep
MA1/10-10.XM5	10512	singleton	Firmicutes	<i>Bacillus licheniformis</i> strain HRBL-15TD17 chromosome, complete genome	CP014781.1	99%	deep
MA1/10-2.XM7	20511	singleton	Alphaproteobacteria	<i>Sphingobium yanoikuyae</i> strain S72 chromosome, complete genome	CP023741.1	100%	middle
Mucin-33.XM15	20513	singleton	Alphaproteobacteria	<i>Pseudovibrio denitrificans</i> strain SCSIO_43753 16S ribosomal RNA gene, partial sequence	MH283837.1	100%	shallow
Mucin-36.XM15	30521	singleton	Gammaaproteobacteria	<i>Vibrio</i> sp. VibC-Oc-063 16S ribosomal RNA gene, partial sequence	KF577116.1	96%	shallow
MA1/10-11.XM5	10512	singleton	Actinobacteria	<i>Demacoccus nishinomiyaensis</i> strain M25, complete genome	CP008889.1	99%	deep
Mucin-11.XM8	12341	singleton	Actinobacteria	<i>Microbulbifer cystodytense</i> 16S rRNA gene, isolate C1	AJ620879.1	98%	middle

GP-3.XM12	10513	singleton	Actinobacteria	<i>Curtobacterium pusillum</i> strain Nc5MA-2 16S ribosomal RNA gene, partial sequence	KP296214.1	99%	shallow
M3-1.XM12	20512	singleton	Actinobacteria	<i>Micrococcus luteus</i> 16S ribosomal RNA gene, partial sequence	KY007582.1	98%	shallow
OLIGO-14.XM15	20312	singleton	Actinobacteria	<i>Microbulbifer</i> sp. GB02-3 16S ribosomal RNA gene, partial sequence	GQ118704.1	97%	shallow
OLIGO-6.XM3	10512	singleton	Alphaproteobacteria	<i>Pseudovibrio denitrificans</i> strain Ab134 16S ribosomal RNA gene, partial sequence	KX990273.1	100%	deep
Mucin-1.XM3	10512	singleton	Alphaproteobacteria	<i>Primorskybacter insulae</i> strain SSK3-2 16S ribosomal RNA, partial sequence	NR_144598.1	99%	deep
Mucin-8.XM7	20522	singleton	Alphaproteobacteria	<i>Ruegeria</i> sp. WJ45-6 16S ribosomal RNA gene, partial sequence	JX853816.1	96%	middle
Mucin-27.XM7	20511	singleton	Alphaproteobacteria	<i>Pseudovibrio</i> sp. strain RKSG039 16S ribosomal RNA gene, partial sequence	MG799441.1	98%	middle
Mucin-7.XM7	10512	singleton	Alphaproteobacteria	<i>Pseudovibrio</i> sp. strain RKSG039 16S ribosomal RNA gene, partial sequence	MG799441.1	100%	middle
Mucin-32.XM9	20531	singleton	Alphaproteobacteria	<i>Pseudovibrio</i> sp. strain RKSG039 16S ribosomal RNA gene, partial sequence	MG799441.1	100%	middle
Mucin-31.XM9	20521	singleton	Alphaproteobacteria	<i>Pseudovibrio</i> sp. strain RKSG039 16S ribosomal RNA gene, partial sequence	MG799441.1	100%	middle
OLIGO-12.XM15	10512	singleton	Alphaproteobacteria	<i>Erythrobacter vulgaris</i> strain 102-Py5 16S ribosomal RNA gene, partial sequence	MG456894.1	99%	shallow
OLIGO-26.XM12	32311	singleton	Alphaproteobacteria	<i>Ruegeria</i> sp. strain CCM43 16S ribosomal RNA gene, partial sequence	MF499123.1	99%	shallow
OLIGO-10.XM14	10511	singleton	Alphaproteobacteria	<i>Pseudovibrio denitrificans</i> strain A-253 16S ribosomal RNA gene, partial sequence	KC751041.1	98%	shallow
Mucin-34.XM15	20521	singleton	Alphaproteobacteria	<i>Pseudovibrio</i> sp. strain Btu15_11 16S ribosomal RNA gene, partial sequence	KY671136.1	97%	shallow
OLIGO-20.XM15	10512	singleton	Alphaproteobacteria	<i>Boseongicola</i> sp. MA-7-27 16S ribosomal RNA gene, partial sequence	KX268607.1	98%	shallow
OLIGO-23.XM3	12313	singleton	Gamma proteobacteria	<i>Alcanivorax</i> sp. MCCC 1A00973 16S ribosomal RNA gene, partial sequence	KU681505.1	97%	deep
OLIGO-4.XM3	20521	singleton	Gamma proteobacteria	<i>Shewanella</i> sp. STAB603 16S ribosomal RNA gene, partial sequence	JF825445.1	97%	deep
MA1/10-1.XM4	10511	singleton	Gamma proteobacteria	<i>Senotrophomonas maltophilia</i> strain CCC10S 16S ribosomal RNA gene, partial sequence	MF375922.1	100%	deep
Mucin-3.XM3	20521	singleton	Gamma proteobacteria	<i>Halomonas salifodinae</i> 16S ribosomal RNA gene, partial sequence	JQ716249.1	97%	deep

Mucin-28.XM7	20531	singleton	Gammaproteobacteria	<i>Alcanivorax</i> sp. MCCC 1A00973 16S ribosomal RNA gene, partial sequence	KU681505.1	99%	middle
CR-10.XM15	10522	singleton	Gammaproteobacteria	<i>Vibrio campbellii</i> CAIM 519 = NBRC 15631 strain ATCC 25920, CAIM 519T chromosome 1, complete sequence	CP015863.1	99%	shallow
OLIGO-16.XM15	10521	singleton	Gammaproteobacteria	<i>Gammaproteobacterium</i> clone S1-5-32 16S ribosomal RNA gene, partial sequence	KF786583.1	97%	shallow
MA1/10-7.XM9	22321	singleton	Firmicutes	<i>Macrococcus canis</i> strain KM45013, complete genome	CP021059.1	100%	middle
MA1/10-3.XM12	20521	singleton	Firmicutes	<i>Bacillus pumilus</i> strain 145 chromosome, complete genome	CP027116.1	100%	shallow
OLIGO-22.XM15	20511	singleton	Firmicutes	<i>Oceanobacillus oncorhynchi</i> strain QTYC25b 16S ribosomal RNA gene, partial sequence	KM974661.2	100%	shallow
OLIGO-11.XM15	10512	1	Alphaproteobacteria	<i>Erythrobacter flavus</i> strain VGI, complete genome	CP022528.1	100%	shallow
GP-2.XM8	22311	2	Actinobacteria	<i>Micrococcus luteus</i> strain SGAir0127 chromosome, complete genome	CP025616.1	99%	middle
Mucin-24.XM5	10512	3	Gammaproteobacteria	<i>Alcanivorax</i> sp. MCCC 1A00973 16S ribosomal RNA gene, partial sequence	KU681505.1	99%	deep
GP-1.XM9	10511	4	Firmicutes	<i>Staphylococcus pasteurii</i> strain JS7 chromosome, complete genome	CP017463.1	99%	middle
OLIGO-25.XM3	20511	11	Alphaproteobacteria	<i>Ruegeria</i> sp. ZGT108 16S ribosomal RNA gene, partial sequence	KP726355.1	99%	deep
OLIGO-5.XM3	10512	11	Alphaproteobacteria	<i>Ruegeria</i> sp. strain RKS040 16S ribosomal RNA gene, partial sequence	MG799442.1	99%	deep
OLIGO-18.XM15	10512	11	Alphaproteobacteria	Marine <i>Alphaproteobacterium</i> L4-30 16S ribosomal RNA gene, partial sequence	KU170446.1	100%	shallow
OLIGO-13.XM15	22331	13	Actinobacteria	<i>Microrubifjer</i> sp. A4B17 gene for 16S rRNA, partial sequence	AB243106.1	99%	shallow
OLIGO-27.XM15	33431	13	Actinobacteria	<i>Microrubifjer</i> sp. A4B17 gene for 16S rRNA, partial sequence	AB243106.1	99%	shallow
OLIGO-7.XM12	32321	13	Gammaproteobacteria	<i>Pelagibacter variabilis</i> partial 16S rRNA gene, strain A4	FM180508.1	99%	shallow
Mucin-22.XM15	24531	14	Alphaproteobacteria	<i>Ruegeria</i> sp. strain RKS062 16S ribosomal RNA gene, partial sequence	MG799449.1	99%	shallow
CR-1.XM5	10511	15	Alphaproteobacteria	<i>Pseudovibrio denitrificans</i> strain Ab134 16S ribosomal RNA gene, partial sequence	KX990273.1	99%	deep
Mucin-25.XM5	20321	15	Alphaproteobacteria	<i>Pseudovibrio</i> sp. strain RKS039 16S ribosomal RNA gene, partial sequence	MG799441.1	100%	deep

Mucin-9.XM7	22541	15	Alphaproteobacteria	<i>Pseudovibrio</i> sp. strain RKSG039 16S ribosomal RNA gene, partial sequence	MG799441.1	99%	middle
Mucin-26.XM7	20331	15	Alphaproteobacteria	<i>Pseudovibrio</i> sp. strain RKSG039 16S ribosomal RNA gene, partial sequence	MG799441.1	99%	middle
CR-3.XM7	10211	15	Alphaproteobacteria	<i>Pseudovibrio</i> sp. strain RKSG039 16S ribosomal RNA gene, partial sequence	MG799441.1	100%	middle
Mucin-29.XM7	10534	15	Alphaproteobacteria	<i>Pseudovibrio</i> sp. strain RKSG039 16S ribosomal RNA gene, partial sequence	MG799441.1	100%	middle
Mucin-10.XM8	24541	15	Alphaproteobacteria	<i>Pseudovibrio</i> sp. strain RKSG039 16S ribosomal RNA gene, partial sequence	MG799441.1	99%	middle
Mucin-12.XM8	10512	15	Alphaproteobacteria	<i>Pseudovibrio</i> sp. strain RKSG039 16S ribosomal RNA gene, partial sequence	MG799441.1	99%	middle
Mucin-30.XM8	20513	15	Alphaproteobacteria	<i>Pseudovibrio</i> sp. strain RKSG039 16S ribosomal RNA gene, partial sequence	MG799441.1	100%	middle
CR-4.XM9	20422	15	Alphaproteobacteria	<i>Pseudovibrio</i> sp. strain RKSG039 16S ribosomal RNA gene, partial sequence	MG799441.1	100%	middle
OLIGO-8.XM12	20512	15	Alphaproteobacteria	<i>Pseudovibrio</i> sp. strain RKSG039 16S ribosomal RNA gene, partial sequence	MG799441.1	100%	shallow
Mucin-14.XM15	10511	15	Alphaproteobacteria	<i>Pseudovibrio</i> sp. strain RKSG039 16S ribosomal RNA gene, partial sequence	MG799441.1	99%	shallow
Mucin-35.XM15	10512	15	Alphaproteobacteria	<i>Pseudovibrio</i> sp. strain RKSG039 16S ribosomal RNA gene, partial sequence	MG799441.1	100%	shallow
OLIGO-24.XM3	12314	16	Alphaproteobacteria	<i>Ruegeria</i> sp. strain RKSG062 16S ribosomal RNA gene, partial sequence	MG799449.1	99%	deep
Mucin-4.XM5	22321	16	Alphaproteobacteria	<i>Ruegeria</i> sp. strain RKSG062 16S ribosomal RNA gene, partial sequence	MG799449.1	99%	deep
Mucin-5.XM5	22341	16	Alphaproteobacteria	<i>Ruegeria</i> sp. strain RKSG062 16S ribosomal RNA gene, partial sequence	MG799449.1	99%	deep
Mucin-20.XM12	20521	16	Alphaproteobacteria	<i>Ruegeria</i> sp. strain RKSG062 16S ribosomal RNA gene, partial sequence	MG799449.1	99%	shallow
OLIGO-17.XM15	20513	16	Alphaproteobacteria	<i>Ruegeria</i> sp. strain RKSG062 16S ribosomal RNA gene, partial sequence	MG799449.1	99%	shallow
Mucin-15.XM15	22341	16	Alphaproteobacteria	<i>Ruegeria</i> sp. strain RKSG062 16S ribosomal RNA gene, partial sequence	MG799449.1	100%	shallow
OLIGO-19.XM15	12513	16	Alphaproteobacteria	<i>Ruegeria</i> sp. strain RKSG062 16S ribosomal RNA gene, partial sequence	MG799449.1	100%	shallow
OLIGO-21.XM15	24514	16	Alphaproteobacteria	<i>Ruegeria</i> sp. strain RKSG062 16S ribosomal RNA gene, partial sequence	MG799449.1	100%	shallow

Mucin-21.XM15	30521	16	Alphaproteobacteria	<i>Alphaproteobacterium</i> sp. clone 12E11 16S ribosomal RNA gene, partial sequence	KC668966.1	99%	shallow
OLIGO-15.XM15	22311	17	Actinobacteria	<i>Microbulbifer</i> sp. GB02-3 16S ribosomal RNA gene, partial sequence	GQ118704.1	99%	shallow
Mucin-13.XM15	20321	17	Actinobacteria	<i>Microbulbifer</i> sp. GB02-3 16S ribosomal RNA gene, partial sequence	GQ118704.1	99%	shallow

B. *A.sventres*

Isolate	CMC	No of Contig/singleton	Phyla/Class	Closest relative	Acc number	% identity	Depth
GP-3.AS4	10512	4	Firmicutes	<i>Staphylococcus pasteurii</i> strain ATCC 51129 16S ribosomal RNA gene, partial sequence	MG757632.1	100%	middle
GP-8.AS4	22311	5	Firmicutes	<i>Staphylococcus epidermidis</i> strain ISLP23 16S ribosomal RNA gene, partial sequence	MF125036.1	100%	middle
GP-6.AS4	10512	12	Firmicutes	<i>Staphylococcus haemolyticus</i> strain M2_0m_PrM_10 16S ribosomal RNA gene, partial sequence	KY742479.1	100%	middle
OLIGO-24.AS4	32331	13	Actinobacteria	<i>Microbulbifer</i> sp. A4B17 gene for 16S rRNA, partial sequence	AB243106.1	99%	middle
OLIGO-35.AS8	10513	14	Alphaproteobacteria	<i>Ruegeria</i> sp. W145-6 16S ribosomal RNA gene, partial sequence	JX853816.1	98%	shallow
Mucin-12.AS3	32331	15	Alphaproteobacteria	<i>Pseudovibrio</i> sp. strain RKSG039 16S ribosomal RNA gene, partial sequence	MG799441.1	99%	middle
Mucin-47.AS3	10522	15	Alphaproteobacteria	<i>Pseudovibrio</i> sp. strain RKSG039 16S ribosomal RNA gene, partial sequence	MG799441.1	100%	middle
OLIGO-37.AS11	22311	16	Alphaproteobacteria	<i>Ruegeria</i> sp. strain RKSG062 16S ribosomal RNA gene, partial sequence	MG799449.1	100%	shallow
Mucin-36.AS7	20321	singleton	Alphaproteobacteria	<i>Ochrobactrum daejeonense</i> strain KINDSS-Mac1 16S ribosomal RNA gene, partial sequence	KY471630.1	100%	shallow
OLIGO-28.AS7	10531	singleton	Alphaproteobacteria	<i>Alphaproteobacterium</i> clone A85 16S ribosomal RNA gene, partial sequence	GQ215680.1	98%	shallow
OLIGO-31.AS7	10512	singleton	Alphaproteobacteria	<i>Halomonas phoceae</i> strain CCUG 5096 16S ribosomal RNA gene, partial sequence	AY922995.1	96%	shallow
OLIGO-34.AS8	10511	singleton	Alphaproteobacteria	<i>Alphaproteobacterium</i> S948 16S ribosomal RNA gene, partial sequence	FJ215570.1	100%	shallow
Mucin-56.AS8	10322	singleton	Alphaproteobacteria	<i>Pseudovibrio</i> sp. FO-BEG1, complete genome	KY671135.1	98%	shallow

Mucin-41.AS11	10531	singleton	Alphaproteobacteria	<i>Pseudovibrio</i> sp. strain RKSG039 16S ribosomal RNA gene, partial sequence	MG799441.1	100%	shallow
GP-10.AS8	10512	singleton	Firmicutes	<i>Pedococcus acidilactici</i> strain NRCC1 16S ribosomal RNA gene, partial sequence	KU504251.1	100%	shallow
Mucin-46.AS2	10521	singleton	Ruegeria	<i>Ruegeria</i> sp. JZ11S69	KC429844.1	99%	middle
Mucin-16.AS4	10531	singleton	Gammaproteobacteria	<i>Vibrio campbellii</i> strain BoB-90 chromosome 1, complete sequence	CP026315.1	98%	middle
M3-1.AS7	10311	singleton	Gammaproteobacteria	<i>Enterobacter ludwigii</i> strain 30ftlb 16S ribosomal RNA gene, partial sequence	MG602668.1	99%	shallow
OLIGO-15.AS2	30321	singleton	Actinobacteria	<i>Microbulbifer</i> sp. A4B17 gene for 16S rRNA, partial sequence	CP029064.1	99%	middle
OLIGO-14.AS2	22331	singleton	Actinobacteria	<i>Microbulbifer</i> sp. A4B17 gene for 16S rRNA, partial sequence	CP029064.1	96%	middle
Mucin-45.AS2	10521	11	Alphaproteobacteria	<i>Ruegeria pomeroyi</i> strain LS80 16S ribosomal RNA gene, partial sequence	FJ937909.1	100%	middle
OLIGO-16.AS2	10512	11	Alphaproteobacteria	<i>Ruegeria pomeroyi</i> strain LS80 16S ribosomal RNA gene, partial sequence	FJ937909.2	99%	middle
Mucin-9.AS2	10531	11	Proteobacteria	<i>Proteobacterium</i> clone L4-30 16S ribosomal RNA gene, partial sequence	KU170446.1	100%	middle
OLIGO-30.AS7	10511	11	Alphaproteobacteria	<i>Ruegeria</i> sp. ZGT108 16S ribosomal RNA gene, partial sequence	KP726355.1	99%	shallow
OLIGO-39.AS11	22311	11	Alphaproteobacteria	<i>Ruegeria</i> sp. strain RKSG208 16S ribosomal RNA gene, partial sequence	MG799470.1	100%	shallow
Mucin-42.AS11	10531	11	Alphaproteobacteria	<i>Ruegeria pomeroyi</i> strain LS80 16S ribosomal RNA gene, partial sequence	FJ937909.1	99%	shallow
M3-4.AS7	20312	12	Firmicutes	<i>Staphylococcus haemolyticus</i> JCM 2416 gene for 16S ribosomal RNA, partial sequence	LC383923.1	100%	shallow
OLIGO-21.AS3	22531	13	Actinobacteria	<i>Microbulbifer epitalgus</i> strain F-104 16S ribosomal RNA gene, partial sequence	NR_041493.1	99%	middle
OLIGO-27.AS7	32531	13	Actinobacteria	<i>Microbulbifer variabilis</i> strain Ni-2088 16S ribosomal RNA gene, partial sequence	NR_041021.1	99%	shallow
OLIGO-29.AS7	32321	13	Actinobacteria	<i>Microbulbifer</i> sp. A4B17 gene for 16S rRNA, partial sequence	AB243106.1	99%	shallow
OLIGO-38.AS11	20411	13	Actinobacteria	<i>Microbulbifer</i> sp. A4B17 gene for 16S rRNA, partial sequence	CP029064.1	99%	shallow
OLIGO-40.AS11	32321	13	Actinobacteria	<i>Microbulbifer</i> sp. A4B17 gene for 16S rRNA, partial sequence	CP029064.1	99%	shallow

OLIGO-36.AS11	22531	13	Actinobacteria	<i>Microbulifer</i> sp. A4B17 gene for 16S rRNA, partial sequence	CP029064.1	99%	shallow
OLIGO-18.AS3	30321	13	Actinobacteria	<i>Microbulifer</i> sp. A4B17 gene for 16S rRNA, partial sequence	CP029064.1	99%	middle
CR-5.AS2	20513	15	Alphaproteobacteria	<i>Pseudovibrio</i> sp. strain RKSG039 16S ribosomal RNA gene, partial sequence	MG799441.1	100%	middle
OLIGO-13.AS2	20511	15	Alphaproteobacteria	<i>Pseudovibrio</i> sp. strain RKSG039 16S ribosomal RNA gene, partial sequence	MG799441.1	99%	middle
Mucin-34.AS3	20331	15	Alphaproteobacteria	<i>Pseudovibrio</i> sp. strain RKSG039 16S ribosomal RNA gene, partial sequence	MG799441.1	99%	middle
Mucin-48.AS3	10521	15	Alphaproteobacteria	<i>Pseudovibrio</i> sp. strain RKSG039 16S ribosomal RNA gene, partial sequence	MG799441.1	99%	middle
OLIGO-17.AS3	20512	15	Alphaproteobacteria	<i>Pseudovibrio</i> sp. strain RKSG039 16S ribosomal RNA gene, partial sequence	MG799441.1	100%	middle
OLIGO-19.AS3	10511	15	Alphaproteobacteria	<i>Pseudovibrio</i> sp. strain RKSG039 16S ribosomal RNA gene, partial sequence	MG799441.1	99%	middle
OLIGO-20.AS3	10512	15	Alphaproteobacteria	<i>Pseudovibrio</i> sp. strain RKSG039 16S ribosomal RNA gene, partial sequence	MG799441.1	99%	middle
Mucin-14.AS4	22531	15	Alphaproteobacteria	<i>Pseudovibrio</i> sp. strain RKSG039 16S ribosomal RNA gene, partial sequence	MG799441.1	99%	middle
Mucin-35.AS4	24531	15	Alphaproteobacteria	<i>Pseudovibrio</i> sp. strain RKSG039 16S ribosomal RNA gene, partial sequence	MG799441.1	99%	middle
Mucin-49.AS4	10521	15	Alphaproteobacteria	<i>Pseudovibrio</i> sp. strain RKSG039 16S ribosomal RNA gene, partial sequence	MG799441.1	99%	middle
Mucin-50.AS4	10521	15	Alphaproteobacteria	<i>Pseudovibrio</i> sp. strain RKSG039 16S ribosomal RNA gene, partial sequence	MG799441.1	100%	middle
Mucin-51.AS4	14531	15	Alphaproteobacteria	<i>Pseudovibrio</i> sp. strain RKSG039 16S ribosomal RNA gene, partial sequence	MG799441.1	100%	middle
OLIGO-22.AS4	10511	15	Alphaproteobacteria	<i>Pseudovibrio</i> denitrificans strain Ab134 16S ribosomal RNA gene, partial sequence	KX990273.1	100%	middle
OLIGO-25.AS7	10512	15	Alphaproteobacteria	<i>Pseudovibrio</i> sp. strain RKSG039 16S ribosomal RNA gene, partial sequence	MG799441.1	99%	shallow
OLIGO-26.AS7	10511	15	Alphaproteobacteria	<i>Pseudovibrio</i> sp. strain RKSG039 16S ribosomal RNA gene, partial sequence	MG799441.1	100%	shallow
Mucin-55.AS7	22331	15	Alphaproteobacteria	<i>Pseudovibrio</i> sp. strain RKSG039 16S ribosomal RNA gene, partial sequence	MG799441.1	99%	shallow
Mucin-18.AS7	22331	15	Alphaproteobacteria	<i>Pseudovibrio</i> sp. strain RKSG039 16S ribosomal RNA gene, partial sequence	MG799441.1	99%	shallow

ucin-19.AS7	20331	15	Alphaproteobacteria	<i>Pseudovibrio</i> sp. strain RKS039 16S ribosomal RNA gene, partial sequence	MG799441.1	99%	shallow
ucin-37.AS7	10512	15	Alphaproteobacteria	<i>Pseudovibrio</i> sp. strain RKS039 16S ribosomal RNA gene, partial sequence	MG799441.1	100%	shallow
ucin-38.AS7	10521	15	Alphaproteobacteria	<i>Pseudovibrio</i> sp. strain RKS039 16S ribosomal RNA gene, partial sequence	MG799441.1	99%	shallow
ucin-52.AS7	10521	15	Alphaproteobacteria	<i>Pseudovibrio</i> sp. strain RKS039 16S ribosomal RNA gene, partial sequence	MG799441.1	100%	shallow
ucin-53.AS7	10522	15	Alphaproteobacteria	<i>Pseudovibrio</i> sp. strain RKS039 16S ribosomal RNA gene, partial sequence	MG799441.1	100%	shallow
ucin-54.AS7	22311	15	Alphaproteobacteria	<i>Pseudovibrio</i> sp. strain RKS039 16S ribosomal RNA gene, partial sequence	MG799441.1	99%	shallow
ucin-21.AS8	10531	15	Alphaproteobacteria	<i>Pseudovibrio</i> sp. strain RKS039 16S ribosomal RNA gene, partial sequence	MG799441.1	99%	shallow
ucin-22.AS8	22331	15	Alphaproteobacteria	<i>Pseudovibrio</i> sp. strain RKS039 16S ribosomal RNA gene, partial sequence	MG799441.1	100%	shallow
ucin-23.AS8	10531	15	Alphaproteobacteria	<i>Pseudovibrio</i> sp. strain RKS039 16S ribosomal RNA gene, partial sequence	MG799441.1	99%	shallow
ucin-24.AS8	22331	15	Alphaproteobacteria	<i>Pseudovibrio</i> sp. strain RKS039 16S ribosomal RNA gene, partial sequence	MG799441.1	99%	shallow
ucin-26.AS8	22331	15	Alphaproteobacteria	<i>Pseudovibrio</i> sp. strain RKS039 16S ribosomal RNA gene, partial sequence	MG799441.1	100%	shallow
ucin-39.AS8	20531	15	Alphaproteobacteria	<i>Pseudovibrio</i> sp. strain RKS039 16S ribosomal RNA gene, partial sequence	MG799441.1	99%	shallow
ucin-40.AS8	10512	15	Alphaproteobacteria	<i>Pseudovibrio</i> sp. strain RKS039 16S ribosomal RNA gene, partial sequence	MG799441.1	99%	shallow
LJGO-33.AS8	10511	15	Alphaproteobacteria	<i>Pseudovibrio</i> sp. strain RKS039 16S ribosomal RNA gene, partial sequence	MG799441.1	99%	shallow
ucin-27.AS11	22531	15	Alphaproteobacteria	<i>Pseudovibrio</i> sp. strain RKS039 16S ribosomal RNA gene, partial sequence	MG799441.1	99%	shallow
ucin-28.AS11	10531	15	Alphaproteobacteria	<i>Pseudovibrio</i> sp. strain RKS039 16S ribosomal RNA gene, partial sequence	MG799441.1	99%	shallow
ucin-29.AS11	20321	15	Alphaproteobacteria	<i>Pseudovibrio</i> sp. strain RKS039 16S ribosomal RNA gene, partial sequence	MG799441.1	99%	shallow

Supplementary Table 7. List of isolates that were selected for antimicrobial screening based on their 16S rRNA gene similarity selection using ContigExpress. Isolates in bold indicate strains that showed antibacterial activity against at least one bacterial indicator strain: EC (*Escherichia coli*), AS (*Aeromonas salmonicida*), BS (*Bacillus subtilis*), SS (*Staphylococcus simulans*). During the first screening, cell free supernatant of isolates was stored at 4°C for 3 days and subsequently the storage was extended for 2 days until re-screening was conducted. Isolates without antibacterial activities were not included for re-screening. Average and standard deviations are based on triplicate measurements. N/D (not detected) indicates that no inhibition was observed.

A. List of isolates from *X. muta* that were included in antimicrobial screening

Isolate Code	No of Contig/singleton	Radius ZOI 1 st /2 nd screening (mm)			
		EC	AS	BS	SS
Mucin-18.XM4	1	N/D	N/D	N/D	N/D
Mucin-6.XM5	2	0.50±0.0/ N/D	0.40±0.0/ ND	N/D	N/D
Mucin-23.XM5	3	N/D	N/D	N/D	0.53±0.25/ 0.86 ± 0.2
Mucin-17.XM4	7	N/D	N/D	N/D	N/D
Mucin-16.XM3	10	N/D	N/D	N/D	N/D
OLIGO-9.XM12	11	N/D	N/D	N/D	N/D
OLIGO-2.XM3	15	0.42±0.0/ N/D	N/D	N/D	N/D
Mucin-19.XM5	singleton	N/D	0.60±0.0/N/D	0.40±0.0/ N/D	N/D
OLIGO-3.XM3	singleton	N/D	N/D	0.83±0.0/ N/D	N/D
MA1/10-6.XM5	singleton	0.83±0.32/ N/D	N/D	0.87±0.08/N /D	N/D
MA1/10-10.XM5	singleton	0.56±0.11/N/D	N/D	N/D	N/D
MA1/10-2.XM7	singleton	N/D	0.42±0.03/N/D	N/D	N/D
Mucin-33.XM15	singleton	0.43±0.0/ N/D	N/D	N/D	N/D
Mucin-36.XM15	singleton	N/D	N/D	N/D	1.32±0.30/N/ D
MA1/10-11.XM5	singleton	N/D	N/D	N/D	N/D
Mucin-11.XM8	singleton	N/D	N/D	N/D	N/D
GP-3.XM12	singleton	N/D	N/D	N/D	N/D
M3-1.XM12	singleton	N/D	N/D	N/D	N/D
OLIGO-14.XM15	singleton	N/D	N/D	N/D	N/D
OLIGO-6.XM3	singleton	N/D	N/D	N/D	N/D
Mucin-1.XM3	singleton	N/D	N/D	N/D	N/D
Mucin-8.XM7	singleton	N/D	N/D	N/D	N/D
Mucin-27.XM7	singleton	N/D	N/D	N/D	N/D
Mucin-7.XM7	singleton	N/D	N/D	N/D	N/D
Mucin-32.XM9	singleton	N/D	N/D	N/D	N/D
Mucin-31.XM9	singleton	N/D	N/D	N/D	N/D
OLIGO-12.XM15	singleton	N/D	N/D	N/D	N/D
OLIGO-10.XM14	singleton	N/D	N/D	N/D	N/D
Mucin-34.XM15	singleton	N/D	N/D	N/D	N/D
OLIGO-20.XM15	singleton	N/D	N/D	N/D	N/D
OLIGO-23.XM3	singleton	N/D	N/D	N/D	N/D
OLIGO-4.XM3	singleton	N/D	N/D	N/D	N/D
MA1/10-1.XM4	singleton	N/D	N/D	N/D	N/D

Mucin-3.XM3	singleton	N/D	N/D	N/D	N/D
Mucin-28.XM7	singleton	N/D	N/D	N/D	N/D
CR-10.XM15	singleton	N/D	N/D	N/D	N/D
OLIGO-16.XM15	singleton	N/D	N/D	N/D	N/D
MA1/10-7.XM9	singleton	N/D	N/D	N/D	N/D
MA1/10-3.XM12	singleton	N/D	N/D	N/D	N/D
OLIGO-22.XM15	singleton	N/D	N/D	N/D	N/D

B. List of isolates from *A. sventres*

Isolate Code	No of Contig/singleton	Radius ZOI 1 st /2 nd screening (mm)			
		EC	AS	BS	SS
GP-3.AS4	4	N/D	N/D	N/D	N/D
GP-8.AS4	5	N/D	N/D	N/D	N/D
GP-6.AS4	12	N/D	N/D	N/D	N/D
OLIGO-24.AS4	13	N/D	N/D	N/D	N/D
OLIGO-35.AS8	14	N/D	0.63±0.0	0.63±0.0	N/A
Mucin-12.AS3	15	N/D	N/D	N/D	0.98±0.10/0.17±0.03
Mucin-47.AS3	15	N/D	N/D	N/D	0.25±0.0 /0.74±0.18
OLIGO-37.AS11	16	N/D	N/D	N/D	N/D
Mucin-36.AS7	singleton	N/D	N/D	N/D	N/D
OLIGO-28.AS7	singleton	N/D	0.6±0.0	N/A	N/D
OLIGO-31.AS7	singleton	N/D	N/D	N/D	N/D
OLIGO-34.AS8	singleton	N/D	N/D	N/D	N/D
Mucin-56.AS8	singleton	0.62±0.12/N/D	N/D	N/D	N/D
Mucin- 41.AS11	singleton	N/D	N/D	N/D	0.42±0.25
GP-10.AS8	singleton	N/D	N/D	N/D	N/D
Mucin-46.AS2	singleton	N/D	N/D	N/D	0.94±0.32
Mucin-16.AS4	singleton	N/D	N/D	N/D	0.51±0.06/ N/D
M3-1.AS7	singleton	N/D	N/D	N/D	N/D
OLIGO-15.AS2	singleton	N/D	N/D	N/D	N/D
OLIGO-14.AS2	singleton	N/D	N/D	N/D	N/D



Chapter 5

Quantifying variations of microbiota and metabolome composition in deep-sea sponges - implications for chemical ecology and bioprospecting

Karin Steffen*, Anak Agung Gede Indraningrat*, Ida Erngren, Jakob Haglöf,
Leontine E. Becking, Hauke Smidt, Igor Yashayaev, Ellen Kenchington, Curt
Pettersson, Paco Cárdenas§ & Detmer Sipkema§ .

* Both authors contributed equally

§ Both authors contributed equally

Manuscript in preparation

Abstract

Marine sponges (phylum Porifera) are the leading biological source for the discovery of novel bioactive compounds from nature. Yet, physico-chemical and biological factors involved in shaping the chemical potential of sponges are poorly understood. A complicating factor is their often rich and species-specific microbiome that has been implicated in bioactive metabolite production. In this study, we aim to investigate the impact of depth on variation in prokaryotic and chemical diversity of the three sponge species *Geodia barretti*, *Stryphnus fortis*, and *Weberella bursa*. Sponges were sampled from 200 m to 1400 m depth. We found that prokaryotic and metabolite composition both varied with depth. Our results show that up to 29 % of the variation in prokaryotic community composition and up to 17% of the variation of the metabolome were attributed to depth. We found that prokaryotic community composition that varied with depth in *W. bursa* came from OTUs affiliated to Gammaproteobacteria and Planctomycetes. While, OTUs that differed significantly with depth in *S. fortis* and *G. barretti* assigned to prokaryotic phyla of Acidobacteria, Chloroflexi, Thaumarchaeota, and SBR1093. Metabolic profiles of sponges were highly host-specific. Concentration of the known bioactive compounds in *G. barretti* (baretin, 8,9-dihydrobaretin and soelterin) was negatively correlated with depth, while positive trend with increasing depth was observed in bioactive compounds associated with *S. fortis* (ianthelline and stryphnusin).

Keywords: sponges, deep-sea, prokaryotic community, metabolome

Introduction

Sponges (Phylum Porifera) are sessile filter-feeding animals found in marine and freshwater habitats and are among the most ancient extant animals [402-404]. Sponges harbour rich and diverse prokaryotic communities, and together host and symbionts are frequently referred to as ‘holobiont’ [405,406]. Extensive 16S ribosomal RNA (rRNA) gene amplicon sequencing surveys showed that a considerable fraction of the prokaryotic communities within sponges is affiliated with so-called sponge-enriched clusters to indicate their specificity for the sponge host environment, although they can also be detected in small quantities in seawater and sediments [24,407]. With regards to host specificity, the members of the prokaryotic communities found within sponges can be divided into two categories: generalists that are detected in many sponge species irrespective of their biogeographic origin and specialists that are observed in particular sponge species [24,406]. In concordance with this picture, the microbiota is acquired by its sponge host both horizontally as well as vertically [19,408,409].

Many studies have tried to elucidate various aspects of the relationships of the sponge-host and its microbiota [19,69]. From a functional perspective, the microbes serve as primary feed to the sponge as well as by increasing bioavailability of nutrients [410-412]. In addition, in a number of cases the microbiota is responsible for chemical defence of the host and thus significantly contributes to the metabolome of the holobiont, notably regarding the production of specialized metabolites [58,281,413].

Sponges have been recognized as one of the prominent sources of novel marine bioactive compounds for decades [42,43,414,415]. With a target or testing system at hand, bioactive compounds are isolated through bioassay-guided screening. Alternatively, the major chemical compound(s) of an organism can be isolated without prior knowledge about its activity and then tested in a wide range of bioassays to assess a bioactivity [416]. However, untargeted metabolomics in sponges is a less common approach for profiling of specialized metabolites and so far, has only been used for chemotaxonomy and chemical discrimination [117,417-421].

In marine habitats, sponges are distributed widely from shallow water to the deep sea. Whereas numerous studies have focused on microbiota and metabolite composition of marine sponges from shallow water, limited information is available from their deep-sea counterparts [69]. A few studies focusing on microbiota composition of sponges from shallow water (< 30 m) to the mesophotic zone (30 – 200 m) indicated that shifts in prokaryotic communities occur across this depth range, presumably influenced by a combination of factors such as nutrient

availability and physicochemical conditions [79-81]. Therefore, it would be intriguing to observe if such patterns would extend beyond the mesophotic zone.

In this study, three boreal demosponges, namely *Geodia barretti* (Bowerbank 1858), *Stryphnus fortis* (Vosmaer 1885), and *Weberella bursa* (Linnaeus, 1758), were sampled along a depth gradient ranging from 244 m to 1481 m below sea level in Davis Strait, North Atlantic. *G. barretti* and *S. fortis* belong to the order Tetractinellida [422], whereas *W. bursa* belongs to the order Polymastiida [423]. The first two are ‘high-microbial abundance’ (HMA) sponges [412] whereas the latter is considered as low microbial abundance (LMA) sponge (N. Boury-Esnault, pers. comm.). Furthermore, *G. barretti* and *S. fortis* are prominent species in North Atlantic sponge grounds [103,111], and particularly *G. barretti* has been a focal species in natural product discovery [115,424]. In this study, 16S rRNA gene amplicon sequencing and mass spectrometry were employed to detect differences in prokaryotic community composition and metabolome profiles of these sponges across the depth range studied here.

Material and Methods

Sampling

Sponge specimens used in this study were collected by the crews of the R/V *Pâmiut* belonging to the Greenland Institute of Natural Resources (GINR), during cruises in the Davis Strait conducted by Fisheries and Oceans Canada, Central and Arctic Region, between 2011 and 2015. Sponges were dredged using Alfredo or Cosmos benthic trawls at depths between 244 m and 1481 m (Figure 1, Figure S1), and geospatial sampling data was recorded. Subsequently each specimen was initially identified on-board, was photographed, and small fragments of the sponge tissues were frozen. The sponges remained on deck or in the laboratory for approximately 30-45 min before they were frozen. The outside temperature usually oscillated around 4-5°C, and the sorting area was approximately 10°C. Upon return to land, samples were shipped to the Bedford Institute of Oceanography (BIO, Dartmouth, Nova Scotia, Canada) where *Geodia barretti*, *Stryphnus fortis* and *Weberella bursa* specimens were identified by M. Best, G. Thompson, L. Anstey and E. Baker. For every specimen, one subsample was freeze-dried for metabolomics and one subsample was kept frozen for 16S rRNA gene amplicon sequencing. Freeze-dried specimens were sent to Uppsala University and stored in a cold room upon arrival, until processed for global metabolite profiling. The remaining frozen subsamples for prokaryotic community analysis were sent to Wageningen University & Research and stored at -20°C until further processing for Illumina MiSeq sequencing. After preliminary

analyses, a few outliers according to Principal Component Analysis of prokaryotic community data were re-identified by P. Cárdenas, and one specimen was removed from the data set as it was another species. Detailed sample information can be found in Supplementary Table 1. Due to the topography of the sampling site, depth and latitude were correlated (Pearson's $\rho=0.429$, $p=0.001$). The maximal geographic diagonal spread across the sampling site is 771 km and depth range is 1237 m.

To establish a potential effect of oceanographic setting (seawater properties, water mass origin, age and mixing history) on sponge prokaryotic community composition and metabolite profile, all oceanographic data available for the study area were assembled. These characteristics include observations available from the World Ocean Database (https://www.nodc.noaa.gov/OC5/WOD/pr_wod.html) maintained by the National Center for Environmental Information (NCEI, formerly National Oceanographic Data Center), as well as by oceanographic surveys conducted by the Bedford Institute of Oceanography of Fisheries and Oceans Canada, including its Atlantic Zone Off-Shelf Monitoring Program (AZOMP, <http://www.bio.gc.ca/science/monitoring-monitorage/azomp-pmzao/azomp-pmzao-en.php>).

All vertical profiles of temperature and salinity obtained from discrete (e.g., water samples and reversing thermometers) and initially continuous and later subsampled measurements were checked for errors and vertically interpolated for every 5 m.

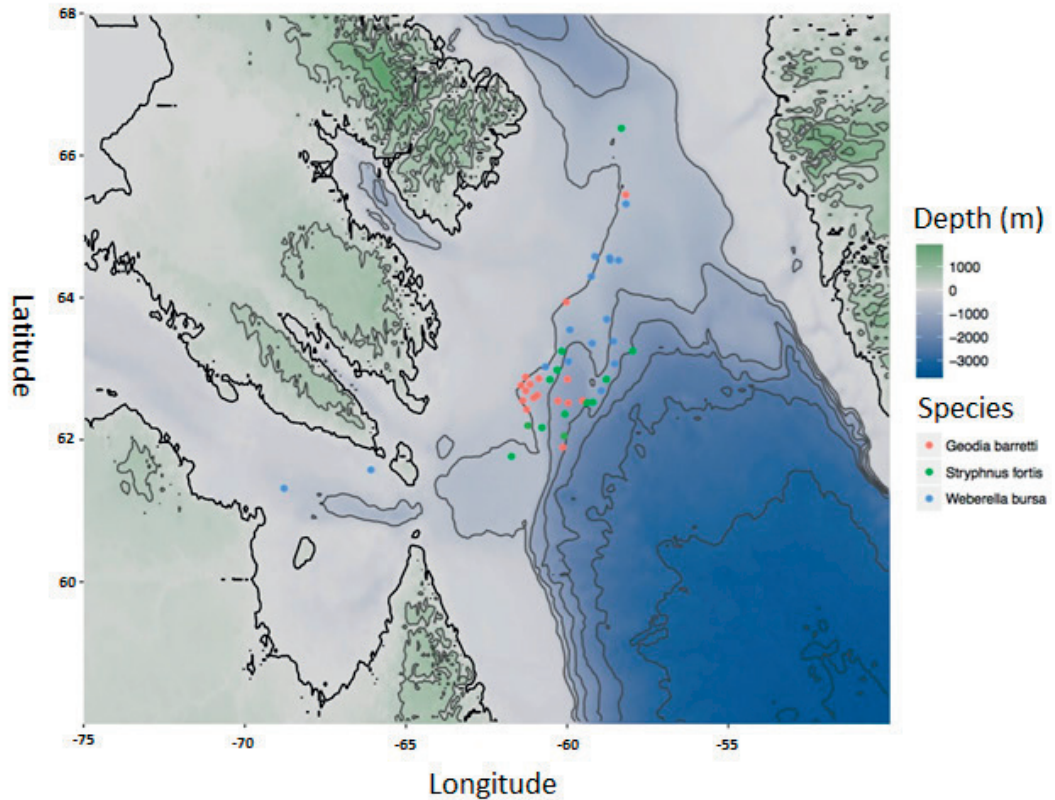


Figure 1. Map of Davis Strait and location where specimens were sampled. Each dot represents a sampling location for one of the three sponge species: red (*G. barretti*), green (*S. fortis*), blue (*W. bursa*). The map was taken from NOAA (<https://www.noaa.gov/>)

DNA extraction and 16S rRNA gene amplicon sequencing

The composition of prokaryotic communities was assessed by Illumina MiSeq amplicon sequencing of the V4 region of the 16S rRNA gene using a two-step amplification procedure. DNA extraction, as well as primer sequences and further details of Illumina MiSeq library preparation were as described in **Chapter 3** of this thesis. Finally, the library was sequenced at GATC Biotech AG (Constance, Germany) by Illumina MiSeq sequencing. Sequencing data was deposited at the NCBI Sequence Read Archive (SRA) with accession number SRP142603 under file numbers SRX3993970 – SRX3993926.

Sequence processing and prokaryotic community analysis

Raw data was analyzed using NG-Tax (Galaxy version 1.0) [309] following procedures as described in **Chapter 3** of this thesis. The impact of depth on prokaryotic community composition was assessed using orthogonal partial least square (OPLS) analysis. Subsequently,

the variable importance in the projection (VIP) was calculated for all OTUs to identify those that contributed most to differences in prokaryotic community composition between different depths, where $VIP > 1$ is considered to indicate a significant contribution to the separation of samples [425-427]. An OTU heatmap for each sponge species was generated in R using pheatmap [316] (version 1.0.8) for the most abundant OTUs ($\geq 0.25\%$) based on average relative abundance in all samples per species. Following a procedure described by Dat *et al* [308], the representative sequences of these most abundant OTUs for each sponge were subjected to a BLAST search against a curated sponge Earth Microbiome Project (EMP) database (<https://github.com/amnona/SpongeEMP>). The sponge microbiome project subOTU sequences that were identical or had one nucleotide mismatch with sequences of the most abundant OTUs were uploaded to the spongeEMP online server (www.spongeemp.com) to identify OTUs that were significantly enriched in sponges [308].

Metabolite extraction

Freeze-dried sponge tissue was ground manually with mortar and pestle, and 50 mg of the powder was extracted in glass vials with 4.5 ml 70% Methanol/MilliQ(MQ) water for one hour on a shaker at low speed. The vials were then centrifuged at 2000 x g for 10 min at 4°C, and 2 ml of the supernatant was dispensed into two glass vials each and dried overnight at 43°C on a savant speed-vac plus sc110A (Thermo Fischer, Waltham, Massachusetts, USA). The dry extracts were kept at -80 °C until further analyses. Metabolites were separated prior to downstream mass spectrometry (MS) analysis using two different chromatographic columns: a hydrophilic interaction liquid chromatography (HILIC) column that retains polar compounds, and a reverse-phase (RP) column that favors retention of non-polar compounds. All samples were processed in randomized order using glass instruments during the extraction.

Mass spectrometry analysis

Dried extracts in glass vials were dissolved in 200 μ L solvent (HILIC: 50 μ L ddH₂O and 175 μ L acetonitrile AcN; RP: 140 μ L ddH₂O and 10 μ L AcN). Upon addition of the organic solvent for HILIC chromatography, all samples separated into two immiscible layers. The vials were centrifuged for 3 min at 2000 x g to yield an even separation. Only the top layer (approximately 150 μ L) was transferred to a Chromacol 03-FISV MS-vial (Thermo Scientific, Waltham, Massachusetts, USA) for MS analyses. For RP chromatography, no layers were observed, and the entire volume of the dissolved sample was used. A five μ L aliquot from each individual

MS-vial for HILIC and RP, respectively, was combined to produce a quality control (QC) sample.

High resolution MS analysis system and settings

The extracts were analyzed back-to-back in positive and negative ionization mode on an Acquity I-Class Ultra Performance Liquid Chromatography UPLC coupled to a G2S Synapt Q-TOF with an electrospray ionization (ESI) ion source (all Waters Corp., Milford, MA, USA). Chromatographic separation in HILIC mode was performed on an Acquity UPLC BEH Amide column (1.7 μm , 2.1 mm inner diameter \times 50 mm, Waters Corp.). Mobile phase A consisted of 95:5 acetonitrile/MQ water with 5 mM ammonium formate and 0.1 % formic acid (FA), and mobile phase B consisted of 40:60 acetonitrile/MQ water with 5 mM ammonium formate and 0.1 % FA. The gradient elution profile was as follows: mobile phase A was decreased non-linearly (slope factor 8, masslynx) from 100 % A to 100 % B over 14 min, 100 % B was held for 2 min and then decreased back to 100 % A over 1 min. The column was re-equilibrated at 100 % A for 6 min for a total runtime of 23 min. Chromatographic separation in RP was performed on an Acquity UPLC BEH C18 column (1.7 μm , 2.1 mm inner diameter \times 50 mm, Waters). Mobile phase A consisted of MQ water with 0.1 % FA, and mobile phase B was AcN with 0.1 % FA. The gradient elution profile started at 95 % A, was decreased linearly over 14 min to 5 % A, and 5 % A was held for 2 min before the column was re-equilibrated at 95 % A for 4 min. The flow rate was set to 0.4 mL/min, the column temperature was set to 40°C, the samples were kept at 8°C and the injection volume was 5 μL in all experiments.

Data acquisition was performed using MS^E mode, and lock mass correction was applied using a solution of leucine enkephalin in both positive and negative mode. Ionization parameters were set as follows in positive/negative mode; the capillary voltage was 1kV/1.5 kV, the cone voltage was 30 V/25 V, the source offset was 50/60 and the source temperature was set to 120°C. Nitrogen was used as desolvation and cone gas with gas flows of 800 l/h and 50 l/h, respectively, and desolvation temperature was set to 500°C/450°C. For MS^E acquisition a collision energy ramp from 20-45 eV was used with argon as collision gas. The instrument was calibrated in the m/z range 50-1500 using sodium formate prior to each analysis.

All study samples were analysed in both RP and HILIC, in positive and negative ionization mode, resulting in four metabolite datasets per sponge specimen. The column and sample cone

was cleaned in between each analysis mode. Prior to each analysis ten QC injections were made to condition the column, and to ensure stable retention times and signal intensities. The study samples were analysed in randomized order with QC injections interspaced every 6th injection.

MS data processing

Raw files were converted to cdf files by Databridge/MassLynx (Waters Corporation, Milford, Massachusetts, USA), sorted according to species and processed with XCMS in R. Peak picking was performed using the `centWave` function with parameters `ppm=8`, `peakwidth` set to `c(5,45)` and the noise parameter set to 2000. Retention time alignment was performed with the `obiwarp` function and the response factor set to 10, grouping was performed with the “group” function and the “fillPeaks” function was used to avoid zero values. This resulted in an average of over 3000 common features among all samples.

The data set was manually curated to remove features eluting in the void (retention time less than 45 s). A raw data set as well as two normalized data sets (Log₁₀-transformed and median fold change normalized) were produced and filtered to only retain features with a coefficient of variation < 30% in the QC samples. After subsequent evaluation, raw data sets were used. Additionally, metadata on sample depth, latitude, longitude, water mass, sampling year, extraction batch, extraction weight and MS injection order was added to the data sets. Finally, data sets produced as described above for both chromatographic methods and both ionization modes, were analysed in R using the packages `vegan` [428], `ggplot2` [313], `xcms` [429] and `ropls` [430].

Results

Prokaryotic community composition

At phylum level, *S. fortis* and *G. barretti* specimens had a similar prokaryotic community composition that was different from that found for *W. bursa* (Figure 2). Acidobacteria, Chloroflexi, Proteobacteria and Thaumarchaeota were the four most pre-dominant phyla found in *S. fortis* and *G. barretti* with an average relative abundance above 10% in all specimens, and accounting for cumulative relative abundances of $70 \pm 2\%$. In addition to these four phyla, ten other phyla with an average relative abundance > 0.25% were observed in all specimens from these two sponges. In contrast, *W. bursa* was represented by only eight microbial phyla with

Proteobacteria constituting the most pre-dominant one, accounting for an average relative abundance of $83\pm 9\%$ in all specimens. When zooming in to the OTU-level, the samples clustered based on host-identity with samples from the HMA sponges *G. barretti* and *S. fortis* being more similar to each other than to *W. bursa* specimens, in line with what was found at phylum level (Figure 3). Only one OTU (OTU4, *Candidatus Nitrosopumilus*) was shared among *S. fortis*, *G. barretti* and *W. bursa*.

For *W. bursa*, microbiota composition of 16 specimens was assessed and yielded 135 OTUs, with 36 OTUs designated as important contributors (VIP score >1) based on OPLS. Depth contributed to 12% (Supplementary Table 2) of the variation of prokaryotic community composition (Supplementary Table 3, $p = 0.009$), and 20 OTUs had a relative abundance of $\geq 0.25\%$ (Figure 4). Further sequence comparison of these 20 OTUs with the sponge EMP database indicated that 11 of these OTUs belonged to sponge-enriched clusters, which were all affiliated to E01-9C-26 (10 OTUs) and Mycobacteria (OTU52) (Figure 4). Relative abundance of OTU0 (Gammaproteobacteria, E01-9C-26), the most abundant OTU in *W. bursa*, did not significantly change with depth (VIP < 1). In contrast, a decreasing relative abundance was observed for OTU6 (Planctomycetes, *Rubripirellula*) in specimens taken below 1000 m depth. However, this OTU was not affiliated with any of the sponge-enriched clusters (Figure 4).

For *S. fortis*, prokaryotic community composition of 15 specimens was assessed and resulted in a total of 461 OTUs with 138 OTUs designated as important contributors (VIP score >1) based on OPLS. Depth contributed to 18% (Supplementary Table 2) of the variation in the prokaryotic community composition of *S. fortis* (Supplementary Table 3, $p = 0.001$), and 89 OTUs had a relative abundance of $\geq 0.25\%$ (Figure 5). In addition, 70% ($n=63$) of these most abundant OTUs were affiliated with sponge-enriched clusters as based on the EMP database. OTU135 (SBR1093) was the predominant OTU in *S. fortis* and its relative abundance decreased in deep specimens. A similar trend was found for other predominant OTUs, including OTU137 (Acidobacteria, subgroup 9, VIP 2.31), OTU146 (Thaumarchaeota, and *Cenarchaeum*, VIP 1.38), which showed higher relative abundances in specimens above 1000 m compared to their deep-water counterparts. Conversely, an increasing trend of relative abundance with depth was observed for OTU337 (Acidobacteria, subgroup 9, VIP 4.28) and thaumarchaeotal (*Cenarchaeum*) OTU138 (VIP 1.46) and OTU454 (VIP 2.49) (Figure 5). In addition, all OTUs that changed significantly with depth, along with abundant OTUs assigned to Chloroflexi, were affiliated with sponge-enriched clusters. However, relative abundance of Chloroflexi OTUs was generally stable across different depths.

For *G. barretti* prokaryotic community composition of 14 specimens yielded a total of 420 OTUs with 139 OTUs designated as important contributors (VIP score >1). Depth accounted for 29% (Supplementary Table 2) of the variation in prokaryotic community composition in *G. barretti* (Supplementary Table 3, $p = 0.001$). Among the most abundant OTUs (Figure 6), 74 OTUs belonged to sponge-enriched clusters. In addition, 60 of these OTUs were also present as pre-dominant OTUs in *S. fortis*. Similar to *S. fortis*, OTU135 (SBR1093) had the highest average relative abundance, but unlike for *S. fortis* this OTU did not vary significantly with depth in *G. barretti* (VIP = 0.15). Decreasing relative abundance in deep specimens was observed for OTU144 (Acidobacteria, subgroup 9, VIP 3.14) and OTU146 (Thaumarchaeota, *Cenarchaeum*, VIP 2.47), whereas OTU138 (Thaumarchaeota, *Cenarchaeum*, VIP 2.88) and OTU337 (Acidobacteria, subgroup 9, VIP 2.50) displayed a higher relative abundance in specimens taken from depths below 1000 m as was also found for *S. fortis*. Furthermore, the majority of Chloroflexi OTUs were assigned to sponge-enriched clusters (Figure 6), but their relative abundance did not vary with depth.

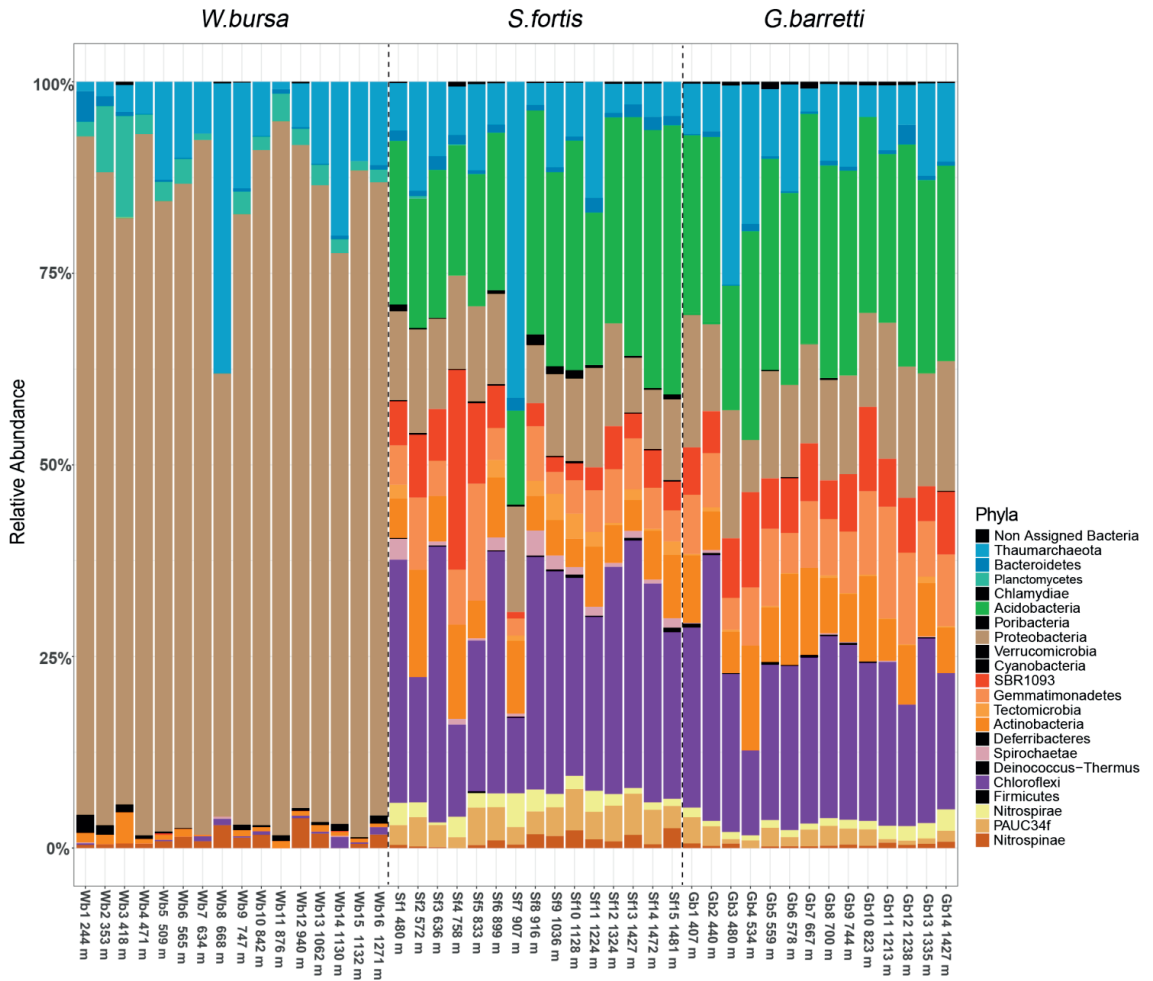


Figure 2. Prokaryotic community composition of *Weberella bursa* (Wb), *Stryphnus fortis* (Sf) and *Geodia barretti* (Gb) at the phylum level based on relative abundance of assigned 16S rRNA gene sequences. Phyla with average relative abundances lower than 0.25% in all samples, i.e. Chlamydiae, Poribacteria, Verrucomicrobia, Cyanobacteria, Deferribacteres, Deinococcus-Thermus and Firmicutes) are coloured in black. Specimens were arranged by decreasing depth from left to right per sponge species.

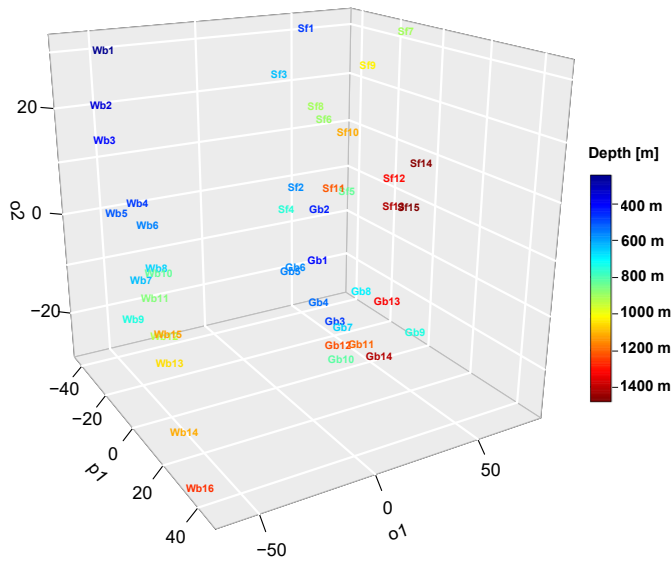


Figure 3. Three dimensional ordination of prokaryotic community composition at the OTU-level for *Weberella bursa* (Wb), *Stryphnus fortis* (Sf) and *Geodia barretti* (Gb) based on the OPLS method. Sponge specimens are coloured based on their depth. Axes o1, o2 and p1 refer to orthogonal 1, orthogonal 2 and predicted variation.

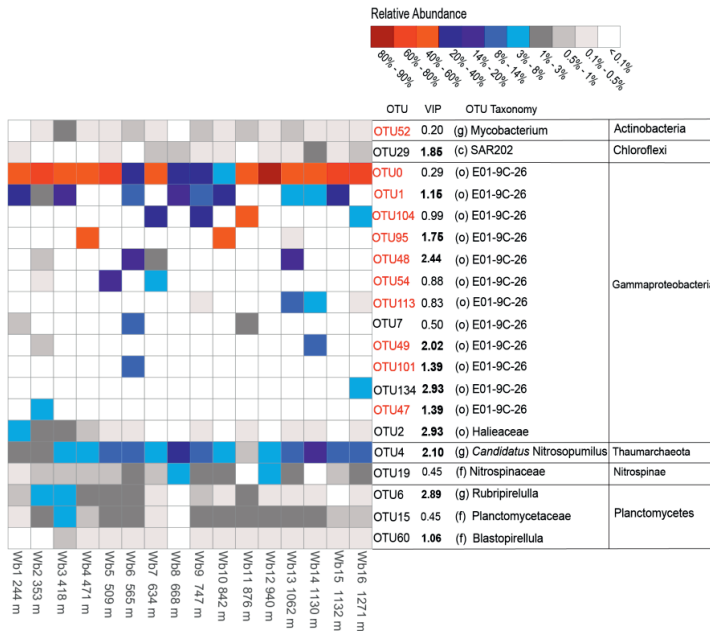


Figure 4. Heatmap with the most abundant OTUs (average relative abundance $\geq 0.25\%$ in all specimens) in *W. bursa*, including their taxonomic affiliation and VIP value. A letter in parentheses indicates the lowest reliably assigned taxonomic level: (c) class, (o) order, (f) family, (g) genus. OTUs highlighted in red were assigned to sponge-enriched clusters and VIP values in bold are > 1 , indicating that these OTUs significantly contribute to the separation of samples in relation to depth as shown in Figure 3.

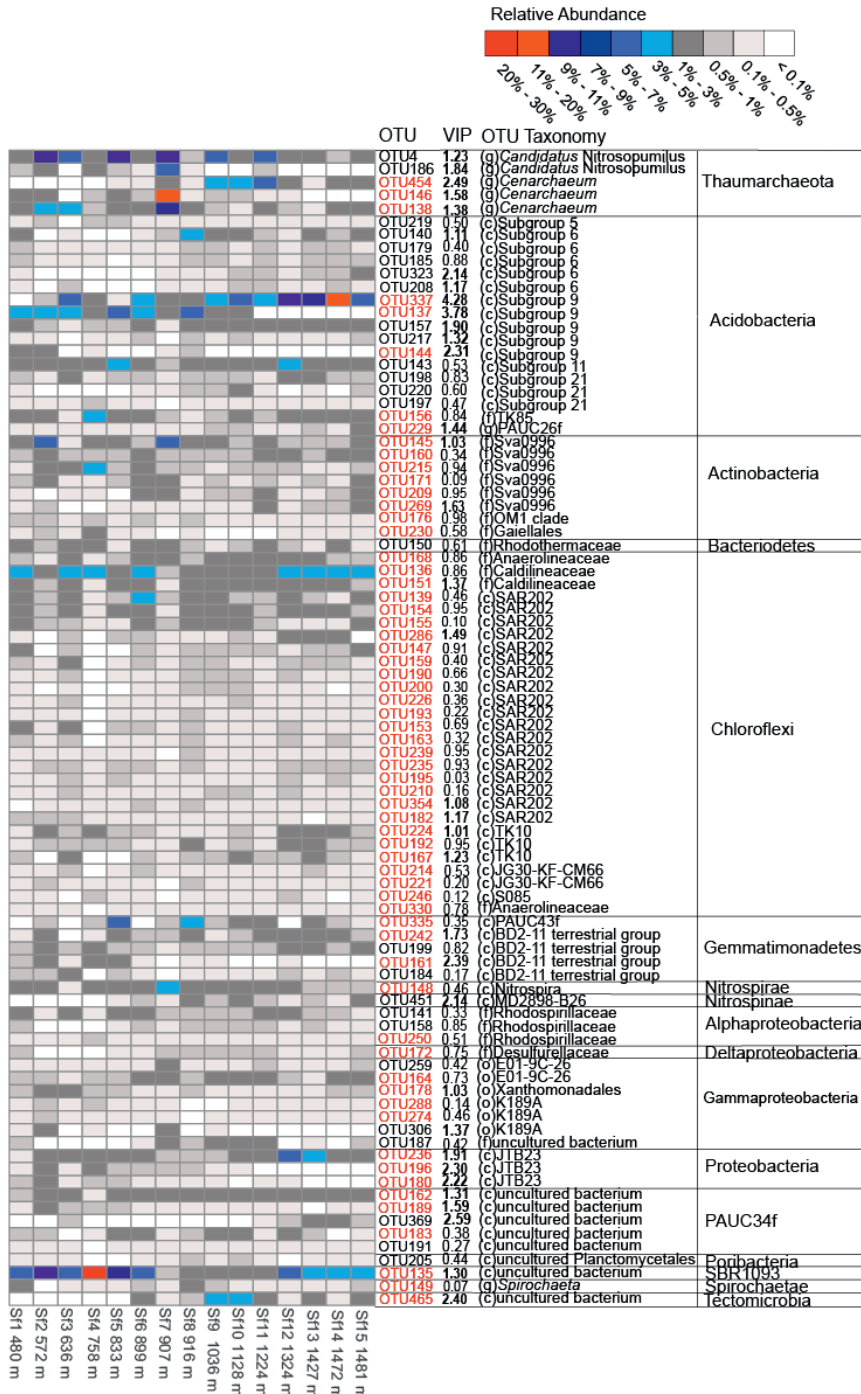


Figure 5. Heatmap with the most abundant OTUs (average relative abundance $\geq 0.25\%$ in all specimens) in *S. fortis*, including their taxonomic affiliation and VIP value. A letter in parentheses indicates the lowest reliably assigned taxonomic level: (c) class, (o) order, (f) family, (g) genus. OTUs highlighted in red were assigned to sponge-enriched clusters and VIP values in bold are > 1 , indicating that these OTUs significantly contribute to the separation of samples in relation to depth as shown in Figure 3.

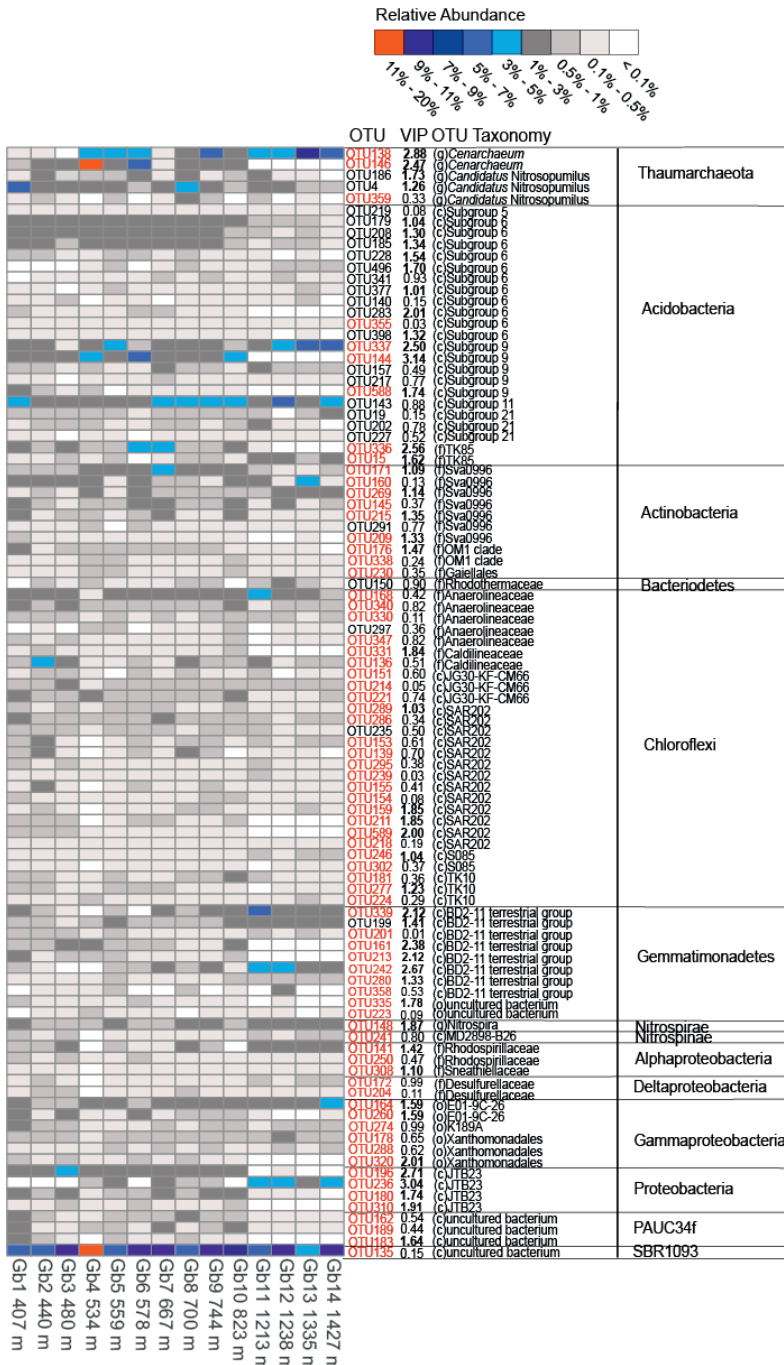


Figure 6. Heatmap with the most abundant OTUs (average relative abundance $\geq 0.25\%$ in all specimens) in *G. barretti*, including their taxonomic affiliation and VIP value. A letter in parentheses indicates the lowest reliably assigned taxonomic level: (c) class, (o) order, (f) family, (g) genus. OTUs highlighted in red were assigned to sponge-enriched clusters and VIP values in bold are > 1 , indicating that these OTUs significantly contribute to the separation of samples in relation to depth as shown in Figure 3.

Metabolic profiling

As we measured the metabolome of the sponge and all its microbiota indiscriminately, we subsequently refer to the holobiont. Multivariate analyses of the holobiont metabolomes with OPLS models showed that the percentage of variation correlating with depth was 17% in *G. barretti*, 14% in *S. fortis* and 12% in *W. bursa* (Supplementary Table 2). Overall, the metabolomes of the three holobionts were significantly different (PERMANOVA, $p=0.001$ in the HILIC positive data set, Supplementary Table 3). The metabolomes of the samples clustered based on host identity (Figure 7), indicating that each holobiont synthesizes a specific set of compounds and that these sets were unique and different from those produced by the other sponge species.

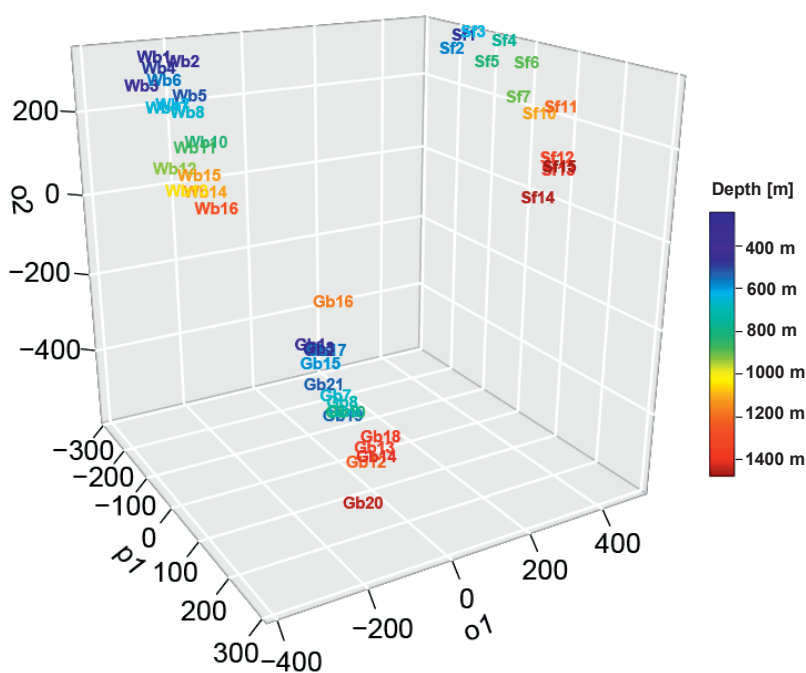


Figure 7. OPLS-based three-dimensional ordination plot of HILIC positive mode metabolite profiles of sponge specimens. Abbreviations with number refer to sponge specimens: Wb (*Weberella bursa*), Gb (*Geodia barretti*), and Sf (*Stryphnus fortis*). Specimens were coloured based on their original depth (in m) as indicated by the colour scale. The axes o1, o2 and p1 refer to orthogonal 1, orthogonal 2 and predicted variation.

Furthermore, investigation of individual variation by comparing chromatograms between representative shallow (200 – 400 m depth) and deep (>1000 m depth) specimens showed that *S. fortis* and *W. bursa* generally had stable metabolite profiles with respect to depth. In contrast, in *G. barretti*, major chromatographic peaks sharply decreased in deep specimens (Figure 8). Metabolomic profiling by targeting retention times of known compounds led to identification

of six bioactive compounds from *G. barretti* holobionts (barettin, 8,9-dihydrobarettin, compound#4, soelterin, 6-bromoconicamin, barretides A and B) and two compounds from *S. fortis* holobionts (ianthelline, stryphnusin) (Figure 9). Unfortunately, no specific bioactive compounds could be identified from metabolite profiles of *W. bursa* holobionts. Overall, the amounts of several of these specific compounds as based on the area under the curve of the chromatograms, significantly correlated with depth (R cor.test reporting Spearman's rho (ρ) and the p-value of significant correlations: barettin $\rho=-0.72$, $p=0.001$; 8,9-dihydrobarettin $\rho=-0.55$, $p=0.02$; soelterin $\rho=-0.70$, $p=0.002$; ianthelline $\rho=0.92$ $p<0.001$, stryphnusin $\rho=0.90$, $p<0.001$). Compounds from *G. barretti* showed either no correlation or a negative correlation with depth, while both compounds from the holobiont *S. fortis* showed a positive correlation with depth.

To select yet unknown metabolites correlated with depth in addition to the known bioactive compounds addressed above, we putatively identified the features (ions with unique mass, charge and retention time) to metabolites with the highest VIPs from the OPLS of the metabolome acquired by HILIC positive mode, and confirmed their identity with standards (Figure 10). Compounds showed different intensities and patterns of positive, negative or no correlation with depth in the three holobionts. Among the identified features with high VIPs, the following metabolites showed a significant correlation with depth in *G. barretti* (arsenobetain $\rho=-0.72$, $p=0.0016$; creatine $\rho=-0.65$, $p=0.010$; carnitine $\rho=-0.67$, $p=0.004$; phosphocholine $\rho=0.71$, $p=0.002$; uranidine $\rho=-0.82$, $p<0.001$), *S. fortis* (creatin $\rho=-0.764$, $p=0.003$; 2-methylbutyroylcarnitine $\rho=0.88$, $p<0.001$), and *W.bursa* (arsenobetain $\rho=0.61$, $p=0.015$, carnitine $\rho=0.53$, $p=0.037$).

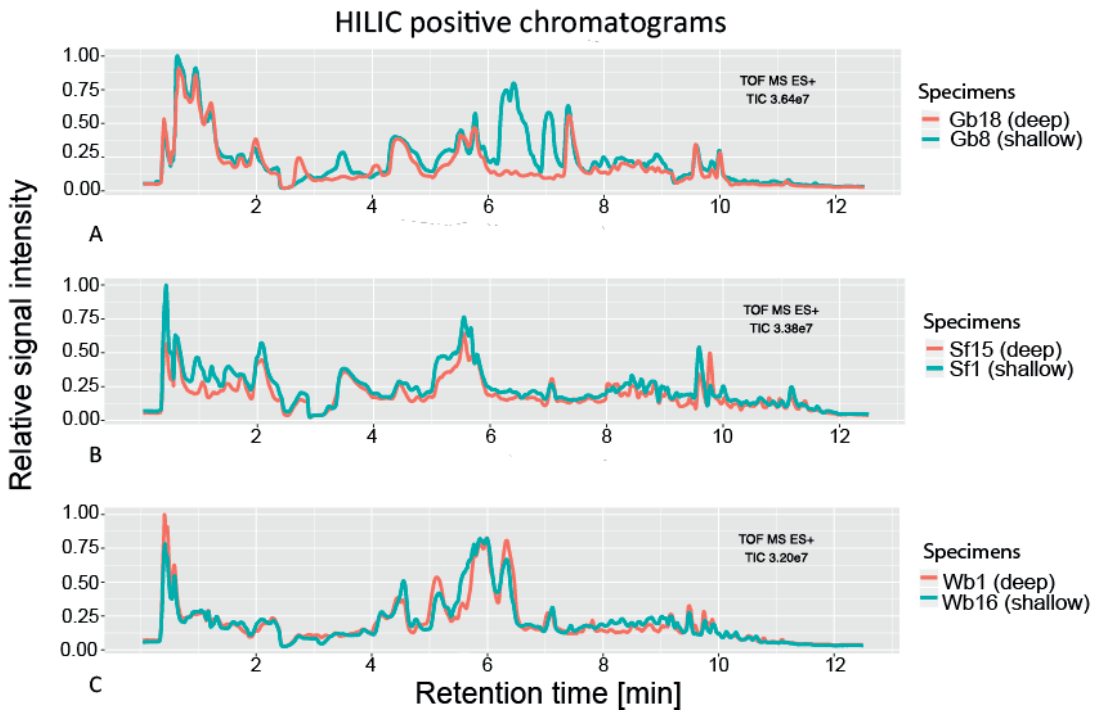


Figure 8. Holobiont metabolic fingerprints from representative shallow and deep specimens of *G. barretti*, *S. fortis* and *W. bursa* based on chromatograms obtained by HILIC column and positive ionization mode.

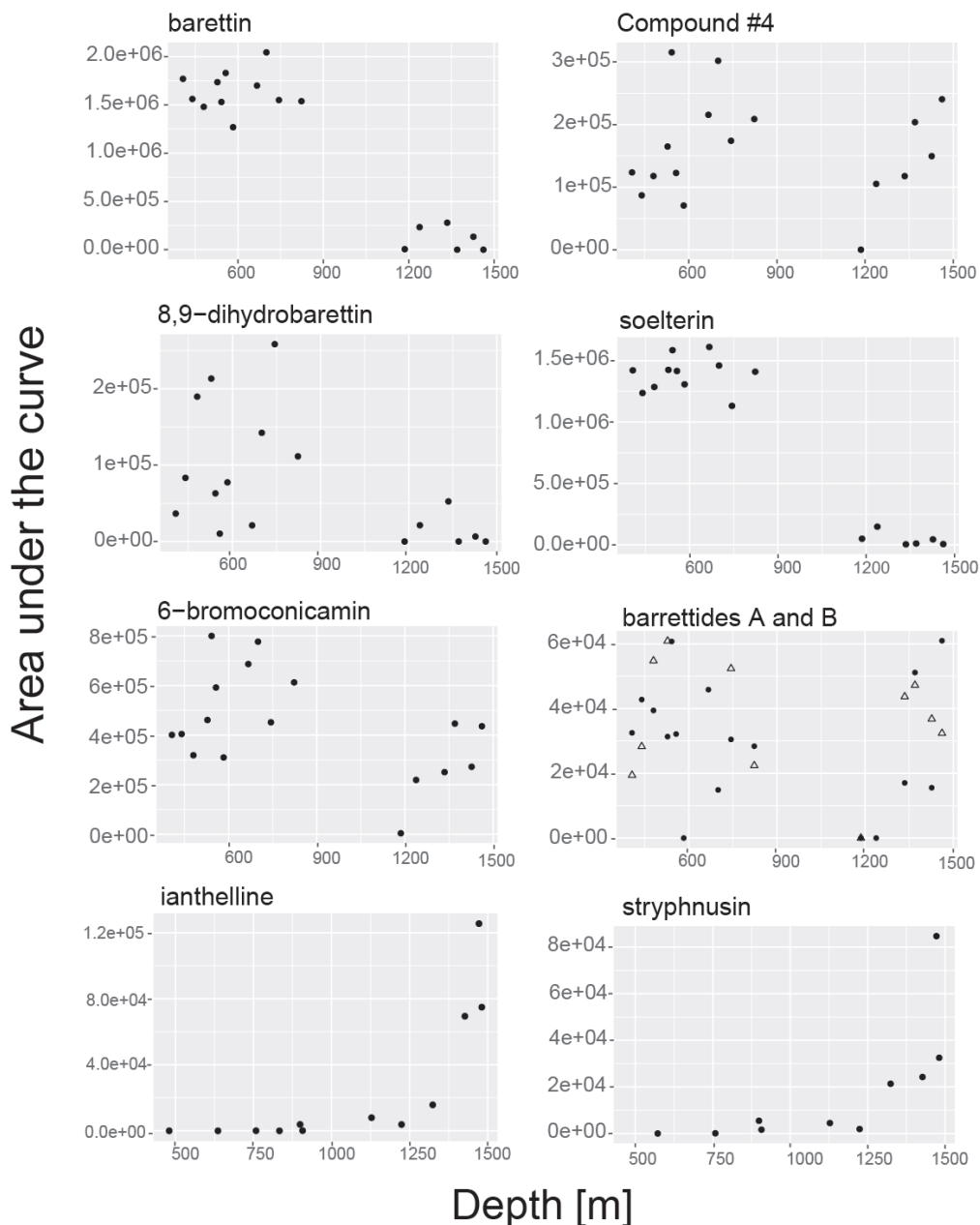


Figure 9. Specific metabolites from *G. barretti*: baretin, compound #4, 8,9-dihydrobaretin,soelterin, 6-bromoconicamin, and the peptides barrettide A (full dots), barrettide B (empty triangles) and *S. fortis* (ianthelline, stryphnusin). Data is extracted from the HILIC positive data set.

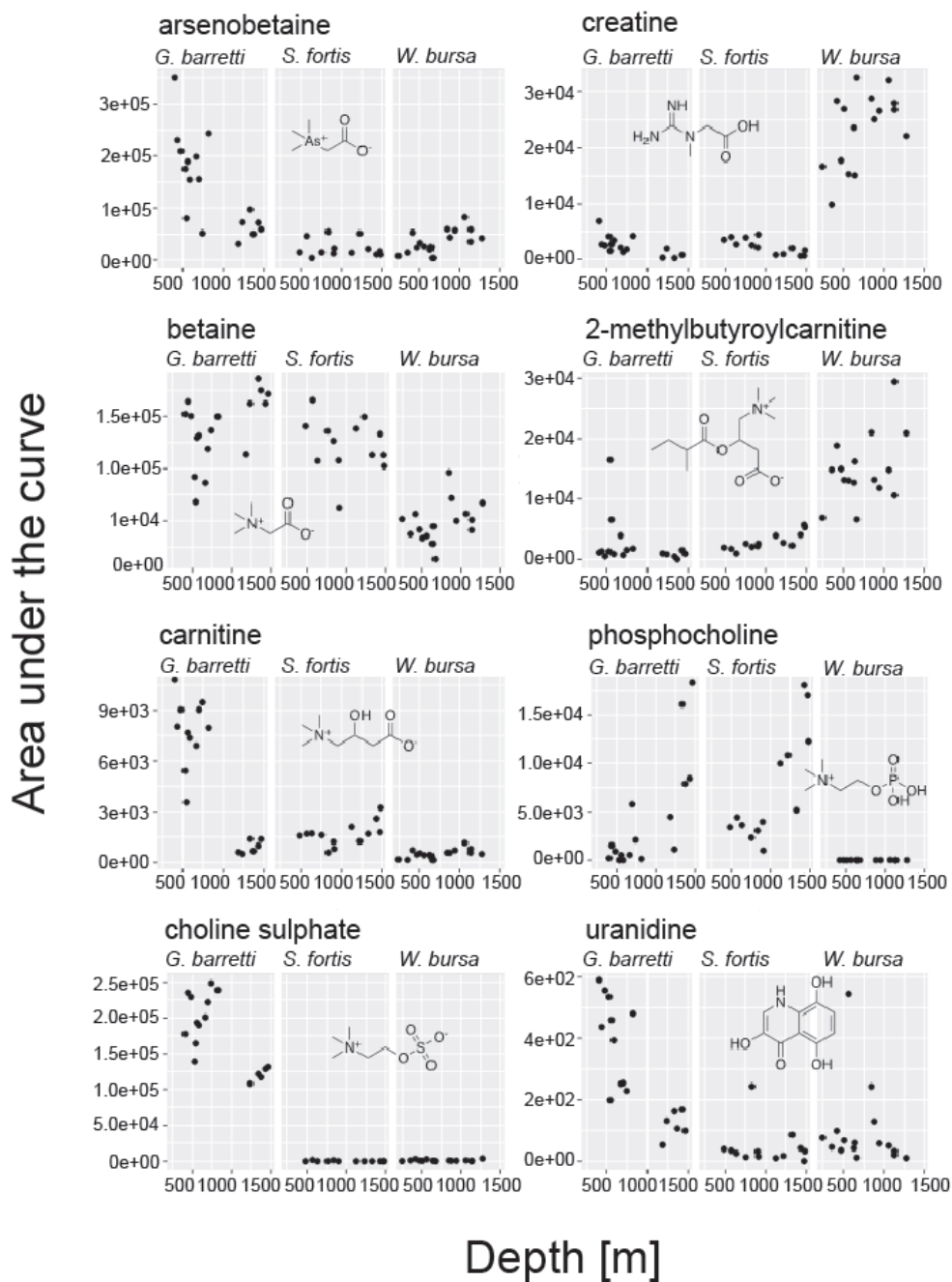


Figure 10. Metabolite concentrations in relation to depth for all three sponge holobionts selected based on the highest scoring VIPs from OPLS of data acquired in HILIC positive mode.

Discussion

Sponge-associated prokaryotes at different depths

At phylum level, the prokaryotic communities associated with the sponge holobionts appeared to be stable across a wide range of depth (400 to 1400 m) (Figure 2). Meanwhile, large numbers of the underlying OTUs varied in relative abundance with depth, or were even not found at all depths along the slope (Figures 3). OPLS models showed that 26% of OTUs in *Weberella bursa*, 30% in *Stryphnus fortis*, and 33% in *Geodia barretti* are designated VIPs, thus correlating with depth. Furthermore, the majority of the most abundant OTUs found in both *G. barretti* and *S. fortis* belongs to sponge-enriched clusters as identified in the sponge microbiome project [25] and represented 14 phyla (Figure 4 and 5). Conversely, in *W. bursa*, the OTUs assigned to sponge-enriched clusters were mainly affiliated with the Gammaproteobacteria (E01-9C-26) (Figure 3).

The prokaryotic communities associated with specimens of *G. barretti* and *S. fortis* were highly similar, as reflected in the composition of their most abundant OTUs. The most abundant OTUs that varied most with depth (VIPs) were affiliated with sponge-enriched clusters and assigned mainly to two phyla, namely the Thaumarchaeota (*Cenarchaeum* and *Candidatus Nitrosopumilus*), and the Acidobacteria (Subgroup 9). As shown for *G. barretti* (Figure 6) and *S. fortis* (Figure 5), a declining trend of relative abundance in specimens retrieved from depths below 1000 m was observed for OTU138 (*Cenarchaeum*). Conversely, OTU146 (*Cenarchaeum*) showed generally higher relative abundances in specimens collected above 1000 m, but was nearly absent in specimens collected below 1000 m in both sponges. Thaumarchaeota are one of the important constituents of prokaryotic communities of sponges and have been associated with nitrogen cycling, and particularly ammonia oxidation [339,431]. The inverse relationship of the relative abundance of the two cenarchaeal OTUs 138 and 146 with depth may indicate that they have each adapted to life at a certain, limited depth range (or associated environmental factors). Similar to Thaumarchaeota, Acidobacteria are a predominant phylum in sponges from shallow to deep-sea habitats [24,84,308,333]. We observed high relative abundance of acidobacterial OTU337 (Subgroup 9) in specimens below 1000 m for both *S. fortis* and *G. barretti*. In contrast, in samples retrieved above 1000 m, OTU137 (Subgroup 9) was more prevalent in *S. fortis* whereas for *G. barretti* it was OTU144 (Subgroup 9). Although the ecological role of Acidobacteria in marine sponges is largely unknown, in terrestrial habitats they are often predicted to play a role in degradation of

recalcitrant organic compounds [332,334]. It is tempting to speculate that in marine sponges Acidobacteria may have a similar role as their terrestrial counterparts.

We also observed a number of Chloroflexi among the most abundant OTUs in both *S. fortis* and *G. barretti* specimens. However, generally these OTUs were observed at rather stable relative abundances across different depths. The most predominant Chloroflexi OTUs found in both sponges were affiliated with sponge-enriched clusters and were mainly assigned to SAR202. A previous study reported that SAR202-Chloroflexi have been associated with sulfite-oxidation and predicted to be important during sulfur turnover in the deep sea [432]. OTU135 assigned to the candidate phylum SBR1093 displayed the highest average relative abundance in both *S. fortis* and *G. barretti* specimens across different depths, however, the functional role of this candidate phylum in sponges remains elusive. A metagenomic reported that SBR1093 genomes harbour genes encoding for carbon fixation via the hydroxypropionate-hydroxybutyrate pathway, but also indicated this phylum is clustered closely with phylotypes of heterotrophs bacteria, *Bradyrhizobiaceae* [433]. Thus, the prevalence of SBR1093 could indicate that this OTU plays a role as a mixotroph in both of *S. fortis* and *G. barretti*. Overall, the prevalence of these sponge-enriched clusters assigned to Thaumarchaeota, Acidobacteria, Chloroflexi and SBR1093 as observed in both HMA sponges indicated that phylogenetically related OTUs, which are likely to have the same role in the sponge holobiont, are hosted by sponges at different depths.

While the abundance of *S. fortis* in the Arctic regions has been well documented [103,111], this study is the first report on prokaryotic communities of *S. fortis*. Additionally, this work also for the first time describes the prokaryotic community composition of *W. bursa*, a typical LMA sponge. The prokaryotic composition of *W. bursa* was in general more stable across different depths than that of the other two sponge species. OTU4 (Thaumarchaeota, *Candidatus Nitrosopumilus*) was the only OTU that was present in all three sponges. However, OTU4 was not detected in the sponge EMP database, which may suggest that this OTU was recruited from the surrounding environment of the deep sea (seawater or sediment) rather than being a sponge symbiont.

In our study, we conceptualized depth as a proxy for other environmental (biotic/abiotic) factors, as depth *per se* would not likely affect the sponge or its microbiome. Previous studies on the impact of depth (0 - 200 m) on sponge prokaryotic communities showed a shift of a predominantly photoautotrophic bacterial community to a more heterotrophic bacterial

community as depth increased, which is mainly linked to the decrease of light intensity with depth [80,81]. However, for our study, light intensity was not likely to affect the microbial community as the shallowest sponges sampled were taken from places beyond light usable for phototrophic microorganisms [70]. Additionally, oceanic depth correlates with hydrostatic pressure (increasing about 1 atm. every 10 m), which was shown to affect enzyme activity and thereby metabolic rates to some extent [434]. Oceanic depth also correlates with temperature and salinity (Supplementary Figure 2), and more importantly, those factors correlated with each other in this study (Pearson's $p=0.44$, $p=0.0015$; Pearson's $p=0.62$, $p<0.001$; and Pearson's $p=0.86$, $p<0.001$ respectively). Interestingly, neither salinity [435] nor temperature [75] on their own were shown to affect sponge microbiota in shallow water. In conjunction, water temperature and salinity are fundamental parameters in oceanography/hydrography characterizing and identifying discrete water masses. Different water masses in the North Atlantic and Arctic were shown to contain specific microbiota [436-438]. This means that rather than biogeography, the affiliation to a particular water mass and thus depth structures oceanic microbiomes. Although the exact positions are subject to strong seasonal and inter-annual changes, three water masses are discernible at our study site in Davis Strait [439], and samples taken from depths below 1000 m are likely to be exposed to two water masses. Previous studies indicated that water masses acts as dispersal barrier for microorganisms in the deep sea, and each water mass harbours specific prokaryotic communities [440-442]. However, our result indicated sponges could maintain their microbiota composition despite of the exposure of different water masses. In this study, no seawater samples were included. However, given the oceanographic variations at our study site [439], the seawater samples taken today might not necessarily adequately reflect microbial exposure of the sponge specimens several decades ago at the time of their larval settlement. Regarding the use of seawater samples to assess the current environmental background, we deem this less important, as despite all specimens in this study being sampled in one locality, overlap in terms of OTUs shared by all three species is virtually non-existent. In addition, it was confirmed that most of the OTUs with high VIP values are indeed those that are generally enriched in marine sponges (and not seawater). However, we acknowledge that the addition of deep seawater samples might have given support to the zonation of certain microbes by water mass, which should be taken into account in future sampling campaigns.

In addition to acquisition of microbes from the water column, the sponge microbiome is partly inherited [278,408,409,443], and once acquired, it appears resistant to changes and various

stressors [77,274,435,444]. To consolidate these findings and explain the pattern of OTU shifts with depth, we therefore propose the adult sponge microbiomes to be structured partly by vertically transmitted microbes, and partly by the microbiome present in the surrounding water mass at the time of larval settlement and early development of the sessile organism. This point prompts future investigations towards elucidating the factors mediating the assembly of sponge host-specific microbiomes in different environments. It is conceivable that there is direct or indirect selection for a functional microbial community (or at least some elements thereof) in the sponge holobiont [24].

Metabolic profiling of sponges from different depths

Concentrations of three metabolites associated with *G. barretti*, baretin, 8,9-dihydrobaretin and soelsterin, were found to be significantly negatively correlated with depth (Figure 9). While soelsterin has not been tested in any assay to our knowledge, baretin and 8,9-dihydrobaretin were found to have several bioactivities [445]. Thus far, their main function is believed to be anti-biofouling, inhibiting settlement of barnacle larvae on the sponge. Interestingly, a third small molecule, 6-bromoconicamin, and the peptides barrettide A and B, all with the same bioactivity, showed no significant trend with depth [115,116,446]. Analogous to that, ianthelline described from *S. fortis* has been shown to inhibit both micro- and macrobiofouling [109] as has been found for other bromotyrosine derivatives [447].

Supposing that all these compounds are indeed involved in anti-biofouling in the sponge, we would expect they would show the same trend, which was not the case as the ianthelline concentration in *S. fortis* increased with depth. This initial contradiction might be resolved by investigating their specific contribution to the anti-biofouling. Biofouling is a complex and sequential process. A surface immersed in water is initially primed by adsorption of organic molecules, subsequently covered by a developing bacterial biofilm and thereafter populated by macrofoulers [448]. Therefore, anti-fouling molecules with different modes of action may be needed. While ianthelline was shown to have a broad antibacterial activity [109], barrettin and 8,9-dihydrobaretin are not cytotoxic [115]. The combination of non-toxic and biofilm formation-inhibiting properties can be modulated by activities affecting quorum sensing (e.g. by quenching or interference) [449,450]. This combination of properties is highly desirable for production of antifouling coatings, as it has been shown that macrofoulers obtain settlement cues from direct contact with biofilms [451,452]. The cyclodipeptides baretin and 8,9-dihydrobaretin belong to the diketopiperazines, whereas 6-bromoconicamin and compound #4

are indoles. Diketopiperazines and indoles have been described as quorum sensing molecules modulating microbial processes, such as biofilm formation and virulence [453]. Ultimately, this bridges bioactivity studies with hypotheses about the processes mediating microbiome composition and maintenance in holobionts. It has been shown that the cnidarian *Hydra vulgaris* is able to interfere with quorum sensing of its major bacterial associate *Curvibacter* sp. [454].

However, the role of the discussed molecules is somewhat more ambiguous. In addition to anti-biofouling activities, baretin, 8,9-dihydrobaretin, 6-bromoconicamine, and stryphnusin are acetylcholinesterase inhibitors [110,455]. Furthermore, baretin, 8,9-dihydrobaretin, 6-bromoconicamine, (and to some extent also compound #4) are also butyrylcholinesterase inhibitors. In the framework of glycerophospholipid metabolism, acetylcholinesterase (EC 3.1.1.7) catalyses the reaction of o-acetylcholine to choline and acetate. Choline is then further enzymatically transformed to phosphocholine by a choline kinase (EC 2.7.1.32). In case baretin, 8,9-dihydrobaretin and ianthelline display their acetylcholinesterase inhibiting effect *in vivo* and throughout the holobionts, we should see an effect downstream of that enzyme. As baretin and 8,9-dihydrobaretin decrease, AChE inhibition should decrease and thus more choline (and phosphocholine) should be observed. In contrast, as ianthelline increases in the deep samples, AChE inhibition should increase and we should observe less choline (and phosphocholine). Our data does not support this hypothesis, as spearman correlation tests between choline and the AChE inhibitors did not produce significant (negative) results (Figure S4). In addition, another interesting bioactivity was established as baretin and 8,9-dihydrobaretin were found to be selective ligands for 5'-HT serotonin receptors [456].

Both ianthelline and stryphnusin showed increasing concentrations in deep-sea *S. fortis* specimens. A previous study suggested that ianthelline was actually not produced by *S. fortis* but by an overgrowing sponge *Hexadella detritifera* [106]. Therefore, it cannot be excluded that ianthelline was not detected in specimens above 1000 m because the epibiont sponge may have been absent on *S. fortis* tissue, while *H. detritifera* tissues were present in specimens below 1000 m. Given that the increasing trend of stryphnusin in the deep specimens resembles the same pattern as that of ianthelline, it could be that also stryphnusin was actually produced by the epibiont sponge. However, future investigation is needed to support this hypothesis.

Among the compounds identified based on their VIP values (Figure 10), six were significantly correlated with depth (arsenobetaine, creatine, 2-methylbutyrylcarnitine, carnitine,

phosphocholine, and uranidine). Interestingly, this correlation was positive in one sponge species and negative in another (e.g. carnitine, arsenobetaine). Arsenobetaine, creatine, betaine, carnitine and choline sulphate are known osmolytes or “compatible solutes” [457-459]. Osmolytes regulate the osmolarity and thus the tonicity of a cell. Osmoconforming organisms generally adapt by synthesising organic molecules compatible with cellular functions and peptides/enzyme activity. The presence of compounds regulating the cells’ response to osmolarity, i.e. salinity of the surrounding seawater, seems logic as salinity increases with depth from 33.29 psu to 34.92 psu across our samples (Supplementary Figure 1, Supplementary Table 1). However, as we observe the holobiont, we cannot easily discern sponge and bacterial adaptations. An interesting observation concerns betaine and arsenobetaine, as the latter decreased with depth in *G. barretti* and increased in *W. bursa* while betaine levels/signals remain stable. The different responses in the sponges are intriguing, as betaine levels remain stable. It has been shown that arsenobetaine is produced in environments where phosphate and arsenate are present as the compounds cannot be distinguished during uptake due to their similar size [460]. The different trends shown by our data challenge that notion. In case of indiscriminate incorporation, we would expect the trend of arsenobetaine to mirror that of betaine. Although quantitative comparisons as (vaguely) reflected by signal intensity should be taken with a pinch of salt, it appears that the major osmolyte among the identified compounds differs by sponge host. In *W. bursa*, creatine is seemingly more abundant than in the other two sponges, whereas arsenobetaine, carnitine and choline sulphate are more abundant in *G. barretti*.

Overall, our findings that both known bioactive compounds (Figure 9) and other newly identified compounds (Figure 10) vary with depth have broad implications. Thus far, factors affecting specialized metabolite production have been enigmatic, inconclusive or contradictory [291,420,421,461]. What seemed to affect production of bioactive compounds was seasonality (correlating with water temperature), however, reproduction did not consistently affect metabolites [417,420,421]. While we have no data on reproductive status of the sponges at the time of sampling, all samples were taken during the same season.

From an ecological point of view, the trends we observe are interesting as they present strong evidence for changes in habitat as perceived by the holobiont. Decrease in bioactive compounds could be either due to biofoulers not being present in the deep North Atlantic (thus the producing microbes are still present but not producing the compound) or the putative microbial producer may be absent or greatly reduced in the sponge holobiont. As we are not

aware of particular overgrowth of *G. barretti* at great depths and we cannot observe new chromatographic peaks, e.g. of a new compound compensating for the loss of barrettin, we hypothesize that indeed the deeper individuals do not need biofouling protection (given that is the true function of the bioactive compounds in Figure 9). Therefore, also from a bioprospecting point of view, it is interesting that depth strongly positively and negatively affects production of known bioactive compounds. This suggests that the deep sea is a source for metabolites not found in shallower water and *vice versa*. In addition, correlations between certain prokaryotic OTUs and secondary metabolite concentrations may help identify the true producers of these metabolites as those are currently mostly unknown.

Conclusion

To our knowledge, this is the most exhaustive survey of sponge specimens sampled at different depths to date. We showed herein that depth has a significant impact on prokaryotes associated with sponges and the metabolome of sponge holobionts. In *W. bursa*, we found the most dominant OTUs that varied with depth assigned to Gammaproteobacteria and Planctomycetes. In both *S. fortis* and *G. barretti*, the most pre-dominant OTUs that varied with depth represented by OTUs affiliated to Acidobacteria, Chloroflexi, Thaumarchaeota, and SBR1093. We observed that metabolite profile in the three deep-sea sponges is highly host-specific as shown by the trend on VIP compounds (arsenobetaine, creatine, 2-methylbutyrylcarnitine, carnitine, phosphocholine, and uranidine) varied among species. With respect on production of secondary metabolites, no clear pattern could be drawn as we found decreasing concentration of bioactive molecules assigned to *G. barretti* (barettin, 8,9-dihydrobarettin and soelterin), but increasing concentration of bioactive compounds associated with *S. fortis* (ianthelline and stryphnusin) was evident as depth increased.

Acknowledgments

Anak Agung Gede Indraningrat received a PhD fellowship from the Indonesia Endowment Fund for Education (LPDP), grant number 20140812021557. This study was financially supported by the SponGES project from the European Union's Horizon 2020 research and innovation programme under grant agreement No 679849.

Supplementary Information

Supplementary Table 1. Detailed sample and metadata information

Species	Depth (m)	Latitude	Longitude	Sample ID	Temperature (°C)	Salinity (PSU)	Year
<i>W. bursa</i>	244	6,157,688	-660,866	Wb1	0,37	33,29	2013
<i>W. bursa</i>	353	61,316,352	-6,878,077	Wb2	2,23	34,13	2011
<i>W. bursa</i>	418	630,277	-6,067,308	Wb3	3,79	34,72	2014
<i>W. bursa</i>	471	6,458,065	-5,913,768	Wb4	1,99	34,47	2013
<i>W. bursa</i>	509	64,298,317	-59,251,742	Wb5	2,32	34,56	2011
<i>W. bursa</i>	565	6,531,817	-5,817,717	Wb6	2,31	34,57	2014
<i>W. bursa</i>	634	6,456,132	-5,868,083	Wb7	3,05	34,70	2014
<i>W. bursa</i>	668	6,452,757	-5,866,903	Wb8	3,86	34,85	2013
<i>W. bursa</i>	747	6,452,541	-58,406,818	Wb9	4,01	34,91	2011
<i>W. bursa</i>	842	6,354,833	-59,918,103	Wb10	4,12	34,91	2011
<i>W. bursa</i>	876	63,696	-5,877,515	Wb11	4,05	34,92	2013
<i>W. bursa</i>	940	6,335,686	-59,225,978	Wb12	3,96	34,91	2011
<i>W. bursa</i>	1,062	6,338,503	-585,631	Wb13	3,79	34,91	2014
<i>W. bursa</i>	1,130	62,690,007	-58,942,747	Wb14	3,77	34,91	2011
<i>W. bursa</i>	1,132	63,101,907	-59,966,512	Wb15	3,82	34,91	2011
<i>W. bursa</i>	1,271	6,306,917	-585,297	Wb16	3,81	34,92	2013
<i>W. bursa</i>	645	6,502,363	-5,817,635	Wb17	2,97	34,71	2013
<i>S. fortis</i>	480	6,219,923	-612,192	Sf1	3,70	34,70	2014
<i>S. fortis</i>	572	6,176,735	-6,172,832	Sf2	4,57	34,89	2013
<i>S. fortis</i>	636	6,638,245	-5,831,742	Sf3	1,93	34,53	2014
<i>S. fortis</i>	758	62,170,797	-60,781,817	Sf4	3,78	34,82	2011
<i>S. fortis</i>	833	6,284,707	-6,053,698	Sf5	4,09	34,89	2014
<i>S. fortis</i>	899	6,298,347	-6,030,927	Sf6	4,08	34,92	2013
<i>S. fortis</i>	907	63,247,158	-60,165,435	Sf7	4,02	34,88	2011
<i>S. fortis</i>	916	6,309,856	-602,211	Sf8	3,88	34,90	2015
<i>S. fortis</i>	1,036	6,265,548	-5,915,816	Sf9	3,64	34,91	2015
<i>S. fortis</i>	1128	6,285,072	-5,878,482	Sf10	3,93	34,92	2013
<i>S. fortis</i>	1224	62,528,587	-59,202,887	Sf11	3,88	34,91	2011
<i>S. fortis</i>	1324	6,236,087	-6,007,323	Sf12	3,59	34,92	2014
<i>S. fortis</i>	1427	620,539	-6,009,182	Sf13	3,78	34,92	2013
<i>S. fortis</i>	1472	63,249,477	-5,796,573	Sf14	3,58	34,92	2011
<i>S. fortis</i>	1481	6,252,163	-5,939,852	Sf15	3,65	34,92	2014
<i>G. barretti</i>	407	6,288,293	-6,129,213	Gb1	2,41	34,49	2013
<i>G. barretti</i>	440	6,276,543	-614,302	Gb2	2,77	34,59	2013
<i>G. barretti</i>	480	6,219,923	-612,192	Gb3	3,70	34,70	2014
<i>G. barretti</i>	534	61,908,942	-63,637,153	Gb4	4,52	34,82	2011
<i>G. barretti</i>	559	648,909	-585,513	Gb5	2,99	34,70	2014
<i>G. barretti</i>	578	61,147,942	-63,560,678	Gb6	4,44	34,82	2011

<i>G. barretti</i>	667	6,268,804	-6,128,264	Gb7	3,73	34,80	2015
<i>G. barretti</i>	700	6,278,033	-6,115,217	Gb8	3,67	34,80	2013
<i>G. barretti</i>	744	625,893	-6,104,198	Gb9	3,87	34,83	2013
<i>G. barretti</i>	823	6,262,814	-60,925,362	Gb10	4,08	34,89	2011
<i>G. barretti</i>	1,213	6,287,086	-586,262	Gb11	3,58	34,92	2015
<i>G. barretti</i>	1,238	6,285,113	-5,999,052	Gb12	N/A	N/A	2013
<i>G. barretti</i>	1,335	625,184	-5,997,052	Gb13	3,60	34,92	2014
<i>G. barretti</i>	1,427	620,539	-6,009,182	Gb14	3,78	34,92	2013
<i>G. barretti</i>	583	6,255,291	-61,373,675	Gb15	3,63	34,75	2011
<i>G. barretti</i>	1,186	6,254,747	-6,028,848	Gb16	3,71	34,92	2014
<i>G. barretti</i>	557	6,242,628	-6,125,654	Gb17	3,65	34,74	2015
<i>G. barretti</i>	1,370	6,224,725	-600,496	Gb18	3,70	34,92	2013
<i>G. barretti</i>	542	65,448	-5,818,323	Gb19	2,05	34,54	2013
<i>G. barretti</i>	1,462	62,551,802	-59,527,228	Gb20	N/A	N/A	2011
<i>G. barretti</i>	528	63,938,048	-60,027,428	Gb21	N/A	N/A	2011

Supplementary Table 2. OPLS model of each sponge based on OTU-level prokaryotic community data (A) and metabolite profiles (B) generated from HILIC positive dataset. Microbiota data was normalised by applying square root of relative abundance. pR2Y, permutation of y response; pQ2, permutation of predictive performance; t1, percentage of explained variation.

A. Microbiota

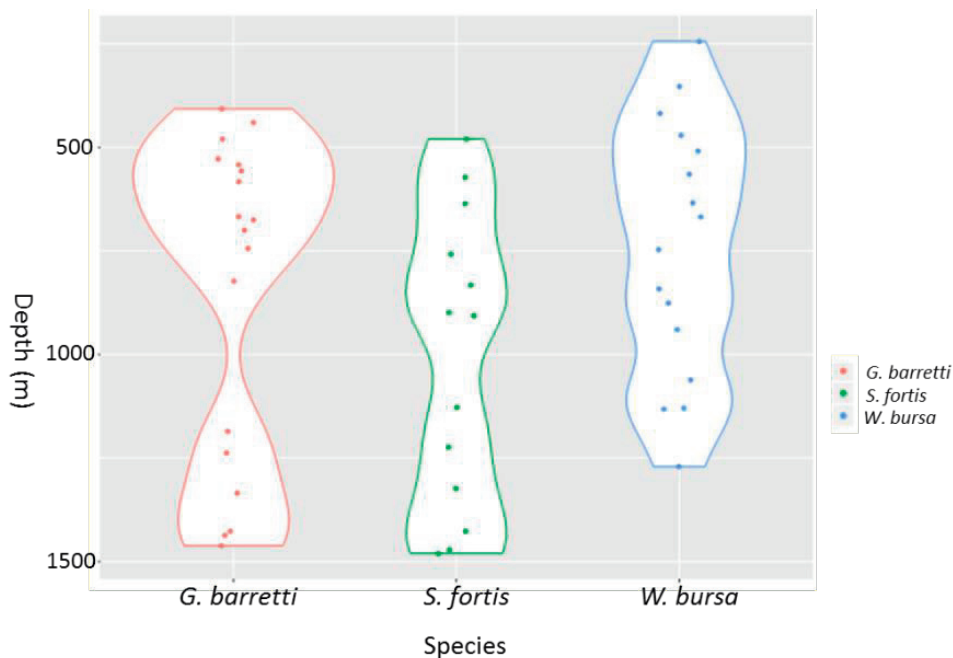
Species	Source of data	pR2Y	pQ2	t1 %	data set
<i>Geodia barretti</i>	OTU table	0.01	0.01	29	14 samples x 420 variables and 1 response
<i>Stryphnus fortis</i>	OTU table	0.01	0.01	18	15 samples x 461 variables and 1 response
<i>Weberella bursa</i>	OTU table	0.16	0.01	12	16 samples x 135 variables and 1 response

B. Metabolome

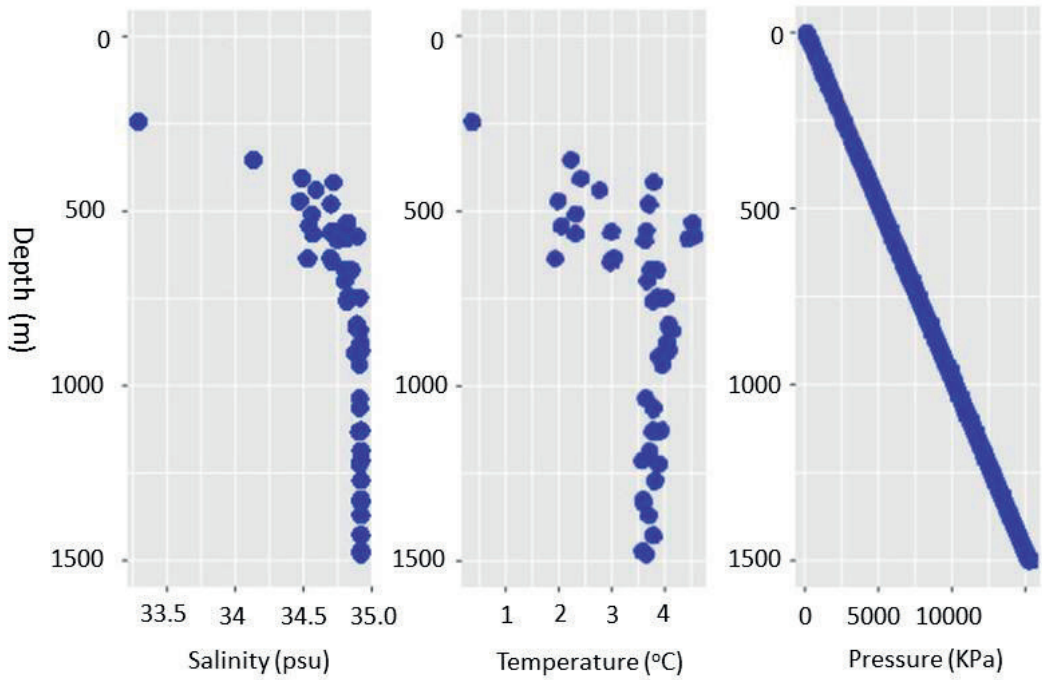
Species	Source of data	pR2Y	pQ2	t1 %	data set
<i>Geodia barretti</i>	HILIC pos	0.01	0.01	17	17 samples x 3507 variables and 1 response
<i>Stryphnus fortis</i>	HILIC pos	0.11	0.01	14	13 samples x 3507 variables and 1 response
<i>Weberella bursa</i>	HILIC pos	0.01	0	12	16 samples x 3507 variables and 1 response

Supplementary Table 3. Permutation ANOVAs of OTU-level prokaryotic community and metabolites based on HILIC positive dataset of *W. bursa*, *S. fortis* and *G. barretti* on parameter depth and other related physicochemical factors: latitude, longitude, year, salinity, and temperature.

Sponge	Parameter	R ²	p value	R ²	p value
<i>W. bursa</i>	Depth	0.14	0.009	0.13	0.003
	Latitude	0.09	0.093	0.15	0.001
	Longitude	0.04	0.69	0.07	0.11
	Year	0.05	0.7	0.1	0.023
	Salinity	0.07	0.27	0.08	0.06
	Temperature	0.05	0.59	0.05	0.26
<i>S. fortis</i>	Depth	0.23	0.001	0.14	0.003
	Latitude	0.08	0.24	0.08	0.37
	Longitude	0.04	0.8	0.07	0.38
	Year	0.06	0.56	0.07	0.35
	Salinity	0.05	0.72	0.09	0.21
	Temperature	0.06	0.48	0.1	0.1
<i>G. barretti</i>	Depth	0.4	0.001	0.22	0.001
	Latitude	0.065	0.18	0.1	0.054
	Longitude	0.09	0.07	0.04	0.69
	Year	0.04	0.37	0.05	0.42
	Salinity	0.06	0.17	0.03	0.84
	Temperature	0.05	0.34	0.06	0.22



Supplementary Figure 1. Distribution pattern of sponge specimens across different depth at the sampling site.



Supplementary Figure 2. Recorded trends of salinity, temperature and pressure across the sampling site.



Chapter 6

General Discussion



Introduction

Oceanic depth stratification links to various biological (e.g. predation, parasitism and competition) and physicochemical factors (e.g. salinity, temperature, light and nutrition), which together influence how organisms adapt to and are distributed in marine ecosystems [70,72]. Sponges are the oldest metazoans and among animals with large bathymetric distribution in oceanic environments spanning from shallow water to the deep sea [3,4,71]. Therefore, sponges are able to adapt to a wide range of environmental conditions related to depth, which could possibly also affect their prokaryotic community and metabolite composition. Alternatively, adaptations in the prokaryotic communities may have allowed sponges to colonize deeper or shallower habitats that would otherwise not be accessible. Sponges and their associated microbes have been regarded as ecologically important taxa in the marine habitat [3,11,19,71], and the sponge holobionts have attracted attention due to their remarkable array of bioactive compounds. A number of studies highlighted that sponge-prokaryotic associations remain stable irrespective of the biogeographical region [74], season [75,76], in response to short-term exposure to sub-lethal temperature [321], nutrient availability [462], pollution [276], and salinity [435]. Additionally, transplantation studies of sponges from shallow water to mesophotic depth and *vice versa* reported stability of microbiota and metabolite composition [78,463]. Conversely, only a few studies investigated sponge-microbiota associations across a natural depth gradient, which mainly covered shallow water to mesophotic depth [79-81], but no study assessed the impact of depth on prokaryotic community and metabolite composition of sponges in the deep sea. In addition, near to no studies have been done on the isolation of bacteria from sponges below shallow water habitats. Thus, it would also be intriguing to know whether depth affects cultivability of sponge-associated bacteria [4,43,282].

This thesis aimed to investigate how depth impacts prokaryotic community composition of marine sponges from shallow water (< 30 m) to mesophotic depth (30-90 m) and extending the survey to the deep sea (> 200 m) using 16S rRNA gene amplicon sequencing based on the Illumina MiSeq platform. This was complemented by a culture-dependent study using a range of different agar media to investigate the recovery of cultivable bacteria of sponges collected from shallow to mesophotic depths. In addition, a literature review was conducted to provide cues on the potential of sponge-associated microbes as antimicrobial producers. Finally, antimicrobial activities of the sponges and their associated microbes, along with sponge

holobiont metabolites were investigated related to depth. Figure 1 provides a brief overview of results obtained from each chapter, which will be further elaborated in the following sections.

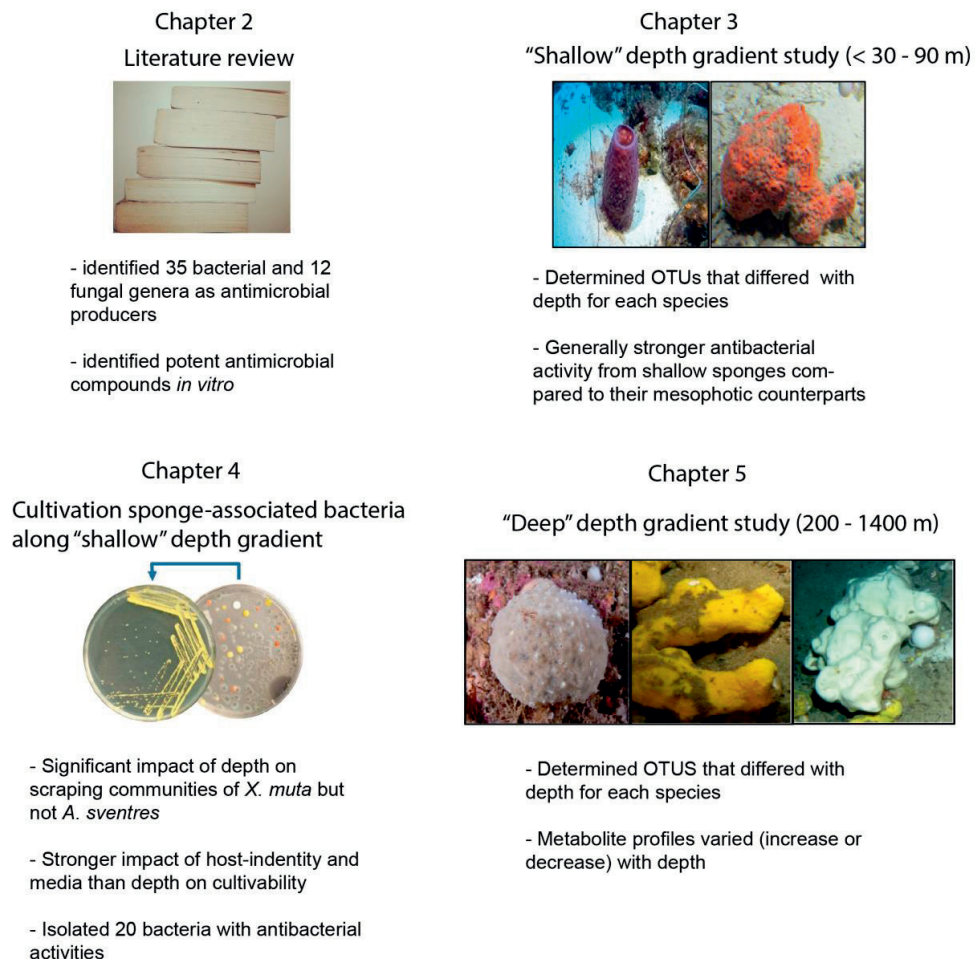


Figure 1. A brief overview of results obtained in Chapters 2 - 5.

Depth influences prokaryotic community composition of marine sponges

We surveyed prokaryotic community composition of sponges *Xestospongia muta* and *Agelas sventres* taken at different depths, ranging from shallow water to mesophotic depth in the Curaçao Sea (**Chapter 3**) and extended our study to the three boreal deep-sea sponges *Weberella bursa*, *Stryphnus fortis* and *Geodia barretti* taken from Davis strait (**Chapter 5**). At phylum level, generally a stable prokaryotic community composition was observed in each sponge species across the depth ranges studied (**Chapter 3**, Figure 1 and **Chapter 5**, Figure

2). However, at OTU level we observed separation of prokaryotic communities based on their depth origin (per species), and determined the most abundant OTUs that significantly contributed to the variation of prokaryotic composition with increasing depth (Table 1).

Table 1. Most abundant OTUs in each sponge with significant differences of relative abundance across different depths.

Sponge	OTU	Taxonomy	Trend with increasing depth
<i>X. muta</i>	OTU200	Cyanobacteria, Subsection I	Decrease
	OTU423	Cyanobacteria, Subsection I	Decrease
	OTU87	Thaumarchaeota, <i>Candidatus Nitrosopumilus</i>	Decrease
	OTU113	Actinobacteria, Sva0996	Decrease
	OTU29	Chloroflexi, SAR2002	Decrease
	OTU81	Chloroflexi, TK10	Decrease
	OTU7	Acidobacteria, Subgroup 6	Increase
	OTU11	Acidobacteria, Subgroup 11	Increase
	<i>A.sventres</i>	OTU503	Acidobacteria, PAUC26f
OTU552		Chloroflexi, SAR202	Decrease
OTU662		Chloroflexi, SAR202	Decrease
OTU591		Proteobacteria (Gammaproteobacteria)	Decrease
OTU527		Proteobacteria (<i>Endozoicomonas</i>)	Increase
OTU514		Thaumarchaeota,	Increase
<i>W. bursa</i>	OTU6	Planctomycetes, <i>Rubripirellula</i>	Decrease
<i>S. fortis</i>	OTU137	Acidobacteria, Subgroup 9	Decrease
	OTU146	Acidobacteria, Subgroup 9	Decrease
	OTU337	Thaumarchaeota, Subgroup 9	Increase
	OTU138	Thaumarchaeota, <i>Cenarchaeum</i>	Increase
	OTU454	Thaumarchaeota, <i>Cenarchaeum</i>	Increase
	OTU135	SBR1093	Decrease
	<i>G. barretti</i>	OTU144	Acidobacteria, Subgroup 9
OTU146		Acidobacteria, Subgroup 9	Decrease
OTU337		Thaumarchaeota, Subgroup 9	Increase
OTU138		Thaumarchaeota, <i>Cenarchaeum</i>	Increase

In both studies, we hypothesized that depth is a proxy for different physicochemical factors (e.g. light, nutrients, salinity, temperature) which may be directly related to the observed differences in sponge-associated prokaryotic community composition. Previously, a number of studies highlighted the strong correlation between depth on abundance and distribution of marine microbiota [283,464,465]. Cyanobacterial OTUs were only abundant in the prokaryotic community of *X. muta* and decreased in relative abundance from the shallow to deeper specimens, which is probably driven by the reduced irradiance at mesophotic depths. Our

results confirm previous holobiont studies on sponges regarding the decline of cyanobacterial OTUs associated with the reduced irradiance at mesophotic depths [79-81]. A previous study on *Callyspongia* spp. reported the prevalence of OTUs affiliated with the genus *Synechococcus* in shallow specimens, which were replaced by members of *Prochlorococcus* at mesophotic depths to indicate specialization of Cyanobacteria towards different light conditions [81]. Our result, however, did not show any replacement by other cyanobacterial OTUs as the relative abundance of Cyanobacteria Subsection I decreased in mesophotic specimens, which may indicate that prokaryotic community composition of *X. muta* was shifted more to heterotrophy as depth increased. Although we also observed differences in the relative abundance (increase or decrease) of taxa other than Cyanobacteria (Table 1), with our current data we cannot fully explain how these differences in the relative abundance of OTUs affect the metabolism of their hosts [25-28]. To this end, the availability of data on organic and inorganic nutrient concentrations is a critical prerequisite for the prediction of differences in the prevalence and abundance of specific heterotrophic bacteria across a depth gradient. For instance, the prevalence of a member of the Thaumarchaeota at all depths may provide cues for the presence of ammonia [466-468], since members of this phylum have been associated with ammonia oxidation and widely observed in sponges both in shallow and deep-sea habitats [84,308,338,405,431].

In both studies, we showed that the majority of the OTUs that significantly changed with depth were affiliated with so called “sponge-enriched clusters”. Sponge-enriched clusters refer to sequences that are highly associated with sponges, but can also be found at low abundance in seawater or sediment [407,469]. Sponge-enriched clusters further can be either “specific”, if they specifically affiliate to one or a few sponge species, or “cosmopolitan”, if they are present in multiple sponge species [24]. Interestingly, sequence comparison of these sponge-enriched cluster-affiliated OTUs using nucleotide BLAST revealed that OTU113 (Actinobacteria, Sva0996) and OTU4 (Nitrospirae, *Nitrospira*) found in *X. muta* were identical with OTU215 and OTU148, respectively, that were present in *G. barretti* and *S. fortis*. Additionally, sequence identification from the sponge EMP database showed that affiliated sequences of these two OTUs are also present in over 30 other sponge species, reinforcing that they might indeed be members of cosmopolitan sponge-enriched clusters [24]. Although ecological functions of sponge-enriched cluster OTUs are largely unknown, they could potentially be important to mediate biochemical processes within their host such as ammonia oxidation (Thaumarchaeota,

Cenarchaeum and *Candidatus Nitrosopumilus*) [308] or degradation of recalcitrant compounds (Chloroflexi, SAR202) [328].

We also observed that prokaryotic community composition of *X. muta*, *A. sventres* and seawater was distinctly separated with only a few overlapping OTUs, confirming the influence of host identity (Figure 2A). Interestingly, a much larger number of overlapping OTUs (Figure 2B) was observed when comparing prokaryotic communities associated with *S. fortis* and *G. barretti* with dominant OTUs shared between both sponges (**Chapter 5**). In contrast, only a small number of OTUs was found to overlap between these two High Microbial Abundance (HMA) sponges and *W. bursa*. The observation that *S. fortis* and *G. barretti* shared OTUs irrespective of depth range may indicate that these OTUs are tightly connected to these HMA sponges due to their co-existence within the deep-sea habitats. It could be that in both sponges these prokaryotic community was transmitted vertically from adult to larvae as previously demonstrated in other sponges for Bacteria [277,470,471] and Archaea [472,473]. However, it could also be that some of these prokaryotic communities initially came from the surrounding environments via horizontal transmission and further reside permanently since both *S. fortis* and *G. barretti* provide ideal niche conditions.

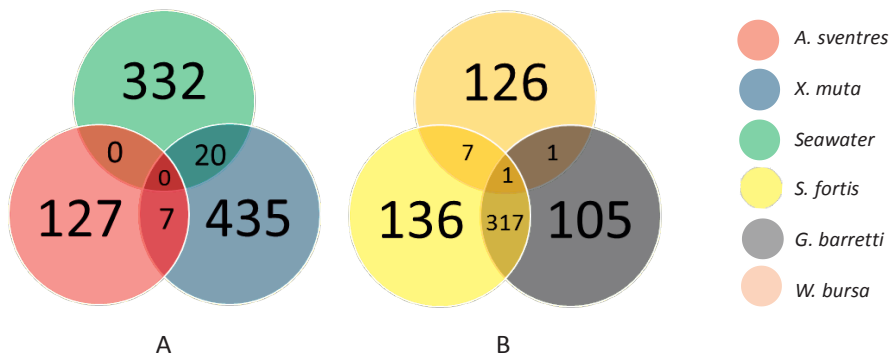


Figure 2. Venn diagram representing the number of unique and shared OTUs in different sample types as described in **Chapter 3** (A) and **Chapter 5** (B).

Our results demonstrated the influence of depth on prokaryotic community composition of marine sponges and determined dominant OTUs for each sponge that differed in relative abundance with increasing depth. However, it is important to note that we rely mainly on amplicon sequencing data and based our analysis on differences in relative abundance of microbial taxa at different levels of taxonomic resolution. Therefore, we could not determine the putative roles of OTUs that differ in prevalence and relative abundance in relation with depth. Additionally, a future depth gradient study on composition and function of prokaryotic

communities of marine sponges should comprehensively capture physicochemical factors associated with depth in order to allow for correlations of microbiota composition and activity with the surrounding environments.

Depth and metabolite variation of marine sponges: how are they connected?

As sessile animals, many sponges rely heavily on chemical defences to protect themselves from predatory fishes, fouling organisms (e.g. barnacles), or other sponge competitors [289,448,474]. Based on the availability of secondary metabolites within their tissues, sponges have been classified into chemically defended species and palatable species [343]. In many cases, these bioactive molecules not only function as feeding deterrent compounds, but also have a broad-spectrum bioactivity including antimicrobial activity [293,294,475].

We investigated the impact of depth on antimicrobial activities of sponge extracts from *X. muta* and *A. sventres* against selected indicator microorganisms, including Gram positive and Gram-negative bacterial strains, a yeast and an oomycete (**Chapter 3**). Our study captured the variability of antimicrobial activities of crude extracts derived from tissues of *X. muta* and *A. sventres* with different depths. The dominant antibacterial activities came mainly from crude extracts of shallow specimens and were particularly strong for *A. sventres*. Although, we did not measure abundance of predatory fishes at the sampling site we assume that the higher antibacterial activities found in shallow sponge specimens could be linked with higher fish predation in the shallow reef habitat. Our assumption is supported by the fact that spongivorous fishes have been reported to be more abundant in shallow water compared to mesophotic depth [73]. It has been confirmed that exposure to spongivorous fishes also induces antimicrobial activities in sponges as a protection against pathogenic infections [318]. Our result confirmed that *A. sventres* is among the well-defended sponge species as commonly observed for members of the genus *Agelas* [343]. Furthermore, we also found antimicrobial activities in *X. muta*, however, as previously reported their bioactivity may vary between individuals, which could be due to site-specific differences in the level of predation [297]. We found a strong anti-*Saprolegnia parasitica* activity, mainly in extracts from deep *X. muta* specimens. *Saprolegnia* spp. including *S. parasitica* are parasites in fish and fish eggs and contribute to an economic loss in aquaculture industry. In addition, these pathogens are generally resistant against a wide range of antifungals [348,476,477]. Our result showed that the crude extract of specimen XM5 at the concentration of 0.5 mg/20 μ L gave the largest recorded radius of the zone of inhibition (13 mm) against *S. parasitica*. By means of comparison, the minimal inhibition concentration

of antifungal malachite green is 0.25 mg/L against *S. parasitica* [478]. In the past, malachite green was widely used as chemical to control infection of *Saprolegnia* spp., however, it was banned world-wide due to its toxic effects [349,350]. Thus, the search for novel compounds to combat these parasites is highly urgent [351]. Irrespective of the higher concentration that was required to inhibit *S. parasitica*, it is important to note that in our study the screening was done using crude extracts that were prepared from a starting tissue sample of only 0.3 gram. Hence, the observed activity from the majority of deep *X. muta* crude-extracts against *S. parasitica* gives a hint on the importance of mesophotic habitats in our quest for novel compounds against parasitic infections. Future studies should aim to elucidate the actual bioactive compound from mesophotic *X. muta* tissue extracts that is responsible for the observed activity against *S. parasitica*.

Metabolite profiling using untargeted metabolomics provides access to the diversity of chemicals produced by an organism without requiring a prior knowledge of a specific compound. Such metabolome analyses have been widely applied in marine organisms to investigate metabolites from corals [479,480], cnidarians [481], jelly fish [482] and sponges [14,418,419]. We applied untargeted metabolomics to assess the variability of metabolite profiles from three boreal sponges, i.e. *W. bursa*, *S. fortis* and *G. barretti*, in relation with depth (**Chapter 5**). We reported that metabolite profiles of each sponge were highly host-specific irrespective of depth. Based on the outcome of untargeted metabolomics, we used standards to identify specific compounds associated with these deep-sea sponges and to assess how they correlated with depth. With regard to these specific compounds, we observed declining concentration of baretin, 8,9-dihydrobaretin and soelsterin in *G. barretti* specimens below 1000 m, whereas concentrations of compounds associated with *S. fortis* (ianthelline and stryphnusin) increased in very deep specimens (1400 m). Given that these compounds yield antibiofouling activity, we would expect they showed the same pattern with respect to increasing depth. As we speculated in **Chapter 5**, the decreasing trend of baretin, 8,9-dihydrobaretin and soelsterin in *G. barretti* could be because the biofouling organism is absent in the deep-sea habitats or relative abundance of the microorganisms responsible for synthesizing these compounds declined in deep specimens. Furthermore, based on the results of a recent study that showed that the compound ianthelline is actually not produced by *S. fortis*, but is synthesized by its epibiont sponge *Hexadella detritifera* [106], it is tempting to speculate that the absence of *H. detritifera* might explain the observed low concentration of ianthelline in *S. fortis* specimens < 1000 m depth. Given that stryphnusin displayed a similar

increasing trend with depth as ianthelline, this compound might also be derived from the epibiont sponge. Further chemical analysis must be done, however, to support this speculation.

Although we could not determine the putative OTUs that could be associated with biosynthesis of active compounds in deep-sea marine sponges, it is interesting to note that a previous metagenomics survey on the deep-sea sponges *Inflatella pellicula*, *Poecillastra compressa* and *Stelletta normani* showed that the sponge microbiome harboured unique genes for biosynthesizing secondary metabolites [63]. Similar metagenomics analyses are currently underway in our laboratory, and should provide new insight into the capacity of the sponges studied here to synthesis bioactive secondary metabolites. Taken together, we showed that depth influences the metabolite profiles in sponges. Although we could not unequivocally identify the exact factor responsible for the observed metabolite variation, it is likely that both biotic (predators or biofouling organisms) and abiotic factors contribute to such variability. Even though we observed stronger antibacterial activities in specimens from shallow water, this pattern was derived from only two sponge species without representatives of deep *A. sventres* specimens. Therefore, we could not fully generalize that antibacterial activities are dominantly present in shallow water and will be absent at mesophotic depths. To draw a stronger conclusion on antimicrobial patterns of marine sponges and their associated microbial communities across different depths, more well-defended species that are present at different depths, e.g. *Agelas* spp, *Aplysina* spp. and *Plakortis angulospiculatus* [73,79,343], should be included in future antimicrobial screening campaigns.

The use of untargeted metabolomics further provides a basis to explore the deep sea especially to detect patterns regarding the differences in metabolite profiles across sponge species and different habitats. In the study described in **chapter 5**, over 3000 features were recorded from metabolites of deep-sea sponges. A more detailed analysis and identification of these features could likely provide hints for novel compounds that are not present in shallow water habitats. In addition, untargeted metabolomics should also be coupled with bioactivity screening in order to confirm whether the presence of a certain molecule correlates to a specific biological function (e.g. anti-biofouling) or possibly refer to different bioactivities. Thus, future bioprospecting campaigns should be expanded to further investigate the chemical diversity and bioactivity of sponges and their associated microorganisms recovered from mesophotic and deep-sea environments.

The impact of depth on cultivability of sponge-associated bacteria

Nearly all isolates reviewed in **chapter 2** were derived from specimens of sponge that inhabit shallow water (<30 m). Conversely, a rather limited number of studies so far has focused to isolate sponge-associated microbes below the shallow habitat, which leaves the true potential of deeper sponge-associated bacteria with respect to antimicrobial activities unknown. In **Chapter 4**, we focused to cultivate sponge-associated bacteria from *X. muta* and *A. sventres* collected from different depths along with assessment of antimicrobial activities of these bacterial isolates. In this chapter, we specifically aimed to obtain bacterial isolates from sponges with strong antimicrobial activities. The experiment was done by preparing replicate plates either to pick individual colonies or to scrape the entire biomass. In general, the cultivable bacterial fraction was mainly affiliated with the phyla Proteobacteria (Alpha-, Gamma-), Firmicutes and Actinobacteria. Similar to previous studies, these cultivable bacteria are not among taxa that are dominantly found from culture-independent studies, suggesting that most of these isolates are not specifically associated with sponges. In addition, we found that sponges from different depths indeed harboured cultivable OTUs that were not cultured from specimens collected in other depth ranges. However, we found that depth did not consistently affect cultivability of sponge-associated bacteria given that significant impact was observed only for the microbial biomass grown on plates inoculated with samples of *X. muta*, whereas depth was insignificant for scraped bacterial communities of *A. sventres*. It should be noted, however, that we cannot exclude that this lack of significant influence of depth was caused by the fact that only samples from shallow and medium depths were included in this study for *A. sventres*.

In line with our cultivation-independent study (**Chapter 3**) we found that host-identity significantly affected the cultivable bacterial fraction of *X. muta* and *A. sventres* as previously reported in cultivation studies of other marine sponges [381,386]. In addition, we could show that variation of the cultivable bacteria from marine sponges was influenced by type of media used. To date, no study has successfully isolated the true symbionts of sponges on agar plates, although the use of various growth media and conditions indeed could increase cultivability of sponge isolates up to 14% [32]. The dominant OTUs that were present in *X. muta* and *A. sventres* (e.g. Actinobacteria sva0996, Chloroflexi SAR202, Acidobacteria subgroup 6) as observed in the culture-independent study (**Chapter 3**, Figure 4) were not among isolates that have been recovered on agar plates. Tremendous efforts have been taken to try to culture the actual sponge-associated bacteria but so far did not succeed [32,35,368-370,372]. Similar to

our study, many cultivation-based studies rely mainly on synthetic agar media without prior knowledge on optimal conditions with respect to required nutrients for the targeted bacteria [483,484]. In the last decade, the advance of sequencing technology, metagenomics, metatranscriptomics, and metaproteomics has provided important insights in genomics of these uncultivated bacteria and may be used to predict their physiological capacities [485]. For instance, the latest metagenomics study described prevalence of Chloroflexi in HMA marine sponges and described that members of this phylum harbour genes that are responsible for complex compound degradation. Based on such genomic information, future cultivation studies should design suitable media that could meet the required physiological conditions of the targeted bacteria [485].

Our results showed 20 isolates with antibacterial activities against at least one of the bacterial indicator strains, whereas no inhibition against the oomycete *Saprolegnia parasitica* was recorded. Nine of these 20 isolates (Table 3, **Chapter 4**) came from four genera (*Pseudovibrio*, *Bacillus*, *Micrococcus* and *Vibrio*) that were identified among prominent isolates previously reported to have antimicrobial activity (**Chapter 2**, Figure 5). It should be noted that in our study we only identified a selected number of representative isolates from larger groups of isolates retrieved from different media and samples. In addition, we only select representative isolates to be screened against indicator strains, while bioactivity of the remaining non-selected isolates has not been determined, and it cannot be excluded that other strains might have other bioactivity profiles. In general, we observed these active isolates displayed weak inhibition against indicator strains, but such weak activities could be because these isolates were grown using the same media used for isolation without further conducting media optimization (e.g. pH, temperature, carbon source) to obtain a higher concentration of metabolites. Since genomic information of the majority of these isolates is already available, optimization of growth media could be done to increase yield of secondary metabolites from the current bacterial isolates since ideal conditions for the production of active compounds can be accommodated [486].

Although in this study we could not isolate bacteria with strong antimicrobial activities, we believe cultivation of sponge-associated bacteria is still relevant in the quest to tapping into their biotechnological potential. However, future cultivation studies cannot rely solely on “classical” cultivation media and should be synchronized with the current data from the *omics* to design media according to the target bacteria.

Outlook

In this thesis, we reported on the prokaryotic community composition of marine sponges based on 16S rRNA gene amplicon sequencing data across different depths and pointed out OTUs for which their relative abundance significantly changed with depth. However, our analysis on prokaryotic community profiles was solely based on their taxonomy and relative abundance and we could not determine the actual functions of these specific OTUs and why they may change their relative abundance with depth. Therefore, an extended study that includes the following points would provide more insight into sponge prokaryotic community functioning along a depth gradient:

Future depth-gradient studies should shift from community profiling based on 16S rRNA gene amplicon sequencing toward metagenomics [487] to obtain better insight into the metabolic capacity of sponge prokaryotic communities. Genomes of specific OTUs of interest can be reconstructed from sponge metagenome data using a sequence composition dependent-binning approach as previously reported for the genome of members of the following taxons: “sponge-associated unclassified lineage” (SAUL) [488], Rhodospirillaceae [489], Gammaproteobacterium [490], Phyllobacteriaceae, the *Nitrospira* genus, the thaumarchaeal order Nitrosopumilales [491], and Chloroflexi [328]. From these reconstructed genomes, a more detailed analysis can be done to investigate whether the increasing trend of specific prokaryotic taxa in the mesophotic zone or in the deep sea is related to a specific biogeochemical cycle, e.g. that of sulphur, nitrogen or phosphorus. Given that we have a number of representative sponge samples taken from different depths, metagenomics would likely provide hints whether the different Thaumarcheota OTUs that were observed at different depth levels all encode ammonia oxidation pathways, or whether the presence of Chloroflexi SAR202 OTUs in shallow water is connected to photoheterotrophy. Moreover, the prevalence of specific metabolic pathways in a metagenome with respect to the depth origin of a sample would provide important cues on the predicted physicochemical conditions of the habitat. To this end, metatranscriptome and metaproteome analyses could provide additional experimental support towards the active expression of specific pathways.

Metagenomics could also be employed to study the diversity of biosynthesis gene clusters encoding for secondary metabolites as previously reported in other studies [57,58,250]. It is intriguing to access whether the higher antibacterial activity found in sponges in the shallow habitat correlates with a higher prevalence of gene clusters encoding for specific secondary

metabolites e.g. polyketide synthases or non-ribosomal peptide synthetases. Additionally, metagenomics could also be applied to investigate whether biosynthesis of barrettin is rather correlated with a specific putative group of archaea or bacteria.

Overall, results provided in this thesis serve as basis for future studies in order to fully unravel ecological and biotechnological potential of sponges and their associated microbes beyond shallow water habitats.



Appendices



References

1. Yin, Z.J.; Zhu, M.Y.; Davidson, E.H.; Bottjer, D.J.; Zhao, F.C.; Tafforeau, P. Sponge grade body fossil with cellular resolution dating 60 Myr before the Cambrian. *Proc. Natl. Acad. Sci.* **2015**, *112*, E1453-E1460.
2. Prozanto, R.; Pisera, A.; Manconi, R. Fossil freshwater sponges: taxonomy, geographic distribution, and critical review. *Acta Palaeontol. Pol.* **2017**, *62*, 467–495.
3. Van Soest, R.W.M.; Boury-Esnault, N.; Vacelet, J.; Dohrmann, M.; Erpenbeck, D.; De Voogd, N.J.; Santodomingo, N.; Vanhoorne, B.; Kelly, M.; Hooper, J.N.A. Global diversity of sponges (Porifera). *Plos One.* **2012**, *7*, 1-23.
4. Hentschel, U.; Piel, J.; Degnan, S.M.; Taylor, M.W. Genomic insights into the marine sponge microbiome. *Nature Rev. Microbiol.* **2012**, *10*, 641-675.
5. Borchellini, C.; Manuel, M.; Alivon, E.; Boury-Esnault, N.; Vacelet, J.; Le Parco, Y. Sponge paraphyly and the origin of Metazoa. *J. Evol. Biol.* **2001**, *14*, 171-179.
6. Gazave, E.; Lapébie, P.; Ereskovsky, A.V.; Vacelet, J.; Renard, E.; Cárdenas, P.; Borchellini, C. No longer Demospongiae: Homoscleromorpha formal nomination as a fourth class of Porifera. *Hydrobiologia.* **2012**, *687*, 3-10.
7. Morrow, C.; Cardenas, P. Proposal for a revised classification of the Demospongiae (Porifera). *Front. Zool.* **2015**, *12*, 1-27.
8. Wehrl, M.; Steinert, M.; Hentschel, U. Bacterial uptake by the marine sponge *Aplysina aerophoba*. *Microb. Ecol.* **2007**, *53*, 355-365.
9. Hentschel, U.; Usher, K.M.; Taylor, M.W. Marine sponges as microbial fermenters. *FEMS Microbiol. Ecol.* **2006**, *55*, 167-177.
10. Vogel, S. Current-induced flow through living sponges in nature. *Proc. Natl. Acad. Sci.* **1977**, *74*, 2069-2071.
11. Bell, J.J. The functional roles of marine sponges. *Estuar Coast Shelf Sci.* **2008**, *79*, 341-353.
12. Maldonado, M.; Ribes, M.; van Duyl, F.C.; Becerro, M.A.; Uriz, M.J.; Maldonado, M.; Turon, X. Chapter three - Nutrient fluxes through sponges: biology, budgets, and ecological implications. In *Advances in marine biology*, Academic Press: 2012; pp 113-182.
13. de Goeij, J.M.; van Oevelen, D.; Vermeij, M.J.A.; Osinga, R.; Middelburg, J.J.; de Goeij, A.F.P.M.; Admiraal, W. Surviving in a marine desert: the sponge loop retains resources within coral reefs. *Science.* **2013**, *342*, 108-110.
14. Fiore, C.L.; Freeman, C.J.; Kujawinski, E.B. Sponge exhalent seawater contains a unique chemical profile of dissolved organic matter. *PeerJ.* **2017**, *5*, 1-22.
15. Phylum Porifera. <https://courses.lumenlearning.com/boundless-biology/chapter/phylum-porifera/> (Access 19-01-2019),
16. Vacelet, J.; Donadey, C. Electron microscope study of the association between some sponges and bacteria. *J. Exp. Mar. Biol. Ecol.* **1977**, *30*, 301-314.
17. Wilkinson, C.R.; Garrone, R.; Vacelet, J. Marine sponges discriminate between food bacteria and bacterial symbionts: electron microscope radioautography and *in situ* evidence. *Proc. R. Soc. Lond., B, Biol. Sci.* **1984**, *220*, 519-528.
18. Moitinho-Silva, L.; Steinert, G.; Nielsen, S.; Hardoim, C.C.P.; Wu, Y.C.; McCormack, G.P.; Lopez-Legentil, S.; Marchant, R.; Webster, N.; Thomas, T., *et al.* Predicting the HMA-LMA Status in marine sponges by Machine Learning. *Front Microbiol.* **2017**, *8*.
19. Taylor, M.W.; Radax, R.; Steger, D.; Wagner, M. Sponge-associated microorganisms: Evolution, ecology, and biotechnological potential. *Microbiol. Mol. Biol. R.* **2007**, *71*, 295-347.
20. Mohamed, N.M.; Saito, K.; Tal, Y.; Hill, R.T. Diversity of aerobic and anaerobic ammonia-oxidizing bacteria in marine sponges. *ISME J.* **2010**, *4*, 38-48.
21. Zhang, F.; Blasiak, L.C.; Karolin, J.O.; Powell, R.J.; Geddes, C.D.; Hill, R.T. Phosphorus sequestration in the form of polyphosphate by microbial symbionts in marine sponges. *P. Natl. Acad. Sci.* **2015**, *112*, 4381-4386.
22. Hentschel, U.; Hopke, J.; Horn, M.; Friedrich, A.B.; Wagner, M.; Hacker, J.; Moore, B.S. Molecular evidence for a uniform microbial community in sponges from different oceans. *Appl. Environ. Microbiol.* **2002**, *68*, 4431-4440.
23. Simister, R.L.; Deines, P.; Botte, E.S.; Webster, N.S.; Taylor, M.W. Sponge-specific clusters revisited: a comprehensive phylogeny of sponge-associated microorganisms. *Environ. Microbiol.* **2012**, *14*, 517-524.

24. Thomas, T.; Moitinho-Silva, L.; Lurgi, M.; Bjork, J.R.; Easson, C.; Astudillo-Garcia, C.; Olson, J.B.; Erwin, P.M.; Lopez-Legentil, S.; Luter, H., *et al.* Diversity, structure and convergent evolution of the global sponge microbiome. *Nat Commun.* **2016**, *7*, 1-12.
25. Moitinho-Silva, L.; Nielsen, S.; Amir, A.; Gonzalez, A.; Ackermann, G.L.; Cerrano, C.; Astudillo-Garcia, C.; Easson, C.; Sipkema, D.; Liu, F., *et al.* The sponge microbiome project. *GigaScience.* **2017**, *6*, 1-7.
26. Fieseler, L.; Horn, M.; Wagner, M.; Hentschel, U. Discovery of the novel candidate phylum "Poribacteria" in marine sponges. *Appl. Environ. Microbiol.* **2004**, *70*, 3724-3732.
27. Lafi, F.F.; Fuerst, J.A.; Fieseler, L.; Engels, C.; Goh, W.W.L.; Hentschel, U. Widespread distribution of Poribacteria in Demospongiae. *Appl Environ Microb.* **2009**, *75*, 5695-5699.
28. Steinert, G.; Gutleben, J.; Atikana, A.; Wijffels, R.H.; Smidt, H.; Sipkema, D. Coexistence of poribacterial phylotypes among geographically widespread and phylogenetically divergent sponge hosts. *Environ. Microbiol. Rep.* **2018**, *10*, 80-91.
29. Schippers, K.J.; Sipkema, D.; Osinga, R.; Smidt, H.; Pomponi, S.A.; Martens, D.E.; Wijffels, R.H. Cultivation of sponges, sponge cells and symbionts: achievements and future prospects. In *Adv Mar Biol*, 2012; pp 273-337.
30. Indraningrat, A.A.G.; Smidt, H.; Sipkema, D. Bioprospecting sponge-associated microbes for antimicrobial compounds. *Mar Drugs.* **2016**, *14*, 1-66.
31. Thoms, C.; Schupp, P. Biotechnological potential of marine sponges and their associated bacteria as producers of new pharmaceuticals (part II). *Journal of International Biotechnology Law.* **2005**, *2*, 257-264.
32. Sipkema, D.; Schippers, K.; Maalcke, W.J.; Yang, Y.; Salim, S.; Blanch, H.W. Multiple approaches to enhance the cultivability of bacteria associated with the marine sponge *Haliclona* (gellius) sp. *Appl. Environ. Microbiol.* **2011**, *77*, 2130-2140.
33. Versluis, D.; McPherson, K.; Passel, M.; Smidt, H.; Sipkema, D. Recovery of previously uncultured bacterial genera from three Mediterranean sponges. *Mar. Biotechnol.* **2017**, *19*, 454-468.
34. Olson, J.B.; Lord, C.C.; McCarthy, P.J. Improved Recoverability of Microbial Colonies from Marine Sponge Samples. *Microbiol Ecol.* **2000**, *40*, 139-147.
35. Steinert, G.; Whitfield, S.; Taylor, M.W.; Thoms, C.; Schupp, P.J. Application of diffusion growth chambers for the cultivation of marine sponge-associated bacteria. *Mar. Biotechnol.* **2014**, *16*, 594-603.
36. Jung, D.; Seo, E.-Y.; Epstein, S.S.; Joung, Y.; Han, J.; Parfenova, V.V.; Belykh, O.I.; Gladkikh, A.S.; Ahn, T.S. Application of a new cultivation technology, I-tip, for studying microbial diversity in freshwater sponges of Lake Baikal, Russia. *FEMS Microbiol Ecol.* **2014**, *90*, 417-423.
37. Davies, J.; Davies, D. Origins and evolution of antibiotic resistance. *Microbiol. Mol. Biol. Rev.* **2010**, *74*, 417-433.
38. White, R.J. The early history of antibiotic discovery: empiricism ruled. In *Antibiotic Discovery and Development*, Dougherty, T.J.; Pucci, M.J., Eds. Springer US: Boston, MA, 2012; pp 3-31.
39. Aminov, R.I. A brief history of the antibiotic era: lessons learned and challenges for the future. *Front Microbiol.* **2010**, *1*.
40. Antimicrobial Resistance: tackling a crisis for the health and wealth of nations. Review on Antimicrobial Resistance: Chaired by Jim O'Neill, 2014, Available online: <http://amr-review.org/Publications>.
41. Taylor, P.L.; Wright, G.D. Novel approaches to discovery of antibacterial agents. *Anim. Health. Res. Rev.* **2008**, *9*, 237-246.
42. Mehbub, M.F.; Lei, J.; Franco, C.; Zhang, W. Marine sponge derived natural products between 2001 and 2010: trends and opportunities for discovery of bioactives. *Mar. Drugs.* **2014**, *12*, 4539-4577.
43. Blunt, J.W.; Copp, B.R.; Keyzers, R.A.; Munro, M.H.G.; Prinsep, M.R. Marine natural products. *Nat. Prod. Rep.* **2017**, *34*, 235-294.
44. Jaspars, M.; De Pascale, D.; Andersen, J.H.; Reyes, F.; Crawford, A.D.; Ianora, A. The marine biodiscovery pipeline and ocean medicines of tomorrow. *J. Mar. Biol. Assoc. U. K.* **2016**, *96*, 151-158.
45. Sipkema, D.; Franssen, M.C.R.; Osinga, R.; Tramper, J.; Wijffels, R.H. Marine sponges as pharmacy. *Mar. Biotechnol.* **2005**, *7*, 142-162.
46. Laport, M.S.; Santos, O.C.S.; Muricy, G. Marine sponges: potential sources of new antimicrobial drugs. *Curr Pharm Biotechnol.* **2009**, *10*, 86-105.
47. Sagar, S.; Kaur, M.; Minneman, K.P. Antiviral lead compounds from marine sponges. *Mar. Drugs.* **2010**, *8*, 2619-2638.
48. Proksch, P.; Edrada-Ebel, R.; Ebel, R. Drugs from the sea - opportunities and obstacles. *Mar. Drugs.* **2003**, *1*, 5.
49. Piel, J. Metabolites from symbiotic bacteria. *Nat Prod Rep.* **2004**, *21*, 519-538.
50. Piel, J. Metabolites from symbiotic bacteria. *Nat Prod Rep.* **2009**, *26*, 338-362.

51. Bringmann, G.; Lang, G.; Mühlbacher, J.; Schaumann, K.; Steffens, S.; Rytik, P.G.; Hentschel, U.; Morschhäuser, J.; Müller, W.E.G. Sorbicillactone A: a structurally unprecedented bioactive novel-type alkaloid from a sponge-derived fungus. In *Sponges (Porifera)*, Müller, W.E.G., Ed. Springer Berlin Heidelberg: Berlin, Heidelberg, 2003; pp 231-253.
52. Phelan, R.W.; Barret, M.; Cotter, P.D.; O'Connor, P.M.; Chen, R.; Morrissey, J.P.; Dobson, A.D.W.; O'Gara, F.; Barbosa, T.M. Subtilomycin: a new Lantibiotic from *Bacillus subtilis* strain MMA7 isolated from the marine sponge *Haliclona simulans*. *Mar. Drugs*. **2013**, *11*, 1878-1898.
53. El-Gendy, M.M.A.; EL-Bondkly, A.M.A. Production and genetic improvement of a novel antimycotic agent, Saadamycin, against Dermatophytes and other clinical fungi from Endophytic Streptomyces sp. Hedaya48. *Journal of Industrial Microbiology & Biotechnology*. **2010**, *37*, 831-841.
54. Waters, A.L.; Peraud, O.; Kasanah, N.; Sims, J.W.; Kothalawala, N.; Anderson, M.A.; Abbas, S.H.; Rao, K.V.; Jupally, V.R.; Kelly, M., et al. An analysis of the sponge *Acanthostrongylophora igens*' microbiome yields an actinomycete that produces the natural product manzamine A. *Frontiers in Marine Science*. **2014**, *1*, 54.
55. Freeman, C.J.; Baker, D.M.; Easson, C.G.; Thacker, R.W. Shifts in sponge-microbe mutualisms across an experimental irradiance gradient. *Mar. Ecol. Prog. Ser.* **2015**, *526*, 41-53.
56. Schirmer, A.; Gadkari, R.; Reeves, C.D.; Ibrahim, F.; DeLong, E.F.; Hutchinson, C.R. Metagenomic analysis reveals diverse polyketide synthase gene clusters in microorganisms associated with the marine sponge *Discodermia dissoluta*. *App. Env. Microbiol.* **2005**, *71*, 4840-4849.
57. Siegl, A.; Hentschel, U. PKS and NRPS gene clusters from microbial symbiont cells of marine sponges by whole genome amplification. *Environ. Microbiol. Rep.* **2010**, *2*, 507-513.
58. Wilson, M.C.; Mori, T.; Ruckert, C.; Uria, A.R.; Helf, M.J.; Takada, K.; Gernert, C.; Steffens, U.A.E.; Heycke, N.; Schmitt, S., et al. An environmental bacterial taxon with a large and distinct metabolic repertoire. *Nature*. **2014**, *506*, 58-62.
59. Alt, S.; Wilkinson, B. Biosynthesis of the novel macrolide antibiotic anthracimycin. *ACS Chem. Biol.* **2015**, *10*, 2468-2479.
60. Yung, P.Y.; Burke, C.; Lewis, M.; Kjelleberg, S.; Thomas, T. Novel antibacterial proteins from the microbial communities associated with the sponge *Cymbastela concentrica* and the green alga *Ulva australis*. *Appl. Environ. Microbiol.* **2011**, *77*, 1512-1515.
61. Sipkema, D. Marine biotechnology: diving deeper for drugs. *Microb Biotechnol.* **2017**, *10*, 7-8.
62. Turk, T.; Avguštin, J.; Batista, U.; Strugar, G.; Kosmina, R.; Čivović, S.; Janussen, D.; Kauferstein, S.; Mebs, D.; Sepčić, K. Biological activities of ethanolic extracts from deep-sea Antarctic marine sponges. *Mar. Drugs*. **2013**, *11*, 1126.
63. Borchert, E.; Jackson, S.A.; O'Gara, F.; Dobson, A.D.W. Diversity of natural product biosynthetic genes in the microbiome of the deep sea sponges *Inflatella pellicula*, *Poecillastra compressa*, and *Stelletta normani*. *Front Microbiol.* **2016**, *7*, 1-11.
64. Baker, E.K.; Puglise, K.A. Mesophotic coral ecosystems — a lifeboat for coral reefs? Harris, P.T., Ed. Nairobi and Arendal, 2016, <http://www.grida.no/publications/88>.
65. Kahng, S.E.; Copus, J.M.; Wagner, D. Recent advances in the ecology of mesophotic coral ecosystems (MCEs). *Curr Opin in Environ Sust.* **2014**, *7*, 72-81.
66. Olson, J.B.; Kellogg, C.A. Microbial ecology of corals, sponges, and algae in mesophotic coral environments. *FEMS Microbiol. Ecol.* **2010**, *73*, 17-30.
67. Thurber, A.R.; Sweetman, A.K.; Narayanaswamy, B.E.; Jones, D.O.B.; Ingels, J.; Hansman, R.L. Ecosystem function and services provided by the deep sea. *Biogeosciences*. **2014**, *11*, 3941-3963.
68. Slattery, M.; Lesser, M.P.; Brazeau, D.; Stokes, M.D.; Leichter, J.J. Connectivity and stability of mesophotic coral reefs. *J. Exp. Mar. Biol. Ecol.* **2011**, *408*, 32-41.
69. Webster, N.S.; Taylor, M.W. Marine sponges and their microbial symbionts: love and other relationships. *Environ. Microbiol.* **2012**, *14*, 335-346.
70. Ramirez-Llodra, E.; Brandt, A.; Danovaro, R.; De Mol, B.; Escobar, E.; German, C.R.; Levin, L.A.; Martínez Arbizu, P.; Menot, L.; Buhl-Mortensen, P., et al. Deep, diverse and definitely different: unique attributes of the world's largest ecosystem. *Biogeosciences*. **2010**, *7*, 2851-2899.
71. Van Soest, R.; Meesters, E.H.W.G.; Becking, L.E. Deep-water sponges (Porifera) from Bonaire and Klein Curaçao, Southern Caribbean. *Zootaxa*. **2014**, *3878*, 404-443.
72. Costello, M.J.; Chaudhary, C. Marine biodiversity, biogeography, deep-sea gradients, and conservation. *Curr. Biol.* **2017**, *27*, R511-R527.
73. Slattery, M.; Gochfeld, D.J.; Diaz, M.C.; Thacker, R.W.; Lesser, M.P. Variability in chemical defense across a shallow to mesophotic depth gradient in the Caribbean sponge *Plakortis angulospiculatus*. *Coral Reefs*. **2016**, *35*, 11-22.
74. Montalvo, N.F.; Hill, R.T. Sponge-associated bacteria are strictly maintained in two closely related but geographically distant sponge hosts. *Appl. Environ. Microbiol.* **2011**, *77*, 7207.

75. Erwin, P.M.; Pita, L.; López-Legentil, S.; Turon, X. Stability of sponge-associated bacteria over large seasonal shifts in temperature and irradiance. *Appl. Environ. Microbiol.* **2012**, *78*, 7358-7368.
76. Erwin, P.M.; Coma, R.; Lopez-Sendino, P.; Serrano, E.; Ribes, M. Stable symbionts across the HMA-LMA dichotomy: low seasonal and interannual variation in sponge-associated bacteria from taxonomically diverse hosts. *FEMS. Microbiol. Ecol.* **2015**, *91*.
77. Cárdenas, C.A.; Bell, J.J.; Davy, S.K.; Hoggard, M.; Taylor, M.W. Influence of environmental variation on symbiotic bacterial communities of two temperate sponges. *FEMS Microbiol Ecol.* **2014**, *88*, 516-527.
78. Thoms, C.; Horn, M.; Wagner, M.; Hentschel, U.; Proksch, P. Monitoring microbial diversity and natural product profiles of the sponge *Aplysina cavernicola* following transplantation. *Mar. Biol.* **2003**, *142*, 685-692.
79. Olson, J.B.; Gao, X.M. Characterizing the bacterial associates of three Caribbean sponges along a gradient from shallow to mesophotic depths. *FEMS Microbiol. Ecol.* **2013**, *85*, 74-84.
80. Morrow, K.M.; Fiore, C.L.; Lesser, M.P. Environmental drivers of microbial community shifts in the giant barrel sponge, *Xestospongia muta*, over a shallow to mesophotic depth gradient. *Environ. Microbiol.* **2016**, *18*, 2025-2038.
81. Steinert, G.; Taylor, M.W.; Deines, P.; Simister, R.L.; de Voogd, N.J.; Hoggard, M.; Schupp, P.J. In four shallow and mesophotic tropical reef sponges from Guam the microbial community largely depends on host identity. *PeerJ.* **2016**, *4*, 1-25.
82. Meyer, B.; Kuever, J. Phylogenetic diversity and spatial distribution of the microbial community associated with the Caribbean deep-water sponge *Polymastia* cf. *corticata* by 16S rRNA, aprA, and amoA Gene analysis. *Microb. Ecol.* **2008**, *56*, 306-321.
83. Brück, W.M.; Brück, T.B.; Self, W.T.; Reed, J.K.; Nitecki, S.S.; McCarthy, P.J. Comparison of the anaerobic microbiota of deep-water *Geodia* spp. and sandy sediments in the Straits of Florida. *ISME J.* **2010**, *4*, 686.
84. Kennedy, J.; Flemer, B.; Jackson, S.A.; Morrissey, J.P.; O'Gara, F.; Dobson, A.D.W. Evidence of a putative deep sea specific microbiome in marine sponges. *Plos One.* **2014**, *9*, 1-13.
85. Vacelet, J.; Bouryèsnault, N. Carnivorous Sponges. *Nature.* **1995**, *373*, 333-335.
86. Vacelet, J.; Fiala, M.; xe; dioni, A.; Fisher, C.R.; Boury-Esnault, N. Symbiosis between methane-oxidizing bacteria and a deep-sea carnivorous cladorhizid sponge. *Mar. Ecol. Prog. Ser.* **1996**, *145*, 77-85.
87. Parra-Velandia, F.J.; Zea, S.; Van Soest, R.W.M. Reef sponges of the genus *Agelas* (Porifera: Demospongiae) from the Greater Caribbean. *Zootaxa.* **2014**, *3794*, 301-343.
88. Lehnert, H.; Soest, R.W.M.V. North Jamaican deep fore-reef sponges. *Beaufortia.* **1996**, *46*, 53-81.
89. Van Soest, R.W.M.; Boury-Esnault, N.; Hooper, J.N.A.; Rützler, K.; de Voogd, N.J.; Alvarez, B.; Hajdu, E.; Pisera, A.B.; Manconi, R.; Schönberg, C., et al. World Porifera database. <http://www.marinespecies.org/porifera> (19-01-2018),
90. Zea, S.; Henkel, T.P.; Pawlik, J.R. The Sponge Guide: a picture guide to Caribbean sponges. www.spongeguide.org (19-01-2018),
91. Zhang, H.W.; Dong, M.L.; Chen, J.W.; Wang, H.; Tenney, K.; Crews, P. Bioactive secondary metabolites from the marine sponge genus *Agelas*. *Mar. Drugs.* **2017**, *15*, 1-29.
92. Assmann, M.; Zea, S.; Kock, M. Sventrin, a new bromopyrrole alkaloid from the Caribbean sponge *Agelas sventres*. *J.Natl.Prod.* **2001**, *64*, 1593-1595.
93. Gloeckner, V.; Wehrl, M.; Moitinho-Silva, L.; Gernert, C.; Schupp, P.; Pawlik, J.R.; Lindquist, N.L.; Erpenbeck, D.; Worheide, G.; Hentschel, U. The HMA-LMA dichotomy revisited: an electron microscopical survey of 56 sponge species. *Biol Bull.* **2014**, *227*, 78-88.
94. Ribes, M.; Dziallas, C.; Coma, R.; Riemann, L. Microbial diversity and putative diazotrophy in high- and low-microbial-abundance mediterranean sponges. *Appl. Environ. Microbiol.* **2015**, *81*, 5683-5693.
95. Bertin, M.; Callahan, M. In *Distribution, abundance and volume of Xestospongia muta at selected sites in the Florida Keys National Marine Sanctuary, Proceedings of the 11th International Coral Reef Symposium*, 7-11 July 2008.
96. McMurray, S.E.; Blum, J.E.; Pawlik, J.R. Redwood of the reef: growth and age of the giant barrel sponge *Xestospongia muta* in the Florida Keys. *Mar Biol.* **2008**, *155*, 159-171.
97. Schmitz, F.J.; Gopichand, Y. (7E, 13 ζ , 15Z)-14,16-dibromo-7,13,15-hexadecatrien-5-ynoic acid. A novel dibromo acetylenic acid from the marine sponge *Xestospongia muta*. *Tetrahedron Lett.* **1978**, *19*, 3637-3640.
98. Patil, A.D.; Kokke, W.C.; Cochran, S.; Francis, T.A.; Tomszek, T.; Westley, J.W. Brominated polyacetylenic acids from the marine sponge *Xestospongia muta*: inhibitors of HIV protease. *J. Nat. Prod.* **1992**, *55*, 1170-1177.

99. Morinaka, B.I.; Skepper, C.K.; Molinski, T.F. Ene-yne tetrahydrofurans from the sponge *Xestospongia muta*. Exploiting a weak CD effect for assignment of configuration. *Org Lett.* **2007**, *9*, 1975-1978.
100. Villegas-Plazas, M.; Wos-Oxley, M.L.; Sanchez, J.A.; Pieper, D.H.; Thomas, O.P.; Junca, H. Variations in microbial diversity and metabolite profiles of the tropical marine sponge *Xestospongia muta* with season and depth. *Microb. Ecol.* **2018**, 1-14
101. Fiore, C.L.; Labrie, M.; Jarett, J.K.; Lesser, M.P. Transcriptional activity of the giant barrel sponge, *Xestospongia muta* holobiont: molecular evidence for metabolic interchange. *Front Microbiol.* **2015**, *6*.
102. Boury-Esnault, N. Family Polymastiidae Gray, 1867. In *Systema Porifera: a guide to the classification of sponges*, Hooper, N.A.J.; Van Soest, R.W.M., Eds. Kluwer Academic: New York, 2002;
103. Murillo, F.J.; Muñoz, P.D.; Cristobo, J.; Rios, P.; González, C.; Kenchington, E.; Serrano, A. Deep-sea sponge grounds of the Flemish Cap, Flemish Pass and the Grand Banks of Newfoundland (Northwest Atlantic Ocean): Distribution and species composition. *Mar. Biol. Res.* **2012**, *8*, 842-854.
104. Plotkin, A.; Gerasimova, E.; Rapp, H.T. Polymastiidae (Porifera: Demospongiae) of the Nordic and Siberian Seas. *J. Mar. Biol. Assoc. U. K.* **2017**, 1-63.
105. Cárdenas, P.; Rapp, H.T. Demosponges from the Northern Mid-Atlantic Ridge shed more light on the diversity and biogeography of North Atlantic deep-sea sponges. *J. Mar. Biol. Assoc. U. K.* **2015**, *95*, 1475-1516.
106. Cárdenas, P. Who produces ianthelline? The Arctic sponge *Stryphnus fortis* or its sponge epibiont *Hexadella dedritifera*: a probable case of sponge-sponge contamination. *J. Chem. Ecol.* **2016**, *42*, 339-347.
107. Cárdenas, P.; Rapp, H.T. Demosponges from the Northern Mid-Atlantic Ridge shed more light on the diversity and biogeography of North Atlantic deep-sea sponges. *J. Mar. Biol.* **2015**, *95*, 1475-1516.
108. Hanssen, K.Ø.; Andersen, J.H.; Stiberg, T.; Engh, R.A.; Svenson, J.; Genevière, A.-M.; Hansen, E. Antitumoral and mechanistic studies of ianthelline isolated from the Arctic sponge *Stryphnus fortis*. *Anticancer Research.* **2012**, *32*, 4287-4297.
109. Hanssen, K.Ø.; Cervin, G.; Trepos, R.; Petitbois, J.; Haug, T.; Hansen, E.; Andersen, J.H.; Pavia, H.; Hellio, C.; Svenson, J. The bromotyrosine derivative ianthelline isolated from the Arctic marine sponge *Stryphnus fortis* inhibits marine micro- and macrobiofouling. *Mar. Biotech.* **2014**, *16*, 684-694.
110. Moodie, L.W.K.; Zuzek, M.C.; Frangez, R.; Andersen, J.H.; Hansen, E.; Olsen, E.K.; Cergolj, M.; Sepcic, K.; Hansen, K.O.; Svenson, J. Synthetic analogs of stryphnusin isolated from the marine sponge *Stryphnus fortis* inhibit acetylcholinesterase with no effect on muscle function or neuromuscular transmission. *Org. Biomol. Chem.* **2016**, *14*, 11220-11229.
111. Beazley, L.I.; Kenchington, E.L.; Murillo, F.J.; Sacau, M.D. Deep-sea sponge grounds enhance diversity and abundance of epibenthic megafauna in the Northwest Atlantic. *ICES J. Mar. Sci.* **2013**, *70*, 1471-1490.
112. Cardenas, P.; Rapp, H.T.; Klitgaard, A.B.; Best, M.; Tholleson, M.; Tendal, O.S. Taxonomy, biogeography and DNA barcodes of *Geodia* species (Porifera, Demospongiae, Tetractinellida) in the Atlantic boreo-arctic region. *Zool. J. Linn. Soc.* **2013**, *169*, 251-311.
113. Hoffmann, F.; Rapp, H.T.; Pape, T.; Peters, H.; Reitner, J. Sedimentary inclusions in the deep-water sponge *Geodia barretti* (Geodiidae, Demospongiae) from the Korsfjord, western Norway. *Sarsia.* **2004**, *89*, 245-252.
114. Lidgren, G.; Bohlin, L.; Bergman, J. Studies of swedish marine organisms VII. A novel biologically active indole alkaloid from the sponge *Geodia baretii*. *Tetrahedron Lett.* **1986**, *27*, 3283-3284.
115. Sjögren, M.; Göransson, U.; Johnson, A.-L.; Dahlström, M.; Andersson, R.; Bergman, J.; Jonsson, P.R.; Bohlin, L. Antifouling activity of brominated cyclopeptides from the marine sponge *Geodia barretti*. *J. Nat. Prod.* **2004**, *67*, 368-372.
116. Carstens, B.B.; Rosengren, K.J.; Gunasekera, S.; Schempp, S.; Bohlin, L.; Dahlström, M.; Clark, R.J.; Göransson, U. Isolation, characterization, and synthesis of the barrettides: disulfide-containing peptides from the marine sponge *Geodia barretti*. *J. Nat. Prod.* **2015**, *78*, 1886-1893.
117. Olsen, E.K.; Söderholm, K.L.; Isaksson, J.; Andersen, J.H.; Hansen, E. Metabolomic Profiling reveals the N-Acyl-Taurine Geodiataurine in extracts from the marine sponge *Geodia macandrewii* (Bowerbank). *J Nat Prod.* **2016**, *79*, 1285-1291.
118. Schöttner, S.; Hoffmann, F.; Cárdenas, P.; Rapp, H.T.; Boetius, A.; Ramette, A. Relationships between host phylogeny, host type and bacterial community diversity in cold-water coral Reef sponges. *Plos One.* **2013**, *8*, e55505.
119. Pita, L.; Fraune, S.; Hentschel, U. Emerging sponge models of animal-microbe symbioses. *Front Microbiol.* **2016**, *7*.
120. Jensen, S.; Fortunato, S.A.V.; Hoffmann, F.; Hoem, S.; Rapp, H.T.; Øvreås, L.; Torsvik, V.L. The relative abundance and transcriptional activity of marine sponge-associated microorganisms emphasizing groups involved in sulfur cycle. *Microb. Ecol.* **2017**, *73*, 668-676.

121. Regina, R.; Friederike, H.; Tore, R.H.; Sven, L.; Christa, S. Ammonia-oxidizing archaea as main drivers of nitrification in cold-water sponges. *Environ. Microbiol.* **2012**, *14*, 909-923.
122. Antimicrobial resistance global report on surveillance. World Health Organization, Geneva, Switzerland, 2014, Available online: <http://www.who.int/drugresistance/documents/surveillancereport/en/>
123. Aminov, R.I. A brief history of the antibiotic era: lessons learned and challenges for the future. *Front Microbiol.* **2010**, *1*, 1-7.
124. Moellering Jr, R.C. Discovering new antimicrobial agents. *International Journal of Antimicrobial Agents.* **2011**, *37*, 2-9.
125. Projan, S.J. Why is big Pharma getting out of antibacterial drug discovery? *Curr. Opin. Microbiol.* **2003**, *6*, 427-430.
126. Fleming, A. On the antibacterial action of cultures of a *Penicillium*, with special reference to their use in the isolation of *B. influenzae*. *Br J Exp Pathol.* **1929**, *10*, 226-236.
127. Gillespie, D.E.; Brady, S.F.; Bettermann, A.D.; Cianciotto, N.P.; Liles, M.R.; Rondon, M.R.; Clardy, J.; Goodman, R.M.; Handelsman, J. Isolation of antibiotics turbomycin A and B from a metagenomic library of soil microbial DNA. *Appl. Environ. Microbiol.* **2002**, *68*, 4301-4306.
128. Ling, L.L.; Schneider, T.; Peoples, A.J.; Spoering, A.L.; Engels, I.; Conlon, B.P.; Mueller, A.; Schaberle, T.F.; Hughes, D.E.; Epstein, S., *et al.* A new antibiotic kills pathogens without detectable resistance. *Nature.* **2015**, *517*, 455-459.
129. Taylor, P.L.; Wright, G.D. Novel approaches to discovery of antibacterial agents. *Anim. Health. Res. Rev.* **2008**, *9*, 237-246.
130. Hughes, C.C.; Fenical, W. Antibacterials from the sea. *Chem. Eur. J.* **2010**, *16*, 12512-12525.
131. Fuerst, J.A. Diversity and biotechnological potential of microorganisms associated with marine sponges. *Appl. Microbiol. Biotechnol.* **2014**, *98*, 7331-7347.
132. Thomas, T.R.A.; Kavlekar, D.P.; LokaBharathi, P.A. Marine drugs from sponge-microbe association—a review. *Mar. Drugs.* **2010**, *8*, 1417-1468.
133. Santos-Gandelman, J.F.; Giambiagi-deMarval, M.; Oelemann, W.M.R.; Laport, M.S. Biotechnological potential of sponge-associated bacteria. *Curr. Pharm. Biotechnol.* **2014**, *15*, 143-155.
134. Graça, A.P.; Viana, F.; Bondoso, J.; Correia, M.I.; Gomes, L.A.G.R.; Humanes, M.; Reis, A.; Xavier, J.; Gaspar, H.; Lage, O. The antimicrobial activity of heterotrophic bacteria isolated from the marine sponge *Erylus deficiens* (Astrophorida, Geodiidae). *Front Microbiol.* **2015**, *6*, 1-10.
135. Hoppers, A.; Stoudenmire, J.; Wu, S.; Lopanik, N.B. Antibiotic activity and microbial community of the temperate sponge, *Haliclona* sp. *J. Appl. Microbiol.* **2015**, *118*, 419-430.
136. Bergmann, W.; Feeney, R.J. The isolation of a new thymine pentoside from sponges. *J. Am. Chem. Soc.* **1950**, *72*, 2809-2810.
137. Bergmann, W.; Feeney, R.J. Contributions to the study of marine products. XXXII. The nucleosides of sponges. I. *J. Org. Chem.* **1951**, *16*, 981-987.
138. Yasuhara-Bell, J.; Lu, Y. Marine compounds and their antiviral activities. *Antiviral Res.* **2010**, *86*, 231-240.
139. Bultel-Poncé, V.; Berge, J.-P.; Debitus, C.; Nicolas, J.-L.; Guyot, M. Metabolites from the sponge-associated bacterium *Pseudomonas* species. *Mar. Biotechnol.* **1999**, *1*, 384-390.
140. Ma, X.H.; Lo, L.T.; Zhu, T.J.; Ba, M.Y.; Li, G.Q.; Gu, Q.Q.; Guo, Y.; Li, D.H. Phenylspirodrimanes with Anti-HIV activity from the sponge-derived fungus *Stachybotrys chartarum* MXH-X73. *J. Nat. Prod.* **2013**, *76*, 2298-2306.
141. Li, Y.; Liu, D.; Cen, S.; Proksch, P.; Lin, W. Isoindolinone-type alkaloids from the sponge-derived fungus *Stachybotrys chartarum*. *Tetrahedron.* **2014**, *70*, 7010-7015.
142. Zhao, Y.; Si, L.; Liu, D.; Proksch, P.; Zhou, D.; Lin, W. Truncateols A–N, new isoprenylated cyclohexanols from the sponge-associated fungus *Truncatella angustata* with anti-H1N1 virus activities. *Tetrahedron.* **2015**, *71*, 2708-2718.
143. Krol, E.; Rychowska, M.; Szweczyk, B. Antivirals - current trends in fighting influenza. *Acta Biochim Pol.* **2014**, *61*, 495-504.
144. Pauletti, P.M.; Cintra, L.S.; Braguine, C.G.; da Silva Filho, A.A.; Silva, M.L.A.e.; Cunha, W.R.; Januário, A.H. Halogenated indole alkaloids from marine invertebrates. *Mar. Drugs.* **2010**, *8*, 1526-1549.
145. Neumann, C.S.; Fujimori, D.G.; Walsh, C.T. Halogenation strategies in natural product biosynthesis. *Chemistry & Biology.* **2008**, *15*, 99-109.
146. Peng, J.X.; Jiao, J.Y.; Li, J.; Wang, W.; Gu, Q.Q.; Zhu, T.J.; Li, D.H. Pyronepolyene C-glucosides with NF-kappa B inhibitory and anti-influenza A viral (H1N1) activities from the sponge-associated fungus *Epicoccum* sp JY40. *Bioorg. Med. Chem. Lett.* **2012**, *22*, 3188-3190.
147. Ma, X.H.; Zhu, T.J.; Gu, Q.Q.; Xi, R.; Wang, W.; Li, D.H. Structures and antiviral activities of butyrolactone derivatives isolated from *Aspergillus terreus* MXH-23. *J. Ocean Univ. China.* **2014**, *13*, 1067-1070.

148. Wang, J.F.; Lin, X.P.; Qin, C.; Liao, S.R.; Wan, J.T.; Zhang, T.Y.; Liu, J.; Fredimoses, M.; Chen, H.; Yang, B., *et al.* Antimicrobial and antiviral sesquiterpenoids from sponge-associated fungus, *Aspergillus sydowii* ZSDS1-F6. *J. Antibiot.* **2014**, *67*, 581-583.
149. Qin, C.; Lin, X.P.; Lu, X.; Wan, J.T.; Zhou, X.F.; Liao, S.R.; Tu, Z.C.; Xu, S.H.; Liu, Y.H. Sesquiterpenoids and xanthenes derivatives produced by sponge-derived fungus *Stachybotry* sp HHI ZSDS1F1-2. *J. Antibiot.* **2015**, *68*, 121-125.
150. Bastos, J.C.S.; Kohn, L.K.; Fantinatti-Garbozzini, F.; Padilla, M.A.; Flores, E.F.; da Silva, B.P.; de Menezes, C.B.A.; Arns, C.W. Antiviral activity of *Bacillus* sp. isolated from the marine sponge *Petromica citrina* against bovine viral diarrhea virus, a surrogate model of the hepatitis C virus. *Viruses*. **2013**, *5*, 1219-1230.
151. Inweregbu, K.; Dave, J.; Pittard, A. Nosocomial infections. *Continuing Education in Anaesthesia, Critical Care & Pain*. **2005**, *5*, 14-17.
152. Weinstein, R.A.; Gaynes, R.; Edwards, J.R.; System, N.N.I.S. Overview of nosocomial infections caused by gram-negative Bacilli. *Clin. Infect. Dis.* **2005**, *41*, 848-854.
153. Nagai, K.; Kamigiri, K.; Arao, N.; Suzumura, K.; Kawano, Y.; Yamaoka, M.; Zhang, H.P.; Watanabe, M.; Suzuki, K. YM-266183 and YM-266184, novel thiopeptide antibiotics produced by *Bacillus cereus* isolated from a marine sponge - I. Taxonomy, fermentation, isolation, physico-chemical properties and biological properties. *J. Antibiot.* **2003**, *56*, 123-128.
154. Suzumura, K.; Yokoi, T.; Funatsu, M.; Nagai, K.; Tanaka, K.; Zhang, H.P.; Suzuki, K. YM-266183 and YM-266184, novel thiopeptide antibiotics produced by *Bacillus cereus* isolated from a marine sponge - II. Structure elucidation. *J. Antibiot.* **2003**, *56*, 129-134.
155. Palomo, S.; Gonzalez, I.; de la Cruz, M.; Martin, J.; Tormo, J.R.; Anderson, M.; Hill, R.T.; Vicente, F.; Reyes, F.; Genilloud, O. Sponge-derived *Kocuria* and *Micrococcus* spp. as sources of the new thiazolyl peptide antibiotic kocurin. *Mar. Drugs*. **2013**, *11*, 1071-1086.
156. Martín, J.; Sousa, T.d.S.; Crespo, G.; Palomo, S.; González, I.; Tormo, J.R.; de la Cruz, M.; Anderson, M.; Hill, R.T.; Vicente, F., *et al.* Kocurin, the true structure of PM181104, an Anti-Methicillin-Resistant *Staphylococcus aureus* (MRSA) thiazolyl peptide from the marine-derived bacterium *Kocuria palustris*. *Mar. Drugs*. **2013**, *11*, 387-398.
157. Schneemann, I.; Nagel, K.; Kajahn, I.; Labes, A.; Wiese, J.; Imhoff, J.F. Comprehensive investigation of marine Actinobacteria associated with the sponge *Halichondria panicea*. *Appl. Environ. Microbiol.* **2010**, *76*, 3702-3714.
158. Schneemann, I.; Kajahn, I.; Ohlendorf, B.; Zinecker, H.; Erhard, A.; Nagel, K.; Wiese, J.; Imhoff, J.F. Mayamycin, a cytotoxic polyketide from a *Streptomyces* strain isolated from the marine sponge *Halichondria panicea*. *J. Nat. Prod.* **2010**, *73*, 1309-1312.
159. Reimer, A.; Blohm, A.; Quack, T.; Greveling, C.G.; Kozjak-Pavlovic, V.; Rudel, T.; Hentschel, U.; Abdelmohsen, U.R. Inhibitory activities of the marine streptomycete-derived compound SF2446A2 against *Chlamydia trachomatis* and *Schistosoma mansoni*. *J. Antibiot.* **2015**, <http://doi.org/10.1038/ja.2015.54>.
160. Vasilevsky, S.; Greub, G.; Nardelli-Haeffliger, D.; Baud, D. Genital *Chlamydia trachomatis*: understanding the roles of innate and adaptive immunity in vaccine research. *Clin. Microbiol. Rev.* **2014**, *27*, 346-370.
161. Li, D.; Xu, Y.; Shao, C.-L.; Yang, R.-Y.; Zheng, C.-J.; Chen, Y.-Y.; Fu, X.-M.; Qian, P.-Y.; She, Z.-G.; de Voogd, N.J., *et al.* Antibacterial bisabolane-type sesquiterpenoids from the sponge-derived fungus *Aspergillus* sp. *Mar. Drugs*. **2012**, *10*, 234-241.
162. Pruksakorn, P.; Arai, M.; Kotoku, N.; Vilchêze, C.; Baughn, A.D.; Moodley, P.; Jacobs Jr, W.R.; Kobayashi, M. Trichoderins, novel aminolipopeptides from a marine sponge-derived *Trichoderma* sp., are active against dormant *Mycobacteria*. *Bioorg. Med. Chem. Lett.* **2010**, *20*, 3658-3663.
163. Pruksakorn, P.; Arai, M.; Liu, L.; Moodley, P.; Jacobs Jr, W.R.; Kobayashi, M. Action-mechanism of Trichoderin A, an anti-dormant *Mycobacterial* aminolipopeptide from marine sponge-derived *Trichoderma* sp. *Biol. Pharm. Bull.* **2011**, *34*, 1287-1290.
164. Oliver, J.D. Recent findings on the viable but nonculturable state in pathogenic bacteria. *FEMS Microbiol. Rev.* **2010**, *34*, 415-425.
165. Coates, A.R.M.; Hu, Y. Novel approaches to developing new antibiotics for bacterial infections. *Br. J. Pharmacol.* **2007**, *152*, 1147-1154.
166. Coates, A.R.M.; Hu, Y. Targeting non-multiplying organisms as a way to develop novel antimicrobials. *Trends Pharmacol. Sci.* **2008**, *29*, 143-150.
167. Eltamany, E.E.; Abdelmohsen, U.R.; Ibrahim, A.K.; Hassanean, H.A.; Hentschel, U.; Ahmed, S.A. New antibacterial xanthone from the marine sponge-derived *Micrococcus* sp. EG45. *Bioorg. Med. Chem. Lett.* **2014**, *24*, 4939-4942.

168. Jayatilake, G.S.; Thornton, M.P.; Leonard, A.C.; Grimwade, J.E.; Baker, B.J. Metabolites from an Antarctic sponge-associated bacterium, *Pseudomonas aeruginosa*. *J. Nat. Prod.* **1996**, *59*, 293-296.
169. Song, F.H.; Ren, B.; Chen, C.X.; Yu, K.; Liu, X.R.; Zhang, Y.H.; Yang, N.; He, H.T.; Liu, X.T.; Dai, H.Q., et al. Three new sterigmatocystin analogues from marine-derived fungus *Aspergillus versicolor* MF359. *Appl. Microbiol. Biotechnol.* **2014**, *98*, 3753-3758.
170. Subramani, R.; Kumar, R.; Prasad, P.; Aalbersberg, W. Cytotoxic and antibacterial substances against multi-drug resistant pathogens from marine sponge symbiont: citrinin, a secondary metabolite of *Penicillium* sp. *Asian. Pac. J. Trop. Biomed.* **2013**, *3*, 291-296.
171. Lee, Y.; Li, H.; Hong, J.; Cho, H.; Bae, K.; Kim, M.; Kim, D.-K.; Jung, J. Bioactive metabolites from the sponge-derived fungus *Aspergillus versicolor*. *Arch Pharmacol Res.* **2010**, *33*, 231-235.
172. Zheng, L.; Chen, H.; Han, X.; Lin, W.; Yan, X. Antimicrobial screening and active compound isolation from marine bacterium NJ6-3-1 associated with the sponge *Hymeniacidon perleve*. *World. J. Microbiol. Biotechnol.* **2005**, *21*, 201-206.
173. Zhang, D.; Yang, X.; Kang, J.S.; Choi, H.D.; Son, B.W. Chlorohydroaspyrones A and B, antibacterial aspyrone derivatives from the marine-derived fungus *Exophiala* sp. *J. Nat. Prod.* **2008**, *71*, 1458-1460.
174. Xie, L.; Ouyang, Y.; Zou, K.; Wang, G.; Chen, M.; Sun, H.; Dai, S.; Li, X. Isolation and difference in anti-*Staphylococcus aureus* bioactivity of curvularin derivatives from fungus *Eupenicillium* sp. *Appl. Biochem. Biotechnol.* **2009**, *159*, 284-293.
175. Santos, O.C.S.; Soares, A.R.; Machado, F.L.S.; Romanos, M.T.V.; Muricy, G.; Giambiagi-deMarval, M.; Laport, M.S. Investigation of biotechnological potential of sponge-associated bacteria collected in Brazilian coast. *Lett. Appl. Microbiol.* **2015**, *60*, 140-147.
176. Sathiyarayanan, G.; Gandhimathi, R.; Sabarathnam, B.; Seghal Kiran, G.; Selvin, J. Optimization and production of pyrrolidone antimicrobial agent from marine sponge-associated *Streptomyces* sp. MAPS15. *Bioprocess. Biosyst. Eng.* **2014**, *37*, 561-573.
177. Karuppiyah, V.; Li, Y.; Sun, W.; Feng, G.; Li, Z. Functional gene-based discovery of phenazines from the actinobacteria associated with marine sponges in the South China Sea. *Appl. Microbiol. Biotechnol.* **2015**, 1-12.
178. Ibrahim, D.; Nazari, T.F.; Kassim, J.; Lim, S.-H. Prodigiosin - an antibacterial red pigment produced by *Serratia marcescens* IBRL USM 84 associated with a marine sponge *Xestospongia testudinaria*. *J. App. Pharm. Sci.* **2014**, *4*, 001-006.
179. Kunz, A.L.; Labes, A.; Wiese, J.; Bruhn, T.; Bringmann, G.; Imhoff, J.F. Nature's Lab for derivatization: new and revised structures of a variety of streptophenazines produced by a sponge-derived *Streptomyces* strain. *Mar. Drugs.* **2014**, *12*, 1699-1714.
180. Manilal, A.; Sabarathnam, B.; Kiran, G.S.; Sujith, S.; Shakir, C.; Selvin, J. Antagonistic potentials of marine sponge associated fungi *Aspergillus clavatus* MFD15. *Asian J of Medi Sci.* **2010**, *2*, 195-200.
181. Choi, E.J.; Kwon, H.C.; Ham, J.; Yang, H.O. 6-Hydroxymethyl-1-phenazine-carboxamide and 1,6-phenazinedimethanol from a marine bacterium, *Brevibacterium* sp. KMD 003, associated with marine purple vase sponge. *J. Antibiot.* **2009**, *62*, 621-624.
182. Viegelmann, C.; Margassery, L.M.; Kennedy, J.; Zhang, T.; O'Brien, C.; O'Gara, F.; Morrissey, J.P.; Dobson, A.D.W.; Edrada-Ebel, R. Metabolomic profiling and genomic study of a marine sponge-associated *Streptomyces* sp. *Mar. Drugs.* **2014**, *12*, 3323-3351.
183. Kobayashi, M.; Aoki, S.; Gato, K.; Matsunami, K.; Kurosu, M.; Kitagawa, I. Marine Natural-Products. 34. Trisindoline, a new antibiotic indole trimer, produced by a bacterium of *Vibrio* sp separated from the marine sponge *Hyrtios-Altum*. *Chem. Pharm. Bull.* **1994**, *42*, 2449-2451.
184. Dashti, Y.; Grkovic, T.; Abdelmohsen, U.R.; Hentschel, U.; Quinn, R.J. Production of induced secondary metabolites by a co-culture of sponge-associated *Actinomyces*, *Actinokineospora* sp. EG49 and *Nocardioopsis* sp. RV163. *Mar. Drugs.* **2014**, *12*, 3046-3059.
185. Jadulco, R.; Brauers, G.; Edrada, R.A.; Ebel, R.; Wray, V.; Sudarsono; Proksch, P. New metabolites from sponge-derived fungi *Curvularia lunata* and *Cladosporium herbarum*. *J. Nat. Prod.* **2002**, *65*, 730-733.
186. Santos, O.C.S.; Pontes, P.V.M.L.; Santos, J.F.M.; Muricy, G.; Giambiagi-deMarval, M.; Laport, M.S. Isolation, characterization and phylogeny of sponge-associated bacteria with antimicrobial activities from Brazil. *Res. Microbiol.* **2010**, *161*, 604-612.
187. Karkowska-Kuleta, J.; Rapala-Kozik, M.; Kozik, A. Fungi pathogenic to humans: molecular bases of virulence of *Candida albicans*, *Cryptococcus neoformans* and *Aspergillus fumigatus*. *Acta Biochim Pol.* **2009**, *56*, 211-224.
188. Van Thiel, D.H.; George, M.; Moore, C.M. Fungal infections: their diagnosis and treatment in transplant recipients. *Int. J. Hepatol.* **2012**, *2012*, 106923.
189. Richardson, M.D. Changing patterns and trends in systemic fungal infections. *J. Antimicrob. Chemoth.* **2005**, *56*, 5-11.

190. Fidel, P.L.; Vazquez, J.A.; Sobel, J.D. *Candida glabrata*: review of epidemiology, pathogenesis, and clinical disease with comparison to *C. albicans*. *Clin. Microbiol Rev.* **1999**, *12*, 80-96.
191. Galimberti, R.; Torre, A.C.; Baztán, M.C.; Rodriguez-Chiappetta, F. Emerging systemic fungal infections. *Clin. Dermatol.* **2012**, *30*, 633-650.
192. El-Gendy, M.A.; El-Bondkly, A.A. Production and genetic improvement of a novel antimycotic agent, Saadamycin, against Dermatophytes and other clinical fungi from endophytic *Streptomyces* sp. Hedaya48. *J. Ind Microbiol. Biotechnol.* **2010**, *37*, 831-841.
193. Nagai, K.; Kamigiri, K.; Matsumoto, H.; Kawano, Y.; Yamaoka, M.; Shimoi, H.; Watanabe, M.; Suzuki, K. YM-202204, a new antifungal antibiotic produced by marine fungus *Phoma* sp. *J. Antibiot.* **2002**, *55*, 1036-1041.
194. McLellan, C.A.; Whitesell, L.; King, O.D.; Lancaster, A.K.; Mazitschek, R.; Lindquist, S. Inhibiting GPI anchor biosynthesis in fungi stresses the endoplasmic reticulum and enhances immunogenicity. *ACS Chemical Biology.* **2012**, *7*, 1520-1528.
195. Butts, A.; Krysan, D.J. Antifungal drug discovery: something old and something new. *Plos Pathogens.* **2012**, *8*.
196. Devi, P.; Wahidullah, S.; Rodrigues, C.; Souza, L.D. The sponge-associated bacterium *Bacillus licheniformis* SABI: A source of antimicrobial compounds. *Mar. Drugs.* **2010**, *8*, 1203-1212.
197. Edrada, R.A.; Heubes, M.; Brauers, G.; Wray, V.; Berg, A.; Grafe, U.; Wohlfarth, M.; Muhlbacher, J.; Schaumann, K.; Sudarsono, *et al.* Online analysis of xestodecalactones A-C, novel bioactive metabolites from the fungus *Penicillium* cf. *montanense* and their subsequent isolation from the sponge *Xestospongia exigua*. *J. Nat. Prod.* **2002**, *65*, 1598-1604.
198. Imamura, N.; Nishijima, M.; Adachi, K.; Sano, H. Novel Antimycin antibiotics, Urauchimycin-a and Urauchimycin-B, produced by marine Actinomycete. *J. Antibiot.* **1993**, *46*, 241-246.
199. Khan, S.T.; Takagi, M.; Shin-ya, K. Diversity, salt requirement, and antibiotic production of Actinobacteria isolated from marine sponges. *Actinomycetologica.* **2010**, *24*, 18-23.
200. Abdelmohsen, U.R.; Pimentel-Elardo, S.M.; Hanora, A.; Radwan, M.; Abou-El-Ela, S.H.; Ahmed, S.; Hentschel, U. Isolation, phylogenetic analysis and anti-infective activity screening of marine sponge-associated Actinomycetes. *Mar. Drugs.* **2010**, *8*, 399-412.
201. Anand, T.P.; Bhat, A.W.; Shouche, Y.S.; Roy, U.; Siddharth, J.; Sarma, S.P. Antimicrobial activity of marine bacteria associated with sponges from the waters off the coast of South East India. *Microbiol Res.* **2006**, *161*, 252-262.
202. Pabel, C.T.; Vater, J.; Wilde, C.; Franke, P.; Hofemeister, J.; Adler, B.; Bringmann, G.; Hacker, J.; Hentschel, U. Antimicrobial activities and matrix-assisted laser desorption/ionization mass spectrometry of *Bacillus* isolates from the marine sponge *Aphysina aerophoba*. *Mar. Biotechnol.* **2003**, *5*, 424-434.
203. Flemer, B.; Kennedy, J.; Margassery, L.M.; Morrissey, J.P.; O'Garra, F.; Dobson, A.D.W. Diversity and antimicrobial activities of microbes from two Irish marine sponges, *Suberites carnosus* and *Leucosolenia* sp. *J. App. Microbiol.* **2012**, *112*, 289-301.
204. Cohen, E.; Koch, L.; Thu, K.M.; Rahamim, Y.; Aluma, Y.; Ilan, M.; Yarden, O.; Carmeli, S. Novel terpenoids of the fungus *Aspergillus insuetus* isolated from the Mediterranean sponge *Psammocinia* sp. collected along the coast of Israel. *Bioorg. Med. Chem.* **2011**, *19*, 6587-6593.
205. Holler, U.; Konig, G.M.; Wright, A.D. Three new metabolites from marine-derived fungi of the genera *Coniothyrium* and *Microsphaeropsis*. *J. Nat. Prod.* **1999**, *62*, 114-118.
206. Ang, K.K.H.; Holmes, M.J.; Higa, T.; Hamann, M.T.; Kara, U.A.K. *In vivo* antimalarial activity of the beta-carboline alkaloid manzamine A. *Antimicrob. Agents Chemother.* **2000**, *44*, 1645-1649.
207. Fattorusso, E.; Tagliatalata-Scafati, O. Marine antimalarials. *Mar. Drugs.* **2009**, *7*, 130-152.
208. Sakai, R.; Higa, T.; Jefford, C.W.; Bernardinelli, G. Manzamine A, a novel antitumor alkaloid from a sponge. *J. Am. Chem. Soc.* **1986**, *108*, 6404-6405.
209. Radwan, M.; Hanora, A.; Khalifa, S.; Abou-El-Ela, S.H. Manzamines. *Cell cycle.* **2012**, *11*, 1765-1772.
210. Eyase, F.L.; Akala, H.M.; Johnson, J.D.; Walsh, D.S. Inhibitory Activity of ferroquine, versus chloroquine, against Western Kenya *Plasmodium falciparum* field isolates determined by a SYBR Green I *in Vitro* Assay. *Am J Trop Med Hyg* **2011**, *85*, 984-988.
211. Rao, K.V.; Santarsiero, B.D.; Mesecar, A.D.; Schinazi, R.F.; Tekwani, B.L.; Hamann, M.T. New manzamine alkaloids with activity against infectious and tropical parasitic diseases from an Indonesian sponge. *J. Nat. Prod.* **2003**, *66*, 823-828.
212. Kobayashi, M.; Chen, Y.-J.; Aoki, S.; In, Y.; Ishida, T.; Kitagawa, I. Four new β -carboline alkaloids isolated from two Okinawan marine sponges of *Xestospongia* sp. and *Haliclona* sp.). *Tetrahedron.* **1995**, *51*, 3727-3736.
213. Rao, K.V.; Kasanah, N.; Wahyuono, S.U.; Tekwani, B.L.; Schinazi, R.F.; Hamann, M.T. Three new manzamine alkaloids from a common Indonesian sponge and their activity against infectious and tropical parasitic diseases. *J. Nat. Prod.* **2004**, *67*, 1314-1318.

214. Hill, R.T.; Hamann, M.; Peraud, O.T.; Kasanah, N. Manzamine producing Actinomycetes. US20050244938 A1, 2005.
215. Peraud, O. Isolation and Characterization of a sponge-associated Actinomycete that produces Manzamines. University of Maryland, 2006.
216. Waters, A.L.; Peraud, O.; Kasanah, N.; Sims, J.; Kothalawala, N.; Anderson, M.A.; Abbas, S.H.; Rao, K.V.; Jupally, V.R.; Kelly, M., *et al.* An analysis of the sponge *Acanthostrongylophora igens*' microbiome yields an actinomycete that produces the natural product manzamine A. *Frontiers in Marine Science*. **2014**, *1*.
217. Pimentel-Elardo, S.M.; Kozytska, S.; Bugni, T.S.; Ireland, C.M.; Moll, H.; Hentschel, U. Anti-parasitic compounds from *Streptomyces* sp. strains isolated from Mediterranean sponges. *Mar. Drugs*. **2010**, *8*, 373-380.
218. Scopel, M.; dos Santos, O.; Frasson, A.P.; Abraham, W.-R.; Tasca, T.; Henriques, A.T.; Macedo, A.J. Anti-Trichomonas vaginalis activity of marine-associated fungi from the South Brazilian Coast. *Exp. Parasitol.* **2013**, *133*, 211-216.
219. Petrin, D.; Delgaty, K.; Bhatt, R.; Garber, G. Clinical and microbiological aspects of *Trichomonas vaginalis*. *Clinical Microbiology Reviews*. **1998**, *11*, 300-317.
220. Inbaneson, S.J.; Ravikumar, S. In vitro antiplasmodial activity of marine sponge *Hyattella intestinalis* associated bacteria against *Plasmodium falciparum*. *Asian Pac J Trop Biomed*. **2011**, *1*, S100-S104.
221. Inbaneson, S.J.; Ravikumar, S. In vitro antiplasmodial activity of marine sponge *Stylissa carteri* associated bacteria against *Plasmodium falciparum*. *Asian Pac J Trop Dis*. **2012**, *2*, 370-374.
222. Inbaneson, S.J.; Ravikumar, S. In vitro antiplasmodial activity of marine sponge *Clathria indica* associated bacteria against *Plasmodium falciparum*. *Asian Pac J Trop Biomed*. **2012**, *2*, S1090-S1095.
223. Inbaneson, S.J.; Ravikumar, S. In vitro antiplasmodial activity of *Clathria vulpina* sponge associated bacteria against *Plasmodium falciparum*. *Asian Pac J Trop Dis*. **2012**, *2*, 319-323.
224. Inbaneson, S.J.; Ravikumar, S. In vitro antiplasmodial activity of bacterium RJAUTHB 14 associated with marine sponge *Haliclona Grant* against *Plasmodium falciparum*. *Paras Res*. **2012**, *110*, 2255-2262.
225. Abdelmohsen, U.R.; Szesny, M.; Othman, E.M.; Schirmeister, T.; Grond, S.; Stopper, H.; Hentschel, U. Antioxidant and anti-protease activities of diazepinomicin from the sponge-associated *Micromonospora* strain RV115. *Mar. Drugs*. **2012**, *10*, 2208-2221.
226. Abdelmohsen, U.R.; Cheng, C.; Viegelmann, C.; Zhang, T.; Grkovic, T.; Ahmed, S.; Quinn, R.J.; Hentschel, U.; Edrada-Ebel, R. Dereplication strategies for targeted isolation of new antitrypanosomal Actinosporins A and B from a marine sponge associated-*Actinokineospora* sp. EG49. *Mar. Drugs*. **2014**, *12*, 1220-1244.
227. Cheng, C.; MacIntyre, L.; Abdelmohsen, U.R.; Horn, H.; Polymenakou, P.N.; Edrada-Ebel, R.; Hentschel, U. Biodiversity, anti-trypanosomal activity screening, and metabolomic profiling of actinomycetes isolated from Mediterranean sponges. *Plos One*. **2015**, *10*, e0138528.
228. Pimentel-Elardo, S.M.; Buback, V.; Gulder, T.A.M.; Bugni, T.S.; Reppart, J.; Bringmann, G.; Ireland, C.M.; Schirmeister, T.; Hentschel, U. New Tetracycline derivatives with anti-Trypanosomal and protease inhibitory activities. *Mar. Drugs*. **2011**, *9*, 1682-1697.
229. Ashforth, E.J.; Fu, C.Z.; Liu, X.Y.; Dai, H.Q.; Song, F.H.; Guo, H.; Zhang, L.X. Bioprospecting for antituberculosis leads from microbial metabolites. *Nat. Prod. Rep.* **2010**, *27*, 1709-1719.
230. Seipke, R.F.; Kaltenpoth, M.; Hutchings, M.I. *Streptomyces* as symbionts: an emerging and widespread theme? *FEMS Microbiol. Rev.* **2012**, *36*, 862-876.
231. Traxler, M.F.; Kolter, R. Natural products in soil microbe interactions and evolution. *Nat. Prod. Rep.* **2015**, *32*, 956-970.
232. Harrington, C.; Reen, F.; Mooij, M.; Stewart, F.; Chabot, J.-B.; Guerra, A.; Glöckner, F.; Nielsen, K.; Gram, L.; Dobson, A., *et al.* Characterisation of Non-Autoinducing Tropolithetic Acid (TDA) Production from Marine Sponge *Pseudovibrio* Species. *Mar. Drugs*. **2014**, *12*, 5960-5978.
233. Keller, N.P.; Turner, G.; Bennett, J.W. Fungal secondary metabolism — from biochemistry to genomics. *Nat. Rev. Micro.* **2005**, *3*, 937-947.
234. Laursen, J.B.; Nielsen, J. Phenazine natural products: biosynthesis, synthetic analogues, and biological activity. *Chemical Reviews*. **2004**, *104*, 1663-1686.
235. Wang, W.; Préville, P.; Morin, N.; Mounir, S.; Cai, W.; Siddiqui, M.A. Hepatitis C viral IRES inhibition by phenazine and phenazine-like molecules. *Bioorg. Med. Chem. Lett.* **2000**, *10*, 1151-1154.
236. Mavrodi, D.V.; Mavrodi, O.V.; Parejko, J.A.; Bonsall, R.F.; Kwak, Y.S.; Paulitz, T.C.; Thomashow, L.S.; Weller, D.M. Accumulation of the Antibiotic Phenazine-1-Carboxylic Acid in the Rhizosphere of Dryland Cereals. *Appl. Environ. Microbiol.* **2012**, *78*, 804-812.
237. Makgatho, M.E.; Anderson, R.; O'Sullivan, J.F.; Egan, T.J.; Freese, J.A.; Cornelius, N.; van Rensburg, C.E.J. Tetramethylpiperidine-substituted phenazines as novel anti-plasmodial agents. *Drug Dev. Res.* **2000**, *50*, 195-202.

238. Gao, X.; Lu, Y.; Xing, Y.; Ma, Y.; Lu, J.; Bao, W.; Wang, Y.; Xi, T. A novel anticancer and antifungus phenazine derivative from a marine actinomycete BM-17. *Microbiol Res.* **2012**, *167*, 616-622.
239. Ozturk, B.; de Jaeger, L.; Smidt, H.; Sipkema, D. Culture-dependent and independent approaches for identifying novel halogenases encoded by *Crambe crambe* (marine sponge) microbiota. *Sci.Rep.* **2013**, *3*.
240. Muller, W.E.G.; Zahn, R.K.; Kurelec, B.; Lucu, C.; Muller, I.; Uhlenbruck, G. Lectin, a possible basis for symbiosis between bacteria and sponges. *J. Bacteriol.* **1981**, *145*, 548-558.
241. Unson, M.D.; Holland, N.D.; Faulkner, D.J. A brominated secondary metabolite synthesized by the cyanobacterial symbiont of a marine sponge and accumulation of the crystalline metabolite in the sponge tissue. *Mar. Biol.* **1994**, *119*, 1-11.
242. Milshteyn, A.; Schneider, J.S.; Brady, S.F. Mining the Metabiome: Identifying Novel Natural Products from Microbial Communities. *Chem Biol.* **2014**, *21*, 1211-1223.
243. Marmann, A.; Aly, A.; Lin, W.; Wang, B.; Proksch, P. Co-cultivation—a powerful emerging tool for enhancing the chemical diversity of microorganisms. *Mar. Drugs.* **2014**, *12*, 1043.
244. Bertrand, S.; Bohni, N.; Schnee, S.; Schumpp, O.; Gindro, K.; Wolfender, J.-L. Metabolite induction via microorganism co-culture: a potential way to enhance chemical diversity for drug discovery. *Biotechnol. Adv.* **2014**, *32*, 1180-1204.
245. Wang, G.-Y.-S.; Graziani, E.; Waters, B.; Pan, W.; Li, X.; McDermott, J.; Meurer, G.; Saxena, G.; Andersen, R.J.; Davies, J. Novel natural products from soil DNA libraries in a *Streptomyces* Host. *Org. Lett.* **2000**, *2*, 2401-2404.
246. Brady, S.F.; Chao, C.J.; Handelsman, J.; Clardy, J. Cloning and heterologous expression of a natural product biosynthetic gene cluster from eDNA. *Org. Lett.* **2001**, *3*, 1981-1984.
247. Chung, E.J.; Lim, H.K.; Kim, J.C.; Choi, G.J.; Park, E.J.; Lee, M.H.; Chung, Y.R.; Lee, S.W. Forest soil metagenome gene cluster involved in antifungal activity expression in *Escherichia coli*. *Appl. Environ. Microb.* **2008**, *74*, 723-730.
248. Simon, C.; Daniel, R. Metagenomic analyses: past and future trends. *App. Environ. Microb.* **2011**, *77*, 1153-1161.
249. Piel, J. Approaches to capturing and designing biologically active small molecules produced by uncultured microbes. *Annu. Rev. Microbiol.* **2011**, *65*, 431-453.
250. Wilson, M.C.; Piel, J. Metagenomic approaches for exploiting uncultivated bacteria as a resource for novel biosynthetic enzymology. *Chem Biol.* **2013**, *20*, 636-647.
251. MacNeil, I.A.; Tiong, C.L.; Minor, C.; August, P.R.; Grossman, T.H.; Loiacono, K.A.; Lynch, B.A.; Phillips, T.; Narula, S.; Sundaramoorthi, R., *et al.* Expression and isolation of antimicrobial small molecules from soil DNA libraries. *J. Mol. Microb. Biotech.* **2001**, *3*, 301-308.
252. He, R.; Wakimoto, T.; Egami, Y.; Kenmoku, H.; Ito, T.; Asakawa, Y.; Abe, I. Heterologously expressed β -hydroxyl fatty acids from a metagenomic library of a marine sponge. *Bioorg. Med. Chem. Lett.* **2012**, *22*, 7322-7325.
253. He, R.; Wang, B.C.; Wakimoto, T.; Wang, M.Y.; Zhu, L.C.; Abe, I. Cyclodipeptides from metagenomic library of a Japanese marine sponge. *J. Brazil. Chem. Soc.* **2013**, *24*, 1926-1932.
254. Ongley, S.E.; Bian, X.; Neilan, B.A.; Müller, R. Recent advances in the heterologous expression of microbial natural product biosynthetic pathways. *Nat. Prod. Rep.* **2013**, *30*, 1121-1138.
255. Baltz, R.H. Molecular engineering approaches to peptide, polyketide and other antibiotics. *Nat. Biotechnol.* **2006**, *24*, 1533-1540.
256. Dobson, A.W.; Jackson, S.; Kennedy, J.; Margassery, L.; Flemer, B.; O'Leary, N.; Morrissey, J.; O'Gara, F. Marine sponges – molecular biology and biotechnology. In *Springer Handbook of Marine Biotechnology*, Kim, S.-K., Ed. Springer Berlin Heidelberg: 2015; pp 219-254.
257. Baltz, R.H. *Streptomyces* and *Saccharopolyspora* hosts for heterologous expression of secondary metabolite gene clusters. *J. Ind. Microbiol Biotechnol.* **2010**, *37*, 759-772.
258. Piel, J. Approaches to capturing and designing biologically active small molecules produced by uncultured microbes. *Annu. Rev. Microbiol.* **2011**, *65*, 431-453.
259. Kennedy, J.; Marchesi, J.R.; Dobson, A.D.W. Metagenomic approaches to exploit the biotechnological potential of the microbial consortia of marine sponges. *Appl. Microbiol. Biotechnol.* **2007**, *75*, 11-20.
260. Piel, J. A polyketide synthase-peptide synthetase gene cluster from an uncultured bacterial symbiont of *Paederus* beetles. *Proc. Natl. Acad. Sci.* **2002**, *99*, 14002-14007.
261. Piel, J.; Butzke, D.; Fusetani, N.; Hui, D.; Platzer, M.; Wen, G.; Matsunaga, S. Exploring the chemistry of uncultivated bacterial symbionts: antitumor polyketides of the pederin family. *J. Nat. Prod.* **2005**, *68*, 472-479.
262. Piel, J.; Hui, D.; Wen, G.; Butzke, D.; Platzer, M.; Fusetani, N.; Matsunaga, S. Antitumor polyketide biosynthesis by an uncultivated bacterial symbiont of the marine sponge *Theonella swinhoei*. *Proc. Natl. Acad. Sci.* **2004**, *101*, 16222-16227.

263. Piel, J.; Hui, D.Q.; Fusetani, N.; Matsunaga, S. Targeting modular polyketide synthases with iteratively acting acyltransferases from metagenomes of uncultured bacterial consortia. *Environ. Microbiol.* **2004**, *6*, 921-927.
264. Piel, J.; Wen, G.; Platzer, M.; Hui, D. Unprecedented diversity of catalytic domains in the first four modules of the putative pederin polyketide synthase. *ChemBioChem.* **2004**, *5*, 93-98.
265. Fisch, K.M.; Gurgui, C.; Heycke, N.; van der Sar, S.A.; Anderson, S.A.; Webb, V.L.; Taudien, S.; Platzer, M.; Rubio, B.K.; Robinson, S.J., *et al.* Polyketide assembly lines of uncultivated sponge symbionts from structure-based gene targeting. *Nat. Chem. Biol.* **2009**, *5*, 494-501.
266. Schirmer, A.; Gadkari, R.; Reeves, C.D.; Ibrahim, F.; DeLong, E.F.; Hutchinson, C.R. Metagenomic analysis reveals diverse polyketide synthase gene clusters in microorganisms associated with the marine sponge *Discodermia dissoluta*. *Appl Environ Microb.* **2005**, *71*, 4840-4849.
267. Rhoads, A.; Au, K.F. PacBio sequencing and its applications. *Genomics, Proteomics & Bioinformatics.* **2015**, *13*, 278-289.
268. Podar, M.; Abulencia, C.B.; Walcher, M.; Hutchison, D.; Zengler, K.; Garcia, J.A.; Holland, T.; Cotton, D.; Hauser, L.; Keller, M. Targeted access to the genomes of low-abundance organisms in complex microbial communities. *Appl. Environ. Microbiol.* **2007**, *73*, 3205-3214.
269. Banik, J.J.; Brady, S.F. Recent application of metagenomic approaches toward the discovery of antimicrobials and other bioactive small molecules. *Curr. Opin. Microbiol.* **2010**, *13*, 603-609.
270. Medema, M.H.; Blin, K.; Cimermancic, P.; de Jager, V.; Zakrzewski, P.; Fischbach, M.A.; Weber, T.; Takano, E.; Breitling, R. antiSMASH: rapid identification, annotation and analysis of secondary metabolite biosynthesis gene clusters in bacterial and fungal genome sequences. *Nucleic Acids Res.* **2011**, *39*, W339-W346.
271. Yun, J.; Ryu, S. Screening for novel enzymes from metagenome and SIGEX, as a way to improve it. *Microb. Cell. Fact.* **2005**, *4*, 8-8.
272. Downey, R.V.; Griffiths, H.J.; Linse, K.; Janussen, D. Diversity and distribution patterns in high southern latitude sponges. *Plos One.* **2012**, *7*, e41672.
273. Hentschel, U.; Fieseler, L.; Wehrl, M.; Gernert, C.; Steinert, M.; Hacker, J.; Horn, M. Microbial Diversity of Marine Sponges. In *Sponges (Porifera)*, Müller, W.E.G., Ed. Springer Berlin Heidelberg: Berlin, Heidelberg, 2003; pp 59-88.
274. Pita, L.; Turon, X.; López-Legentil, S.; Erwin, P.M. Host rules: spatial stability of bacterial communities associated with marine sponges (*Ircinia* spp.) in the Western Mediterranean Sea. *FEMS. Microbiol Ecol.* **2013**, *86*, 268-276.
275. Haroim, C.C.P.; Costa, R. Temporal dynamics of prokaryotic communities in the marine sponge *Sarcotragus spinosulus*. *Mol Ecol.* **2014**, *23*, 3097-3112.
276. Gantt, S.E.; Lopez-Legentil, S.; Erwin, P.M. Stable microbial communities in the sponge *Crambe crambe* from inside and outside a polluted Mediterranean harbor. *FEMS Microbiol. Lett.* **2017**, *364*.
277. Enticknap, J.J.; Kelly, M.; Peraud, O.; Hill, R.T. Characterization of a culturable Alphaproteobacterial symbiont common to many marine sponges and evidence for vertical transmission via sponge larvae. *App. Env. Microbiol.* **2006**, *72*, 3724-3732.
278. Schmitt, S.; Tsai, P.; Bell, J.; Fromont, J.; Ilan, M.; Lindquist, N.; Perez, T.; Rodrigo, A.; Schupp, P.J.; Vacelet, J., *et al.* Assessing the complex sponge microbiota: core, variable and species-specific bacterial communities in marine sponges. *ISME J.* **2012**, *6*, 564-576.
279. Keren, R.; Mayzel, B.; Lavy, A.; Polishchuk, I.; Levy, D.; Fakra, S.C.; Pokroy, B.; Ilan, M. Sponge-associated bacteria mineralize arsenic and barium on intracellular vesicles. *Nat Commun.* **2017**, *8*.
280. Horn, H.; Slaby, B.M.; Jahn, M.T.; Bayer, K.; Moitinho-Silva, L.; Förster, F.; Abdelmohsen, U.R.; Hentschel, U. An Enrichment of CRISPR and other defense-related features in marine sponge-associated microbial metagenomes. *Front Microbiol.* **2016**, *7*.
281. Slaby, B.M.; Hackl, T.; Horn, H.; Bayer, K.; Hentschel, U. Metagenomic binning of a marine sponge microbiome reveals unity in defense but metabolic specialization. *ISME J.* **2017**, *11*, 2465-2478.
282. Piel, J. Metabolites from symbiotic bacteria. *Nat. Prod. Rep.* **2009**, *26*, 338-362.
283. Sunagawa, S.; Coelho, L.P.; Chaffron, S.; Kultima, J.R.; Labadie, K.; Salazar, G.; Djahanschiri, B.; Zeller, G.; Mende, D.R.; Alberti, A., *et al.* Structure and function of the global ocean microbiome. *Science.* **2015**, *348*.
284. Bongaerts, P.; Frade, P.R.; Hay, K.B.; Englebort, N.; Latijnhouwers, K.R.W.; Bak, R.P.M.; Vermeij, M.J.A.; Hoegh-Guldberg, O. Deep down on a Caribbean reef: lower mesophotic depths harbor a specialized coral-endosymbiont community. *Sci.Rep.* **2015**, *5*.
285. Brazeau, D.A.; Lesser, M.P.; Slattery, M. Genetic structure in the coral, *Montastraea cavernosa*: assessing genetic differentiation among and within mesophotic reefs. *Plos One.* **2013**, *8*, 1-12.

286. Gonzalez-Zapata, F.L.; Bongaerts, P.; Ramirez-Portilla, C.; Adu-Oppong, B.; Walljasper, G.; Reyes, A.; Sanchez, J.A. Holobiont diversity in a reef-building coral over its entire depth range in the mesophotic zone. *Front. Mar. Sci.* **2018**, 1-13.
287. Lesser, M.P.; Marc, S.; Michael, S.; Michiko, O.; D., G.R.; Andrea, G. Photoacclimatization by the coral *Montastraea cavernosa* in the mesophotic zone: light, food, and genetics. *Ecology*. **2010**, *91*, 990-1003.
288. Vermeij, M.J.A.; Bak, R.P.M. How are coral populations structured by light? marine light regimes and the distribution of *Madracis*. *Mar. Ecol. Prog. Series*. **2002**, *233*, 105-116.
289. Pawlik, J.R.; Chanas, B.; Toonen, R.J.; Fenical, W. Defenses of Caribbean sponges against predatory Reef Fish. I. chemical deterrence. *Mar. Ecol. Prog. Series* **1995**, *127*, 183-194.
290. Loh, T.L.; Pawlik, J.R. Chemical defenses and resource trade-offs structure sponge communities on Caribbean coral reefs. *Proc. Natl. Acad. Sci.* **2014**, *111*, 4151-4156.
291. Page, M.; West, L.; Northcote, P.; Battershill, C.; Kelly, M. Spatial and temporal variability of cytotoxic metabolites in populations of the New Zealand sponge *Mycale hentscheli*. *J. Chem. Ecol.* **2005**, *31*, 1161-1174.
292. Webster, N.S. Sponge disease: a global threat? *Environ. Microbiol.* **2007**, *9*, 1363-1375.
293. Newbold, R.W.; Jensen, P.R.; Fenical, W.; Pawlik, J.R. Antimicrobial activity of Caribbean sponge extracts. *Aquat. Microb. Ecol.* **1999**, *19*, 279-284.
294. Sarah, R.K.; Garo, E.; Paul, R.J.; Timothy, P.H.; William, F.; Joseph, R.P. Effects of Caribbean sponge extracts on bacterial attachment. *Aquat. Microb. Ecol.* **2005**, *31*, 175-182.
295. McMurray, S.E.; Finelli, C.M.; Pawlik, J.R. Population dynamics of giant barrel sponges on Florida coral reefs. *J. Exp. Mar. Biol. Ecol.* **2015**, *473*, 73-80.
296. Deignan, L.K.; Pawlik, J.R.; López-Legentil, S. Evidence for shifting genetic structure among Caribbean giant barrel sponges in the Florida Keys. *Mar. Biol.* **2018**, *165*, 106.
297. Chanas, B.; Pawlik, J.R. Variability in the chemical defense of the Caribbean reef sponge *Xestospongia muta*. *Proceedings of the 8th International Coral Reef Symposium*. **1997**, *2*, 1363-1368.
298. Fiore, C.L.; Jarett, J.K.; Lesser, M.P. Symbiotic prokaryotic communities from different populations of the giant barrel sponge, *Xestospongia muta*. *Microbiologyopen*. **2013**, *2*, 938-952.
299. Iwai, S.; Weinmaier, T.; Schmidt, B.L.; Albertson, D.G.; Poloso, N.J.; Dabbagh, K.; DeSantis, T.Z. Piphillin: improved prediction of metagenomic content by direct inference from human microbiomes. *Plos One*. **2016**, *11*.
300. Erpenbeck, D.; List-Armitage, S.; Alvarez, B.; Degnan, B.M.; Worheide, G.; Hooper, J.N.A. The systematics of Raspailiidae (Demospongiae : Poecilosclerida : Microcionina) re-analysed with a ribosomal marker. *J. Mar. Biol. Assoc. UK*. **2007**, *87*, 1571-1576.
301. Meyer, C.P.; Geller, J.B.; Paulay, G. Fine scale endemism on coral reefs: Archipelagic differentiation in turbinid gastropods. *Evolution*. **2005**, *59*, 113-125.
302. Kearse, M.; Moir, R.; Wilson, A.; Stones-Havas, S.; Cheung, M.; Sturrock, S.; Buxton, S.; Cooper, A.; Markowitz, S.; Duran, C., et al. Geneious Basic: An integrated and extendable desktop software platform for the organization and analysis of sequence data. *Bioinformatics*. **2012**, *28*, 1647-1649.
303. Erpenbeck, D.; Voigt, O.; Gultas, M.; Worheide, G. The sponge genetree server-providing a phylogenetic backbone for poriferan evolutionary studies. *Zootaxa*. **2008**, 58-60.
304. Tamura, K.; Stecher, G.; Peterson, D.; Filipiński, A.; Kumar, S. MEGA6: Molecular Evolutionary Genetics analysis version 6.0. *Mol. Biol. Evol.* **2013**, *30*, 2725-2729.
305. Parada, A.E.; Needham, D.M.; Fuhrman, J.A. Every base matters: assessing small subunit rRNA primers for marine microbiomes with mock communities, time series and global field samples. *Environ. Microbiol.* **2016**, *18*, 1403-1414.
306. Apprill, A.; McNally, S.; Parsons, R.; Weber, L. Minor revision to V4 region SSU rRNA 806R gene primer greatly increases detection of SAR11 bacterioplankton. *Aquat. Microb. Ecol.* **2015**, *75*, 129-137.
307. van Lingen, H.J.; Edwards, J.E.; Vaidya, J.D.; van Gastelen, S.; Saccenti, E.; van den Bogert, B.; Bannink, A.; Smidt, H.; Plugge, C.M.; Dijkstra, J. Diurnal dynamics of gaseous and dissolved metabolites and microbiota composition in the bovine rumen. *Front Microbiol.* **2017**, *8*.
308. Dat, T.T.H.; Steinert, G.; Thi Kim Cuc, N.; Smidt, H.; Sipkema, D. Archaeal and bacterial diversity and community composition from 18 phylogenetically divergent sponge species in Vietnam. *PeerJ*. **2018**, *6*, 1-23.
309. Ramiro-Garcia, J.; Hermes, G.; Giatsis, C.; Sipkema, D.; Zoetendal, E.; Schaap, P.; Smidt, H. NG-Tax, a highly accurate and validated pipeline for analysis of 16S rRNA amplicons from complex biomes *F1000Research*. **2016**, *5*, 1-44.
310. Yilmaz, P.; Parfrey, L.W.; Yarza, P.; Gerken, J.; Pruesse, E.; Quast, C.; Schweer, T.; Peplies, J.; Ludwig, W.; Glöckner, F.O. The SILVA and "All-species Living Tree Project (LTP)" taxonomic frameworks. *Nucleic. Acids. Res.* **2014**, *42*, 643-648.

311. McMurdie, P.J.; Holmes, S. phyloseq: An R package for reproducible interactive analysis and graphics of microbiome census data. *Plos One*. **2013**, *8*, e61217.
312. Lahti, L.; Shetty, A.S.; Blake, T.; Salojarvi, J. microbiome R package. **2017**, <http://microbiome.github.com/microbiome>.
313. Wickham, H. *ggplot2: Elegant Graphics for Data Analysis*. Springer-Verlag New York: 2016, <http://ggplot2.org>.
314. Paradis, E.; Claude, J.; Strimmer, K. APE: Analyses of Phylogenetics and Evolution in R language. *Bioinformatics*. **2004**, *20*, 289-290.
315. Kembel, S.W.; Cowan, P.D.; Helmus, M.R.; Cornwell, W.K.; Morlon, H.; Ackerly, D.D.; Blomberg, S.P.; Webb, C.O. Picante: R tools for integrating phylogenies and ecology. *Bioinformatics*. **2010**, *26*, 1463-1464.
316. Kolde, R. *heatmap: Pretty Heatmaps*, R package version 1.0.8.; 2015.
317. Parks, D.H.; Tyson, G.W.; Hugenholtz, P.; Beiko, R.G. STAMP: statistical analysis of taxonomic and functional profiles. *Bioinformatics*. **2014**, *30*, 3123-3124.
318. Rohde, S.; Nietzer, S.; Schupp, P.J. Prevalence and mechanisms of dynamic chemical defenses in tropical sponges. *Plos One*. **2015**, *10*, 1-19.
319. Lesser, M.P.; Slattery, M.; Leichter, J.J. Ecology of mesophotic coral reefs. *J. Exp. Mar. Biol Ecol*. **2009**, *375*, 1-8.
320. Webster, N.S.; Cobb, R.E.; Negri, A.P. Temperature thresholds for bacterial symbiosis with a sponge. *ISME J*. **2008**, *2*, 830.
321. Simister, R.; Taylor, M.W.; Tsai, P.; Fan, L.; Bruxner, T.J.; Crowe, M.L.; Webster, N. Thermal stress responses in the bacterial biosphere of the Great Barrier Reef sponge, *Rhopaloeides odorabile*. *Environ. Microbiol*. **2012**, *14*, 3232-3246.
322. Goodbody-Gringley, G.; Marchini, C.; Chequer, A.D.; Goffredo, S. Population structure of *Montastraea cavernosa* on shallow versus mesophotic reefs in Bermuda. *Plos One*. **2015**, *10*, 1-17.
323. Flombaum, P.; Gallegos, J.L.; Gordillo, R.A.; Rincón, J.; Zabala, L.L.; Jiao, N.; Karl, D.M.; Li, W.K.W.; Lomas, M.W.; Veneziano, D., et al. Present and future global distributions of the marine Cyanobacteria. *Proc. Natl. Acad. Sci*. **2013**, *110*, 9824-9829.
324. Ma, Y.; Zeng, Y.; Jiao, N.; Shi, Y.; Hong, N. Vertical distribution and phylogenetic composition of bacteria in the Eastern Tropical North Pacific Ocean. *Microbiol Res*. **2009**, *164*, 624-633.
325. Thacker, R.W. Impacts of shading on sponge-Cyanobacteria symbioses: a comparison between host-specific and generalist associations. *Integr. Comp. Biol*. **2005**, *45*, 369-376.
326. Erwin, P.M.; Thacker, R.W. Phototrophic nutrition and symbiont diversity of two Caribbean sponge-cyanobacteria symbioses. *Mar Ecol Prog Series*. **2008**, *362*, 139-147.
327. Freeman, C.J.; Thacker, R.W. Complex interactions between marine sponges and their symbiotic microbial communities. *Limnology and Oceanography*. **2011**, *56*, 1577-1586.
328. Bayer, K.; Jahn, M.T.; Slaby, B.M.; Moitinho-Silva, L.; Hentschel, U. Marine sponges as Chloroflexi hot spots: genomic insights and high-resolution visualization of an abundant and diverse symbiotic clade. *mSystems*. **2018**, *3*, e00150-00118.
329. Schmitt, S.; Deines, P.; Behnam, F.; Wagner, M.; Taylor, M.W. Chloroflexi bacteria are more diverse, abundant, and similar in high than in low microbial abundance sponges. *FEMS Microbiol. Ecol*. **2011**, *78*, 497-510.
330. Nowicka, B.; Kruk, J. Powered by light: Phototrophy and photosynthesis in prokaryotes and its evolution. *Microbiol Res*. **2016**, *186-187*, 99-118.
331. Ward, L.M.; Hemp, J.; Shih, P.M.; McGlynn, S.E.; Fischer, W.W. Evolution of phototrophy in the Chloroflexi phylum driven by horizontal gene transfer. *Front Microbiol*. **2018**, *9*, 260.
332. Kielak, A.M.; Barreto, C.C.; Kowalchuk, G.A.; van Veen, J.A.; Kuramae, E.E. The ecology of Acidobacteria: moving beyond genes and genomes. *Front Microbiol*. **2016**, *7*, 744-744.
333. O'Connor-Sánchez, A.; Rivera-Domínguez, A.J.; Santos-Briones, C.d.l.; López-Aguiar, L.K.; Peña-Ramírez, Y.J.; Prieto-Davo, A. Acidobacteria appear to dominate the microbiome of two sympatric Caribbean Sponges and one Zoanthid. *Biol. Res*. **2014**, *47*, 67-67.
334. Quaiser, A.; López-García, P.; Zivanovic, Y.; Henn, M.R.; Rodriguez-Valera, F.; Moreira, D. Comparative analysis of genome fragments of Acidobacteria from deep Mediterranean plankton. *Environ. Microbiol*. **2008**, *10*, 2704-2717.
335. Nelson, C.E.; Carlson, C.A.; Ewart, C.S.; Halewood, E.R. Community differentiation and population enrichment of Sargasso Sea bacterioplankton in the euphotic zone of a mesoscale mode-water eddy. *Environ. Microbiol*. **2014**, *16*, 871-887.
336. Fortunato, C.S.; Eiler, A.; Herfort, L.; Needoba, J.A.; Peterson, T.D.; Crump, B.C. Determining indicator taxa across spatial and seasonal gradients in the Columbia River coastal margin. *ISME J*. **2013**, *7*, 1899.

337. Seo, J.-H.; Kang, I.; Yang, S.-J.; Cho, J.-C. Characterization of spatial distribution of the bacterial community in the South Sea of Korea. *Plos One*. **2017**, *12*, 1-18.
338. Jackson, S.A.; Flemer, B.; McCann, A.; Kennedy, J.; Morrissey, J.P.; O'Gara, F.; Dobson, A.D.W. Archaea Appear to dominate the microbiome of *Inflatella pellicula* deep sea sponges. *Plos One*. **2014**, *8*, 1-8.
339. Zhang, F.; Pita, L.; Erwin, P.M.; Abaid, S.; López-Legentil, S.; Hill, R.T. Symbiotic archaea in marine sponges show stability and host specificity in community structure and ammonia oxidation functionality. *FEMS Microbiol. Ecol.* **2014**, *90*, 699-707.
340. Ijichi, M.; Hamasaki, K. Distinctive physiological response of shallow and deep ecotypes of ammonia-oxidizing marine archaea in seawater cultures. *Plankton and Benthos Research*. **2017**, *12*, 259-265.
341. Neave, M.J.; Apprill, A.; Ferrier-Pagès, C.; Voolstra, C.R. Diversity and function of prevalent symbiotic marine bacteria in the genus Endozoicomonas. *Appl. Microbiol. Biotechnol.* **2016**, *100*, 8315-8324.
342. Helber, S.B.; Hoesjmakers, D.J.J.; Muhando, C.A.; Rohde, S.; Schupp, P.J. Sponge chemical defenses are a possible mechanism for increasing sponge abundance on reefs in Zanzibar. *Plos One*. **2018**, *13*, 1-26.
343. Pawlik, J.R. The chemical ecology of sponges on Caribbean reefs: natural products shape natural systems. *Bioscience*. **2011**, *61*, 888-898.
344. Chanas, B.; Pawlik, J.R.; Lindel, T.; Fenical, W. Chemical defense of the Caribbean sponge *Agelas clathrodes* (Schmidt). *J. Exp. Mar. Bio. Ecol.* **1997**, *208*, 185-196.
345. Dunlap, M.; Pawlik, J.R. Spongivory by parrotfish in Florida mangrove and reef habitats. *Mar. Ecol.* **1998**, *19*, 325-337.
346. Xuefeng, Z.; Tunhai, X.; Xian-Wen, Y.; Riming, H.; Bin, Y.; Lan, T.; Yonghong, L. Chemical and biological aspects of marine sponges of the genus *Xestospongia*. *Chem. Biodiv.* **2010**, *7*, 2201-2227.
347. Earle, G.; Hintz, W. New approaches for controlling *Saprolegnia parasitica*, the causal agent of a devastating fish disease. *Trop. Life Sci Res.* **2014**, *25*, 101-109.
348. Hu, X.G.; Liu, L.; Hu, K.; Yang, X.L.; Wang, G.X. In Vitro Screening of Fungicidal Chemicals for Antifungal Activity against *Saprolegnia*. *J. World. Aquacult. Soc.* **2013**, *44*, 528-535.
349. Srivastava, S.; Sinha, R.; Roy, D. Toxicological effects of malachite green. *Aquat. Toxicol.* **2004**, *66*, 319-329.
350. Stamatii, A.; Nebbia, C.; Angelis, I.D.; Albo, A.G.; Carletti, M.; Rebecchi, C.; Zampaglioni, F.; Dacasto, M. Effects of malachite green (MG) and its major metabolite, leucomalachite green (LMG), in two human cell lines. *Toxicol. In Vitro.* **2005**, *19*, 853-858.
351. Takada, K.; Kajiwara, H.; Imamura, N. Oridamycins A and B, anti-*Saprolegnia parasitica* indolosesquiterpenes isolated from *Streptomyces* sp. KS84. *J. Nat. Prod.* **2010**, *73*, 698-701.
352. Takahashi, K.; Sakai, K.; Nagano, Y.; Sakaguchi, S.O.; Lima, A.O.; Pellizari, V.H.; Iwatsuki, M.; Takishita, K.; Nonaka, K.; Fujikura, K., et al. Cladomarine, a new anti-saprolegniasis compound isolated from the deep-sea fungus, *Penicillium coralligerum* YK-247. *J. Antibiot.* **2017**, *70*, 911-914.
353. Langille, M.G.I.; Zaneveld, J.; Caporaso, J.G.; McDonald, D.; Knights, D.; Reyes, J.A.; Clemente, J.C.; Burkpile, D.E.; Vega Thurber, R.L.; Knight, R., et al. Predictive functional profiling of microbial communities using 16S rRNA marker gene sequences. *Nature Biotechnol.* **2013**, *31*, 814.
354. ABhauer, K.P.; Wemheuer, B.; Daniel, R.; Meinicke, P. Tax4Fun: predicting functional profiles from metagenomic 16S rRNA data. *Bioinformatics.* **2015**, *31*, 2882-2884.
355. Wilson, M.C.; Nam, S.-J.; Gulder, T.A.M.; Kauffman, C.A.; Jensen, P.R.; Fenical, W.; Moore, B.S. Structure and biosynthesis of the marine streptomycete ansamycin ansalactam A and its distinctive branched chain polyketide extender unit. *J. Am. Chem. Soc.* **2011**, *133*, 1971-1977.
356. Kim, T.K.; Hewavitharana, A.K.; Shaw, P.N.; Fuerst, J.A. Discovery of a new source of rifamycin antibiotics in marine sponge Actinobacteria by phylogenetic prediction. *Appl Environ. Microbiol.* **2006**, *72*, 2118-2125.
357. Trindade-Silva, A.E.; Rua, C.P.J.; Andrade, B.G.N.; Vicente, A.C.P.; Silva, G.G.Z.; Berlink, R.G.S.; Thompson, F.L. Polyketide synthase gene diversity within the microbiome of the sponge endemic to the Southern Atlantic Ocean. *Appl. Environ. Microbiol.* **2013**, *79*, 1598-1605.
358. Della Sala, G.; Hochmuth, T.; Costantino, V.; Teta, R.; Gerwick, W.; Gerwick, L.; Piel, J.; Mangoni, A. Polyketide genes in the marine sponge *Plakortis simplex*: a new group of mono-modular type I polyketide synthases from sponge symbionts. *Env. Microbiol. Rep.* **2013**, *5*, 809-818.
359. Kudo, F.; Eguchi, T. Chapter 20 Biosynthetic enzymes for the aminoglycosides butirosin and neomycin. In *Methods in Enzymology*, Academic Press: 2009; pp 493-519.
360. Cushnie, T.P.T.; Cushnie, B.; Lamb, A.J. Alkaloids: an overview of their antibacterial, antibiotic-enhancing and antivirulence activities. *Int. J. Antimicrob. Agents* **2014**, *44*, 377-386.

361. Krstin, S.; Peixoto, H.S.; Wink, M. Combinations of alkaloids affecting different molecular targets with the saponin digitonin can synergistically enhance trypanocidal activity against *Trypanosoma brucei brucei*. *Antimicrob Agents Ch*. **2015**, *59*, 7011-7017.
362. Lackner, G.; Peters, E.E.; Helfrich, E.J.N.; Piel, J. Insights into the lifestyle of uncultured bacterial natural product factories associated with marine sponges. *Proc. Natl. Acad. Sci*. **2017**, *114*, 347-356.
363. Mori, T.; Cahn, J.K.B.; Wilson, M.C.; Meoded, R.A.; Wiebach, V.; Martinez, A.F.C.; Helfrich, E.J.N.; Albersmeier, A.; Wibberg, D.; Dätwyler, S., *et al.* Single-bacterial genomics validates rich and varied specialized metabolism of uncultivated sponge symbionts. *Proc. Natl. Acad. Sci*. **2018**, *115*, 1718-1723.
364. Waters, A.L.; Peraud, O.; Kasanah, N.; Sims, J.W.; Kothalawala, N.; Anderson, M.A.; Abbas, S.H.; Rao, K.V.; Jupally, V.R.; Kelly, M., *et al.* An analysis of the sponge *Acanthostrongylophora igens'* microbiome yields an actinomycete that produces the natural product manzamine A. *Front. Mar. Sci*. **2014**, *1*, 1-28.
365. Santos, O.C.S.; Pontes, P.V.M.L.; Santos, J.F.M.; Muricy, G.; Giambiagi-deMarval, M.; Laport, M.S. Isolation, characterization and phylogeny of sponge-associated bacteria with antimicrobial activities from Brazil. *Res Microbiol*. **2010**, *161*, 604-612.
366. Tabares, P.; Pimentel-Elardo, S.M.; Schirmeister, T.; Hunig, T.; Hentschel, U. Anti-protease and immunomodulatory activities of bacteria associated with Caribbean sponges. *Mar. Biotechnol*. **2011**, *13*, 883-892.
367. Joint, I.; Muhling, M.; Querellou, J. Culturing marine bacteria - an essential prerequisite for biodiscovery. *Microb Biotechnol*. **2010**, *3*, 564-575.
368. Hentschel, U.; Schmid, M.; Wagner, M.; Fieseler, L.; Gernert, C.; Hacker, J. Isolation and phylogenetic analysis of bacteria with antimicrobial activities from the Mediterranean sponges *Aplysina aerophoba* and *Aplysina cavernicola*. *FEMS Microbiol. Ecol*. **2001**, *35*, 305-312.
369. Matobole, R.M.; van Zyl, L.J.; Parker-Nance, S.; Davies-Coleman, M.T.; Trindade, M. Antibacterial activities of bacteria isolated from the marine sponges *Isodictya compressa* and *Higginsia a bidentifera* collected from Algoa Bay, South Africa. *Mar. Drugs*. **2017**, *15*, 47.
370. Muscholl-Silberhorn, A.; Thiel, V.; Imhoff, J.F. Abundance and bioactivity of cultured sponge-associated bacteria from the mediterranean sea. *Microb. Ecol*. **2008**, *55*, 94-106.
371. Zhou, X.F.; Xu, T.H.; Yang, X.W.; Huang, R.M.; Yang, B.; Tang, L.; Liu, Y.H. Chemical and biological aspects of marine sponges of the genus *Xestospongia*. *Chem. Biodiv*. **2010**, *7*, 2201-2227.
372. Montalvo, N.F.; Davis, J.; Vicente, J.; Pittiglio, R.; Ravel, J.; Hill, R.T. Integration of culture-based and molecular analysis of a complex sponge-associated bacterial community. *Plos One*. **2014**, *9*, 1-8.
373. Zhang, H.; Zhang, W.; Jin, Y.; Jin, M.; Yu, X. A comparative study on the phylogenetic diversity of culturable actinobacteria isolated from five marine sponge species. *Antonie van Leeuwenhoek*. **2008**, *93*, 241-248.
374. Santavy, D.L.; Colwell, R.R. Comparison of bacterial communities associated with the Caribbean Sclerosponge *Ceratoporella nicholsoni* and ambient seawater. *Mar. Ecol. Prog. Ser*. **1990**, *67*, 73-82.
375. Santavy, D.L.; Willenz, P.; Colwell, R.R. Phenotypic study of bacteria associated with the Caribbean Sclerosponge, *Ceratoporella nicholsoni*. *App. Env. Microbiol*. **1990**, *56*, 1750-1762.
376. Olson, J.B.; McCarthy, P.J. Associated bacterial communities of two deep-water sponges. *Aquat. Microb. Ecol*. **2005**, *39*, 47-55.
377. Leung, B.; Liu, S. Science Buddies: Interpreting Plates. <https://www.sciencebuddies.org/science-fair-projects/references/interpreting-agar-plates> (30 April 2016).
378. Oksanen, J.; Blanchet, F.G.; Friendly, M.; Kindt, R.; Legendre, P.; McGlenn, D.; Minchin, P.R.; O'Hara, R.B.; Simpson, G.L.; Solymos, P.M., *et al.* vegan: Community Ecology Package. **2018**, <https://CRAN.R-project.org/package=vegan>.
379. Lane, D.J. 16S/23S rRNA Sequencing. In *Nucleic Acid Techniques in Bacterial Systematic*, Stackebrandt, E.; Goodfellow, M., Eds. John Wiley and Sons: New York, 1991; pp 115-175.
380. Versluis, D.; Nijssen, B.; Naim, M.A.; Koehorst, J.J.; Wiese, J.; Imhoff, J.F.; Schaap, P.J.; van Passel, M.W.J.; Smidt, H.; Sipkema, D. Comparative genomics highlights symbiotic capacities and high metabolic flexibility of the marine genus *Pseudovibrio*. *Genome Biol Evol*. **2018**, *10*, 125-142.
381. Hardoim, C.C.P.; Cardinale, M.; Cuccio, A.C.B.; Esteves, A.I.S.; Berg, G.; Xavier, J.R.; Cox, C.J.; Costa, R. Effects of sample handling and cultivation bias on the specificity of bacterial communities in keratose marine sponges. *Front Microbiol*. **2014**, *5*, 1-15.
382. Graça, A.P.; Bondoso, J.; Gaspar, H.; Xavier, J.R.; Monteiro, M.C.; de la Cruz, M.; Oves-Costales, D.; Vicente, F.; Lage, O.M. Antimicrobial activity of heterotrophic bacterial communities from the marine sponge *Erylus discophorus* (Astrophorida, Geodiidae). *Plos One*. **2013**, *8*, 1-10.
383. Lai, Q.; Wang, J.; Gu, L.; Zheng, T.; Shao, Z. *Alcanivorax marinus* sp. nov., isolated from deep-sea water. *Int. J. Syst. Evol. Microbiol*. **2013**, *63*, 4428-4432.

384. Wang, G.; Barrett, N.H.; McCarthy, P.J. Draft genome sequence of deep-sea *Alteromonas* sp. strain V450 isolated from the marine sponge *Leiodermatium* sp. *Genome. Announc.* **2017**, *5*, 1-2.
385. Kyoung Kwon, K.; Hye Oh, J.; Yang, S.-H.; Seo, H.-S.; Lee, J.-H. Alcanivorax gelatiniphagus sp. nov., a marine bacterium isolated from tidal flat sediments enriched with crude oil. *Int. J. Syst. Evol. Microbiol.* **2015**, *65*, 2204-2208.
386. Esteves, A.I.S.; Amer, N.; Nguyen, M.; Thomas, T. Sample processing impacts the viability and cultivability of the sponge microbiome. *Front Microbiol.* **2016**, *7*, 1-17.
387. Romano, S. Ecology and biotechnological potential of bacteria belonging to the genus. *Appl. Environ. Microbiol.* **2018**, *84*.
388. Margassery, L.M.; Kennedy, J.; O’Gara, F.; Dobson, A.D.; Morrissey, J.P. Diversity and antibacterial activity of bacteria isolated from the coastal marine sponges *Amphilectus fucorum* and *Eurypon major*. *Letts. Appl. Microbiol.* **2012**, *55*, 2-8.
389. Brinkmann, C.; Kearns, P.; Evans-Illidge, E.; Kurtböke, D. Diversity and bioactivity of marine bacteria associated with the sponges *Candidaspongia flabellata* and *Rhopaloeides odorabile* from the Great Barrier Reef in Australia. *Diversity.* **2017**, *9*, 1-26.
390. Mohamed, N.M.; Cicirelli, E.M.; Kan, J.; Chen, F.; Fuqua, C.; Hill, R.T. Diversity and quorum-sensing signal production of Proteobacteria associated with marine sponges. *Environ. Microbiol.* **2008**, *10*, 75-86.
391. Zan, J.; Cicirelli, E.M.; Mohamed, N.M.; Sibhatu, H.; Kroll, S.; Choi, O.; Uhlson, C.L.; Wysoczynski, C.L.; Murphy, R.C.; Churchill, M.E.A., et al. A complex LuxR–LuxI type quorum sensing network in a roseobacterial marine sponge symbiont activates flagellar motility and inhibits biofilm formation. *Mol. Microbiol.* **2012**, *85*, 916-933.
392. Quévrain, E.; Domart-Coulon, I.; Pernice, M.; Bourguet-Kondracki, M.-L. Novel natural parabens produced by a *Microbulbifer* bacterium in its calcareous sponge host *Leuconia nivea*. *Environ. Microbiol.* **2009**, *11*, 1527-1539.
393. Ruiz, B.; Chavez, A.; Forero, A.; Garcia-Huante, Y.; Romero, A.; Sanchez, M.; Rocha, D.; Sanchez, B.; Rodriguez-Sanoja, R.; Sanchez, S., et al. Production of microbial secondary metabolites: regulation by the carbon source. *Crit. Rev. Microbiol.* **2010**, *36*, 146-167.
394. Ranglová, K.; Krejčová, P.; Kubec, R. The effect of storage and processing on antimicrobial activity of *Tulbaghia violacea*. *S. Afr. J. Bot.* **2015**, *97*, 159-164.
395. Laher, F.; Aremu, A.O.; Van Staden, J.; Finnie, J.F. Evaluating the effect of storage on the biological activity and chemical composition of three South African medicinal plants. *S. Afr. J. Bot.* **2013**, *88*, 414-418.
396. Pilasombut, K.; Rumjuankiat, K.; Ngamyeesoon, N.; Duy, L.N.D. *In vitro* characterization of bacteriocin produced by lactic acid bacteria isolated from Nem Chua, a traditional Vietnamese fermented pork. *Korean. J. Food. Sci. An.* **2015**, *35*, 473-478.
397. Harrington, C.; Reen, F.J.; Mooij, M.J.; Stewart, F.A.; Chabot, J.-B.; Guerra, A.F.; Glöckner, F.O.; Nielsen, K.F.; Gram, L.; Dobson, A.D.W., et al. Characterisation of non-autoinducing tropodithietic acid (TDA) production from marine sponge *Pseudovibrio* species. *Mar. Drugs.* **2014**, *12*, 5960-5978.
398. Crowley, S.P.; O’Gara, F.; O’Sullivan, O.; Cotter, P.D.; Dobson, A.D.W. Marine *Pseudovibrio* sp as a novel source of antimicrobials. *Mar. Drugs.* **2014**, *12*, 5916-5929.
399. Penesyan, A.; Marshall-Jones, Z.; Holmstrom, C.; Kjelleberg, S.; Egan, S. Antimicrobial activity observed among cultured marine epiphytic bacteria reflects their potential as a source of new drugs. *FEMS Microbiol. Ecol.* **2009**, *69*, 113-124.
400. Pereira, L.B.; Palermo, B.R.Z.; Carlos, C.; Ottoboni, L.M.M. Diversity and antimicrobial activity of bacteria isolated from different Brazilian coral species. *FEMS Microbiol. Lett.* **2017**, *364*, 1-8.
401. Saurav, K.; Bar-Shalom, R.; Haber, M.; Burgsdorf, I.; Oliviero, G.; Costantino, V.; Morgenstern, D.; Steindler, L. In search of alternative antibiotic drugs: quorum-quenching activity in sponges and their bacterial isolates. *Front Microbiol.* **2016**, *7*, 1-18.
402. Simion, P.; Philippe, H.; Baurain, D.; Jager, M.; Richter, D.J.; Di Franco, A.; Roue, B.; Satoh, N.; Quéinnec, E.; Ereskovsky, A., et al. A Large and consistent phylogenomic dataset supports sponges as the sister group to all other animals. *Curr. Biol.* **2017**, *27*, 958-967.
403. Dohrmann, M.; Wörheide, G. Dating early animal evolution using phylogenomic data. *Sci.Rep.* **2017**, *7*, 1-6.
404. Zumberge, J.A.; Love, G.D.; Cárdenas, P.; Sperling, E.A.; Gunasekera, S.; Rohrsen, M.; Grosjean, E.; Grotzinger, J.P.; Summons, R.E. Demosponge steroidal biomarker 26-methylstigmastane provides evidence for neoproterozoic animals. *Nature Ecol. Evol.* **2018**, *2*, 1709-1714.
405. Rodríguez-Marconi, S.; De la Iglesia, R.; Diez, B.; Fonseca, C.A.; Hajdu, E.; Trefault, N. Characterization of bacterial, archaeal and eukaryote symbionts from Antarctic sponges reveals a high diversity at a three-domain level and a particular signature for this ecosystem. *Plos One.* **2015**, *10*, 1-19.

406. Pita, L.; Rix, L.; Slaby, B.M.; Franke, A.; Hentschel, U. The sponge holobiont in a changing ocean: from microbes to ecosystems. *Microbiome*. **2018**, *6*, 1-18.
407. Taylor, M.W.; Tsai, P.; Simister, R.L.; Deines, P.; Botte, E.; Ericson, G.; Schmitt, S.; Webster, N.S. 'Sponge-specific' bacteria are widespread (but rare) in diverse marine environments. *ISME J.* **2012**, *7*, 438-443.
408. Sipkema, D.; de Caralt, S.; Morillo, J.A.; Al-Soud, W.A.; Sørensen, S.J.; Smidt, H.; Uriz, M.J. Similar sponge-associated bacteria can be acquired via both vertical and horizontal transmission. *Environ. Microbiol.* **2015**, *17*, 3807-3821.
409. Webster, N.S.; Taylor, M.W.; Behnam, F.; Lückner, S.; Rattei, T.; Whalan, S.; Horn, M.; Wagner, M. Deep sequencing reveals exceptional diversity and modes of transmission for bacterial sponge symbionts. *Environ. Microbiol.* **2010**, *12*, 2070-2082.
410. Weisz, J.B.; Hentschel, U.; Lindquist, N.; Martens, C.S. Linking abundance and diversity of sponge-associated microbial communities to metabolic differences in host sponges. *Mar. Biol.* **2007**, *152*, 475-483.
411. Li, Z.-Y.; Wang, Y.-Z.; He, L.-M.; Zheng, H.-J. Metabolic profiles of prokaryotic and eukaryotic communities in deep-sea sponge *Neamphius huxleyi* indicated by metagenomics. *Sci.Rep.* **2014**, *4*, 3895.
412. Leys, S.P.; Kahn, A.S.; Fang, J.K.H.; Kutti, T.; Bannister, R.J. Phagocytosis of microbial symbionts balances the carbon and nitrogen budget for the deep-water boreal sponge *Geodia barretti*. *Limnol. Oceanogr.* **2018**, *63*, 187-202.
413. Thoms, C.; Schupp, P.J. Chemical defense strategies in sponges: a review. In *Porifera research: biodiversity, innovation and sustainability*, 2007; Vol. 28, pp 627-637.
414. Leal, M.C.; Puga, J.; Serôdio, J.; Gomes, N.C.M.; Calado, R. Trends in the discovery of new marine natural products from invertebrates over the last two decades – where and what are we bioprospecting? *Plos One*. **2012**, *7*, 1-15.
415. Rangel, M.; Falkenberg, M. An overview of the marine natural products in clinical trials and on the market. *J. Coast. Life. Med.* **2015**, *3*, 421-428.
416. Samuelsson, G.; Bohlin, L. *Drugs of Natural Origin: A Treatise of Pharmacognosy, Seventh Edition*. 7th ed.; Swedish Pharmaceutical Press: 2017.
417. Ivanisevic, J.; Thomas, O.P.; Pedel, L.; Pérez, N.; Ereskovsky, A.V.; Culioli, G.; Pérez, T. Biochemical trade-offs: evidence for ecologically linked secondary metabolism of the sponge *Oscarella balibalo*. *Plos One*. **2011**, *6*, 1-11.
418. Pérez, T.; Ivanisevic, J.; Dubois, M.; Pedel, L.; Thomas, O.P.; Tokina, D.; Ereskovsky, A.V. *Oscarella balibalo*, a new sponge species (Homoscleromorpha: Plakinidae) from the Western Mediterranean sea: cytological description, reproductive cycle and ecology. *Mar. Ecol.* **2011**, *32*, 174-187.
419. Reveillaud, J.; Allewaert, C.; Pérez, T.; Vacelet, J.; Banaigs, B.; Vanreusel, A. Relevance of an integrative approach for taxonomic revision in sponge taxa: case study of the shallow-water Atlanto-Mediterranean *Hexadella* species (Porifera: Ianthellidae: Verongida). *Invertebr. Syst.* **2012**, *26*, 230-248.
420. Reverter, M.; Perez, T.; Ereskovsky, A.V.; Banaigs, B. Secondary metabolome variability and inducible chemical defenses in the Mediterranean sponge *Aplysina cavernicola*. *J. Chem. Ecol.* **2016**, *42*, 60-70.
421. Reverter, M.; Tribalat, M.-A.; Pérez, T.; Thomas, O.P. Metabolome variability for two Mediterranean sponge species of the genus *Haliclona*: specificity, time, and space. *Metabolomics*. **2018**, *14*, 1-12.
422. Cárdenas, P.; Xavier, J.R.; Reveillaud, J.; Schander, C.; Rapp, H.T. Molecular phylogeny of the Astrophorida (Porifera, Demospongiae) reveals an unexpected high level of spicule homoplasy. *Plos One*. **2011**, *6*, 1-18.
423. Plotkin, A.; Gerasimova, E.; Rapp, H.T. Polymastiidae (Porifera: Demospongiae) of the Nordic and Siberian Seas. *J. Mar. Biol. Assoc. U. K.* **2018**, *98*, 1273-1335.
424. Lind, K.; Hansen, E.; Østerud, B.; Eilertsen, K.-E.; Bayer, A.; Engqvist, M.; Leszczak, K.; Jørgensen, T.; Andersen, J. Antioxidant and anti-inflammatory activities of baretin. *Mar. Drugs*. **2013**, *11*, 2655-2666.
425. Galindo-Prieto, B.; Eriksson, L.; Trygg, J. Variable influence on projection (VIP) for orthogonal projections to latent structures (OPLS). *J. Chemom.* **2014**, *28*, 623-632.
426. Eriksson, L.; Johansson, E.; Kettaneh-Wold, N.; Trygg, J.; Wikström, C.; Wold, S. *Multi- and megavariable data analysis (part 2)*. Second ed. ed.; 2006Vol. Vol. *Advanced Applications and Method Extensions*.
427. Ogawa, T.; Hirose, Y.; Honda-Ogawa, M.; Sugimoto, M.; Sasaki, S.; Kibi, M.; Kawabata, S.; Ikebe, K.; Maeda, Y. Composition of salivary microbiota in elderly subjects. *Sci.Rep.* **2018**, *8*, 414.
428. Oksanen, J.; Blanchett, F.G.; Kindt, R.; Legendre, P.; Minchin, P.R.; O'Hara, R.B.; Simpson, G.L.; Solymos, P.; Stevens, M.H.M.; Wagner, H. *Vegan: community ecology package*. R Package Version 3.5.0. 2016.

429. Smith, C.A.; Want, E.J.; O'Maille, G.; Abagyan, R.; Siuzdak, G. XCMS: processing mass spectrometry data for metabolite profiling using nonlinear peak alignment, matching, and identification. *Anal. Chem.* **2006**, *78*, 779-787.
430. Thévenot, E.A.; Roux, A.; Xu, Y.; Ezan, E.; Junot, C. Analysis of the human adult urinary metabolome variations with age, body mass index, and gender by implementing a comprehensive workflow for univariate and OPLS statistical analyses. *J. Proteome. Res.* **2015**, *14*, 3322-3335.
431. Radax, R.; Hoffmann, F.; Rapp, H.T.; Leininger, S.; Schleper, C. Ammonia-oxidizing archaea as main drivers of nitrification in cold-water sponges. *Environ. Microbiol.* **2012**, *14*, 909-923.
432. Mehrshad, M.; Rodriguez-Valera, F.; Amoozegar, M.A.; López-García, P.; Ghai, R. The enigmatic SAR202 cluster up close: shedding light on a globally distributed dark ocean lineage involved in sulfur cycling. *ISME J.* **2018**, *12*, 655-668.
433. Wang, Z.; Guo, F.; Liu, L.; Zhang, T. Evidence of carbon fixation pathway in a bacterium from candidate phylum SBR1093 revealed with genomic analysis. *Plos One.* **2014**, *9*, 1-9.
434. Gerringer, M.E.; Drazen, J.C.; Yancey, P.H. Metabolic enzyme activities of abyssal and hadal fishes: pressure effects and a re-evaluation of depth-related changes. *Deep Sea Res. Part I Oceanogr. Res. Pap.* **2017**, *125*, 135-146.
435. Glasl, B.; Smith, C.E.; Bourne, D.G.; Webster, N.S. Exploring the diversity-stability paradigm using sponge microbial communities. *Sci.Rep.* **2018**, *8*, 1-9.
436. Galand, P.E.; Potvin, M.; Casamayor, E.O.; Lovejoy, C. Hydrography shapes bacterial biogeography of the deep Arctic Ocean. *ISME J.* **2009**, *4*, 564-576.
437. Fu, Y.; Keats, K.F.; Rivkin, R.B.; Lang, A.S. Water mass and depth determine the distribution and diversity of Rhodobacterales in an Arctic marine system. *FEMS Microbiol. Ecol.* **2013**, *84*, 564-576.
438. Frank, A.H.; Garcia, J.A.L.; Herndl, G.J.; Reinthaler, T. Connectivity between surface and deep waters determines prokaryotic diversity in the North Atlantic Deep Water. *Environ. Microbiol.* **2016**, *18*, 2052-2063.
439. Yashayaev, I. Hydrographic changes in the Labrador Sea, 1960–2005. *Prog. Oceanogr.* **2007**, *73*, 242-276.
440. Müller, O.; Wilson, B.; Paulsen, M.L.; Rumińska, A.; Armo, H.R.; Bratbak, G.; Øvreås, L. Spatiotemporal dynamics of ammonia-oxidizing Thaumarchaeota in distinct Arctic water masses. *Front. Microbiol.* **2018**, *9*, 1-13.
441. Djurhuus, A.; Boersch-Supan, P.H.; Mikalsen, S.-O.; Rogers, A.D. Microbe biogeography tracks water masses in a dynamic oceanic frontal system. *R Soc Open Sci.* **2017**, *4*, 1-14.
442. Agogue, H.; Lamy, D.; Neal, P.R.; Sogin, M.L.; Herndl, G.J. Water mass-specificity of bacterial communities in the North Atlantic revealed by massively parallel sequencing. *Mol. Ecol.* **2011**, *20*, 258-274.
443. Fieth, R.A.; Gauthier, M.-E.A.; Bayes, J.; Green, K.M.; Degnan, S.M. Ontogenetic changes in the bacterial symbiont community of the tropical demosponge *Amphimedon queenslandica*: metamorphosis is a new beginning. *Front. Mar. Sci.* **2016**, *3*, 1-20.
444. Weigel, B.L.; Erwin, P.M. Effects of reciprocal transplantation on the microbiome and putative nitrogen cycling functions of the intertidal sponge, *Hymeniacidon heliophila*. *Sci.Rep.* **2017**, *7*, 1-12.
445. Bohlin, L.; Cárdenas, P.; Backlund, A.; Göransson, U. 35 Years of Marine Natural Product Research in Sweden: Cool Molecules and Models from Cold Waters. In *Blue Biotechnology: From Gene to Bioactive Product*, Müller, W.E.G.; Schröder, H.C.; Wang, X., Eds. Springer International Publishing: Cham, 2017; pp 1-34.
446. Sjogren, M.; Jonsson, P.R.; Dahlstrom, M.; Lundalv, T.; Burman, R.; Goransson, U.; Bohlin, L. Two brominated cyclic dipeptides released by the coldwater marine sponge *Geodia barretti* act in synergy as chemical defense. *J. Nat. Prod.* **2011**, *74*, 449-454.
447. Ortlepp, S.; Sjögren, M.; Dahlström, M.; Weber, H.; Ebel, R.; Edrada, R.; Thoms, C.; Schupp, P.; Bohlin, L.; Proksch, P. Antifouling activity of bromotyrosine-derived sponge metabolites and synthetic analogues. *Mar. Biotechnol.* **2007**, *9*, 776-785.
448. Müller, W.E.G.; Wang, X.; Proksch, P.; Perry, C.C.; Osinga, R.; Gardères, J.; Schröder, H.C. Principles of biofouling protection in marine sponges: a model for the design of novel biomimetic and bio-inspired coatings in the marine environment? *Mar. Biotechnol.* **2013**, *15*, 375-398.
449. Gilles, B.; Tom, C. Quorum sensing inhibitors as anti-biofilm agents. *Curr. Pharm. Des.* **2015**, *21*, 5-11.
450. Le Norcy, T.; Niemann, H.; Proksch, P.; Tait, K.; Linossier, I.; Réhel, K.; Hellio, C.; Fay, F. Sponge-inspired dibromohemibastadin prevents and disrupts bacterial biofilms without toxicity. *Mar. Drugs.* **2017**, *15*, 1-18.
451. Hadfield, M.G. Biofilms and marine invertebrate larvae: what bacteria produce that larvae use to choose settlement sites. *Annu. Rev. Mar. Sci.* **2011**, *3*, 453-470.

476. Liu, Y.; Zachow, C.; Raaijmakers, J.; de Bruijn, I. Elucidating the diversity of aquatic *Microdochium* and *Trichoderma* species and their activity against the fish pathogen *Saprolegnia diclina*. *Int. J. Mol. Sci.* **2016**, *17*, 140.
477. Shin, S.; Kulatunga, D.C.M.; Dananjaya, S.H.S.; Nikapitiya, C.; Lee, J.; De Zoysa, M. *Saprolegnia parasitica* isolated from rainbow trout in Korea: characterization, anti-*Saprolegnia* activity and host pathogen interaction in Zebrafish disease model. *Mycobiology.* **2017**, *45*, 297-311.
478. Willoughby, L.G.; Roberts, R.J. Towards strategic use of fungicides against *Saprolegnia parasitica* in salmonid fish hatcheries. *J. Fish. Dis.* **1992**, *15*, 1-13.
479. Quinn Robert, A.; Vermeij Mark, J.A.; Hartmann Aaron, C.; Galtier d'Auriac, I.; Benler, S.; Haas, A.; Quistad Steven, D.; Lim Yan, W.; Little, M.; Sandin, S., *et al.* Metabolomics of reef benthic interactions reveals a bioactive lipid involved in coral defence. *Proc. R. Soc. Lond., B, Biol. Sci.* **2016**, *283*, 1-10.
480. Sogin, E.M.; Anderson, P.; Williams, P.; Chen, C.-S.; Gates, R.D. Application of 1H-NMR metabolomic profiling for reef-building corals. *Plos One.* **2014**, *9*, e111274.
481. Garrett, T.A.; Schmeitzel, J.L.; Klein, J.A.; Hwang, J.J.; Schwarz, J.A. Comparative lipid profiling of the cnidarian *Aiptasia pallida* and its dinoflagellate symbiont. *Plos One.* **2013**, *8*, e57975.
482. Stabili, L.; Rizzo, L.; Fanizzi, F.P.; Angilè, F.; Del Coco, L.; Girelli, C.R.; Lomartire, S.; Piraino, S.; Basso, L. The Jellyfish *Rhizostoma pulmo* (Cnidaria): biochemical composition of ovaries and antibacterial lysozyme-like activity of the oocyte lysate. *Mar. Drugs.* **2018**, *17*, 17.
483. Stewart, E.J. Growing unculturable bacteria. *J. Bacteriol.* **2012**, *194*, 4151-4160.
484. Vartoukian, S.R.; Palmer, R.M.; Wade, W.G. Strategies for culture of 'unculturable' bacteria. *FEMS Microbiol. Lett.* **2010**, *309*, 1-7.
485. Gutleben, J.; Chaib De Mares, M.; van Elsas, J.D.; Smidt, H.; Overmann, J.; Sipkema, D. The multi-omics promise in context: from sequence to microbial isolate. *Crit. Rev. Microbiol.* **2018**, *44*, 212-229.
486. Jacob, J.; Rajendran, R.U.; Priya, S.H.; Purushothaman, J.; Saraswathy Amma, D.K.B.N. Enhanced antibacterial metabolite production through the application of statistical methodologies by a *Streptomyces nogalater* NIIST A30 isolated from Western Ghats forest soil. *Plos One.* **2017**, *12*, 1-21.
487. Handelsman, J. Metagenomics: application of genomics to uncultured microorganisms. *Microbiol. Mol. Biol. Rev.* **2004**, *68*, 669-685.
488. Astudillo-García, C.; Slaby, B.M.; Waite, D.W.; Bayer, K.; Hentschel, U.; Taylor, M.W. Phylogeny and genomics of SAUL, an enigmatic bacterial lineage frequently associated with marine sponges. *Environ. Microbiol.* **2018**, *20*, 561-576.
489. Karimi, E.; Slaby, B.M.; Soares, A.R.; Blom, J.; Hentschel, U.; Costa, R. Metagenomic binning reveals versatile nutrient cycling and distinct adaptive features in alphaproteobacterial symbionts of marine sponges. *FEMS Microbiol Ecol.* **2018**, *94*.
490. Gauthier, M.-E.A.; Watson, J.R.; Degnan, S.M. Draft genomes shed light on the dual bacterial symbiosis that dominates the microbiome of the coral reef sponge *Amphimedon queenslandica*. *Front. Mar. Sci.* **2016**, *3*.
491. Moitinho-Silva, L.; Díez-Vives, C.; Batani, G.; Esteves, A.I.S.; Jahn, M.T.; Thomas, T. Integrated metabolism in sponge-microbe symbiosis revealed by genome-centered metatranscriptomics. *ISME J.* **2017**, *11*, 1651.

Summary

This thesis aims to investigate the impact of depth on prokaryotic community composition and metabolite profiles, including antimicrobial activities, in marine sponges. Understanding both the prokaryotic community and metabolite profiles of sponges in relation to depth will provide important insights for marine ecology and future bioprospecting efforts of bioactive compounds from the sponge holobiont. A brief overview of prokaryotic community composition in sponges from shallow water to the deep sea and motivation of this research is provided in **chapter 1**. **Chapter 2** gives a comprehensive literature review on antimicrobial activities (antiviral, antibacterial, antifungal and antiprotozoal) of microbial isolates from marine sponges. The most potent antimicrobial compounds against microbial targets documented to date based on *in vitro* tests are: 2-undecyl-4-quinolone (human immunodeficiency virus 1 (HIV-1), truncateol M (influenza A virus), thiopeptide YM-266183 (nosocomial Gram positive bacteria), sydonic acid (*Escherichia coli*), naphthacene glycoside SF2446A2 (*Chlamydia trachomatis*), manzamine A (*Plasmodium* spp. and *Leishmania donovani*), valinomycin and staurosporine (*Trypanosoma brucei*), and saadamycin (*Candida albicans* and dermatophytic fungi). Furthermore, we identified *Streptomyces*, *Pseudovibrio*, *Bacillus*, *Aspergillus* and *Penicillium* as the leading producers of currently known antimicrobial compounds.

In **chapter 3**, the impact of depth on prokaryotic community composition and antimicrobial activities of two demosponges, *Xestospongia muta* and *Agelas sventres*, was investigated. Sponges were sampled from three depth categories: shallow (< 30 m), medium (30 – 60m) and deep (60 – 90 m) from the Curaçao Sea. Our findings showed that specific OTUs assigned to Cyanobacteria, Chloroflexi, Acidobacteria, Actinobacteria, Proteobacteria and Thaumarchaeota contributed to the significant variance in prokaryotic community composition observed along the depth gradient. Shallow sponge specimens generally yielded higher antibacterial activities compared to deep specimens. Based on this study, we hypothesized that the observed differences in prokaryotic community composition and antimicrobial activities may be caused by different physicochemical conditions (light and nutrient availability) along the depth gradient.

In **chapter 4**, cultivability of sponge-associated bacteria of *X. muta* and *A. sventres* collected from different depths in the Curaçao Sea was investigated. We observed that the source of inoculum (sponge species) and the cultivation medium had more pronounced impact on the

prokaryotic community recovered than the depth from which the sample was collected. Subsequently, antimicrobial screening of 41 and 20 bacterial isolates from *X. muta* and *A. sventres*, respectively, led to identification of ten isolates from *X. muta* and eight isolates from *A. sventres* with biological activity against at least one of the bacterial indicator strains: *Escherichia coli*, *Aeromonas salmonicida*, *Bacillus subtilis*, and *Staphylococcus simulans*, whereas no inhibition of the oomycete *Saprolegnia parasitica* or the yeast *Candida oleophila* was observed.

It is intriguing how depth impacts prokaryotic community composition and metabolite profiles of deep-sea sponges. In **chapter 5**, we studied microbiota composition and metabolome of the three deep-sea sponges *Weberella bursa*, *Stryphnus fortis* and *Geodia baretii* collected along a depth range of 200 – 1400 m in Davis Strait. The most predominant OTUs that varied with depth (increased, decreased or stable) in *S. fortis* and *G. baretii* could be assigned to Acidobacteria, Chloroflexi, Thaumarchaeota, and SBR1093. In contrast, in *W. bursa*, the most predominant OTUs that varied with depth were affiliated with Gammaproteobacteria and Planctomycetes. Furthermore, we found that secondary metabolite concentrations associated with these deep-sea sponges also varied with depth. As depth increased we observed that concentrations of anti-biofouling compounds known to be produced by *G. baretii* (barettin, 8,9-dihydrobarettin and soelterin) decreased significantly, whereas concentrations of known compounds in *S. fortis* (ianthelline and stryphnusin) substantially increased in deep specimens.

Finally, **chapter 6** elaborates and integrates findings obtained from the different research chapters. At two different geographic locations and across different depth ranges, we observed that depth significantly affected prokaryotic community composition at OTU level and at the same time also influenced metabolite profiles and antimicrobial activities in shallow as well as deep-sea sponges. In contrast, depth did not consistently affect cultivability of sponge-associated bacteria as opposed to the source of inocula and the growth media. Future research should be focused on metagenomics in combination with innovative cultivation strategies in order to obtain a clearer insight on prokaryotic community composition and diversity of secondary metabolite biosynthesis gene clusters of sponges across depth gradients.

Nederlandse samenvatting

Het doel van deze thesis is om de impact van diepte op prokaryotische compositie samenstellingen en metabolische profielen te onderzoeken, inclusief antimicrobiële activiteiten, in zee sponzen. Het begrijpen van zowel de prokaryotische samenstelling en metabolische profielen van sponzen in relatie tot diepte zal belangrijke inzichten geven voor zee ecologie en toekomstige bio exploratie inspanningen van bioactieve stoffen afkomstig van de spons holobiont. Een kort overzicht van prokaryotische compositie samenstellingen in sponzen afkomstig van ondiep water tot de diepe zee en motivatie van dit onderzoek is voorzien in **hoofdstuk 1**. Hoofdstuk 2 geeft een uitvoerig literatuur review over antimicrobiële activiteiten (antiviraal, antibacterieel, antifungaal en antiprotozoaal) van microbiële isolaten van zee sponzen. De meest potente antimicrobiële stoffen tegen microbiële doelwitten zover gedocumenteerd gebaseerd op *in vitro* testen zijn: 2-undecyl-4-quinolone (human immunodeficiency virus 1 (HIV-1), truncateol M (influenza A virus), thiopeptide YM-266183 (nosocomiaal Gram positieve bacteriën), sydonic acid (*Escherichia coli*), naphthacene glycoside SF2446A2 (*Chlamydia trachomatis*), manzamine A (*Plasmodium* spp. and *Leishmania donovani*), valinomycin en staurosporine (*Trypanosoma brucei*), and saadamycin (*Candida albicans* en dermatofytische schimmels). Overigens, we hebben *Streptomyces*, *Pseudovibrio*, *Bacillus*, *Aspergillus* en *Penicillium* geïdentificeerd als de belangrijkste producenten van antimicrobiële stoffen die we vandaag de dag kennen.

In **hoofdstuk 3**, het effect van diepte op prokaryotische compositie samenstelling en microbiële activiteiten van twee demosponzen, *Xesospongia muta* en *Agelas sventres*, was onderzocht. Sponzen waren bemonsterd vanaf drie diepte categorieën: ondiep (< 30 m), medium (30 – 60m) en diep (60 – 90 m) van de zee van Curaçao. Onze bevindingen lieten zien dat specifieke OTUs die toegekend zijn tot Cyanobacteriën, Chloroflexi, Acidobacteriën, Actinobacteriën, Proteobacteriën en Thaumarchaeota bijdroegen aan de significante variatie in prokaryotische compositie samenstelling die geobserveerd zijn langs de diepte gradient.

In **hoofdstuk 4**, werd de cultiveerbaarheid van spons-geassocieerde bacteriën van *X. muta* en *A. sventres* die verzameld zijn van verscheidene dieptes in de zee van Curaçao onderzocht. We hebben geobserveerd dat de bron van het inoculum (spons soort) en het groei medium een belangrijkere impact had op de gevonden prokaryotische samenstelling dan de diepte waarvan het monster was verzameld. Vervolgens, antimicrobiële screening van 41 en 20 bacteriële isolaten van *X. muta* en *A. sventres*, respectievelijk, lijdde tot identificatie van tien isolaten van

X. muta en acht isolaten van *A. sventres* met biologische activiteit tegen ten minste een van de bacteriële indicator strengen: *Escherichia coli*, *Aeromonas salmonicida*, *Bacillus subtilis*, en *Staphylococcus simulans*, waarbij geen inhibitie van de oomyceet *Saprolegnia parasitica* of de gist *Candida oleophila* was geobserveerd.

Het is intrigerend hoe diepte de samenstelling van prokaryotische gemeenschappen en metabolietprofielen van diepzee-sponzen beïnvloedt. In **hoofdstuk 5**, hebben we de microbiota-samenstelling en het metabooloom van de drie diepzeesponzen *Weberella bursa*, *Stryphnus fortis* en *Geodia baretii* verzameld op een diepte van 200 – 1400 m in Davis Strait. De meest overheersende OTUs die varieerden met diepte (verhoogd, verlaagd of stabiel) in *S. fortis* en *G. barretti* konden worden toegewezen aan Acidobacteria, Chloroflexi, Thaumarchaeota, en SBR 1093. In *W. bursa* daarentegen, de meest overheersende OTUs die varieerden met diepte, waren gelieerd met Gammaproteobacteria en Planctomycetes. Bovendien vonden we dat secundaire metabolietconcentraties geassocieerd met deze diepzeesponzen ook met de diepte varieerden. Naarmate de diepte toenam, zagen we dat concentraties van anti-biofoulingverbindingen waarvan bekend is dat ze geproduceerd worden door *G. barretti* (baretin, 8,9-dihydrobaretin en soelterin) significant afnamen, terwijl concentraties van bekende verbindingen in *S. fortis* (ianthelline en stryphnusin) substantieel toenamen in diepe exemplaren.

Ten slotte worden in **hoofdstuk 6** de bevindingen uit de verschillende hoofdstukken uitgewerkt en geïntegreerd. Op twee verschillende geografische locaties en over verschillende dieptebereiken, zagen we dat diepte de prokaryotische samenstelling van de gemeenschap op OTU-niveau significant beïnvloedde en tegelijkertijd ook de metabolietprofielen en antimicrobiële activiteiten in ondiepe- als ook diepzee-sponzen beïnvloedde. Daartegenover staat dat diepte niet consistent de kweekbaarheid van met spons geassocieerde bacteriën beïnvloedt, in tegenstelling tot de bron van inocula en de groeimedia. Toekomstig onderzoek moet gericht zijn op metagenomica in combinatie met innovatieve teeltstrategieën om een duidelijker inzicht te krijgen in de samenstelling van prokaryotische gemeenschappen en de diversiteit van secundaire metaboliet biosynthese genenclusters of sponzen over diepte gradiënten.

Ringkasan Bahasa Indonesia

Thesis ini bertujuan untuk meneliti pengaruh kedalaman terhadap komposisi prokaryotes dan profil metabolit meliputi aktivitas antimikroba pada hewan spons. Pemahaman akan komposisi prokaryotes dan profil metabolit terkait dengan kedalaman akan memberikan tambahan informasi yang penting untuk ekologi laut dan upaya biospeksi senyawa aktif dari spons holobiont. Gambaran singkat mengenai komposisi komunitas prokaryotes pada sponges dari habitat yang dangkal hingga ke laut dalam dan latar belakang dari penelitian ini diuraikan pada Bab 1. Bab 2 memberikan tinjauan pustaka menyeluruh tentang aktivitas antimikroba (antivirus, antibakteri, antijamur dan antiprotozoa) oleh mikroba yang diisolasi dari spons. Senyawa dengan aktivitas terbaik yang tercatat pada pustaka berdasarkan uji *in vitro* meliputi: 2-undecyl-4-quinolone (human immunodeficiency virus 1 (HIV-1), truncateol M (influenza A virus), thiopeptide YM-266183 (nosocomial Gram positive bacteria), sydonic acid (*Escherichia coli*), naphthacene glycoside SF2446A2 (*Chlamydia trachomatis*), manzamine A (*Plasmodium* spp. and *Leishmania donovani*), valinomycin and staurosporine (*Trypanosoma brucei*), and saadamycin (*Candida albicans* and jamur dermatophytic). Selanjutnya, kami mengidentifikasi *Streptomyces*, *Pseudovibrio*, *Bacillus*, *Aspergillus* and *Penicillium* sebagai penghasil utama senyawa antimikroba.

Pada bab 3 mempelajari pengaruh kedalaman terhadap komunitas prokaryotik dan aktivitas antimikroba dari dua demosponges, *Xestospongia muta* and *Agelas sventres*. Sampling spons dilakukan pada tiga kategori kedalaman yaitu: dangkal (< 30 m), sedang (30 – 60m) and dalam (60 – 90 m) di laut Curaçao. Hasil penelitian menunjukkan spesifik OTUs yang berafiliasi pada Cyanobacteria, Chloroflexi, Acidobacteria, Actinobacteria, Proteobacteria and Thaumarchaeota secara signifikan berkontribusi pada variasi komunitas prokaryotik spons. Spons dari habitat dangkal secara umum menghasilkan aktivitas antibakteri yang lebih kuat dibandingkan spesimen dari laut yang lebih dalam. Berdasarkan hasil ini, kami berhipotesis bahwa perbedaan pada komunitas prokaryotik dan aktivitas antimikroba dapat dipengaruhi oleh kondisi fisik dan kimia (cahaya dan ketersediaan nutrisi) sepanjang gradient kedalaman.

Bab 4 mempelajari kultivabiliti dari bakteri yang berasosiasi dengan dua spons *X. muta* and *A. sventres* yang dikoleksi dari laut Curaçao. Kami mengamati asal inokulum (jenis spons) dan media kultivasi memiliki efek yang lebih kuat daripada efek dari kedalaman dimana sampel diperoleh. Selanjutnya, aktivitas antimikroba terhadap 41 and 20 isolat bakteri dari *X. muta* and *A. sventres* berturut-turut, mengidentifikasi sepuluh isolat bakteri dari *X. muta* dan delapan

isolat dari *A. sventres* dengan daya hambat terhadap setidaknya satu dari bakteri indikator: *Escherichia coli*, *Aeromonas salmonicida*, *Bacillus subtilis*, and *Staphylococcus simulans*. Sementara tidak ada daya hambat teramati pada oomycete *Saprolegnia parasitica* atau yeast *Candida oleophila*.

Sangat menarik untuk mengetahui bagaimana kedalaman mempengaruhi komposisi prokaryotik dan profil metabolit pada spons di laut dalam. Pada bab 5, kami mempelajari komposisi mikroba dan metabolit dari tiga spons laut dalam *Weberella bursa*, *Stryphnus fortis* and *Geodia barretti* yang dikoleksi sepanjang kedalaman 200 – 1400 m di selat Davis. OTUs yang mendominasi dengan variasi sepanjang kedalaman (meningkat, menurun atau stabil) pada *S. fortis* and *G. barretti* dapat diasosiasikan terhadap Acidobacteria, Chloroflexi, Thaumarchaeota, and SBR1093. Sebaliknya, pada *W. bursa*, dominan OTUs yang berubah sesuai dengan kedalaman berasal dari Gammaproteobacteria and Planctomycetes. Selanjutnya, kami menemukan konsentrasi metabolit sekunder yang berasosiasi dengan ketiga spons ini juga bervariasi mengikuti kedalaman. Semakin kedalaman laut meningkat, kami mengamati konsentrasi senyawa anti-biofouling yang umum diproduksi oleh *G. barretti* (barettin, 8,9-dihydrobarettin and soelterin) menurun secara signifikan. Sementara konsentrasi dari senyawa yang berasosiasi dengan *S. fortis* (ianthelline and stryphnusin) secara substansial meningkat pada specimens di laut yang lebih dalam.

Pada akhirnya, bab 6 mengelaborasi dan mengintegrasikan hasil-hasil yang diperoleh dari bab-bab sebelumnya. Pada dua lokasi geografis dan kedalaman yang berbeda, kami menemukan bahwa kedalaman memiliki pengaruh signifikan terhadap komposisi prokaryotik pada tingkat OTU dan pada waktu yang bersamaan juga mempengaruhi komposisi metabolit dan aktivitas antibacterial baik di laut dangkal maupun laut dalam. Sebaliknya, kedalaman tidak secara konsisten mempengaruhi kultivabiliti dari sponge yang berasosiasi dengan spons, apabila dibandingkan dengan sumber inokulum dan media pertumbuhan. Penelitian di masa yang akan datang disarankan untuk lebih mengarah pada metagenomik yang dikomplementasikan dengan strategi kultivasi yang lebih inovatif untuk memperoleh gambaran yang lebih mendalam terhadap komposisi prokaryotik dan keanekaragaman gen kluster yang mengkode metabolit sekunder pada spons.

Acknowledgements

I would like to acknowledge many people for their support both directly and indirectly for the completion of my PhD which I fully indebted. First, I would like to thank **Indonesia Endowment Fund for Education (LPDP)** that provided me grant to pursue PhD at Wageningen University.

Next, I would like to thank my promotor **Hauke** your guidance and support during my PhD project. In every discussion, you always come with valuable input and provide me with critical insight to improve quality of experiments and manuscripts. **Detmer**, I can't ask more for a PhD supervisor. Thank you for your guidance, patience, and critical inputs to ensure I am still on track on my PhD trajectory. **Lisa**, thanks for feedbacks, helps and motivations that you provide me to reach this finish line.

I was lucky to be a PhD student at the Laboratory of Microbiology when **Willem** still chaired the group. Your leadership and vision are truly inspiring. I will always remember the “mantra” that each scientist should do science following a circle to be “good, better, and best”.

I would like to thank my paranymphs, **Hugo** and **Nuning**, for accompanying me during the final stage of my PhD. Thanks to both of you for helping me arranging submission of my thesis and all related documents while I was in Bali. **Hugo** “the man”, I will for sure miss your sense of humor and the “drops” from your candy jar. **Nuning**, thank you for always share stories from life to career and to be a travel buddy while we explored cities in the Netherlands and Europe.

My lab works would not run so smoothly without technical supports from our lab technicians. I would like to thank **Ineke, Wilma, Steven, Tom, Ton, and Monika** for your help every time I need some assistance. I also enjoyed chats and jokes we had in and outside the lab. I would also like to thank **Anja** for your support related to administration. **Philippe**, I always fascinate with your ideas to arrange the lab to be a better place to do research. **Sjon** and **Wim** thanks for your help every time I got problems with my PC and laptop. **Bart** thanks for your assistance every time I needed help on Bioinformatics.

Life during PhD will be so much fun when we have office mates to share stories and jokes with. I would like to thank Dennis, Peng, Jie, and Thomas to whom I shared office when the lab was still in the Dreijen. **Dennis**, it was an honoured being your paranymph and your

badminton partner. I would also like to thank my office mates at the room 6075 in the Helix building: **Tika, Alex, Hugo, Carrie, and Klaudyna**. I will miss all the fun we had and our irregular office lunch with KFC menu.

I was lucky to be part of such vibrant group in MolEco, one of the most diverse groups with people from many nationalities. I enjoyed all the social events (MolEco cakes, Christmas Dinner, Lab trips) and every scientific discussion we had during MolEco and PhD meetings. I would also like to thank all friends and colleagues from Bacgen, MicFys, and SSB for your kindness and friendship. For me, our PhD trip to Germany, Sweden, and Denmark in 2017 is one of the memorable experiences we shared as a group. I would like to thank **Emmy** (and all native Dutch “teachers”) to run the Dutch lunch every Wednesday where international PhD students and guests can practice Dutch actively. Although, my Dutch proficiency has not improved so much from “Ik spreek een beetje Nederland”, I enjoyed every session during the Dutch lunch time when we discussed various topics.

I was happy to supervise **Sebastian, Ina, and Mandy** during their thesis project. Results of their works have contributed on chapter 4 of my PhD thesis. I wish you the best of luck!

I would also like to thank the members of the marine group: **Tika, Johanna, Jie, Menia, Georg, Dat, Catarina, and Leire** for every discussion and support. **Tika**, we joined the marine group as master students and later also as PhD students in the same office. Thanks for sharing all the ups and downs during the PhD time. I wish you the best of luck and look forward to have research collaboration with you in Indonesia. **Johanna** “spongie”, you are the star of the marine group, with your easy-going personality, contagious laugh, yet critical feedback on every discussion, you are the source of happiness for us :). Look forward to meet you when visiting Bali to enjoy “Bir Bintang”, “Kopi Luwak” and “Marlboro Putih”. **Jie** “shifu”, we not only worked in the same labs under the same supervisors, but also shared corridor at Asserpark 8B for 3.5 years. Thanks for your friendship and I wish you all the best. **Menia**, our trip to Porto during the SponGES general meeting in 2018 together with my wife, **Vassia, Beate, and Kathrin** was enjoyable and so much fun. Hope to repeat it somewhere in the future. **Dat** “boss”, let’s meet in the future either in Vietnam or Indonesia. **Georg** thanks for your input and advice for chapter 3 of this thesis and also to share your expertise in microbial ecology. Our collaboration during preparing the practical course was so much fun. **Catarina and Leire**, let me know when you guys plan to dive or surf in Bali :)

My field trip to Curaçao was one of the unforgettable experiences in my life. I would like to thank **Adriaan “Dutch” Schrier** to facilitate me with the submarine to sample sponges. **Laureen**, thanks for arranging my trip so that I have pleasant stay in Curaçao. I would like to thank all the pilots of the submarine: **Bruce, Barbara, Barry, and Tico** for your help during the sampling. Also, I would like to thank technical supports from **Manuel** and **Joe** during setting up the lab. **Jasper** and **Ben**, my sampling trip would not be so smooth without your help and advice.

It was so great experiences for me to join two general meetings of SponGES in London and Porto to learn how the project was organized, and importantly to meet many renowned scientists in the field of sponges and marine microbiology. **Ellen, Paco** and **Karin**, I am happy to collaborate with you for the manuscript in Chapter 5, also thanks for your feedbacks during discussion and preparation of the manuscript.

I’ve spent six years in Wageningen for pursuing master and PhD. During this period of time, I met many Indonesian friends in PPI Wageningen which I shared many sweet memories with. Came from different provinces in Indonesia, we have blended as family that support each other during our stay in Wageningen. Thanks for your friendship: Om **John, Nela**, mb **Dian, Titis**, teteh **Dewi**, mb **Tika, Wardah**, Bang **Zein, Emil** and family, mb **Eka**, mb **Linda, Nuning**, mb **Nila**, mas **Anto** dan family, bang **Reo**, Pak **Dikky**, Mas **Fajar**, Uni **Eli**, Pak **Eko**, Kang **Dadan, Belinda**, kang **Yuda, Hachi, Gumi, Gendis, Wiwid**, mb **Vitri**, mas **Ika**, mb **Dican**, mb **Evi, Anissa** and family, mb **Arita**, bang **Jimmy**, bang **Odie** dan mb **Melly**, rekan-rekan master dan PhD Indonesia di Wageningen. Wherever you are now, I wish you all the best of luck. Terima kasih banyak :)

I would also like to thank people I call “family” during my stay in the Netherlands. All your kindness I cannot repay. Dankjewel tante **Jane** en Om **Donny** op Maastricht. Hartelijk bedankt voor de familie Smit: Ibu **Trees, Heine, Melle, Tim** en **Evan**. Thanks for inviting me to every celebrations in the family. Dankjewel voor de familie **van Harten**: mb **Dewi, Anthony, Ratih**, with you all I could feel Balinese atmosphere while far away from home with Balinese foods and spiritual trips we did to Pura Agung Shanti Buana in Belgium. Matur Suksma. I would also like to thanks mb **Eka**, kang **Yusuf** and **Kirana** for your friendship and hospitality.

Ajik, my dad **I Gusti Agung Ketut Suarjana** matur suksma untuk doa dan dukungan yang selalu diberikan kepada tiang. Ibu, my late mother, **Dewa Ayu Oka Mas** you passed away when I was 2.5 years old when I had only few memories about you. You are my prime

inspiration and motivation for pursuing postgraduate study abroad. My sister, **Gung Mas**, I can't ask more for a sister. Thanks for everything you have done to support me. Also, I would like to thank my brother in law, bli **Wayan Rubianta** and my two nephews, **Nanda** and **Danis** for their immense support towards me. Matur suksma katur tiang ring keluarga di Karangasem: Uwak **De Radnyan**, Bulik **Sueni**, Biang **Ayu**, Aji **Suradnya**, Aji **Surawan**, sepupu-sepupu lan keluarga besar di Bangli atas doa dan dukungan selama ini.

I would like to thank family from my wife side. My late mother in law **Ni Putu Arya Widiasih**, thanks for being a good friend and a mother to me. Mum, you will always be missed. Ayah **Ketut Suparjaya**, matur suksma untuk segala doa dan dukungan kepada tiang, semoga ayah sehat selalu. Terima kasih kepada adik-adik ipar dan pasangan mereka masing-masing: **Darpita&Adi**, **Antari&Dekha**, serta **Wulandari&Ngurah** atas bantuan dan dukungannya selama ini. Ucapan terimakasih juga saya haturkan kepada Bu **Ade** sekeluarga di Panjer, Bu **Ayu**, **Zila**, dan Om **Wid**, juga keluarga besar di Saelus atas segala doa dan dukungan kepada saya dan Titi selama ini.

Terima kasih yang sebesar-sebesarannya saya haturkan pada segenap pimpinan yayasan Kesejahteraan KORPRI Provinsi Bali, Rektor Universitas Warmadewa, Dekan Fakultas Kedokteran dan Ilmu Kesehatan Warmadewa, segenap kolega dosen dan pegawai atas segala dukungan yang diberikan semenjak saya bergabung di FKIK Universitas Warmadewa dan selama saya merampungkan PhD thesis ini.

I would like to thank my classmates "HIMABIO 2004" and lecturers at the study program of Biology, Udayana University, for the encouragement and support when I planned to pursue my postgraduate study abroad. I would like to thank my former bachelor supervisors: Pak **Yan** and Pak **Sujaya** for providing me recommendation letters when I applied both MSc and PhD fellowship.

Last but not least. I would like to thank my wife **Dharmesti**. Looking back, it's funny how our relationship grows from tutor-student, brother-sister, fiancée, husband-wife, and just recently as colleague at Warmadewa University. Thanks for always be my special supporter in every sad and happy moments. My life is complete with you by myside.

Co-author Affiliations

Hauke Smidt¹

Detmer Sipkema¹

Leontine E. Becking^{2,3}

Sebastian Micheller¹

Ida Erngren⁵

Mandy Runderkamp¹

Jakob Haglöf⁵

Ina Sauerland¹

Igor Yashayaev⁶

Georg Steinert^{1*}

Ellen Kenchington⁶

Benjamin Mueller⁴

Curt Pettersson⁵

Jasper de Goeij⁴

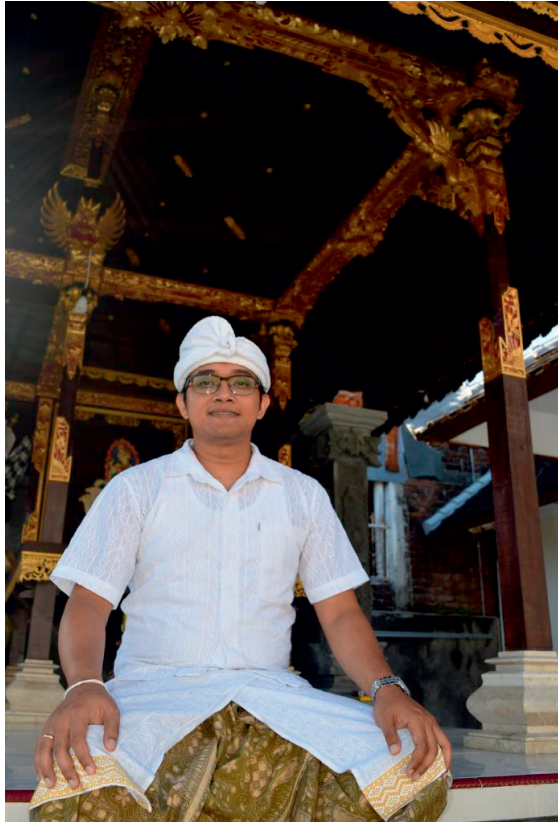
Paco Cárdenas⁵

Karin Steffen⁵

1. Laboratory of Microbiology, Wageningen University & Research, Stippeneng 4, 6708 WE, Wageningen, Netherlands.
 2. Marine Animal Ecology Group, Wageningen University & Research, Droevendaalsesteeg 1, 6708 PB, Wageningen, The Netherlands.
 3. Wageningen Marine Research, Wageningen University & Research, Ankerpark 27, 1781 AG, Den Helder, The Netherlands.
 4. Department of Freshwater and Marine Ecology, University of Amsterdam, Postbus 94240, 1090 GE, Amsterdam, The Netherlands.
 5. Pharmacognosy, Department of Medicinal Chemistry, Uppsala University, Husargatan 3, Uppsala 751 23, Sweden.
 6. Department of Fisheries and Oceans, Bedford Institute of Oceanography, Dartmouth, Canada
- * Present address: GEOMAR Helmholtz Centre for Ocean Research, Division of Marine Microbiology. Düsternbrooker Weg 20 D-24105, Kiel, Germany.

About the author

Anak Agung Gede Indraningrat was born in Denpasar, Bali, Indonesia at 18 November 1985. In August 2008, he completed bachelor degree in Biology at Udayana University in Bali. In 2010, he was among the 50 awardees of the International Fellowship Program in Indonesia sponsored by the Ford Foundation. With the Fellowship, he continued master of Biotechnology at Wageningen University and Research (WUR) in September 2011 with specialization in cellular and molecular. He completed his major thesis at the Laboratory of Microbiology under supervision Kyle McPherson M.Sc, Dr Detmer



Sipkema and Prof. Dr Hauke Smidt on detection of halogenase activity in sponge-associated microbes. He stayed at the same lab for his minor thesis to work on characterization of argonaute protein under supervision of Daan Swarts M.Sc and Prof. Dr John van der Oost, and completed his master degree in July 2013. In September 2014, he returned to Laboratory of Microbiology WUR as a PhD candidate after securing a fellowship from the Indonesian Endowment Fund for Education (LPDP) to conduct research on sponge microbiology under supervision of Dr Detmer Sipkema, Dr Leontine E. Becking and Prof. Dr Hauke Smidt. His PhD research focused on analysing the impact of depth on prokaryotic composition and biomolecules variation of marine sponges, which the result is presented in this thesis. In September 2018, he returned to Bali to join Faculty of Medicine and Health Sciences Warmadewa University as a lecturer and researcher.

List of Publications

Indraningrat, A.A.G., Smidt, H., Sipkema, D. Bioprospecting sponge-associated microbes for antimicrobial compounds. *Marine Drugs*. **2016**, *14*, 1-66.

Indraningrat, A.A.G., Micheller, S., Runderkamp, M., Sauerland, I., Becking, L.E., Smidt, H., Sipkema, D. Cultivation and antimicrobial screening of sponge-associated bacteria from *Agelas sventres* and *Xestospongia muta* collected from different depths. Submitted to *Marine Drugs*.

Indraningrat, A.A.G., Steinert, G., Becking, L.E., Mueller, B., de Goeij, J., Smidt, H., Sipkema, D. Depth affects sponge prokaryotic communities and their antimicrobial activities in two Demosponges, *Xestospongia muta* and *Agelas sventres*. Manuscript in preparation.

Steffen, K*, **Indraningrat, A.A.G***, Erngren, I., Haglöf, J., Becking, L.E., Smidt, H., Yashayaev, I., Kenchington, E., Pettersson, C., Cárdenas, P., Sipkema, D. Quantifying variations of microbiota and metabolome composition in deep-sea sponges - implications for chemical ecology and bioprospecting. Manuscript in preparation. *Both authors contributed equally.

Overview of Completed Training Activities

Discipline Specific Activities

Courses

PADI OWD, Karangasem, Indonesia	2015
Design experiment, Wageningen, NL	2016

Meetings

3rd WUR PhD Symposium, Wageningen, NL – oral presentation	2016
1st Acroporanet, Wageningen, NL – oral presentation	2016
1 st WISE, Wageningen, NL – poster presentation	2016
1 st COMBI conference 2016, Denpasar, Indonesia – oral presentation	2016
2 nd WISE, Wageningen, NL – poster presentation	2017
Blue Symposium: Sponge, Corals and the World, Blanes, Spain – oral presentation	2017
SponGES General Meeting, London UK, – pitch presentation	2017
SponGES General Meeting, Porto, Portugal – oral presentation	2018
WUR– Indonesian Network Scientific Exposure, Bogor, Indonesia, – poster presentation	2018

General Courses

VLAG PhD week, Baarlo, NL	2015
Project and time management, Wageningen, NL	2014
The Essential of Scientific Writing and Presenting, Wageningen, NL	2014
Scientific writing, Wageningen, NL	2016
R-course, Wageningen, NL	2016
Writing Grant Proposal, Wageningen, NL	2017

Optionals

Preparation of research proposal, Wageningen, NL	2014
Molecular Ecology group meetings, Wageningen, NL	2014-2018
Laboratory of Microbiology PhD Meetings, Wageningen, NL	2014-2018
Laboratory of Microbiology PhD Trip to Germany, Sweden and Denmark	2017

The research described in this thesis was financially supported by Indonesian Endowment for Education (LPDP) under grant agreement number 20140812021557 for Anak Agung Gede Indraningrat. Additional financial supports were also given by the SponGES project from the European Union's Horizon 2020 research and innovation programme under grant agreement No 679849, Substation Curaçao for submersible dives and the Rufford Foundation under grant number 17660-1.

Colophon

Cover: silhouet of marine sponges across different depths

Cover design: Sigit Pamungkas and Anak Agung Gede Indraningrat

Printed by: DigiForce || ProefschriftMaken

Financial support from LPDP and Laboratory of Microbiology, Wageningen University for printing this thesis is gratefully acknowledged.

